

University of Alberta

Biosynthetic Studies of Resorcylic Acid Lactones, Hypothemycin, Radicicol, and Dehydrocurvularin

by

Zhizeng Gao

A thesis submitted to the Faculty of Graduate Studies and Research
in partial fulfillment of the requirements for the degree of

Doctor of Philosophy

Department of Chemistry

©Zhizeng Gao

Fall, 2013

Edmonton, Alberta

Permission is hereby granted to the University of Alberta Libraries to reproduce single copies of this thesis and to lend or sell such copies for private, scholarly or scientific research purposes only. Where the thesis is converted to, or otherwise made available in digital form, the University of Alberta will advise potential users of the thesis of these terms.

The author reserves all other publication and other rights in association with the copyright in the thesis and, except as herein before provided, neither the thesis nor any substantial portion thereof may be printed or otherwise reproduced in any material form whatsoever without the author's prior written permission.

Abstract

Fungal polyketides, a vast source for pharmaceutical industries, are biosynthesized by multifunctional iterative polyketide synthases (PKS). The biosynthesis employs complex programming rules, which are currently unresolved. To decode the programming rules, the biosynthesis of three polyketides, hypothemycin, radicicol and dehydrocurvularin were investigated via heterologous reconstitution of corresponding PKSs in *Saccharomyces cerevisiae* strain BJ5464-NpgA. The biosyntheses of hypothemycin and radicicol share significant similarity. They both employ a pair of highly reducing PKS (HRPKS) and non-reducing PKS (NRPKS): the HRPKSs (Hpm8 and Rdc5) construct the reduced portions of the PKS-product backbones, whereas the NRPKSs (Hpm3 and Rdc1) synthesize the aromatic portions. To determine the distribution of reactions between HRPKS and NRPKS in the two biosynthetic systems, putative biosynthetic intermediates (**27** for hypothemycin and **149** for radicicol) were synthesized as their *S*-*N*-acetylcysteamine (SNAC) thioesters. We found that hypothemycin biosynthesis employs a 6+3 distribution of reactions, but radicicol biosynthesis uses a 5+4 distribution of reactions.

The substrate-dependent stereospecificity of Hpm8 ketoreductase (KR) was investigated by incubating Hpm8 with a series of β -keto SNAC thioesters. The KR domain stereospecificity was found to be dependent only on substrate chain lengths; the KR domain reduced the β -keto groups of diketides (4 carbon) to L-hydroxyl groups, but reduced all other β -keto intermediates to D-hydroxyl groups. This unprecedented, switchable stereospecificity suggests that iterative PKSs are more complex than previous thought, and that the substrate-PKS

interactions play a significant role in iterative PKS programming. To fully investigate the substrate-HRPKS interactions, a series of ^{13}C -labeled, partially assembled precursors were synthesized and assayed with Hpm8 and Hpm3. Our data suggest that Hpm8 prefers substrates resembling biosynthetic intermediates after the reductive modifications.

The putative gene cluster of dehydrocurvularin was uncovered via genomic sequencing of producing strain *Alternaria cinerariae*. A pair of HRPKS (Dhc3) and NRPKS (Dhc5) was identified, analogous to hypothemycin and radicicol biosynthesis. Both PKS genes were cloned into expression plasmids, and the gene products were successfully expressed and purified from BJ5464-NpgA. *In vivo* reconstitution of DHC production in BJ5464-NpgA containing genes encoding Dhc3 and Dhc5 was not successful. Other cryptic enzymes may be involved in the biosynthesis of DHC.

Acknowledgements

I would like to express my sincere gratitude to my Ph.D. supervisor Professor John C. Vederas. His infectious enthusiasm of science has profoundly influenced me and his immense knowledge has always guided me overcome the field of obstacles. Moreover, the Vederas group has always been a warm and supportive family. I would also like to express my thanks to Professor Yi Tang (UCLA) and his graduate students Dr. Hui Zhou, Dr. Kangjian Qiao, and Ms. Jingjing Wang for the fruitful collaborations on hypothemycin and radicicol biosynthesis projects. I sincerely thank Mr. Gareth Lambkin for his mentoring on the molecular biology techniques.

I would like to thank Dr. Marco van Belkum and Dr. Brandon Findlay for their efforts in proofreading this thesis, as well as Mr. Gareth Lambkin and Mr. Justin Thuss for proofreading part of thesis. I would like to thank Ms. Amy Norquay for her hard work on synthesis of a ^{13}C -labeled substrate. I am especially grateful to Dr. Dave Dietrich, Dr. Jennifer Chaytor, Dr. Jesse Li, and Dr. Wei Liu for their insightful suggestions and encouragement on my research projects. I would like to thank support staff in the NMR services, mass spectral services, and analytical services for their assistance with my research projects. Finally I want to thank my family and friends for their support. I am especially gratefully to my wife Vicky for her unfailing support and encouragement.

Table of Content

Chapter 1: Introduction.....	1
1.1 Background of polyketides.....	1
1.2 PKS programming.....	3
1.2.1 Type I PKS	7
1.2.1.1 Type I modular PKS.....	7
1.2.1.2 Type I iterative PKS	11
1.2.1.2.1 HRPKSs programming	12
1.2.1.2.2 NRPKSs programming.....	18
1.2.2 Type II PKSs	20
1.2.3 Type III PKSs.....	22
Chapter 2: Biosynthetic Studies of Hypothemycin	26
2.1 Introduction.....	26
2.2 <i>In vitro</i> reconstitution of two iterative PKSs for DHZ biosynthesis.....	29
2.2.1 Introduction.....	29
2.2.2 Results and discussion	30
2.2.2.1 <i>In vitro</i> reconstitution of Hpm8	30
2.2.2.2 <i>In vitro</i> reconstitution of DHZ biosynthesis.....	33
2.2.2.3 Kinetic parameters of Hpm8 and Hpm3 <i>in vitro</i>	36
2.2.2.4 Distribution of labor between Hpm8 and Hpm3	37
2.2.2.5 Probing the function of the SAT domain.....	39
2.2.3 Conclusions	43
2.3 Hpm8 KR domain stereospecificity.....	45

2.3.1 Introduction.....	45
2.3.2 Results and discussion	48
2.3.2.1 Synthesis of SNAC thioesters	48
2.3.2.1.1 Synthesis of diketides 30, 30D and 30L.....	48
2.3.2.1.2 Synthesis of tetraketides 35, 35D and 35L.....	49
2.3.2.1.3 Syntheses of triketides 32, 32D and 32L.	54
2.3.2.1.4 Synthesis of triketides 31, 31D and 31L, tetraketides 33, 33D and 33L, 34, 34D and 34L, and pentaketides 36, 36D and 36L.	55
2.3.2.1.5 Synthesis of hexaketides 37, 37D and 37L	57
2.3.2.2 Stereospecificity of Hpm8 KR domain at diketide and tetraketide stages.....	58
2.3.2.3 Probing stereospecificity of Hpm8 KR at other ketide stages	60
2.3.2.4 Domain swaps between Hpm8 KR and Rdc5 KR.....	61
2.3.2.5 Stereospecificity of chimeric Hpm8 toward β -keto SNAC thioesters	66
2.3.2.6 Activities of chimeric Hpm8 and Hpm3 <i>in vivo</i>	67
2.3.2.6.1 Identity of 79.....	68
2.3.2.6.2 Probing epimerization activity of Hpm3.....	71
2.3.2.6.3 Rational for production of <i>epi</i> -DHZ by Hpm8B2, Hpm8B4 or Hpm8B7	72
2.3.3 Conclusions.....	73
2.4 Investigation of HRPKS functions using partially assembled intermediates	76

2.4.1 Introduction.....	76
2.4.2 Results and discussion	82
2.4.2.1 Synthesis of SNAC thioesters	82
2.4.2.1.1 Synthesis of ¹³ C-labeled diketide 95	82
2.4.2.1.2 Synthesis of ¹³ C-labeled diketide 96, triketides 97 and 98, and tetraketides 100 and 101	82
2.4.2.1.3 Synthesis of ¹³ C-labeled triketide 99	85
2.4.2.1.4 Synthesis of ¹³ C-labeled pentaketide 102	85
2.4.2.1.5 Synthesis of ¹³ C-labeled pentaketide 103	86
2.4.2.1.5.1 Conjugated reduction of 125 with Hantzsch esters ...	87
2.4.2.1.5.2 Conjugated reduction of 125 with NaBH ₄ and InCl ₃ . 88	
2.4.2.1.6 Synthesis of unnatural triketides 104 and 105	90
2.4.2.2 Incorporation of ¹³ C-labeled partially assemble precursors... 91	
2.4.2.2.1 Incorporation of triketide 99.....	92
2.4.2.2.2 Incorporation of other ¹³ C-labeled ketide intermediates ...	96
2.4.2.3 Incorporation of unnatural precursors 97, 30D, 104, 105.....	100
2.4.2 Conclusions	102
Chapter 3: Biosynthetic Studies of Radicicol.....	104
3.1 Introduction of radicicol.....	104
3.2 Results and discussion	108
3.2.1 Expressions of Rdc5 and Rdc1 and their activities.....	108
3.2.2 Polyketide chain length control of Rdc5 and Rdc1	112
3.2.2.1 6+3 combination and 5+4 combination	112

3.2.2.2 Synthesis of pentaketide SNAC thioester 149	114
3.2.2.3 Incorporation of 149	117
3.2.3 Functions of the Rdc1 TE domain	119
3.2.3.1 Knock-out of the TE domain of Rdc5	119
3.2.3.2 Probing the stereoselectivity of the TE domain	123
3.2.4 Function of Rdc2	126
3.2.4.1 Rdc2 transforms (<i>R</i>)-monocillin II to pochonin D	126
3.2.4.2 Substrate specificity of Rdc2	128
3.3 Conclusion	130
Chapter 4: Biosynthetic studies of dehydrocurvularin	132
4.1 Introduction	132
4.1.1 Introduction to curvularins and their biological activities	132
4.1.2 Previous biosynthetic studies of dehydrocurvularin	134
4.1.3 Project Goals	138
4.2 Results and discussion	139
4.2.1 Gene cluster for dehydrocurvularin	139
4.2.2 Proposed biosynthesis of dehydrocurvularin.	144
4.2.3 Plasmid construction	146
4.2.3.1 Plasmids constructed (Collaboration with Mr. Gareth Lambkin)	146
4.2.3.2 Plasmid construction	151
4.2.3.2.1 Dhc3 plasmid construction	152
4.2.3.2.2 Dhc5 plasmid construction	153

4.3 Conclusions.....	157
Chapter 5: Experimental	161
5.1 General synthetic procedures	161
5.1.1 Reagents, solvents, and purifications	161
5.1.2 Compound characterization	162
5.2 Synthesis and characterization of compounds	163
4-(Methoxymethoxy)-6-methyl-2 <i>H</i> -pyran-2-one (9)	163
6-(Bromomethyl)-4-(methoxymethoxy)-2-pyrone (10)	164
Dimethyl (4-(methoxymethoxy)-2-oxo-2 <i>H</i> -pyran-6-yl)	
methylphosphonate (11)	164
(<i>S</i>)-methyl 3-(<i>tert</i> -butyldimethylsilyloxy)butanoate (14)	165
(<i>S</i>)-3-(<i>tert</i> -butyldimethylsilyloxy)butanal (15).....	166
(<i>S</i> , <i>E</i>)-6-(4-(<i>tert</i> -Butyldimethylsilyloxy)pent-1-enyl)-4-	
(methoxymethoxy)-2 <i>H</i> -pyran-2-one (12)	167
(<i>S</i> , <i>E</i>)-4-Hydroxy-6-(4-hydroxypent-1-enyl)-2 <i>H</i> -pyran-2-one (8).....	168
(<i>S</i>)- <i>tert</i> -Butyldimethyl(pent-4-en-2-yloxy)silane (17)	169
(<i>S</i> , <i>E</i>)-5-(<i>tert</i> -Butyldimethylsilyloxy)hex-2-enal (18)	169
(4 <i>S</i> , 8 <i>S</i> , <i>E</i>)-8-(<i>tert</i> -Butyldimethylsilyloxy)nona-1,5-dien-4-ol (19)	170
(5 <i>S</i> , 9 <i>S</i> , <i>E</i>)-5-Allyl-2, 2, 3, 3, 9, 11, 11, 12, 12-nonamethyl-4, 10-dioxa-3,	
11-disilatridec-6-ene (20)	171
(2 <i>E</i> , 5 <i>S</i> , 6 <i>E</i> , 9 <i>S</i>)-Ethyl 5,9-bis(<i>tert</i> -butyldimethylsilyloxy) deca-2,6-	
dienoate (21)	172

(5 <i>S</i> , 9 <i>S</i> , <i>E</i>)-Methyl 5,9-bis(<i>tert</i> -butyldimethylsilyloxy)dec-6-enoate (22)	173
(5 <i>S</i> , 9 <i>S</i> , <i>E</i>)-5, 9-bis(<i>tert</i> -Butyldimethylsilyloxy)dec-6-enal (23)	174
<i>S</i> -2-Acetamidoethyl 2-(diethoxyphosphoryl)ethanethioate (25)	175
(2 <i>E</i> , 7 <i>S</i> , 8 <i>E</i> , 11 <i>S</i>)- <i>S</i> -2-Acetamidoethyl 7,11-bis(<i>tert</i> -butyldimethylsilyloxy)dodeca-2,8-dienethioate (26)	176
(2 <i>E</i> , 7 <i>S</i> , 8 <i>E</i> , 11 <i>S</i>)- <i>S</i> -2-Acetamidoethyl 7,11-dihydroxydodeca-2,8-dienethioate (27)	177
(<i>S</i>)-4-benzyl-3-((3 <i>R</i> ,7 <i>S</i> , <i>E</i>)-7-(<i>tert</i> -butyldimethylsilyloxy)-3-hydroxyoct-4-enoyl)oxazolidin-2-one (39) and (<i>S</i>)-4-benzyl-3-((3 <i>S</i> ,7 <i>S</i> , <i>E</i>)-7-(<i>tert</i> -butyldimethylsilyloxy)-3-hydroxyoct-4-enoyl)oxazolidin-2-one (40) ...	178
(3 <i>R</i> , 7 <i>S</i> , <i>E</i>)-7-(<i>tert</i> -Butyldimethylsilyloxy)-3-hydroxy-1-((<i>S</i>)-4-isopropyl-2-thioxothiazolidin-3-yl)oct-4-en-1-one (56) and (3 <i>S</i> , 7 <i>S</i> , <i>E</i>)-7-(<i>tert</i> -Butyldimethylsilyloxy)-3-hydroxy-1-((<i>S</i>)-4-isopropyl-2-thioxothiazolidin-3-yl)oct-4-en-1-one (57)	180
(3 <i>R</i> , 7 <i>S</i> , <i>E</i>)- <i>S</i> -2-Acetamidoethyl 7-(<i>tert</i> -butyldimethylsilyloxy)-3-hydroxyoct-4-enethioate (41)	182
(3 <i>S</i> , 7 <i>S</i> , <i>E</i>)- <i>S</i> -2-Acetamidoethyl 7-(<i>tert</i> -butyldimethylsilyloxy)-3-hydroxyoct-4-enethioate (42)	183
(3 <i>R</i> , 7 <i>S</i> , <i>E</i>)- <i>S</i> -2-Acetamidoethyl 3,7-dihydroxyoct-4-enethioate (35L).	183
(3 <i>S</i> , 7 <i>S</i> , <i>E</i>)- <i>S</i> -2-Acetamidoethyl 3,7-dihydroxyoct-4-enethioate (35D).	184
(<i>S</i> , <i>E</i>)- <i>S</i> -2-Acetamidoethyl 7-(<i>tert</i> -Butyldimethylsilyloxy)-3-oxooct-4-enethioate and (<i>S</i> , 4 <i>E</i>)- <i>S</i> -2-Acetamidoethyl 7-(<i>tert</i> -butyldimethylsilyloxy)-3-hydroxyocta-2, 4-dienethioate (58)	185

(<i>S, E</i>)- <i>S</i> -2-Acetamidoethyl 7-hydroxy-3-oxooct-4-enethioate and (<i>S, 4E</i>)- <i>S</i> -2-Acetamidoethyl 3,7-dihydroxyocta-2, 4-dienethioate (35).....	186
(3 <i>S, 5S</i>)-5-(<i>tert</i> -butyldimethylsilyloxy)-3-hydroxy-1-((<i>S</i>)-4-isopropyl-2-thioxothiazolidin-3-yl)hexan-1-one (65) and (3 <i>R, 5S</i>)-5-(<i>tert</i> -butyldimethylsilyloxy)-3-hydroxy-1-((<i>S</i>)-4-isopropyl-2-thioxothiazolidin-3-yl)hexan-1-one (66)	187
(3 <i>S, 5S</i>)- <i>S</i> -2-acetamidoethyl 3,5-dihydroxyhexanethioate (32L)	189
(3 <i>R, 5S</i>)- <i>S</i> -2-acetamidoethyl 3, 5-dihydroxyhexanethioate (32D).....	190
(<i>S</i>)- <i>S</i> -2-Acetamidoethyl 5-(<i>tert</i> -butyldimethylsilyloxy)-3-oxohexanethioate and (<i>S</i>)- <i>S</i> -2-Acetamidoethyl 5-(<i>tert</i> -butyldimethylsilyloxy)-3-hydroxyhex-2-enethioate (67).....	190
(<i>S</i>)- <i>S</i> -2-Acetamidoethyl 5-hydroxy-3-oxohexanethioate and (<i>S</i>)- <i>S</i> -2-Acetamidoethyl 3,5-dihydroxyhex-2-enethioate (32)	192
(<i>S</i>)-3-Hydroxy-1-((<i>S</i>)-4-isopropyl-2-thioxothiazolidin-3-yl)hexan-1-one (68) and (<i>R</i>)-3-Hydroxy-1-((<i>S</i>)-4-isopropyl-2-thioxothiazolidin-3-yl)hexan-1-one (69).....	192
(<i>S</i>)- <i>S</i> -2-Acetamidoethyl 3-hydroxyhexanethioate (31L)	194
(<i>R</i>)- <i>S</i> -2-Acetamidoethyl 3-hydroxyhexanethioate (31D)	195
<i>S</i> -2-Acetamidoethyl 3-oxohexanethioate and <i>S</i> -2-Acetamidoethyl 3-hydroxyhex-2-enethioate (31)	195
(<i>S</i>)-3-Hydroxy-1-((<i>S</i>)-4-isopropyl-2-thioxothiazolidin-3-yl)octan-1-one (70) and (<i>R</i>)-3-Hydroxy-1-((<i>S</i>)-4-isopropyl-2-thioxothiazolidin-3-yl)octan-1-one (71)	196
(<i>S</i>)- <i>S</i> -2-Acetamidoethyl 3-hydroxyoctanethioate (33L).....	198

(<i>R</i>)-<i>S</i>-2-Acetamidoethyl 3-hydroxyoctanethioate (33D)	198
<i>S</i>-2-acetamidoethyl 3-oxooctanethioate and <i>S</i>-2-Acetamidoethyl 3-	
hydroxyoct-2-enethioate (33)	199
(<i>R</i>, <i>E</i>)-3-Hydroxy-1-((<i>S</i>)-4-isopropyl-2-thioxothiazolidin-3-yl)oct-4-en-1-	
one (72) and (<i>S</i>, <i>E</i>)-3-Hydroxy-1-((<i>S</i>)-4-isopropyl-2-thioxothiazolidin-3-	
yl)oct-4-en-1-one (73)	200
(<i>R</i>, <i>E</i>)-<i>S</i>-2-Acetamidoethyl 3-hydroxyoct-4-enethioate (34D)	201
(<i>S</i>, <i>E</i>)-<i>S</i>-2-Acetamidoethyl 3-hydroxyoct-4-enethioate (34L).....	202
(<i>E</i>)-<i>S</i>-2-Acetamidoethyl 3-oxooct-4-enethioate and (4<i>E</i>)-<i>S</i>-2-	
Acetamidoethyl 3-hydroxyocta-2,4-dienethioate (34).....	203
(<i>S</i>)-3-Hydroxy-1-((<i>S</i>)-4-isopropyl-2-thioxothiazolidin-3-yl)decan-1-one	
(74) and (<i>R</i>)-3-Hydroxy-1-((<i>S</i>)-4-isopropyl-2-thioxothiazolidin-3-	
yl)decan-1-one (75).....	204
(<i>S</i>)-<i>S</i>-2-Acetamidoethyl 3-hydroxydecanethioate (36L)	205
(<i>R</i>)-<i>S</i>-2-Acetamidoethyl 3-hydroxydecanethioate (36D)	206
<i>S</i>-2-Acetamidoethyl 3-oxodecanethioate and <i>S</i>-2-Acetamidoethyl 3-	
hydroxydec-2-enethioate (36).....	206
(<i>S</i>)-1-((<i>S</i>)-4-Benzyl-2-thioxothiazolidin-3-yl)-3-hydroxydodecan-1-one	
(77) and (<i>R</i>)-1-((<i>S</i>)-4-Benzyl-2-thioxothiazolidin-3-yl)-3-	
hydroxydodecan-1-one (78).....	207
(<i>S</i>)-<i>S</i>-2-Acetamidoethyl 3-hydroxydodecanethioate (37D).....	209
(<i>R</i>)-<i>S</i>-2-Acetamidoethyl 3-hydroxydodecanethioate (37L)	209
<i>S</i>-2-Acetamidoethyl 3-oxododecanethioate and <i>S</i>-2-Acetamidoethyl 3-	
hydroxydodec-2-enethioate (37)	210

MOM-DHZ (80)	211
(3R,7S)-7,14,16-trihydroxy-3-methyl-3,4,5,6,7,8,9,10,11,12-decahydro- 1H-benzo[c][1]oxacyclotetradecin-1-one (83).....	212
(R)-tert-Butyldimethyl(pent-4-en-2-yloxy)silane (86)	213
(R, E)-5-(tert-Butyldimethylsilyloxy)hex-2-enal (87).....	213
(4S, 8R, E)-8-(tert-Butyldimethylsilyloxy)nona-1,5-dien-4-ol (88)	214
(5S, 9R, E)-5-Allyl-2, 2, 3, 3, 9, 11, 11, 12, 12-nonamethyl-4, 10-dioxa-3, 11-disilatridec-6-ene (89)	215
(2E, 5S, 6E, 9R)-Ethyl 5,9-bis(tert-butyldimethylsilyloxy) deca-2,6- dienoate (90)	215
(5S, 9R, E)-Methyl 5,9-bis(tert-butyldimethylsilyloxy)dec-6-enoate (91)	216
(5S, 9R, E)-5, 9-bis(tert-Butyldimethylsilyloxy)dec-6-enal (92).....	217
(2E, 7S, 8E, 11R)-S-2-Acetamidoethyl 7,11-bis(tert- butyldimethylsilyloxy)dodeca-2,8-dienethioate (93)	218
(2E, 7S, 8E, 11R)-S-2-Acetamidoethyl 7,11-dihydroxydodeca-2,8- dienethioate (94)	219
5-([1- ¹³ C]-1-Hydroxyethylidene)-2,2-dimethyl-1,3-dioxane-4,6- dione1(108).....	220
S-2-Acetamidoethyl [3- ¹³ C]-3-oxobutanethioate and S-2-Acetamidoethyl [3- ¹³ C]-3-hydroxybut-2-enethioate (95)	221
(S)-[1- ¹³ C]-1-(4-benzyl-2-thioxothiazolidin-3-yl)ethanone (109)	222

(<i>S</i>)-[1- ¹³ C]-1-((<i>S</i>)-4-Benzyl-2-thioxothiazolidin-3-yl)-3-hydroxybutan-1-one (110) and (<i>R</i>)-[1- ¹³ C]-1-((<i>S</i>)-4-Benzyl-2-thioxothiazolidin-3-yl)-3-hydroxybutan-1-one (111)	223
(<i>S</i>)- <i>S</i> -(2-Acetamidoethyl) [1- ¹³ C]-3-hydroxybutanethioate (96)	224
(3 <i>S</i> , 5 <i>S</i>)-[1- ¹³ C]-1-((<i>S</i>)-4-Benzyl-2-thioxothiazolidin-3-yl)-5-(<i>tert</i> -butyldimethylsilyloxy)-3-hydroxyhexan-1-one (112) and (3 <i>R</i> , 5 <i>S</i>)-[1- ¹³ C]-1-((<i>S</i>)-4-Benzyl-2-thioxothiazolidin-3-yl)-5-(<i>tert</i> -butyldimethylsilyloxy)-3-hydroxyhexan-1-one (113)	225
(3 <i>S</i> , 5 <i>S</i>)- <i>S</i> -(2-Acetamidoethyl) [1- ¹³ C]-3,5-dihydroxyhexanethioate (97)	227
(3 <i>R</i> , 5 <i>S</i>)- <i>S</i> -2-Acetamidoethyl [1- ¹³ C]-3,5-dihydroxyhexanethioate (98)	228
(3 <i>R</i> , 7 <i>S</i> , <i>E</i>)- [1- ¹³ C]-1-((<i>S</i>)-4-Benzyl-2-thioxothiazolidin-3-yl)-7-(<i>tert</i> -butyldimethylsilyloxy)-3-hydroxyoct-4-en-1-one (114) and (3 <i>S</i> , 7 <i>S</i> , <i>E</i>)-[1- ¹³ C]-1-((<i>S</i>)-4-Benzyl-2-thioxothiazolidin-3-yl)-7-(<i>tert</i> -butyldimethylsilyloxy)-3-hydroxyoct-4-en-1-one (115)	229
(3 <i>S</i> , 7 <i>S</i> , <i>E</i>)- <i>S</i> -2-Acetamidoethyl [1- ¹³ C]-3,7-dihydroxyoct-4-enethioate (101)	230
(<i>S</i> , <i>E</i>)- <i>S</i> -2-Acetamidoethyl [1- ¹³ C]-7-(<i>tert</i> -butyldimethylsilyloxy)-3-oxooct-4-enethioate and (<i>S</i> , 2 <i>Z</i> , 4 <i>E</i>)- <i>S</i> -2-Acetamidoethyl [1- ¹³ C]-7-(<i>tert</i> -butyldimethylsilyloxy)-3-hydroxyocta-2,4-dienethioate (116)	231
(<i>S</i> , <i>E</i>)- <i>S</i> -2-Acetamidoethyl [1- ¹³ C]-7-hydroxy-3-oxooct-4-enethioate and (<i>S</i> , 2 <i>Z</i> , 4 <i>E</i>)- <i>S</i> -2-Acetamidoethyl [1- ¹³ C]-3,7-dihydroxyocta-2,4-dienethioate (100)	233

[1- ¹³ C]-2-(Diethoxyphosphoryl)acetic acid (118):	234
<i>S</i> -2-Acetamidoethyl [1- ¹³ C]-2-(diethoxyphosphoryl)ethanethioate (119)	234
(<i>S, E</i>)- <i>S</i> -2-Acetamidoethyl [1- ¹³ C]-(5-(<i>tert</i> -butyldimethylsilyloxy)hex-2- enethioate (120)	236
(<i>S, E</i>)- <i>S</i> -2-Acetamidoethyl [1- ¹³ C]-5-hydroxyhex-2-enethioate (99).....	237
<i>S</i> -2-Acetamidoethyl [1- ¹³ C]-prop-2-enethioate (122).....	238
(2 <i>E, 5S, 6E, 9S</i>)- <i>S</i> -2-Acetamidoethyl [1- ¹³ C]-5,9-bis(<i>tert</i> - butyldimethylsilyloxy)deca-2,6-dienethioate (123)	239
(2 <i>E, 5S, 6E, 9S</i>)- <i>S</i> -2-Acetamidoethyl [1- ¹³ C]-5,9-dihydroxydeca-2,6- dienethioate (102)	240
(<i>E</i>)- <i>S</i> -(2-acetamidoethyl) but-2-enethioate (125).....	240
(5 <i>S, 9S, E</i>)- <i>S</i> -2-Acetamidoethyl [1- ¹³ C]-5,9-bis(<i>tert</i> - butyldimethylsilyloxy)dec-6-enethioate (124).....	241
(5 <i>S, 9S, E</i>)- <i>S</i> -2-Acetamidoethyl [1- ¹³ C]-5,9-dihydroxydec-6-enethioate (103).....	242
(<i>S,E</i>)- <i>S</i> -2-Acetamidoethyl 5-(<i>tert</i> -butyldimethylsilyloxy)hex-2-enethioate (129).....	243
(<i>S</i>)- <i>S</i> -2-Acetamidoethyl 5-(<i>tert</i> -butyldimethylsilyloxy)hexanethioate (130)	244
(<i>S</i>)- <i>S</i> -2-Acetamidoethyl 5-hydroxyhexanethioate (105).....	245
(<i>R, E</i>)- <i>S</i> -2-Acetamidoethyl 5-hydroxyhex-2-enethioate (104)	245
(<i>S,5E,11E</i>)-14,16-dihydroxy-3-methyl-3,4,9,10-tetrahydro-1 <i>H</i> - benzo[<i>c</i>][1]oxacyclotetradecine-1,7(8 <i>H</i>)-dione (133)	246

2, 4-bis(Methoxymethoxy)-6-methylbenzaldehyde (138)	247
2,4-bis(Methoxymethoxy)-6-methylbenzoic acid (139).....	248
(<i>R</i>)-Pent-4-en-2-yl 2,4-bis(methoxymethoxy)-6-methylbenzoate (140)	249
(<i>E</i>)- <i>N</i> -Methoxy- <i>N</i> -methylhepta-2,6-dienamide (146).....	250
(<i>R</i> , <i>E</i>)-Pent-4-en-2-yl 2,4-bis(methoxymethoxy)-6-(2-oxoocta-3,7-	
dienyl)benzoate (141)	251
MOM-(<i>R</i>) monocillin II (142)	252
(<i>R</i>)-monocillin II (135)	253
(<i>R</i>)-methyl 3-(<i>tert</i> -butyldiphenylsilyloxy)butanoate (151).....	254
(<i>R</i>)-3-(<i>tert</i> -butyldiphenylsilyloxy)butanal (152)	254
(<i>R</i> , <i>E</i>)-Methyl 7-(<i>tert</i> -butyldiphenylsilyloxy)oct-4-enoate (155).....	255
(<i>R</i> , <i>E</i>)-7-(<i>tert</i> -Butyldiphenylsilyloxy)oct-4-enal (156).....	256
(<i>R</i> , 2 <i>E</i> , 6 <i>E</i>)- <i>S</i> -2-Acetamidoethyl 9-(<i>tert</i> -butyldiphenylsilyloxy)deca-2,6-	
dienethioate (157)	256
(<i>R</i> , 2 <i>E</i> , 6 <i>E</i>)- <i>S</i> -2-Acetamidoethyl 9-hydroxydeca-2, 6-dienethioate (149)	
.....	257
(<i>S</i>)-methyl 3-(<i>tert</i> -Butyldiphenylsilyloxy)butanoat (159).....	258
(<i>S</i>)-3-(<i>tert</i> -butyldiphenylsilyloxy)butanal (160)	259
(<i>S</i> , <i>E</i>)-Methyl 7-(<i>tert</i> -butyldiphenylsilyloxy)oct-4-enoate (161)	259
(<i>S</i> , <i>E</i>)-7-(<i>tert</i> -Butyldiphenylsilyloxy)oct-4-enal (162)	260
(<i>S</i> , 2 <i>E</i> , 6 <i>E</i>)- <i>S</i> -2-Acetamidoethyl 9-(<i>tert</i> -butyldiphenylsilyloxy)deca-2,6-	
dienethioate (163)	261
(<i>S</i> , 2 <i>E</i> , 6 <i>E</i>)- <i>S</i> -2-Acetamidoethyl 9-hydroxydeca-2,6-dienethioate(164)	262
(<i>S</i>)-hept-6-en-2-ol (176).....	263

(<i>S, E</i>)- <i>S</i> -2-Acetamidoethyl 7-hydroxyoct-2-enethioate (177)	264
5.3 Biological procedures.....	265
5.3.1 Strain and general techniques for DNA manipulation	265
5.3.2 Isolation of <i>A. cinerariae</i> genomic DNA & total RNA, and the construction of cDNA library	265
5.3.4 Plasmid constructions.....	266
5.3.5 Protein Expression	270
Chapter 6: References.....	272
Appendix: X-ray crystal structure of dehydrocurvularin (5)	304

List of Schemes

Scheme 1-1 Degradation of dehydroacetic acid to form orcinol.....	3
Scheme 1-2 Proposed mechanism for the starter unit priming of HRPKSs.....	14
Scheme 1-3 A) Biosynthesis of tenellin by TENS. B) Biosynthesis of desmethylbassianin by DMBS.....	15
Scheme 1-4 Proposed mechanism of loading of a starter unit from the SAT domain to the KS domain.	19
Scheme 2-1 Synthesis of the proposed pyrone 8	33
Scheme 2-3 Synthesis of diketides (A) 30 and (B) 30D and 30L	49
Scheme 2-4 Original synthetic routes toward synthesis of 30D and 30L	50
Scheme 2-5 Synthesis of tetraketides 35 , 35D and 35L	53
Scheme 2-6 Syntheses of triketides 32 , 32D and 32L	55
Scheme 2-7 General synthetic scheme for four β -keto SNAC thioesters and eight β -hydroxyl SNAC thioesters.....	56
Scheme 2-8 Synthesis of hexaketides 37 , 37D and 37L	57
Scheme 2-9 General scheme of biosynthesis of (<i>R</i>)-monocillin II, a precursor toward radicicol.	62
Scheme 2-10 Attempts to synthesize 79 from 5 via a Mitsunobu reaction.	69
Scheme 2-11 Synthesis of 83 , an enantiomer of α -zearalanol.	70
Scheme 2-12 Synthesis of 94	72
Scheme 2-13 Synthesis of ^{13}C -labeled diketide 95	82
Scheme 2-14 Synthesis of (A) 109 , (B) diketide 96 , (C) triketides 97 and 98 , and (D) tetraketides 100 and 101	84

Scheme 2-15 Synthesis of ^{13}C -labeled triketide 99	85
Scheme 2-16 Synthesis of ^{13}C -labeled pentaketide 102	86
Scheme 2-17 Retrosynthesis of pentaketide 103	86
Scheme 2-18 Synthesis of 125	86
Scheme 2-19 Conjugate reduction by NADPH and Hantzsch ester.....	87
Scheme 2-20 Synthesis of ^{13}C -labeled pentaketide 103	90
Scheme 2-21 Synthesis of unnatural precursors (A) 104 and (B) 105	91
Scheme 2-22 Synthesis of 133 from DHZ.	95
Scheme 3-1 Synthesis of (<i>R</i>)-monocillin II (135).	110
Scheme 3-2 Retrosynthesis of pentaketide 149	114
Scheme 3-3 Three-component cross metathesis.....	115
Scheme 3-4 An alternative synthesis of pentaketide 149	116
Scheme 3-5 Mechanism of the Johnson-Claisen rearrangement.....	117
Scheme 3-6 Mechanisms of formation of 135 and 158	123
Scheme 3-7 Synthesis of 164	124
Scheme 4-1 Degradation of DHC to confirm the stereochemistry.....	133
Scheme 4-2 Intact incorporation of acetate units into DHC in <i>A. cinerariae</i>	135
Scheme 4-3 Incorporation of partially assembled precursors into dehydrocurvularin.	136
Scheme 4-4 Synthesis of tetraketide 173	156

List of Figures

Figure 1-1 Examples of polyketides and their biological activities.....	2
Figure 1-2 General biosynthesis of polyketides and fatty acids.	4
Figure 1-3 Programming of PKSs. The solid arrows represent the programmed pathway. The dash arrows show possible pathways.	7
Figure 1-4 Biosynthesis of erythromycin A.....	9
Figure 1-5 Production of a 16-membered macrolide by iteratively using of module 4 of DEBS2. The red ketide is from the additional round of iteration in module 4.	11
Figure 1-6 Domain architectures of HRPKS and mFAS.	13
Figure 1-7 Domain swaps between TENS and DMBS. The blue domains are from TENS; and the orange domains are from DMBS. ⁵¹	17
Figure 1-8 Activities of PKS4 from <i>G. fujikuroi</i> . A) Production of 1 by PKS4. B) Production of 2 by TE-less PKS4. C) Production of 3 and 4 by minimal PKS4.	20
Figure 1-9 Biosynthesis aromatic polyketides by type II PKSs.....	21
Figure 1-10 Type III PKSs promoted biosynthesis.....	23
Figure 1-11 Biosynthesis of chalcone and stilbene by CHS and STS respectively.	24
Figure 2-1 Typical RALs: hypothemycin, zearalenone, radicicol, LL-783,277, LLZ1640-2 and aigialomycin D.	26
Figure 2-2 Hypothemycin gene cluster in <i>H. subiculosus</i>	28
Figure 2-3 Proposed biosynthesis of hypothemycin.	28

Figure 2-4 Domain architecture of Hpm8 and Hpm3. KS: ketosynthase; MAT: malonyl-CoA:acyltransferase; ACP: acyl carrier protein; KR: ketoreductase; DH: dehydratase; ER: enoyl reductase; SAT: starter unit:ACP transacylase; PT: product template; TE: thioesterase.	29
Figure 2-5 Mechanisms of the formation of pyrones 6 , 7 and 8 . Black arrows represent the programmed pathway for biosynthesis of DHZ. Red arrows show the derailment pathway when Hpm3 is absent.	31
Figure 2-6 Formation of dehydrozearalenol (predicted and experimental). The structure highlight in the red box is the crystal structure of DHZ (5).	35
Figure 2-7 Kinetic analysis of Hpm8 and Hpm3 performed by the Tang group. A) The initial velocity of the biosynthesis of 5 at different Hpm8 concentrations. The concentration of Hpm3 is maintained at 5 μ M; (B) The initial velocity of the synthesis of 5 at different Hpm3 concentrations. Three different concentrations of Hpm8 are used at (i) 10 μ M, (ii) 20, and (iii) 30 μ M.	37
Figure 2-8 Transition states of asymmetrical allylboration.	39
Figure 2-9 Synthesis of 5 by (A) Hpm8 and Hpm3 from malonyl-CoA and NADPH; (B) Hpm8 and Hpm3-SAT ⁰ from malonyl-CoA and NADPH; (C) Hpm3 from malonyl-CoA and 27 ; D) Hpm3-SAT ⁰ from malonyl-CoA and 27	40
Figure 2-10 (A) Proposed biosynthesis of zearalenone. (B) Proposed biosynthesis of DHZ from Hpm8 and PKS13.	41
Figure 2-11 Specificity of the SAT domain. (A) Communication between Hpm8 and PKS13. (B) Production of 5 from 27 by mutant PKSH1. (C) Communication between Hpm8 and mutant PKS13.	42

Figure 2-12 Production of unnatural polyketide 29 by swapping the SAT domain.	43
Figure 2-13 KR domain of Hpm8 reduces the β -keto groups of the diketide and tetraketide with different stereospecificity during the biosynthesis of DHZ. The structure in the red box is the Newman projection of the hexaketide intermediate.....	46
Figure 2-14 β -keto SNAC thioesters used to probe stereochemical control of the Hpm8 KR domain.	48
Figure 2-15 Possible transition states of aldol reactions containing: (A) α - substituted enolate; and (B) α -unsubstituted enolate.	51
Figure 2-16 Transition states of Crimmins' auxiliary promoted aldol reaction. .	54
Figure 2-17 (A) <i>In vivo</i> ketoreduction of 30 tethered to ACP; and (B) <i>in vitro</i> reduction of 30 tethered to SNAC by the Hpm8 KR domain.	59
Figure 2-18 The stereospecificity of Hpm8 KR at the tetraketide stage.....	60
Figure 2-19 The stereospecificity of the Hpm8 KR domain at the triketide, pentaketide and tetraketide stages.....	61
Figure 2-20 The HPLC traces of the <i>in vivo</i> metabolites profiles from the <i>S.</i> <i>cerevisiae</i> co-transformants expressing Hpm3 and (i) Hpm8 (ii) Hpm8_Lys ²⁰⁸⁸ Asp, (iii) Hpm8_Ser ²¹¹³ Ala, (iv) Hpm8_Tyr ²¹²⁶ Ala or (v) Hpm8_Tyr ²¹¹⁸ Phe. The chromatograms above are obtained by monitoring at 320 nm. Mutations of Lys ²⁰⁸⁸ , Ser ²¹¹³ and Tyr ²¹²⁶ abolish the activities of Hpm8.....	63

Figure 2-21 (A) Cartoon view of the homology model of Hpm8_cKR. The catalytic residues Ser²¹¹³, Lys²⁰⁸⁸ and Tyr²¹²⁶ are shown as sticks in red. (B) The topology diagram of the model structure of Hpm8_cKR. The $\alpha_4\beta_5\alpha_5\alpha_6$ motif is highlighted in salmon. (C) Illustration of the swapping regions between Hpm8_cKR and Rdc5_cKR in different chimeric HRPKSs. In the schematic chimeric enzymes, the backbone is based on Hpm8. The substituting regions derived from Rdc5 are displayed in red lines. * indicates the positions of the three catalytic residues. 65

Figure 2-22 (A) Production of DHZ by Hpm8B5, Hpm8B8 and Hpm8B9; and (B) Production of *epi*-DHZ and DHZ by Hpm8B2, Hpm8B4 and Hpm8B7. 68

Figure 2-23 CD spectra of **83** (line a) and **84** (line b). 70

Figure 2-24 The fourteen intermediates en route to the hexaketide intermediate transferred to Hpm3 for production of DHZ. The four red structures are ready precursors, and the ten black structures between the acetyl unit and the hexaketide are unready precursors. 79

Figure 2-25 Feeding experiments involving advanced precursors or analogs. (A) incorporation of ¹³C labeled precursors; the red structures are ready precursors; and (B) incorporation of precursor analogs. 81

Figure 2-26 Incorporation of ¹³C-labeled precursors in a pre-loading assay. 92

Figure 2-27 LC-MS of the triketide **99** assay. (A) LC trace of triketide **99** assay (top); LC trace of control assay without substrate addition (bottom); (B) MS

spectrum of peak 1 of triketide 99 assay (left); MS spectrum of peak 1 of control assay (right); (B) UV spectrum of peak 1 from triketide 99	93
Figure 2-28 UV and MS spectra of 131 , 132 and 133 . (A) UV spectra of 131 and 132 (top); UV spectra of 133 (bottom). (B) MS spectra of 131 , 132 and 133 and their proposed structures.	94
Figure 2-29 ^{13}C NMR spectrum of ^{13}C -labeled DHZ (upper) and DHZ standard (bottom).	96
Figure 2-30 Three type of interactions between substrates and Hpm8. (A) ready precursor; (B) β -keto unready precursor; and (C) other unready precursor.	100
Figure 3-1 Resorcylic acid lactones (RALs): radicicol, zearalenone, and hypothemycin, (<i>R</i>)-monocillin II, Pochonin D.	104
Figure 3-2 The gene cluster of radicicol in <i>Pochonia chlamydosporia</i>	106
Figure 3-3 Domain architectures of Rdc5 and Rdc1. KS: ketosynthase; MAT: malonyl-CoA:acyltransferase; ACP: acyl carrier protein; KR: ketoreductase; DH: dehydratase; ER: enoyl reductase; SAT: starter unit:ACP transacylase; PT: product template; TE: thioesterase.	107
Figure 3-4 Proposed biosynthesis of radicicol (134).	108
Figure 3-5 <i>In vivo</i> reconstitution of biosynthesis of 135 . LC-MS profiles of organic extract from trace i) BJ5464-NpgA expressing Rdc1; trace ii) BJ5464-NpgA/ pKJ61 expressing Rdc5; trace iii) BJ5464-NpgA co-expressing Rdc5 and Rdc1.	109

Figure 3-6 Origin of the C5'-C6' *cis*-double bond. Rdc5 generates a single bond at C5'-C6'. The *cis*-double bond of C5'-C6' is introduced by post-PKS modifications..... **112**

Figure 3-7 Distribution of labor between Rdc5 and Rdc1. (A) 6+3 combination; and (B) 5+4 combination. Ketide units added by Rdc1 are shown in red. . **113**

Figure 3-8 Precursor-directed feeding using SNAC substrates. **A)** LC-MS profiles of organic extracts from strain harboring Rdc1 and trace i without substrate feeding; *trace ii*, supplementation with the pentaketide SNAC **164**; trace iii, supplementation with the pentaketide SNAC **149**. **B)** Chiral HPLC separation of the enantiomers **135** and **165** on a Lux 3 µm cellulose-1 column (Phenomenex): trace i, **165**; trace ii, **135**; trace iii, co-injection of a mixture of **165** and **135**. All traces are monitored at 300 nm. **118**

Figure 3-9 Reconstitution of Rdc1-S1889A *in vivo* and *in vitro*. (A) HPLC analysis (300 nm) of polyketides synthesized by (i) expressing Rdc1-S1889A and Rdc5 *in vivo* and (ii) incubating Rdc1-S1889A with compound **149** *in vitro*. (B) UV spectrum and compound structure of **158**. (B) Structures of isocoumarin compounds SMA76b and SMA76c. **120**

Figure 3-10 Circular dichroism (CD) spectra of (*S*)-monocillin II (**165**, upper) and (*R*)-monocillin II (**135**, bottom) **125**

Figure 3-11 LC-MS profiles for production of chlorinated RALs from the following: trace i, BJ5464-NpgA expressing Rdc5, Rdc1, and Rdc2; trace ii, *in vitro* assay of 50 µM Rdc2 incubated with 1 mM **135**, 100 µM FAD, 2 mM NADPH, 50 mM NaCl, and 10 µM SsuE (flavin reductase). *Inset* in

trace i shows observed [M-H] ⁺ MS spectrum of 136 , and <i>inset</i> in trace ii shows the observed [M-H] ⁺ MS spectrum of 166	127
Figure 3-12 LC-MS profiles for production of 167 from the following: trace i, BJ5464-NpgA expressing Hpm8, Hpm3, and Rdc2; trace ii, <i>in vitro</i> assay of 50 μM Rdc2 incubated with 1 mM DHZ, 100 μM FAD, 2 mM NADPH, 50 mM NaCl, and 10 μM SsuE. <i>Inset</i> in trace ii shows observed [M - H] ⁺ MS spectrum of 167	128
Figure 4-1 Curvularin-type natural products.	132
Figure 4-2 Proposed biosynthesis of dehydrocurvularin.	135
Figure 4-3 A) Production of DHC when supplying AtCuRS2 with L-5. B) Production of 175 when supplying AtCuRS2 with 174	138
Figure 4-4 Distinct cyclization mechanisms during the formation of 5 and 168 . C2-C7 cyclization yields RALs, while C3-C8 cyclization yields DALs....	139
Figure 4-5 RAL-type compounds: <i>cis</i> -resorcyllide, hypothemycin, radicicol, zearalenone, dehydrozearalenol and monocillin II.	140
Figure 4-6 Gene cluster of dehydrocurvularin biosynthesis.	142
Figure 4-7 (A) . Three conserved residues (Phe ¹⁴⁵⁵ , Tyr ¹⁵⁷⁶ , and Trp ¹⁵⁸⁴) promote DAL-type cyclization. (B). Mutations of the three residues to Tyr ¹⁴⁵⁵ , Phe ¹⁵⁷⁶ , and Leu ¹⁵⁸⁴ lead to RAL-type cyclization.	144
Figure 4-8 Proposed biosynthetic pathway for DHC.....	145
Figure 4-9 Synthesis of the first strain of cDNA. Red boxes represent introns.	146

Figure 4-10 pXK30 and pKOS518-120A plasmids. Amp is the ampicillin resistance gene. ADH2p is the ADH2 promoter sequences. ADH2t is the ADH2 terminator sequences.	147
Figure 4-11 Construction of an expression plasmid by TAR in <i>S. cerevisiae</i> . ..	148
Figure 4-12 A) Construction of Dhc3 expression plasmid from <i>dhc3-1</i> , <i>dhc3-2</i> and linearized pKOS518-120A. B) Construction of the Dhc5 expression plasmid from <i>dhc5</i> and linearized pXK30.	150
Figure 4-13 6% SDS-PAGE gel of proteins purified from <i>S. cerevisiae</i> BJ5464-NpgA containing <i>hpm3</i> and <i>dhc3</i> after Ni-NTA chromatography. Lane 1: Protein Marker. Lane 2: Dhc3 elution. Lane 3: concentrated Dhc3. Lane 4: Hpm3 elution. Lane 5: concentrated Hpm3.	151
Figure 4-14 An alternative way to construct Dhc3 expression plasmid.	153
Figure 4-15 Construction of Dhc5 expression plasmid from gDNA and cDNA.	154
Figure 4-16 6% SDS-PAGE gel of proteins purified from <i>S. cerevisiae</i> BJ5464-NpgA containing <i>dhc5</i> after Ni-NTA chromatography. Lane 1: concentrated Dhc5 (no mutation). Lane 2: Concentrated Dhc5 (1 mutation). Lane 3: Protein Marker.	155
Figure 4-17 6% SDS-PAGE gel of proteins purified from <i>S. cerevisiae</i> BJ5464-NpgA containing <i>hpm3</i> and <i>dhc3</i> after Ni-NTA chromatography. Lane 1: Protein Marker. Lane 2: concentrated Hpm3. Lane 3: concentrated Dhc3.	156

List of Tables

Table 2-1 Summary of the synthesis of triketides 31 , 31D and 31L , tetraketides 33 , 33D and 33L , 34 , 34D and 34L , and pentaketides 36 , 36D and 36L	56
Table 2-2 NMR data ^a comparison between 79 and 5	68
Table 2-3 Conditions employed for conjugate reduction of 125 to 126 with Hantzsch ester.	88
Table 2-4 Conditions employed for conjugated reduction of 125 to 126 with NaBH ₄ -InCl ₃	89
Table 2-5 Incorporation of partially assembled precursors.....	97
Table 2-6 Incorporation of partially assembled precursors analogs.	101
Table 3-1 NMR assignment of 158^a	121
Table 3-2 NMR assignment of 167^a	129
Table 5-1 Primers used for cloning.....	266

List of Abbreviations

[α]	specific rotation
A	adenylation domain
Å	angstrom
AcOH	acetic acid
ACP	acyl carrier protein
AIBN	2,2'-azobis(2-methylpropionitrile)
AT	acyl transferase
ATP	adenosine-5'-triphosphate
<i>n</i> -BuLi	<i>n</i> -butyl lithium
<i>c</i>	concentration in g mL ⁻¹ (for optical rotation)
C	condensation domain
CD	circular dichroism
cDNA	complementary DNA
CHS	chalcone synthase
CLC	Claisen cyclase
CMeT	C-methyltransferase domain
CoA	coenzyme A
δ	chemical shift in parts per million downfield from TMS
d	doublet (in NMR)
DAL	dihydroxyphenylacetic acid lactone
DBU	1,8-diazabicyclo[5.4.0]undec-7-ene
DCC	1,3-dicyclohexylcarbodiimide

DEBS	6-deoxyerythronolide synthase
DH	dehydratase
DHC	dehydrocurvularin
DHZ	dehydrozearalenol
DIBAL	diisobutyl aluminum hydride
DIPEA	<i>N, N</i> -diisopropylethylamine
DKC	Dieckmann cyclase
DMAP	4-(dimethylamino)pyridine
DMBS	desmethylbassianin synthase
DMSO	dimethylsulfoxide
DMF	dimethylformamide
DMP	Dess-Martin periodinane
eq	equivalents(s)
ER	enoyl reductase
EtOAc	ethyl acetate
FAS	fatty acid synthase
FT-ICR-MS	fourier transform ion cyclotron resonance mass spectrum
FTIR	Fourier transform infrared spectroscopy
GC-MS	gas chromatography coupled with liquid chromatography
HREI	high-resolution electron impact
HRES	high-resolution electrospray
HRPKS	highly reducing polyketide synthase
HWE	Horner-Wadsworth-Emmons
iNOS	inducible nitric-oxide synthase

IR	infrared
<i>J</i>	coupling constant in hertz
kDa	kilo Daltons
KR	ketoreductase
KS	ketosynthase
LiHMDS	lithium hexamethyldisilazane
LDA	lithium diisopropylamide
LC-MS	liquid chromatography coupled with mass spectrometry
m	multiplet
<i>m/z</i>	mass to charge ratio
MAT	malonyl-CoA:ACP transacylase
Me	methyl
MeT	methyl transferase
MFS	major facilitator family
MOM	methoxy methyl
MS	mass spectrometry
MSAS	6-methylsalicylic acid synthase
NADPH	β-nicotinamide adenine dinucleotide phosphate
NaHMDS	sodium hexamethyldisilazane
NBS	<i>N</i> -bromosuccinimide
NMR	nuclear magnetic resonance
NTA	nitrilotriacetic acid
NRPKS	non-reducing polyketide synthase
NRPS	non-ribosomal peptide synthetase

PCR	polymerase chain reaction
Ph	phenyl
PR-PKS	partially reducing polyketide synthase
PKS	polyketide synthase
ppm	parts per million
Ppant	phosphopantetheine
PT	product template
q	quartet
quant.	quantitative yield
R	reduction domain
RAL	resorcylic acid lactone
RT-PCR	reverse transcription polymerase chain reaction
s	singlet
SAM	<i>S</i> -adenosyl- <i>L</i> -methionine
SNAC	<i>N</i> -acetylcysteamine
SAT	starter unit:ACP transacylase
STS	stilbene synthase
<i>t</i> -BuOH	<i>tert</i> -butanol
t	triplet
TAR	transformation associated recombination
TBAF	tetrabutylammonium fluoride
TBDMS	<i>tert</i> -butyldimethylsilyl
TBDPS	<i>tert</i> -butyldiphenylsilyl
TE	thioesterase

TENS	tenellin synthetase
TH	thioester hydrolase domain
THF	tetrahydrofuran
TLC	thin layer chromatography
TFA	trifluoroacetic acid
TS	transition state
UV	ultraviolet spectroscopy

Chapter 1: Introduction

1.1 Background of polyketides

Polyketides are a large group of structural diverse secondary metabolites that occur in various organisms (bacteria, fungi, plants and protists), and display a variety of biological activities.¹⁻⁵ This class of natural products plays a profound role in human medicine, as antibiotics (erythromycin A), anticancer drugs (doxorubicin), cholesterol-lowering agents (lovastatin), antifungals (amphotericin B), and immunosuppressant drugs (rapamycins) (**Figure 1-1**).^{3, 4} It is estimated that polyketide-based therapeutics represent 20% of the top-selling drugs in the worldwide market with total annual revenues of over than US \$20 billion.³ An attractive aspect of polyketides is that they are naturally drug-like. More than 20 polyketide drugs have been commercialized, and there are only about 7000 polyketide structures known. So the “hit rate” of polyketides is approximately 0.3%, which is significantly higher than that of a typical High-Throughput screening of synthetic compound libraries.³

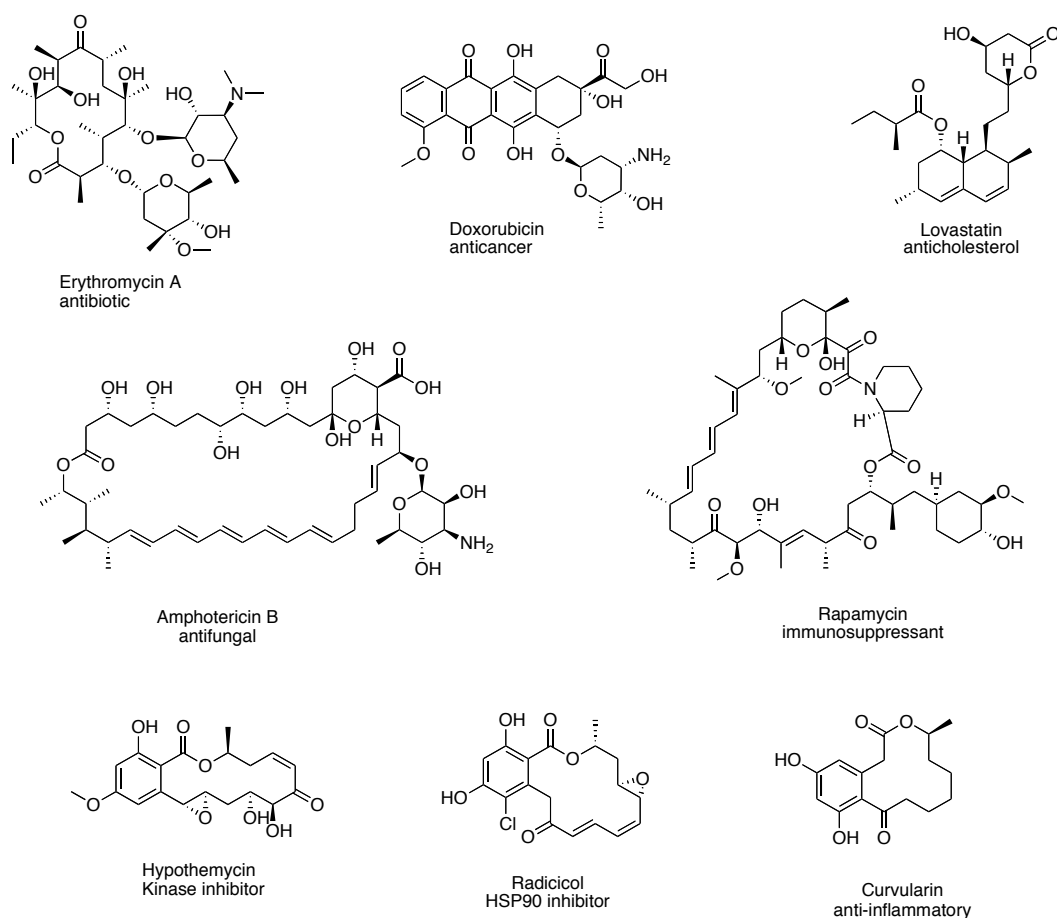
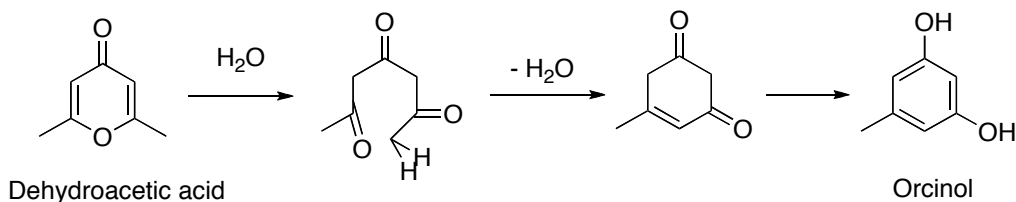


Figure 1-1 Examples of polyketides and their biological activities.

The word “polyketide” was originally coined by a British chemist, John Norman Collie, to represent the polyketomethylene group, $-(CH_2.CO)_n$.^{6, 7} In 1893, when he tried to degrade dehydroacetic acid with barium hydroxide, orcinol was formed as one of the products.⁸ He proposed that dehydroacetic acid was opened by water to form a polyketone intermediate, which then condensed again to generate the aromatic compound orcinol (**Scheme 1-1**). After many similar chemical explorations, the reactivity of the $-(CH_2.CO)_n-$ group (which Collie referred to as a “ketide” group) inspired his proposal that fats and oils might be derived from simple ketides.^{6, 9}



Scheme 1-1 Degradation of dehydroacetic acid to form orcinol.

However, this proposal was not prevalent until Arthur Birch first incorporated ^{14}C -labeled acetate into 6-methylsalicylic acid,¹⁰ which firmly established the “Collie-Birch polyketide hypothesis” that polyketides are derived from simple acetate units. This pioneering work, together with other stable isotope-labeling methodologies (^{13}C , ^2H , ^3H , ^{18}O) combined with rapidly developed NMR and mass spectrometry, paved the way for biosynthetic studies of polyketides.^{1, 11, 12}

1.2 PKS programming

Polyketide synthases (PKS) are enzymes responsible for formation of polyketides. PKSs share significant structural similarity with fatty acid synthases (FAS).¹³ FASs and PKSs employ the same set of domains to assemble fatty acids and polyketides, respectively, from simple acetate units as shown in **Figure 1-2**.

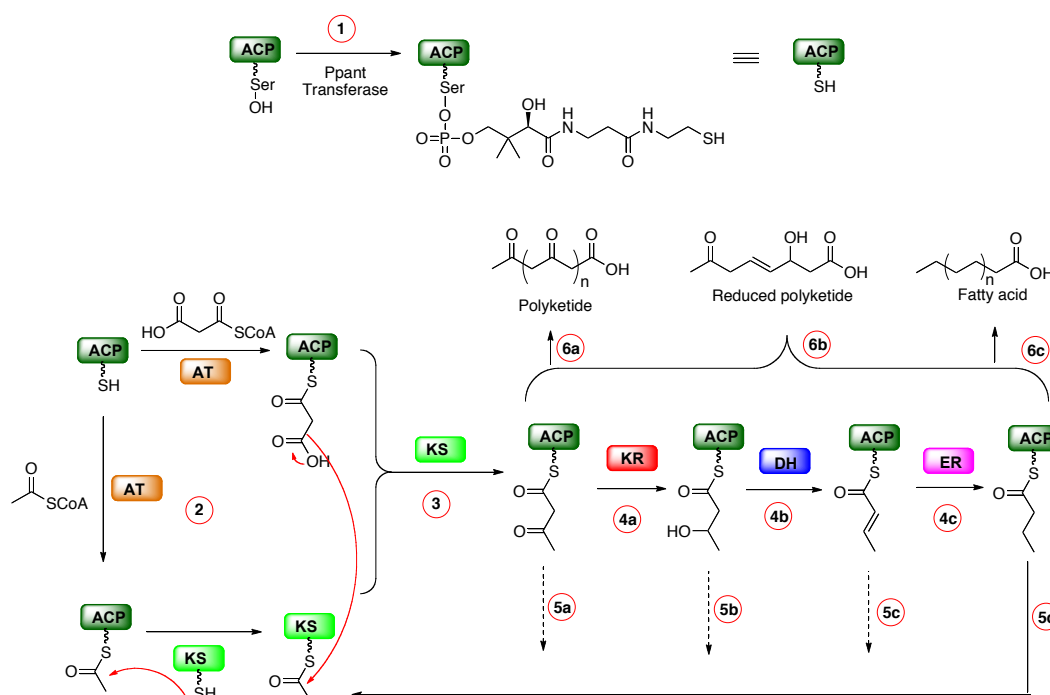


Figure 1-2 General biosynthesis of polyketides and fatty acids.

1. The first step of the assembly of polyketides and fatty acids is activation of acyl carrier protein (ACP). In the activation, a phosphopantetheine (Ppant) moiety is attached to a serine residue of ACP. A Ppant transferase enzyme facilitates this process.¹⁴⁻¹⁶ The Ppant arm is about 18Å long and flexible enough to enable the growing polyketide chain to reach the active sites of other domains for elongations and modifications.¹⁷

2. The acyltransferase (AT) domain catalyzes the priming of the starter unit (usually acetyl-CoA) and the extension unit (usually malonyl-CoA) to the ketosynthase (KS) domain and the ACP domain, respectively. For a FAS, a single AT domain promotes both acetyl- and malonyl-priming.¹³ The acetyl and malonyl units are competitively loaded to the Ppant thiol group of the ACP domain, where only the acetyl unit is transferred to the KS domain by transthioesterification.^{18, 19}

For PKSs, a fungal PKS usually employs a single AT domain to prime both the starter and extension units on the ACP domain; while a bacterial PKS typically uses different AT domains to facilitate the starter and extension units priming. Nevertheless, the starter unit of PKSs and FASs is generally not directly priming on the KS domain.

3. The KS domain catalyzes the decarboxylative Claisen condensation to furnish a β -keto intermediate tethered to the ACP domain.²⁰

4. PKSs differ from FASs in the fourth step. For the biosynthesis of a fatty acid, the β -keto intermediate from the step 3 undergoes three sequential reductions (4a, 4b, and 4c) exerted by the ketoreductase (KR) domain, the dehydratase (DH) domain, and the enoyl reductase (ER) domain. In contrast, the β -keto intermediate from a PKS can skip any reduction step (4a, 4b, or 4c) and be transferred back to the KS domain (5a, 5b, 5c, or 5d) for further chain elongations.¹

5. After the reductive modifications are completed, the intermediate is transferred back to the KS domain as a new starter unit, and this also makes the ACP domain available for loading of another malonyl-CoA as a new extender unit. Then the enzymes perform the Claisen condensation again (step 3). From here, a production cycle is established (step 3 - step 4 - step 5 - step 3).

6. Once a desired product is generated, the thioesterase (TE) domain usually terminates the chain elongation and offloads the product from the enzymes. If all β -keto intermediates skip all the reductions (pathway 5a), unmodified polyketides are formed (6a) and further cyclization steps can lead to

aromatic polyketides; if β -keto intermediates skip some of the reductions (combinations of pathway 5a, 5b, 5c, and 5d), reduced polyketides are generated with great diversity (6b); if all β -keto intermediates undergo all the reductive steps (pathway 5d), saturated fatty acids are produced (6c).

It is obvious that PKSs employ more complex programming rules than FASs, thus generating more structurally diverse natural products. The term “programmed PKS” has been introduced to describe “*control of the variables that determine the structure of the product of a specific PKS*”.²¹ There are several aspects of PKS programming. Taking the biosynthesis of 6-deoxyerythronolide B as an example (**Figure 1-3**), the first programming feature is the selection of the starter units. The 6-deoxyerythronolide PKSs (DEBS) specifically use propionyl-CoA as the starter unit instead of acetyl-CoA. The second feature is the choice of the extender units. DEBS specifically use (2*S*)-methylmalonyl-CoA as the extender unit.²² The third feature is the control of the reductive modifications of the β -keto groups of the growing chain. During the first round of chain extension, DEBS specifically reduce the β -keto group to (*R*)- β -hydroxyl, which then serves as a starter unit for the second chain extension. This feature represents two levels of programming: (1) Control of the oxidation stages of the β -position; and (2) stereochemical control of the ketoreduction. The fourth feature is regulation of cyclization of the nascent carbon chain. A 14-membered macrolactone is produced instead of other possible isomers.

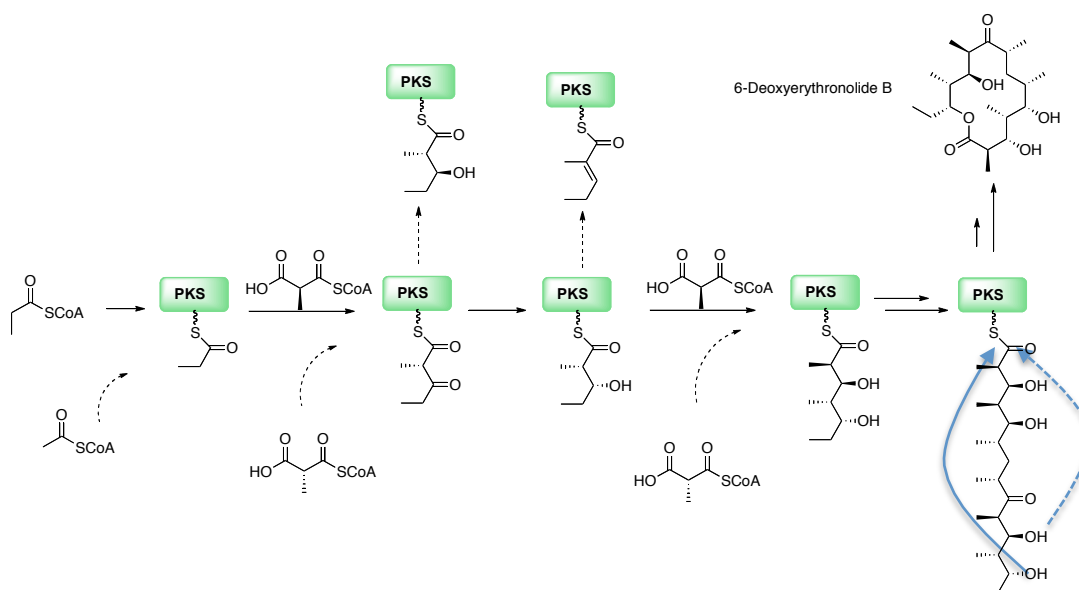


Figure 1-3 Programming of PKSs. The solid arrows represent the programmed pathway. The dash arrows show possible pathways.

Understanding of PKSs programming has been significantly advanced with crystallizations of individual PKS domains and development of genetic techniques.^{13, 23} Here the PKSs programming is discussed in terms of the three types of PKS,²³ with the focus on the Type I PKSs.

1.2.1 Type I PKS

Type I PKS enzymes are large, multi-functional, multi-domain megasynthases. Type I PKSs can be subdivided into two groups: modular²⁴ (mainly in bacteria) and iterative²³ (mainly in fungi) PKSs.

1.2.1.1 Type I modular PKS

Thirty years ago, a PKS enzyme was essentially a “black box” assembling polyketides.¹² It had been suggested that polyketides could be synthesized in a way resembling that of fatty acid biosynthesis, where a saturated chain was first

produced.¹² Then intensive “post-PKSs modifications” such as, C-methylation, cytochrome P-450 oxidation and rearrangements were exerted on the resulting saturated chain to generate a fully functionalized polyketide.

The mysterious programming of polyketide biosynthesis was first uncovered by Peter Leadlay and Leonard Katz’s landmark work on erythromycin PKSs.²⁵⁻²⁸ The *ery* gene cluster, responsible for erythromycin A production in *Saccharopolyspora erythraea*, encodes three PKSs (DEBS1, DEBS2, and DEBS3), and each PKS consists of two modules (**Figure 1-4**). Each module houses a full set of domains capable of performing one round of chain extension. In addition to module 1 and module 2, DEBS1 also has a loading module which only has two domains, the AT domain and the ACP domain. The loading module selects the starter unit propionyl-CoA, and transfers it to the KS domain of module 1. The ACP domain of module 1 is charged with methylmalonyl-CoA, which reacts with propionyl-CoA in the module 1 KS domain active-site cavity to form a β -keto intermediate. The KR domain stereospecifically reduces the β -keto intermediate to a β -hydroxyl intermediate. Because DH and ER are missing in module 1, no further reductive modifications can be exerted on the β -hydroxyl intermediate, and it is transferred to the KS domain of module 2. The chain extension and reductive modifications continue in module 2, 3, 4, 5, and 6, until a heptaketide is formed. The heptaketide is transferred to the TE domain of module 6, where a macrolactonization reaction is initiated to release 6-deoxyerythronolide B as a PKS product. 6-Deoxyerythronolide B undergoes two sequential glycosylations to form erythromycin A.

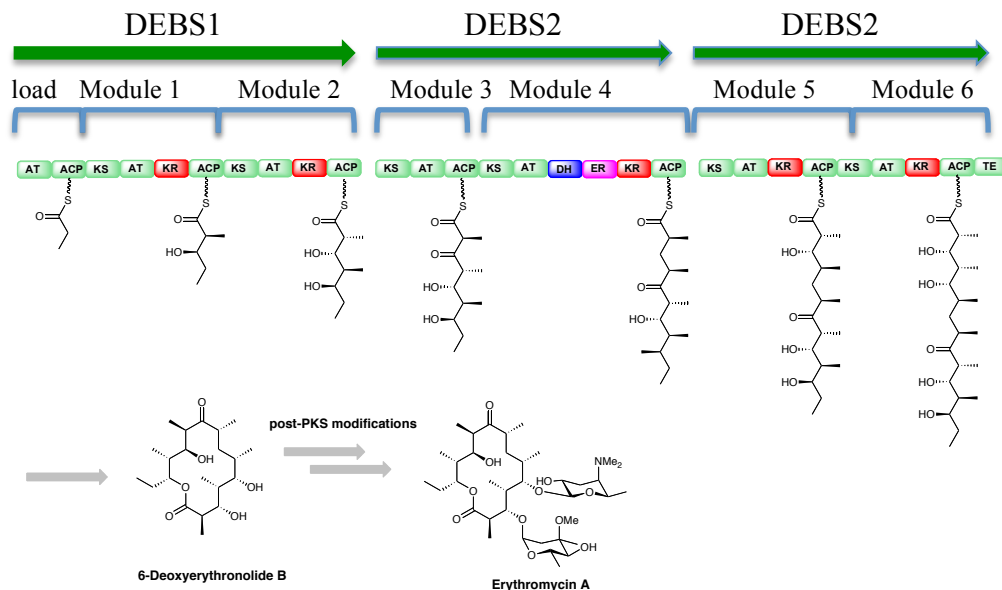


Figure 1-4 Biosynthesis of erythromycin A.

The programming of modular PKSs is seemingly encoded in the gene sequence, where the modules are arranged co-linearly with the products. Since the programming is the order and composition of modules, it is possible to predict a reasonable structure for the PKS product at the genetic level. In the programming, the AT domains govern the selection of the starter and extender units. The AT domains exclusively recruit (2*S*)-methylmalonyl-CoA for the biosynthesis of erythromycin.²² Extensive studies suggested that the KS domain catalyzes Claisen condensations with an inversion of configuration at C2 of the (2*S*)-methylmalonyl-CoA to yield a D-configured methyl group on intermediates.^{29, 30} The L-configured methyl groups of erythromycin are generated by epimerizations of the D-configured methyl groups, which are catalyzed by KR prior to the ketoreduction.^{31, 32} Control of the oxidation levels of the β -keto groups is achieved by elimination of certain processing domains in each module. The KR domains

are programmed to generate either *R* or *S*-configured β -hydroxyl groups. The intrinsic stereospecificity of ketoreduction is believed to be mediated by a Leu-Asp-Asp triad.^{33, 34} With the triad, the KR domain produces *S*-hydroxyl in the product; without the triad, a product with an *R*-hydroxyl is formed. The TE domain is programmed to facilitate cyclization of the heptaketide intermediate. Crystal structures of the DEBS TE domain suggest that a 20-Å-long substrate-binding channel passes through the entire domain, in which a macrolactonization reaction releases the PKS product.³⁵

However, not every type I modular PKS follows the aforementioned programming. A group of type I modular PKSs, the *trans*-AT type PKSs, utilize a single stand-alone AT or tandem AT enzymes instead of the common *cis*-AT domain for selection of the starter and extender units.³⁶ In addition, aberrant polyketide products can be produced by module skipping or stuttering (iterative use).³⁷ For example, in addition to 6-deoxyerythronolide B, a 16-membered octaketide macrolide was also isolated when *S. erythraea* strain No. 5 was cultured.³⁸ Detailed studies suggested that the 16-membered macrolide was an aberrant PKS product where the module 4 was iteratively used twice (**Figure 1-5**). Presumably because it is located at the end of the DEBS2 and its communication with module 5, which is located in a different PKS, is not very effective.

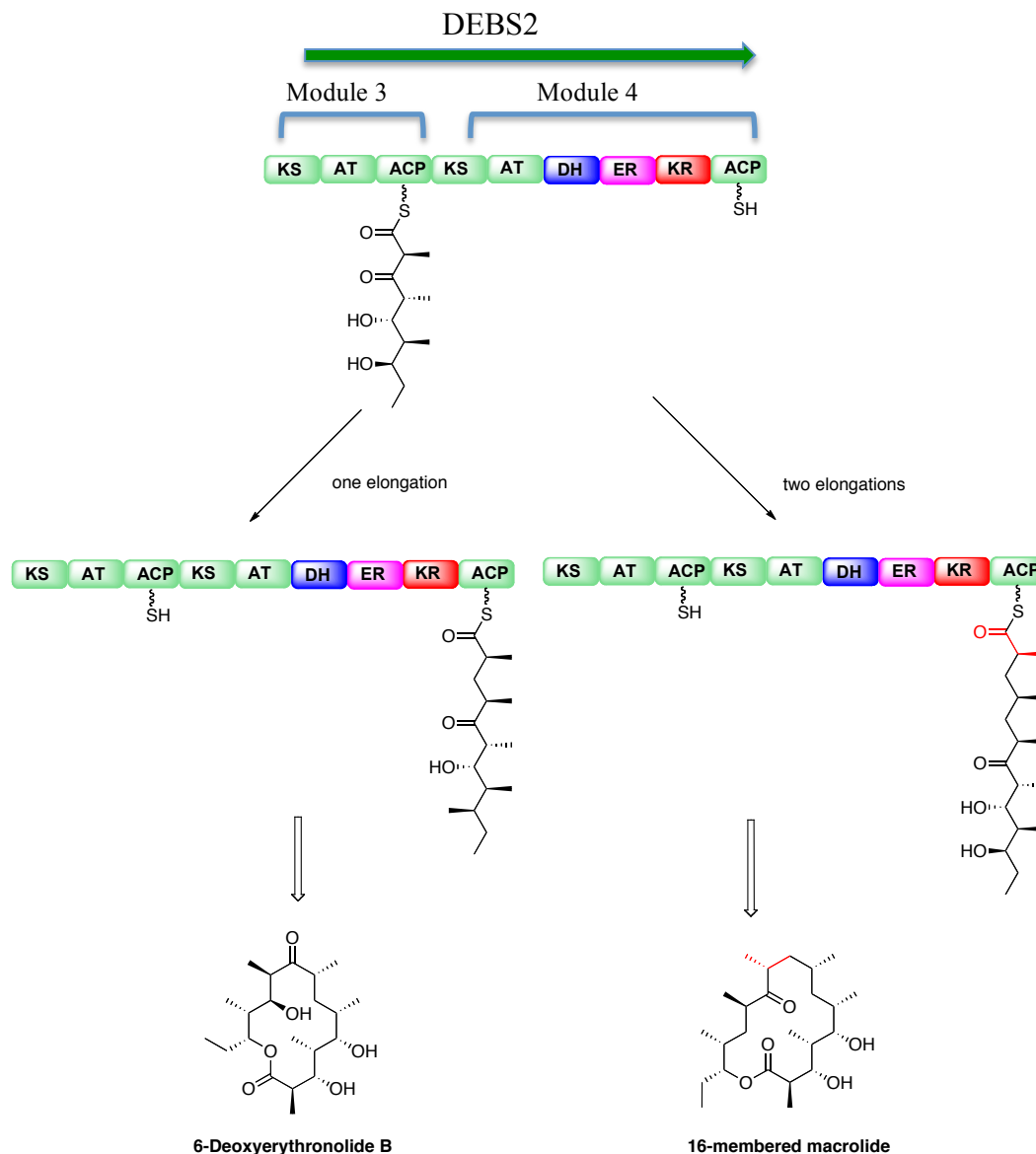


Figure 1-5 Production of a 16-membered macrolide by iteratively using of module 4 of DEBS2. The red ketide is from the additional round of iteration in module 4.

1.2.1.2 Type I iterative PKS

Type I iterative PKSs are predominately employed by fungi. The domain architecture of iterative PKSs resembles that of modular PKSs.²³ However, a iterative PKS only consists of one set of domains utilized repetitively during each

round of chain elongation, which renders the prediction of PKS products at the genetic level impractical.

Type I iterative PKSs can be divided into three groups²³ based on the presence of processing domains (KR, DH, and ER): highly reducing (HR) PKSs, partially reducing (PR) PKSs, and non-reducing (NR) PKSs. HRPKSs house a full set of processing domains, while NRPKSs have no processing domains. It has been found that HRPKSs and NRPKSs are able to collaboratively synthesize polyketides, such as hypothemycin and radicicol.³⁹⁻⁴¹ HRPKSs and NRPKSs are the main focus of this dissertation. On the other hand, PRPKSs usually contain a single KR domain or KR-DH didomain. PRPKSs are rare; an example is the 6-methylsalicylic acid synthase (6-MSAS) that was actually the first cloned and purified fungal PKS.⁴²⁻⁴⁶ A conserved domain search suggested that two processing domains (KR and DH) are present in 6-MSAS. However, the DH domain was recently revised to be a thioester hydrolase (TH) domain.⁴⁷

1.2.1.2.1 HRPKSs programming

In sharp contrast to the collinearity feature of modular PKSs, the programming of iterative PKSs is enigmatic. The domain architecture of HRPKSs shares great similarities with that of mammalian FASs (mFAS) (**Figure 1-6**). In the crystal structure of one mFAS,⁴⁸ one can find two essential domains, the KS and AT domains; and three processing domains, the KR, DH, and ER domains. However, ACP and TE do not appear in the crystal structure because of flexibility. In addition, two pseudo-domains are also found in the crystal structure: CMeT^o, a C-methyltransferase pseudo-domain with the *S*-adenosyl methionine

(SAM) binding motif truncated; and KR_s, a structural pseudo-domain of the KR domain. The whole crystal structure of a type I iterative PKS is not available yet; however, bioinformatics analysis suggests type I iterative PKSs possess the same set of domains as FASs except the CMeT domain is active in some PKSs.⁴⁹

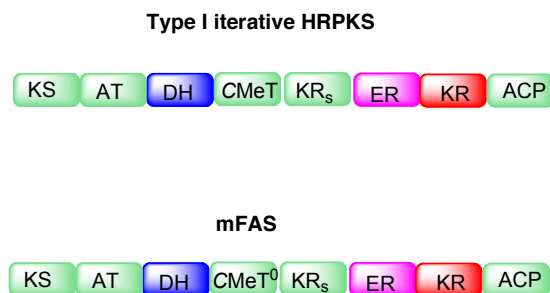
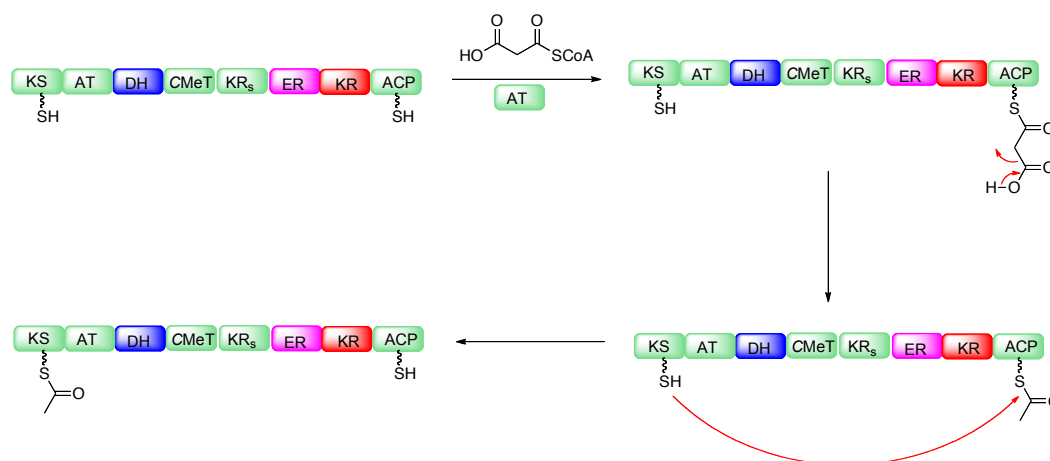


Figure 1-6 Domain architectures of HRPKS and mFAS.

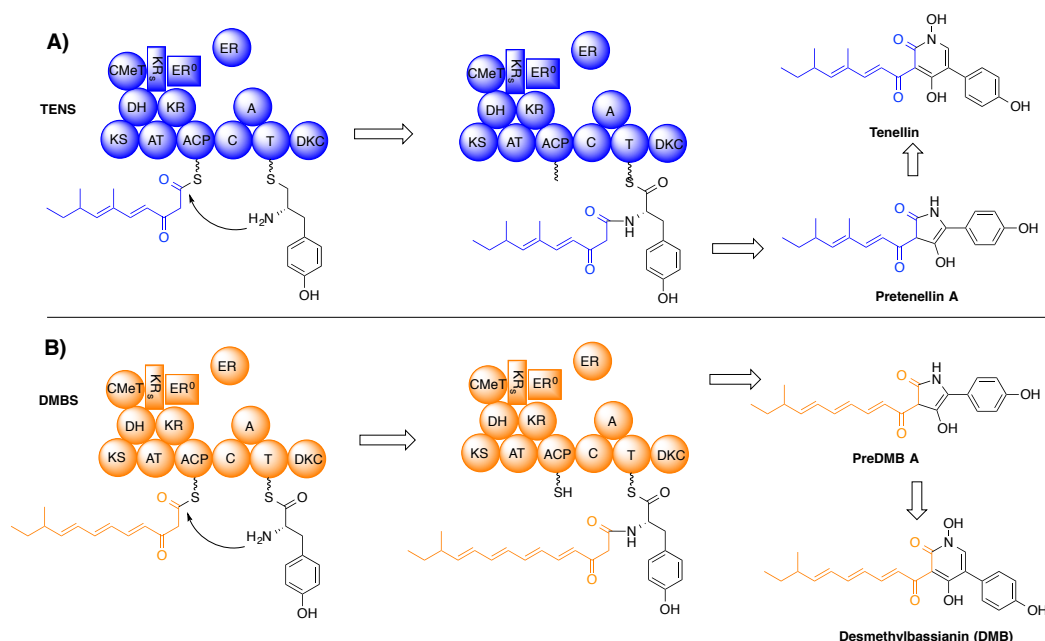
The complicated programming rules of HRPKSs are cryptically encoded in the amino acid sequence, and the mechanisms of the programming are not completely understood yet. Ma *et al.*⁵⁰ claimed that the starter unit priming of fungal HRPKSs is predominantly via decarboxylation of malonyl-ACP (**Scheme 1-2**). Their work on minimal LovB (lovastatin polyketide synthase B) constructs suggested that acetyl-CoA, compared to malonyl-CoA, is strongly discriminated by the AT domain. Moreover, the KS domain of LovB cannot mediate a thioester exchange to directly prime the acetyl unit. Thus, it appears that the starter unit for fungal HRPKSs is predominately derived from decarboxylation of malonyl-ACP.



Scheme 1-2 Proposed mechanism for the starter unit priming of HRPKSs.

In addition to catalyzing a specific round of chain elongations by a single set of domains, HRPKSs also selectively use processing domains (CMeT, KR, DH, and ER) to modify β -keto intermediates during each round of chain elongation. Recently domain swaps conducted in the Cox and Simpson lab shed light on the nature of iterative PKS programming.⁵¹ The domain swaps were performed in two structurally related fungal PKSs, the tenellin synthetase (TENS)⁵² and desmethylbassianin synthetase (DMBS).⁵³ These two PKSs produce polyketides only differing in a ketide group and a methyl group: TENS produces a pentaketide with two methyl groups; while DMBS produces a hexaketide with one methyl group. Analogous to lovastatin biosynthesis,⁵⁴ both biosyntheses employ *trans*-acting ER domains.⁵³ In addition, both the polyketides are fused with a tyrosine by a single module of a nonribosomal peptide synthetase (NRPS) housing of the condensation (C), adenylation (A), thiolation (T) and Dieckmann cyclase (DKC) domains. Furthermore, the offloaded PKS products

undergo post-PKS modifications to form tenellin and desmethylbassianin (Scheme 1-4).



Scheme 1-3 A) Biosynthesis of tenellin by TENS. B) Biosynthesis of desmethylbassianin by DMBS.

Switching the KS-AT-DH tridomain of DMBS to that of TENS did not alter the fermentation products.⁵¹ However, replacing of the CMeT-KR_s domain of TENS with that of DMBS successfully generated a pentaketide with one methyl group, together with a small portion of the doubly methylated product, pretenellin A (**Figure 1-7A**). The product alteration suggested that CMeT-KR_s primarily controls the methylation pattern, which is expected; but other portions of the enzymes also play a minor role. Swapping TENS KR to DMBS KR significantly altered the PKS products: hexaketides with one and two C-methyl groups arise together with the previous detected pentaketides (**Figure 1-7B**). The scrambled chain length and C-methylation pattern strongly indicated that KR is

involved in the regulation of both polyketide chain length and methylation. Co-swapping of the KR-ER⁰ and CMeT-KR_s domains of TENS with counterparts of DMES completely abolished the double *C*-methylation and also dramatically suppressed pentaketide production, suggesting that the KR and CMeT-KR_s domains collaboratively control *C*-methylation and chain length (**Figure 1-7C**). The existence of a small amount of pentaketide implied KR and CMeT-KR_s are not the sole determinants of chain length. Indeed, including further KS, DH and AT completely switched the function of TENS to that of DMBS, suggesting that they may also participate in the chain length control (**Figure 1-7D**).

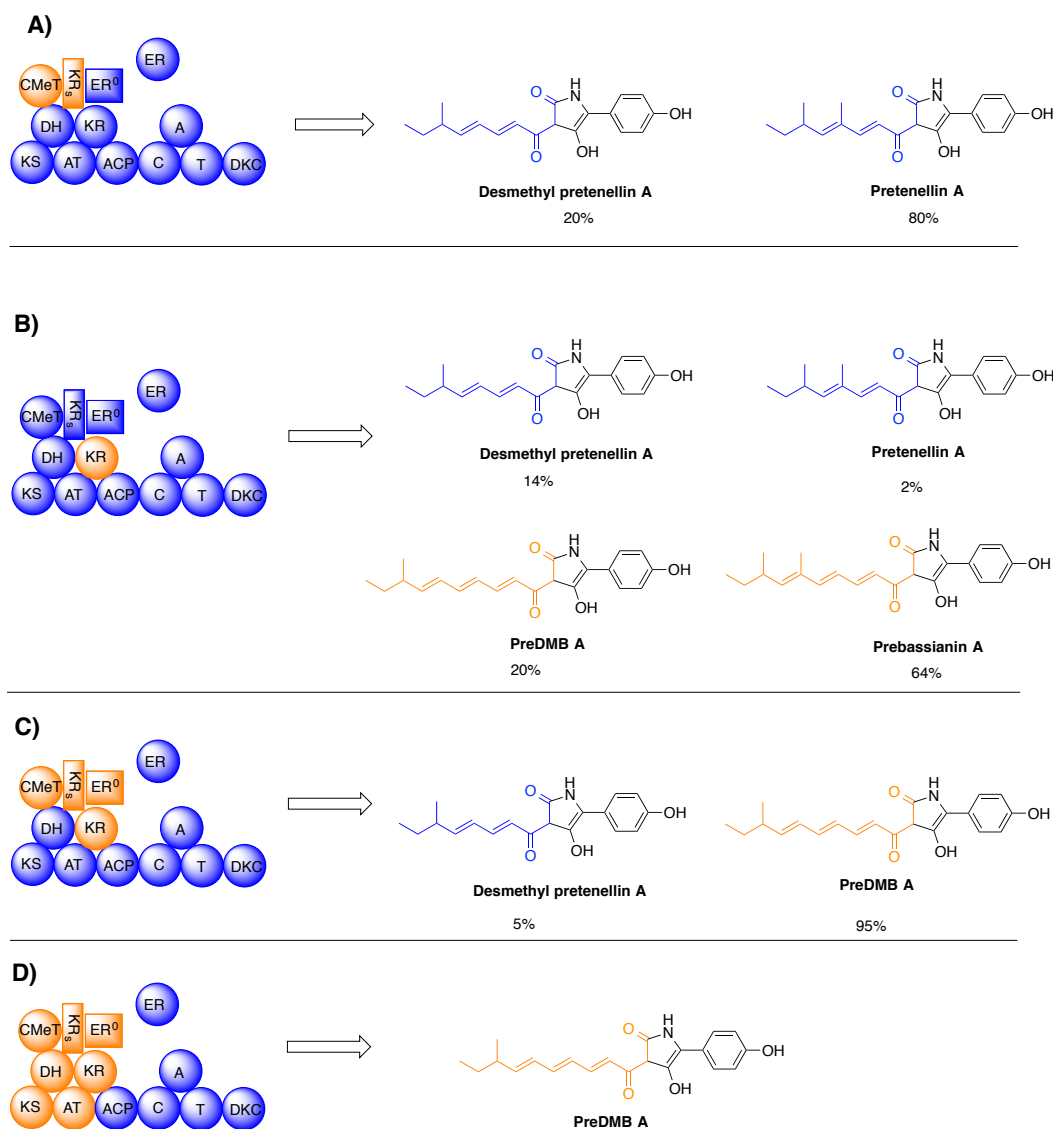


Figure 1-7 Domain swaps between TENS and DMBS. The blue domains are from TENS; and the orange domains are from DMBS.⁵¹

Furthermore, an additional degree of programming complexity of the KR domain has been unraveled.⁵⁵ The KR domain of Hpm8, the HRPKS for hypothemycin biosynthesis, is capable of reducing different β -keto intermediates with opposite stereospecificity based on chain length, which will be discussed in detail in Chapter 2. Type I KR domains appear to be involved in controlling chain

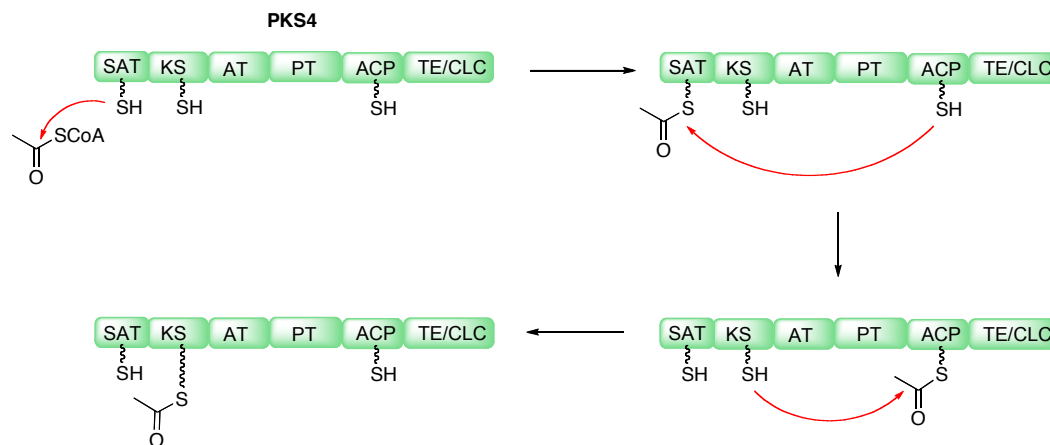
length and C-methylation,⁵¹ tuning stereospecificity based on chain length,⁵⁵ and epimerizing the C2 methyl group of biosynthetic intermediates (modular PKS).^{31,}
³² These multiple functions indicate that KR are much more sophisticatedly programmed than previous thought. Completely deciphering the KR domain programming will be a great springboard toward fully decoding the mechanisms of polyketide synthesis.

1.2.1.2.2 NRPKSs programming

NRPKSs have four commonly encountered domain, KS, AT, ACP, and TE (which is also called the Claisen cyclase (CLC) domain, because it catalyzes a Claisen-type cyclization.²³). In addition, enzyme deconstruction analysis of NRPKSs by the Udvary-Merski algorithm⁵⁶ revealed two additional domains: starter unit:ACP transacylase (SAT)⁵⁷ and the product template (PT).^{58, 59} The programming of NRPKSs is less complicated compared to that of HRPKSs due to the absence of the processing domains (KR, DH, and ER).

The AT domain of NRPKS attaches an extension unit to the ACP domain; while the SAT domain loads a starter unit to the KS domain. The SAT domain is located at the *N*-terminus of NRPKS, and it shares secondary-structural similarity with the AT domain.⁵⁷ It is common that the SAT domain recruits a partially assembled polyketide intermediate from its partnered enzymes such as FASs, HRPKSs.^{40, 41, 58, 60} Pioneering work⁵⁷ in the Townsend lab suggested that the starter polyketide intermediate recruited by SAT is first transferred to the ACP domain, and then delivered to the KS domain by transthioesterification (**Scheme 1-5**). For example, PKS4, a NRPKS from *Gibberella fujikuroi*, uses its SAT

domain to load acetyl-CoA to the KS domain via the ACP domain. The AT domain only loads malonyl-CoA.⁶¹ However, when the SAT domain is mutated or the media lack acetyl-CoA (**Figure 1-8**), decarboxylation of malonyl-ACP serves as an alternative source for the acetyl unit, analogous to HRPKSs.⁶¹



Scheme 1-4 Proposed mechanism of loading of a starter unit from the SAT domain to the KS domain.

The KS domain appears to control chain length, while the PT and TE/CLC domains control cyclization of the nascent polyketide chain.⁶⁰ For example, PKS4 from *G. fujikuroi* is responsible for the production of Sma76a (**1**),⁶² as shown in **Figure 1-8**. Without the TE/CLC domain, TE-less PKS4 generated product **2** (C2-C7 and C8-C1 cyclizations), suggesting that the TE/CLC domain is responsible for the Claisen condensation (C10-C1).⁶³ Elimination of the PT domain in the minimal PKS led to the formation of products **3** and **4**, suggesting that the PT domain is essential for C2-C7 cyclization. On the other hand, the absence of the SAT, the PT and TE/CLC domains in the minimal PKS did not affect production of the nonaketide intermediates, indicating that the KS domain might be responsible for the chain length control.

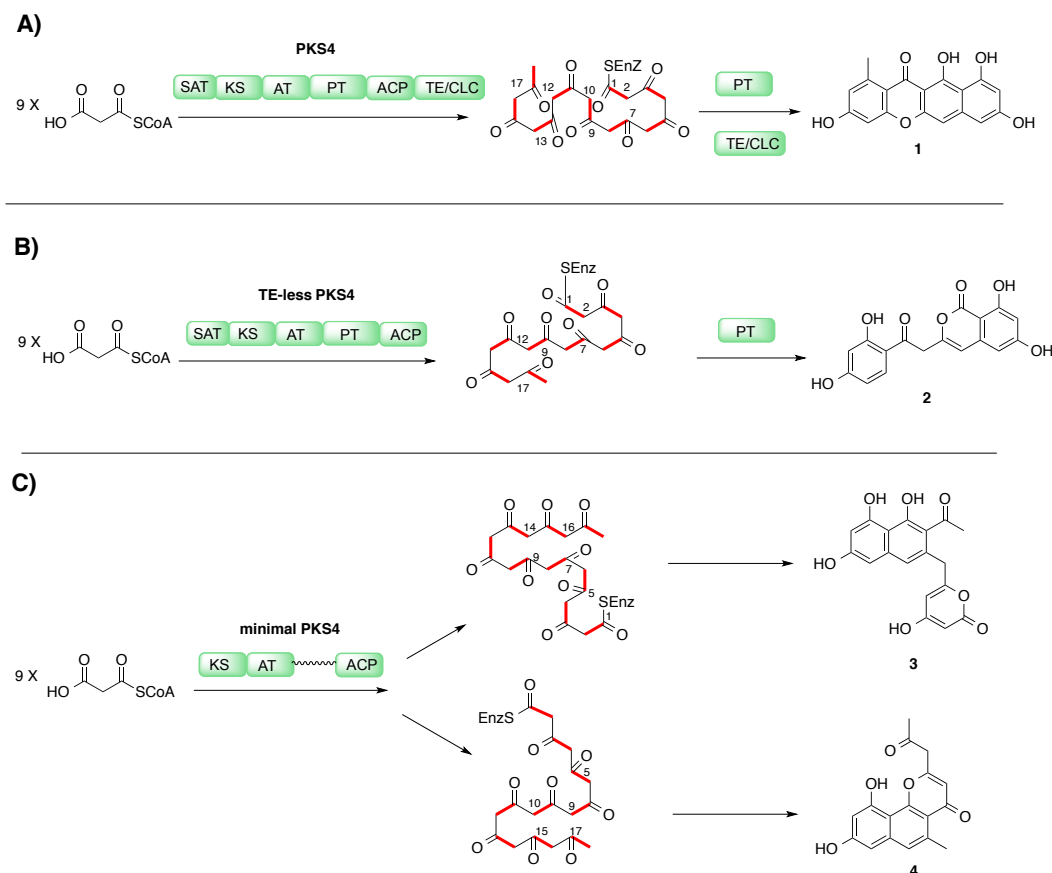


Figure 1-8 Activities of PKS4 from *G. fujikuroi*. A) Production of **1** by PKS4. B) Production of **2** by TE-less PKS4. C) Production of **3** and **4** by minimal PKS4.

1.2.2 Type II PKSs

In contrast to type I PKS megasynthases, Type II PKS enzymes are relatively small dissociable proteins (domains) analogous to type II bacterial and plant FASs.⁶⁴ The minimal type II PKS consists of the KS α , KS β , and ACP domains. In contrast to the active KS α domain, the KS β domain possesses a glutamine instead of a cysteine in the active site. KS β forms a heterodimer with KS α to catalyze the iterative decarboxylative Claisen condensation of malonyl-CoA extender units. In addition, it has been shown that KS β also primarily

governs the chain length of the growing polyketide chain.⁶⁴ So KS_β is also called “chain length factor” (CLF).⁶⁵ Since the AT domain is absent in most type II PKSs, the ACP domain is hypothesized to recruit extender unit by self-priming of malonyl-CoA. ACP-tethered malonyl-CoA undergoes decarboxylation to form an acetyl unit, which can then be transferred to KS_α as starter units, similar as that of HRPKSs. Bisang *et al.* reported that the glutamine residue of KS_β is involved in decarboxylation of malonyl-CoA tethered to the ACP domain.⁶⁶ Because they lack reductive processing domains, type II PKSs usually produce aromatic polyketides such as the anticancer drug doxorubicin, through regioselective cyclization (catalyzed by cyclases), aromatization (catalyzed by aromatases) and post-PKS modifications of nascent polyketide chains.

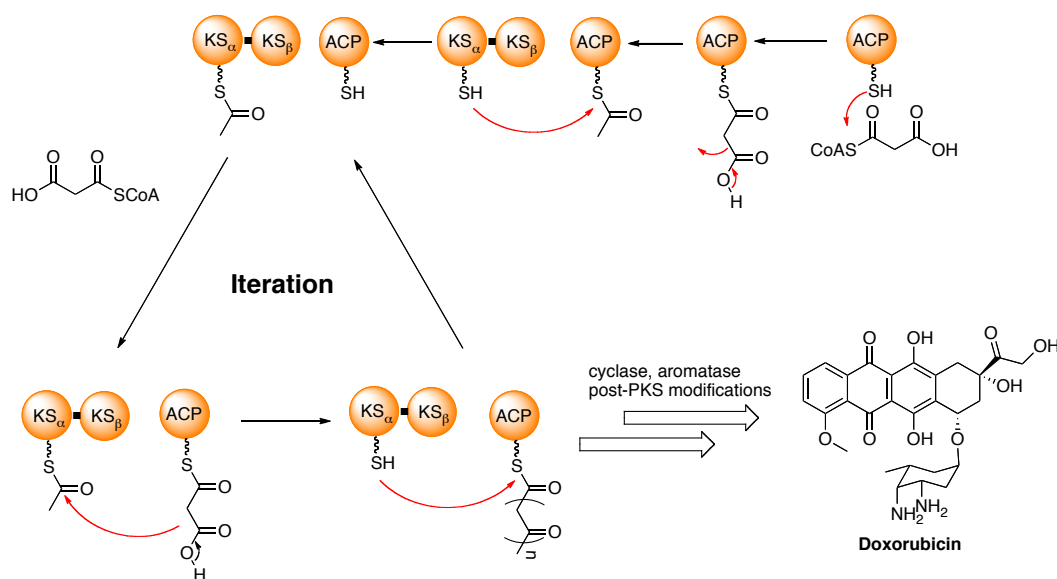


Figure 1-9 Biosynthesis aromatic polyketides by type II PKSs.

1.2.3 Type III PKSs

Type III PKS is a unique type of PKS that does not use the ACP domain. Instead of using multi-domain megasynthases for synthesizing polyketides, Type III PKSs only house a KS domain, which forms a homodimer for polyketide biosynthesis.^{67, 68} This KS domain performs multiple reactions: recruitment of a starter unit, iterative Claisen condensation of malonyl-CoA, cyclization and aromatization of nascent polyketide chain. Type III PKSs directly use malonyl-CoA as the extender unit, in contrast with type I and type II PKSs, which require that the CoA thioesters be tethered to the ACP domain first. As shown in **Figure 1-10**, the KS domain promotes Claisen condensation of malonyl-CoA to form a freestanding CoA thioester derivative, which can be recaptured by the KS domain through transthioesterification. The KS-tethered chain then serves as a starter unit for the next round of chain extension. So every round of chain elongation requires the intermediate to offload, which is different than in other PKS systems. In addition, because there are no reductive processing domains present, type III PKSs usually produce aromatic polyketides such as chalcone, a key intermediate en route to flavonoids. The shape and volume of the cavity of the KS domain governs the starter unit selection, chain length control and cyclization, because all reactions occur in the same KS domain active site.

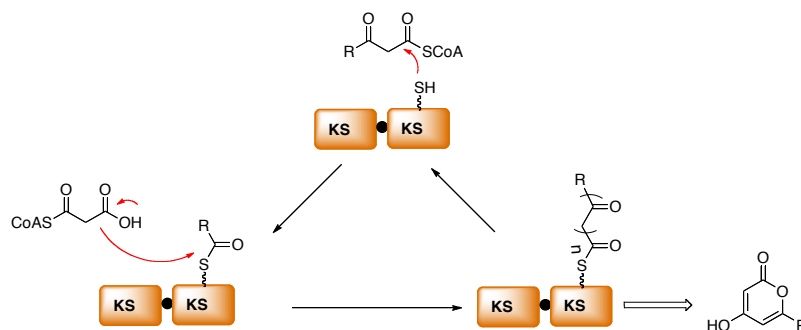


Figure 1-10 Type III PKSs promoted biosynthesis.

Two well-documented type III PKSs are chalcone synthase (CHS) and stilbene synthase (STS).⁶⁹ CHS and STS both extend the *p*-coumaroyl-CoA starter unit three times with malonyl-CoA to afford an identical tetraketide-CoA intermediate, which is recaptured by the KS domain (**Figure 1-11**). Inside the KS domain cavity, CHS and STS fold the tetraketide into different conformations, leading to two cyclization products, chalcone and stilbene, respectively.⁷⁰ CHS catalyzes a C6/C1 Claisen-type cyclization to generate the chalcone scaffold; STS promotes a C2/C7 aldol-type cyclization to produce the stilbene backbone, after a decarboxylation reaction. Interestingly, STS displays thioesterase activity and can offload the tetraketide as a free acid. Crystal structures of STS suggest that residues Glu192, Thr132, and Thr132 are arranged in an “aldol switch” conformation to mediate an aldol-type cyclization, prior to decarboxylation to generate stilbene. CHS also contains these three residues, but they are not in compatible distances to form the “aldol switch” hydrogen bond network. Thus, Austin *et al.* suggested that cyclization of the nascent polyketide chain is facilitated electronically instead of by the shape of the active-site cavity in CHS and STS.⁷⁰

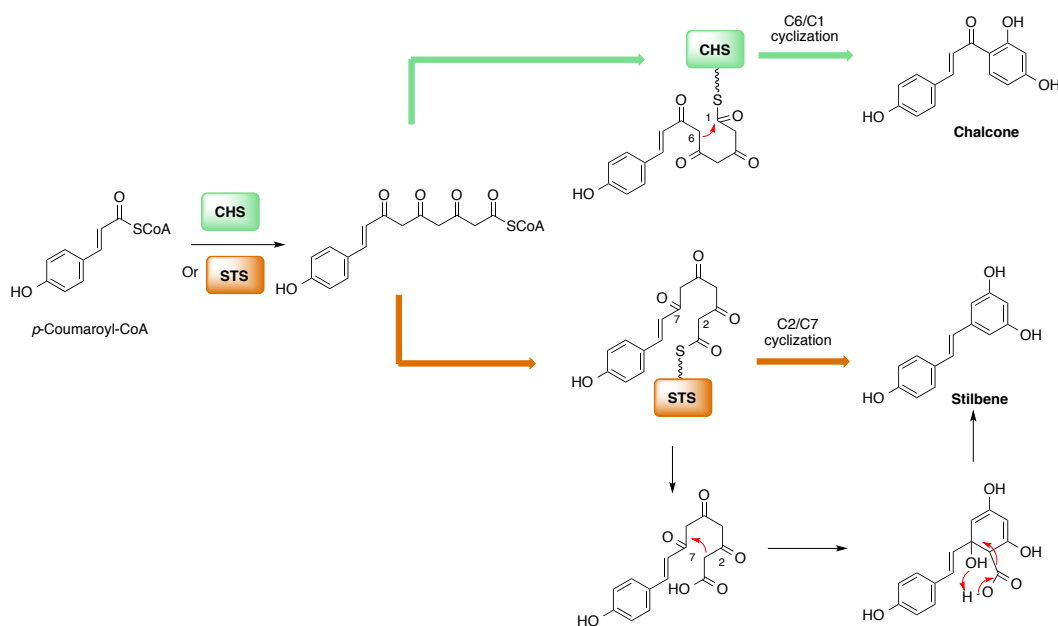


Figure 1-11 Biosynthesis of chalcone and stilbene by CHS and STS respectively.

In summary, our understanding of polyketide biosynthesis has been advanced dramatically, especially in the field of type I modular PKSs (bacterial). However, the knowledge of the mechanisms of fungal PKSs is still weak because of the cryptic programming. To advance our understanding of fungal PKSs, the biosynthesis of three fungal polyketides (hypothemycin, radicicol and dehydrocurvularin) is studied in detail in this dissertation. In chapter 2, the biosynthesis of hypothemycin will be addressed via heterologous expression of corresponding PKSs (Hpm8 and Hpm3) and subsequent probing their functions with chemically synthesized putative intermediates. Chapter 2 contains three main sections. In Section 2.2, the *in vitro* activities of Hpm8 and Hpm3 were demonstrated by formation of the first PKS product, dehydrozearalenol. In Section 2.3, the substrate-dependent stereospecificity of Hpm8 KR domain will be discussed. In Section 2.4, the functions of Hpm8 were probed by *in vitro*

incorporation of ^{13}C -labeled precursors. In Chapter 3, the biosynthesis of radicicol will be discussed. The two PKSs for radicicol biosynthesis, Rdc5 and Rdc1, were heterologously expressed and the *in vitro* activities were demonstrated by formation of the first PKS product, (*R*)-monocillin II. In addition, the distribution of labors between Rdc5 and Rdc1 was probed by feeding a putative SNAC thioesters **149**. In Chapter 4, the biosynthesis of dehydrocurvularin was investigated via genomic sequencing of producing strain *Alternaria cinerariae*. Two iterative PKS were identified from the genomic sequences. The two PKS genes were cloned into expression plasmids, and the gene products were successfully expressed.

Chapter 2: Biosynthetic Studies of Hypothemycin*

2.1 Introduction

Resorcylic acid lactones (RALs) are fungal polyketides that contain a resorcyate core (2,4-dihydroxybenzoate) fused in a reduced 14-membered macrolactone (**Figure 2-1**). Hypothemycin, a RAL, was first isolated from *Hypomyces trichothecoides* in 1980, but the proposed structure was not correct.⁷¹ Later, the structure and stereochemistry of hypothemycin was established by both X-ray crystallography⁷² and chemical synthesis.^{73, 74}

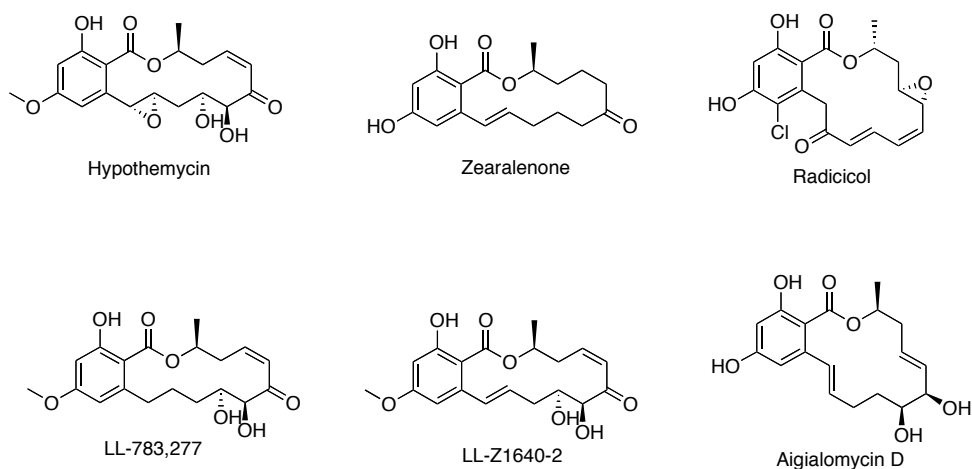


Figure 2-1 Typical RALs: hypothemycin, zearalenone, radicicol, LL-783,277, LLZ1640-2 and aigialomycin D.

* A version of this chapter has been published.

1. Zhou, H.; Qiao, K.; Gao, Z.; Meehan, M. J.; Li, J. W.; Zhao, X.; Dorrestein, P. C.; Vederas, J. C.; Tang, Y. *J. Am. Chem. Soc.* **2010**, *132*, 4530-4531. (**Section 2.2**)
2. Zhou, H.; Gao, Z.; Qiao, K.; Wang, J.; Vederas, J. C.; Tang, Y. *Nat. Chem. Biol.* **2012**, *8*, 331-333. (**Section 2.3**)
3. Gao, Z.; Wang, J.; Norquay, A. K.; Qiao, K.; Tang, Y.; Vederas, J. C. *J. Am. Chem. Soc.* **2013**, *135*, 1735-1738. (**Section 2.4**)

Hypothemycin displays interesting biological activities. It has moderate antifungal⁷⁵ and antimalarial⁷¹ activity. More importantly, it has recently been recognized as an anti-cancer candidate because it suppresses proliferation of human cells and inhibits tumor growth in animals.⁷⁶⁻⁷⁹ More detailed studies suggested that hypothemycin irreversibly inhibits a subset of protein kinases by covalently binding to the ATP-binding site.^{80, 81} A structural-bioinformatics analysis revealed that the ATP-binding site houses a conserved Cys residue, which can attack the *cis*-enone of hypothemycin in a Michael addition fashion.^{80,81}

Reeves *et al.* have recently sequenced the hypothemycin gene cluster from *Hypomyces subiculosus* (**Figure 2-2**).³⁹ A pair of HRPKS and NRPKS (Hpm8 and Hpm3) are proposed to synthesize an advanced intermediate, (6*S'*, 10*S'*)-*trans*-7', 8'-dehydrozearalenol (DHZ, **5**), from nine acetate units (**Figure 2-3**). Hpm8 is responsible for synthesizing a reduced hexaketide, which is transferred downstream to Hpm3 for another three rounds of chain elongation (without reductive modifications). The resulting nonaketide undergoes a regioselective Dieckmann condensation, then macrolactonizes to release DHZ as the first PKS product. DHZ is further decorated by post-PKS modifications to generate aigialomycin C via *O*-methylation (Hpm5), epoxidation (Hpm9), and hydroxylation (Hpm1). Aigialomycin C undergoes another round of post-PKS modifications, hydroxylation (Hpm1), isomerization (Hpm2) and oxidation (Hpm7), to finally afford hypothemycin. Interestingly, the *cis*-enone functional

group, which is important for the biological activity of hypothemycin, is generated by a post-PKS modification (Hpm2) in the presence of glutathione.

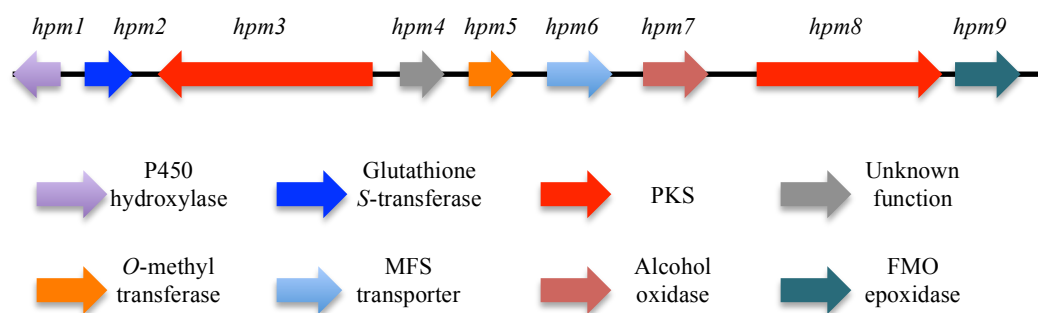


Figure 2-2 Hypothemycin gene cluster in *H. subiculosus*.

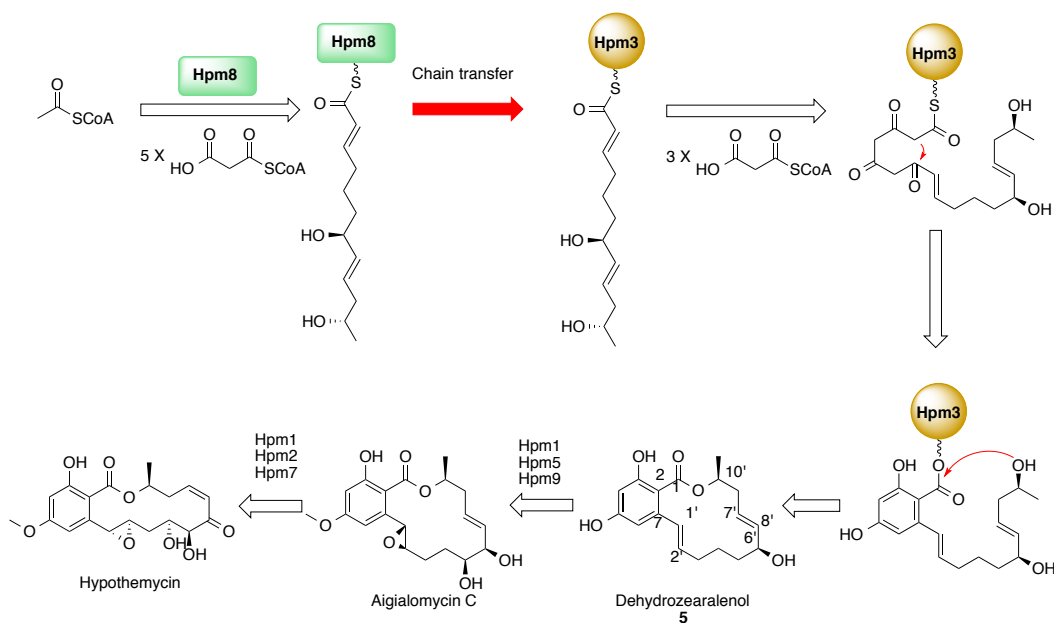


Figure 2-3 Proposed biosynthesis of hypothemycin.

2.2 *In vitro* reconstitution of two iterative PKSs for DHZ biosynthesis*

2.2.1 Introduction

Hpm8 is a type I iterative HRPKS, consisting of a set of domains similar to a FAS: KS, MAT (malonyl-CoA:acyl transferase), DH, core, ER, KR, and ACP (Figure 2-4). The KS, MAT and ACP domains are responsible for chain elongations, while KR, DH and ER are processing domains that tailor the β -positions of ACP-tethered intermediates. The core domain contains two parts: KR_s and inactive CMeT.⁴⁹ Hpm3 is a characteristic iterative NRPKS containing KS, MAT, ACP, PT, SAT and TE (Figure 2-4). The SAT domain is proposed to facilitate the transfer of the hexaketide intermediate between Hpm8 and Hpm3. The PT domain is believed to catalyze the regioselective Dieckmann condensation of the nascent polyketide intermediate. Finally, the TE domain is involved in the release of DHZ via macrolactonization.

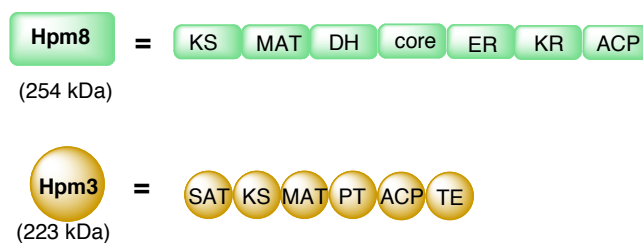


Figure 2-4 Domain architecture of Hpm8 and Hpm3. KS: ketosynthase; MAT: malonyl-CoA:acyltransferase; ACP: acyl carrier protein; KR: ketoreductase; DH: dehydratase; ER: enoyl reductase; SAT: starter unit:ACP transacylase; PT: product template; TE: thioesterase.

* This is a collaborative project with the Tang group. I was responsible for synthesis and characterizations of intermediates and products, whereas our collaborators, Professor Yi Tang and co-workers, were in charge of protein expression and purification, as well as the biological assay.

Although the biosynthesis of DHZ has been confirmed by co-expression of Hpm8 and Hpm3 in *Saccharomyces cerevisiae* BJ5464-NpgA,³⁹ *in vitro* reconstitution of Hpm3 and Hpm8 is needed to fully characterize the proposed biosynthesis. In addition, the proposed intermediate that is transferred from Hpm8 to Hpm3 has not been identified in previous studies. Characterization of this hexaketide intermediate and decoding the chain transferring mechanism will enhance our understanding of the programming of fungal PKSs.

2.2.2 Results and discussion

2.2.2.1 *In vitro* reconstitution of Hpm8

Hpm8 was expressed and purified from *S. cerevisiae* BJ5464-NpgA by our collaborators. BJ5464-NpgA is a genetically modified strain housing an phosphopantetheinyl transferase gene, *npga*, which enables heterologous expression of intact and phosphopantetheinylated PKSs.^{82, 83} The activities of Hpm8 were first probed by incubation with 2 mM of malonyl-CoA. The *in vitro* reaction was then quenched by the addition of EtOAc with 1% AcOH. LC-MS analysis of the organic extract reveals a main product **6** (**Figure 2-5**). Compound **6** has identical retention time, UV spectrum, and mass spectrum with 4-hydroxy-6-methyl-2-pyrone, which was also observed when LovB (HRPKS) was incubated with malonyl-CoA.⁵⁴ The formation of **6** can be rationalized as follows. Hpm8 self-primes a starter unit by the decarboxylation of malonyl-CoA.⁵⁰ The KS domain catalyzes a chain elongation to form a β -keto diketide. Next, Hpm8 is programmed to reduce the β -keto group with the KR domain in the presence of NADPH. However, the *in vitro* reaction was not supplied with NADPH. To

offload the intermediate from the enzyme, Hpm8 elongates the intermediate once to afford a triketide, which undergoes enolization and cyclization to release **6**. The formation of **6** therefore strongly suggests that Hpm8 is active *in vitro* and able to use malonyl-CoA as a starter unit.⁵⁰

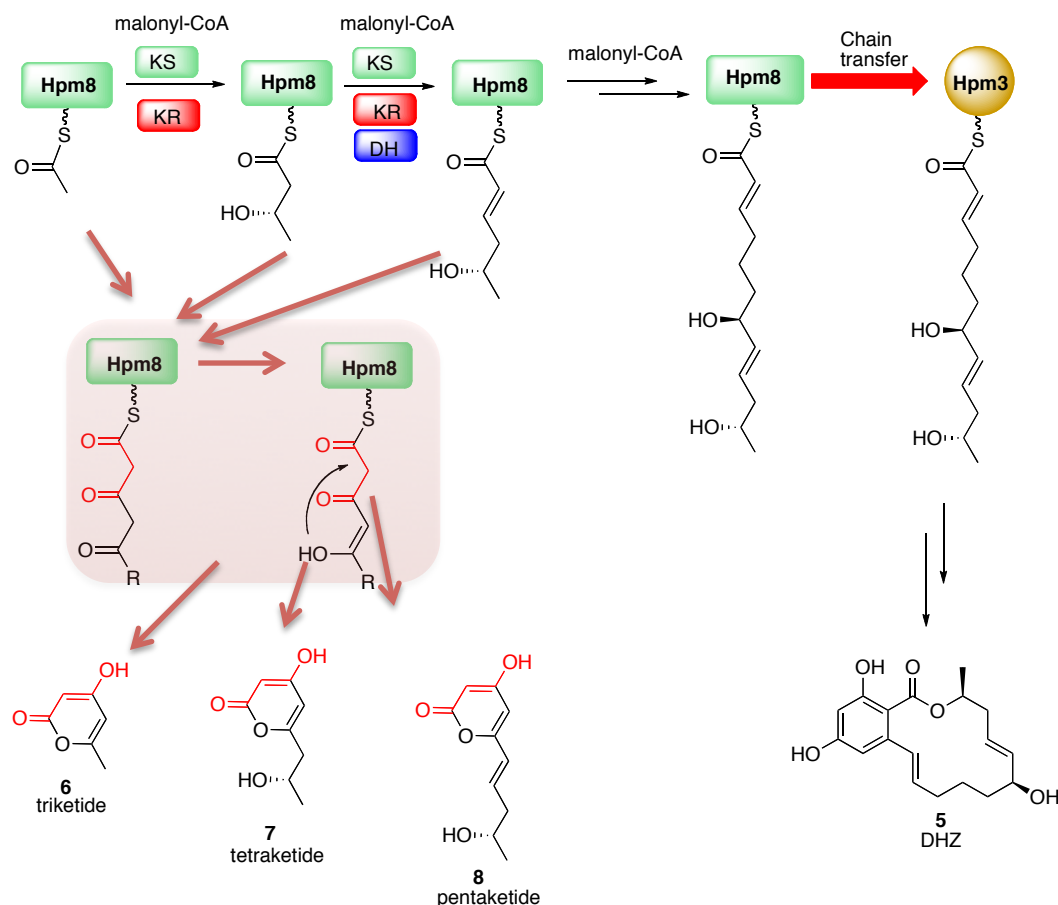


Figure 2-5 Mechanisms of the formation of pyrones **6**, **7** and **8**. Black arrows represent the programmed pathway for biosynthesis of DHZ. Red arrows show the derailment pathway when Hpm3 is absent.

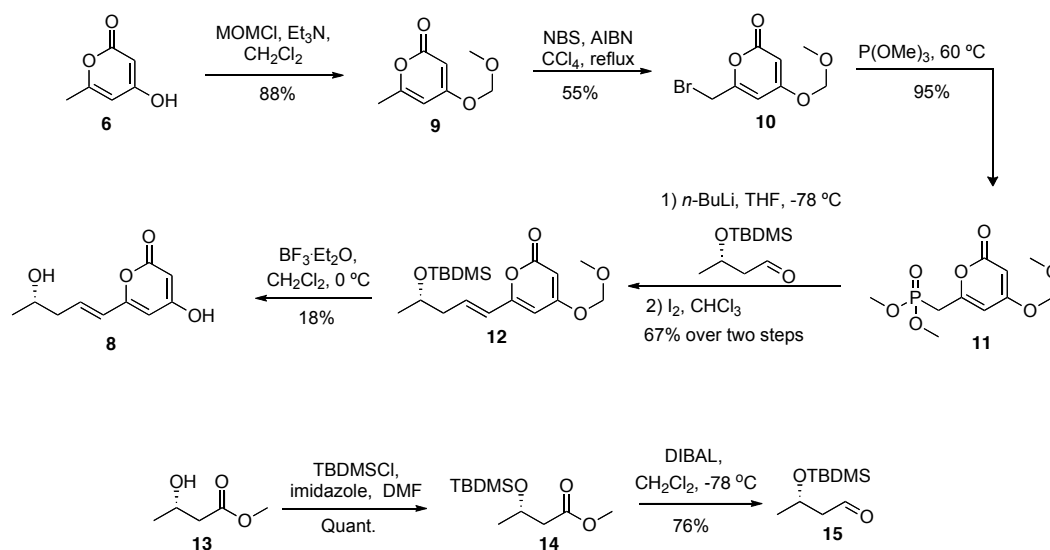
When NADPH is added to enable the functions of the processing domains, this generates two new products **7** and **8**, as well as **6**, in the *in vitro* reaction of Hpm8 (**Figure 2-5**). However, the completed hexaketide acyl intermediate is not observed, even with mild base hydrolysis or butylamine-mediated aminolysis.

Therefore, Hpm3 may be required for proper formation of the hexaketide by Hpm8.

The UV absorbance of **7** and **8** is similar to that of **6**, suggesting they are derailed pyrone products of Hpm8. In addition, the mass of **7** (m/z 170) and **8** (m/z 196) indicate that they might be a tetraketide and pentaketide, respectively. Therefore, structures **7** and **8** were proposed to be a tetraketide pyrone with the first ketide unit reduced to a hydroxyl group, and a pentaketide pyrone with the first ketide as a hydroxyl group and the second ketide reduced to a double bond, respectively (**Figure 2-5**). The proposed structures are consistent with the hypothesis that they are shunt products produced during the biosynthesis of the hexaketide intermediate.

Two authentic standards were chemically synthesized to confirm the proposed structures of **7** and **8**. Compound **7** was synthesized by a previous graduate student in our group, Dr. Jesse Li. Compound **8** was prepared as shown in **Scheme 2-1**. Protection of commercially available pyrone **6** with methyl chloromethyl ether (MOMCl) in the presence of Et₃N provided **9**, which was brominated with *N*-bromosuccinimide (NBS), using AIBN as a radical initiator to afford **10**. Compound **10** underwent an Arbuzov reaction with trimethyl phosphite to yield **11**, which reacted with aldehyde **15** to furnish **12** ($E/Z = 3:1$). Compound **15** was obtained in two steps: *tert*-butyldimethyl silyl (TBDMS) protection of commercially available **13** and subsequent reduction of the methyl ester with one equivalent of diisobutylaluminium hydride (DIBAL). Complete isomerization of the double bond of **12** to the *E*-configuration was achieved with a catalytic

amount of I₂. Deprotection of the MOM and TBDMS protecting groups with boron trifluoride etherate (BF₃•Et₂O) in one pot furnished the desired product **8**. Chemically synthesized pyrone **7** and **8** have identical LC-MS and UV profiles as the products isolated from the *in vitro* assay. Therefore **7** and **8** are confirmed to be *in vitro* shunt products from Hpm8. The production of **7** and **8** also indicates that the processing domains, at least KR and DH, are functional *in vitro*.



Scheme 2-1 Synthesis of the proposed pyrone **8**.

2.2.2.2 *In vitro* reconstitution of DHZ biosynthesis

Hpm3 was also expressed and purified from *S. cerevisiae* BJ5464-NpgA by our collaborators, using a method similar to produce Hpm8. Supplementation of acetyl- and malonyl-CoA to Hpm3 does not generate any detectable amount of polyketides, suggesting that Hpm3 cannot self-prime either acetyl- or malonyl-CoA to initiate the polyketide biosynthesis. When Hpm3, together with Hpm8, is supplied with 2 mM NADPH and 2 mM malonyl-CoA, a new peak (*m/z* 317, [M-

H]⁻) with a UV absorbance pattern similar to resorcylic acid is detected by LC-MS in the organic extract. This new compound **5** has an identical retention time, UV absorbance and mass fragmentation pattern as that of DHZ. Furthermore, culturing BJ5464-NpgA harboring both Hpm8 and Hpm3 expression plasmids produces **5** with a titer of 20 mg/L. The NMR spectrum of **5** is consistent with the proposed structure of DHZ. Moreover, crystallization of **5** was achieved by slowly evaporating a 3:1 hexanes/acetone solution of **5** (**Figure 2-6**). Surprisingly, the crystal structure shows that the configurations of C-10' and C-6' are both *S* (C-6' is *S*-configuration because the double bond takes a high priority during the stereochemistry assignment). The stereochemistry of C-6' was initially proposed to be *R* based on the fact that the single Hpm8 KR domain reduces β-keto groups with the same facial selectivity (**Figure 2-6**). How the single active site of Hpm8 KR generates opposite stereo configurations will be discussed in Section 2.3.

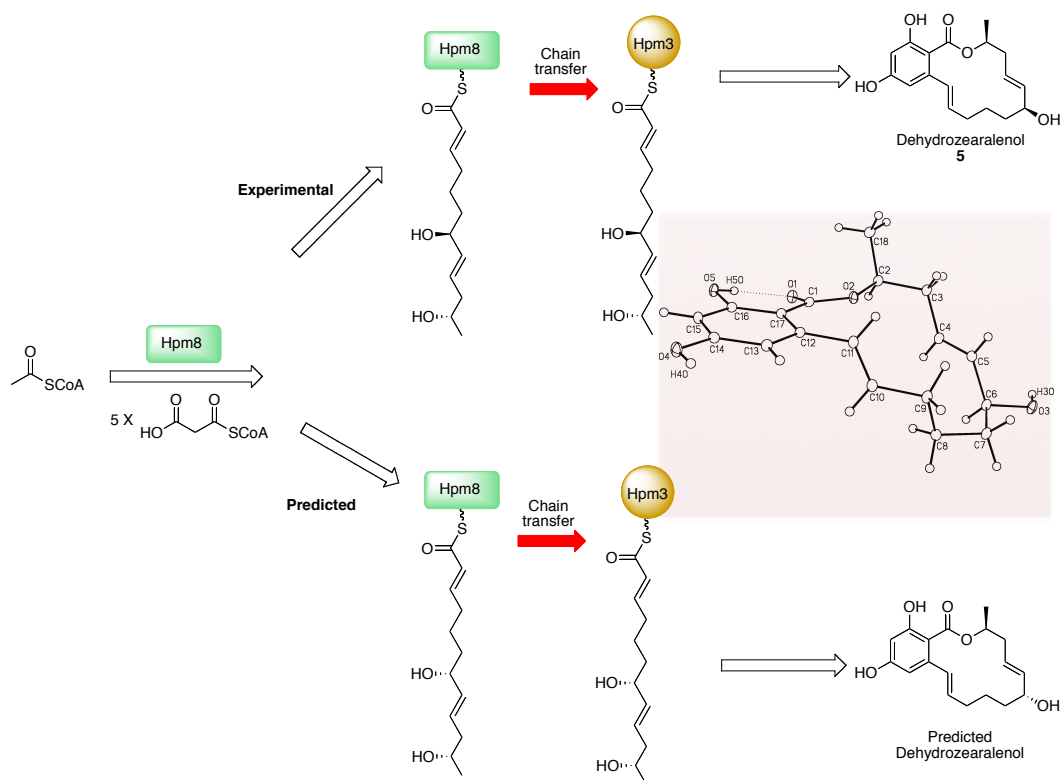


Figure 2-6 Formation of dehydrozearalenol (predicted and experimental). The structure highlight in the red box is the crystal structure of DHZ (**5**).

The production of **5** indicates that the two tandem iterative PKSs are fully active *in vitro*. This *in vitro* biosynthesis represents more than 30 catalytic steps, which can be divided into three stages: 1) Hpm8 first synthesizes a reduced hexaketide intermediate tethered to the ACP domain. This process is achieved by programmed iterative uses of the functional domains of Hpm8; 2) the hexaketide is transferred to Hpm3; and 3) Hpm3 further elongates and modifies the hexaketide to form DHZ. It is remarkable that these complicated processes could be reproduced *in vitro* cleanly, as the reaction mixture only contains a single RAL-type polyketide. However, a small amount of the shunt products, **6**, **7** and **8** is still observed in the Hpm8 and Hpm3 assay. This indicates that, under assay

conditions, intermediates have a tendency to derail off the enzyme system as pyrone products, possibly because the relative amounts of Hpm8 and Hpm3 are not optimal.

2.2.2.3 Kinetic parameters of Hpm8 and Hpm3 *in vitro*

To assess the kinetics of Hpm8 and Hpm3 during the biosynthesis of **5**, the product level was quantified using [2-¹⁴C]-malonyl-CoA and radioactive thin-layer chromatography by the Tang group. When the concentration of Hpm3 is fixed at 5 μ M, production of **5** is proportional to the concentration of Hpm8 (**Figure 2-7A**), with an apparent rate constant of 0.11 min⁻¹. Alternatively, when the concentration of Hpm8 is fixed at 10, 20 and 30 μ M, the velocities of formation of **5** are essentially steady at 1.1 μ M min⁻¹, 2.0 μ M min⁻¹ and 3.9 μ M min⁻¹, respectively, suggesting that the production of **5** is independent of the concentration of Hpm3 in the tested range. These two experiments indicate that Hpm8 is the rate-determining step during the biosynthesis of **5** *in vitro*. This is reasonable since Hpm8 catalyzes more elongation steps, and these steps are programmed much more complicatedly than Hpm3. Rapid scavenging of the hexaketide intermediate and subsequent releasing of **5** also provides an additional driving-force for production of the hexaketide intermediate by Hpm8.

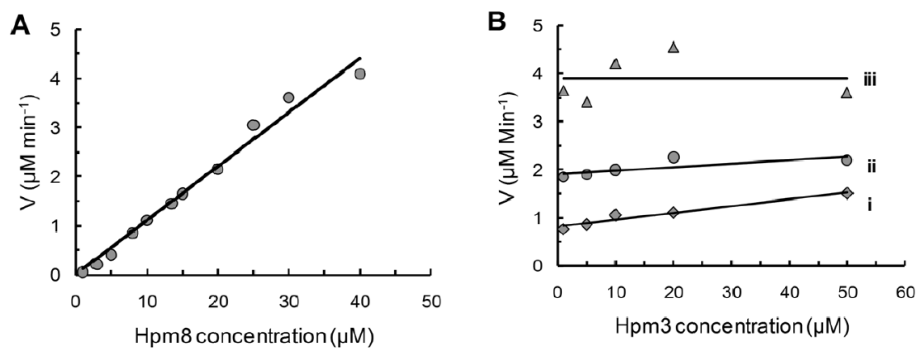


Figure 2-7 Kinetic analysis of Hpm8 and Hpm3 performed by the Tang group. A) The initial velocity of the biosynthesis of **5** at different Hpm8 concentrations. The concentration of Hpm3 is maintained at 5 μM ; (B) The initial velocity of the synthesis of **5** at different Hpm3 concentrations. Three different concentrations of Hpm8 are used at (i) 10 μM , (ii) 20, and (iii) 30 μM .

2.2.2.4 Distribution of labor between Hpm8 and Hpm3

As mentioned above, a hexaketide is proposed to transfer from Hpm8 to Hpm3 as a starter unit for synthesis of **5**. However, the hexaketide is not observed in an *in vitro* reaction of Hpm8, malonyl-CoA and NADPH. Thus, the presence of this hexaketide intermediate is still ambiguous. To determine the final product formed by Hpm8, the potential hexaketide intermediate in its *S*-*N*-acetylcysteamine (SNAC) thioester form (**27**) was synthesized (**Scheme 2-2**). Compound **27** is synthesized as a SNAC thioester because SNAC can mimic the Ppant arm attached to the ACP domain, and thus be recognized by PKSs.⁸⁴

The synthesis started with the protection of (*S*)-pent-4-en-2-ol with TBDMSCl, followed by cross metathesis with crotonaldehyde in the presence of Grubbs II catalyst to afford conjugated aldehyde **18**. Allylboration of aldehyde **18** followed by another TBDMS protection furnished protected diol **20**. The terminal alkene selectively underwent cross metathesis with ethyl acrylate using Grubbs II

catalyst to yield conjugated ester **21**. Regioselective reduction of the conjugated double bond with magnesium in MeOH furnished transesterification product **22**, which was immediately reduced to aldehyde **23** with one equivalent of DIBAL. Compound **23** underwent a Horner-Wadsworth-Emmons (HWE) reaction under the Masamune-Roush condition (LiBr, Et₃N)⁸⁵ with **25** to provide **26**. Phosphonate **25** was a product from a coupling reaction between *N*-acetylcysteamine (HSNAC) and 2-(diethoxyphosphoryl)acetic acid using *N,N'*-dicyclohexylcarbodiimide (DCC) and 4-dimethylaminopyridine (DMAP) as coupling reagents. Under the Masamune–Roush condition, the Li⁺ ion coordinates with the carbonyl groups of **25** to lower the pK_a of the α-proton, allowing a weak base such as Et₃N to deprotonate the phosphonate and initiate the HWE reaction. Initial attempts to deprotect the TBDMS groups of **26** with *tetra-N*-butylammonium fluoride (TBAF) or HCl were not successful. Both strong basic and acid conditions resulted in the decomposition of **26**. Therefore, a mild acidic condition, AcOH/H₂O/THF = 3:3:1,⁸⁶ was employed to remove the protecting groups of **26** and afford the desired product **27**.

The key reaction in the synthesis of **27** is the asymmetrical allylation of aldehyde **18** using (-)-Ipc₂B(allyl)borane. Two possible six-membered transition states (TS) can be proposed for the allylation (**Figure 2-8**). In TS B, the methylene of the alkyl group suffers steric clashing with the methyl group from the pinene group.⁸⁷ Therefore TS A is more favorable, and leads to formation of **19** in this synthesis.

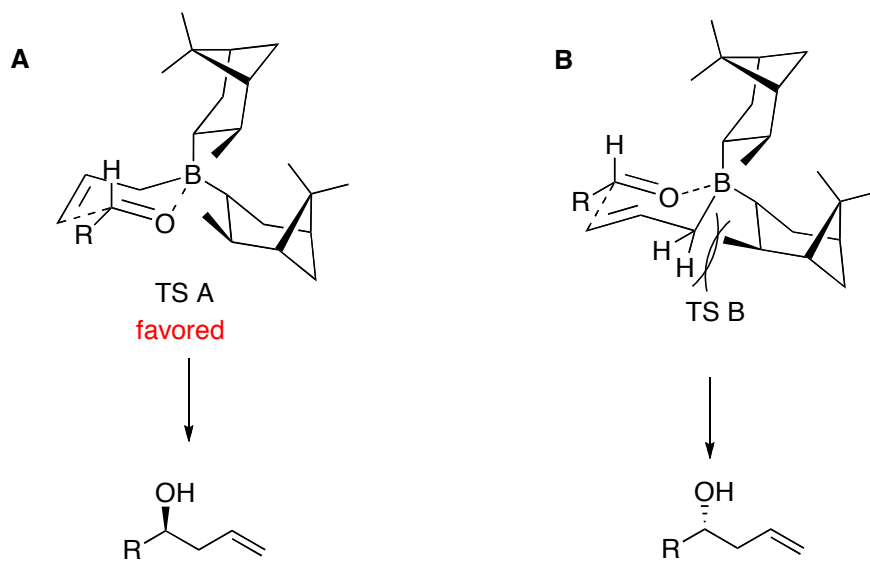


Figure 2-8 Transition states of asymmetrical allylboration.

Chemically synthesized **27** was supplied to an *in vitro* assay containing Hpm3 and malonyl-CoA. LC-MS analysis of the organic extract suggests that **5** is synthesized by Hpm3 in excellent yield, almost as a single peak in the HPLC trace. The successful transformation from **27** to **5** by Hpm3 suggests that the hexaketide is the final advanced acyl intermediate transferred from Hpm8. Therefore, the distribution of effort between Hpm8 and Hpm3 is same as predicted: Hpm8 produces a hexaketide, then Hpm3 extends the hexaketide three times, followed by regioselective cyclization and macrolactonization to release the first PKS product.

2.2.2.5 Probing the function of the SAT domain

The transacylation of the hexaketide from Hpm8 to Hpm3 is most likely facilitated by Hpm3 SAT, analogous to norsolorinic acid biosynthesis.⁵⁷ To probe the role of the SAT domain in the synthesis of **5**, the active site Ser121 was

mutated to alanine by the Tang group to furnish a mutant Hpm3-SAT⁰. As expected, the biosynthesis of **5** is completely abolished when Hpm3 was replaced with mutant Hpm3-SAT⁰ in an *in vitro* assay containing Hpm8, malonyl-CoA and NADPH (**Figure 2-9B**). Therefore, the SAT domain is essential for the chain transfer between Hpm8 and Hpm3. Surprisingly, Hpm3-SAT⁰ is able to prime **27** as a starter unit to initiate the biosynthesis of **5** with a yield comparable to the wild type (**Figure 2-9D**), indicating that recruitment of **27** could be independent of the SAT domain, and possibly be by direct priming on the KS domain.

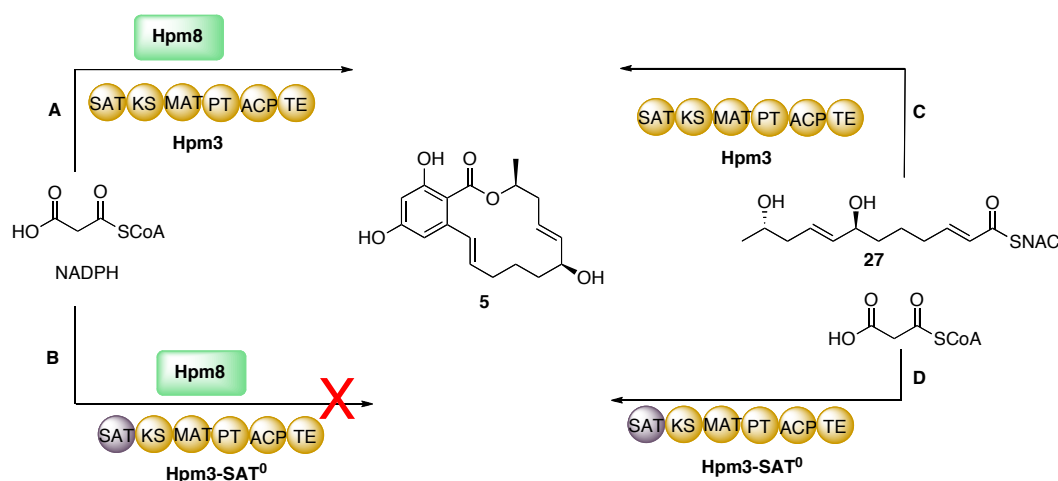


Figure 2-9 Synthesis of **5** by (A) Hpm8 and Hpm3 from malonyl-CoA and NADPH; (B) Hpm8 and Hpm3-SAT⁰ from malonyl-CoA and NADPH; (C) Hpm3 from malonyl-CoA and **27**; D) Hpm3-SAT⁰ from malonyl-CoA and **27**.

To examine the specificity of the SAT domain involved in the protein interactions between Hpm8 and Hpm3, zearalenone PKS13⁸⁸ was paired with Hpm8. PKS13 is a NRPKS responsible for the synthesis of zearalenone with PKS4 (HRPKS) (**Figure 2-10**). Similar to the DHZ biosynthesis, PKS4 synthesizes a hexaketide intermediate, and then PKS13 transforms it into zearalenone. The only differences between the two hexaketides produced by

PKS4 and Hpm8 are the functional groups at the C4'-C5' and C6' positions: a single bond and a ketone group (PKS4) VS. a double bond and a hydroxyl group (Hpm8) (**Figure 2-10**).

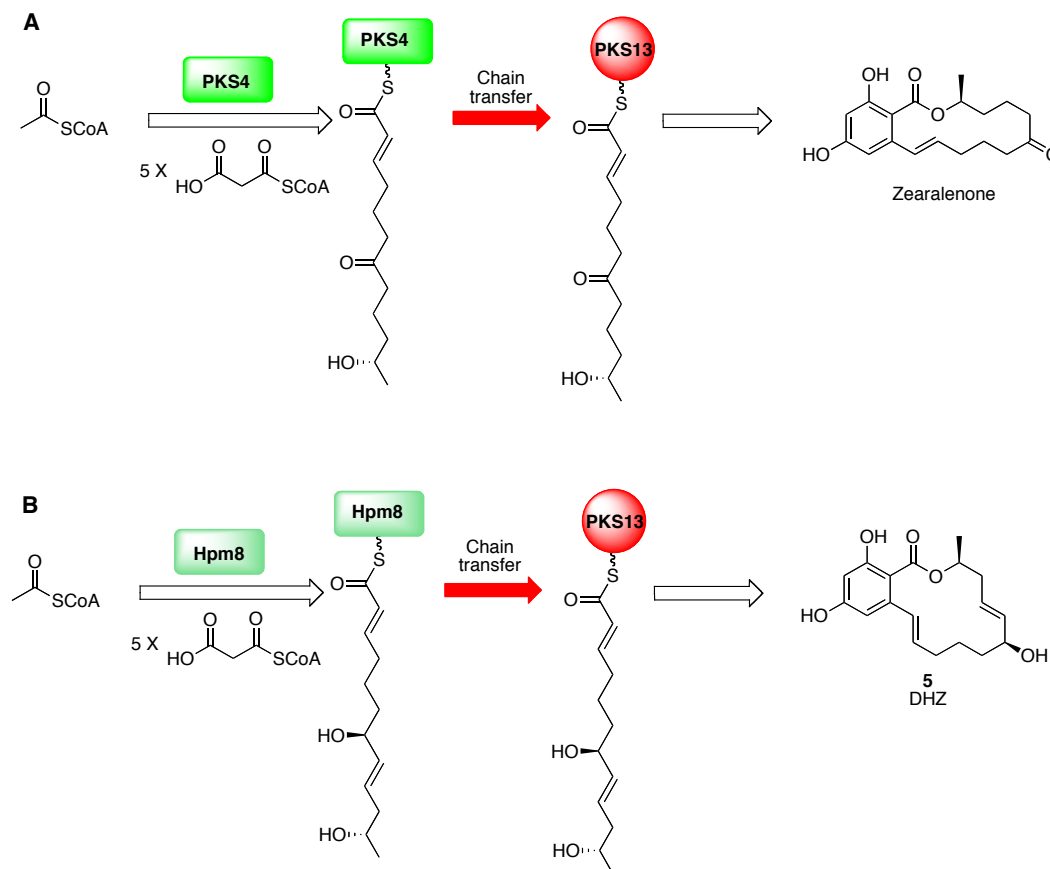


Figure 2-10 (A) Proposed biosynthesis of zearalenone. (B) Proposed biosynthesis of DHZ from Hpm8 and PKS13.

However, Hpm8 fails to communicate with PKS13 to synthesize **5**, suggesting that interactions between Hpm8 and Hpm3 are specific (**Figure 2-11A**). Replacement of Hpm3 SAT with PKS13 SAT generated the mutant PKSH1. The mutant is catalytically active as demonstrated by the production of **5** in the presence of **27** and malonyl-CoA (**Figure 2-11B**). However, the mismatched SAT domain cannot establish communication between Hpm8 and

PKSH1, indicating that the SAT domain is specific to its native partner (**Figure 2-11C**).

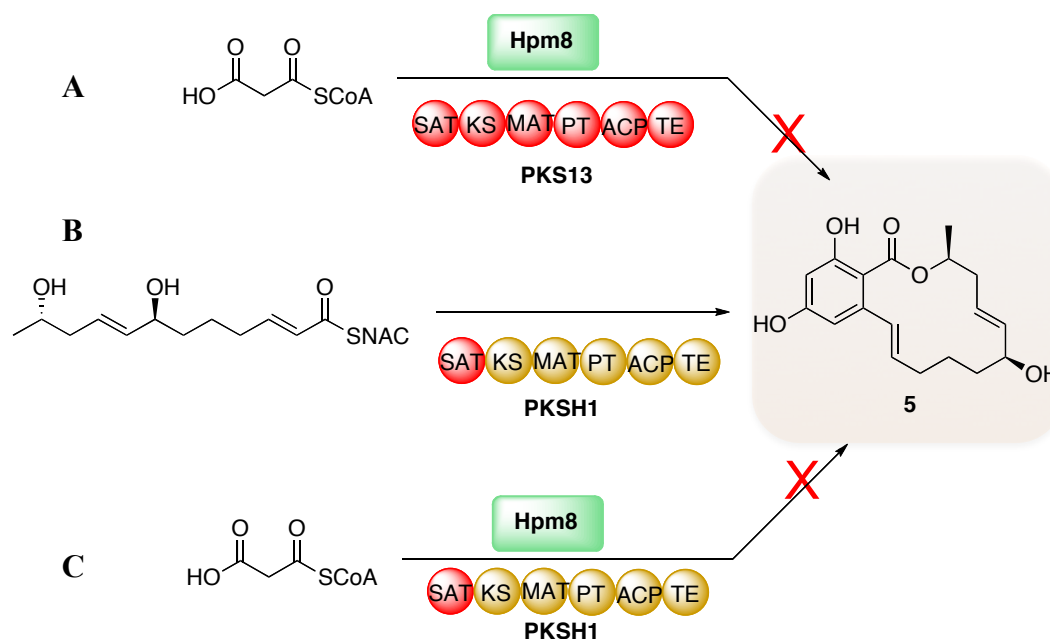


Figure 2-11 Specificity of the SAT domain. (A) Communication between Hpm8 and PKS13. (B) Production of **5** from **27** by mutant PKS13. (C) Communication between Hpm8 and mutant PKS13.

It would be interesting to see if an interaction can be established between Hpm8 and PKS13 by swapping PKS13 SAT with Hpm3 SAT. Unfortunately the construct PKSH2, in which the PKS13 SAT domain is replaced with the counterpart of Hpm3, is not catalytically active. However, this idea has been tested in the asperfuranone biosynthesis.⁸⁹ When the SAT domain of an NPRKS, asperfuranone synthase E (AfoE), is replaced with StcA (sterigmatocystin synthase A) SAT, AfoE can collaborate with StcJ and StcK (partnered FASs for sterigmatocystin biosynthesis) to produce an unnatural natural product **29** (**Figure 2-12**). These results indicate that the SAT-mediated chain transferring reactions

are highly specific, and this specificity can be employed to generate natural product analogs.

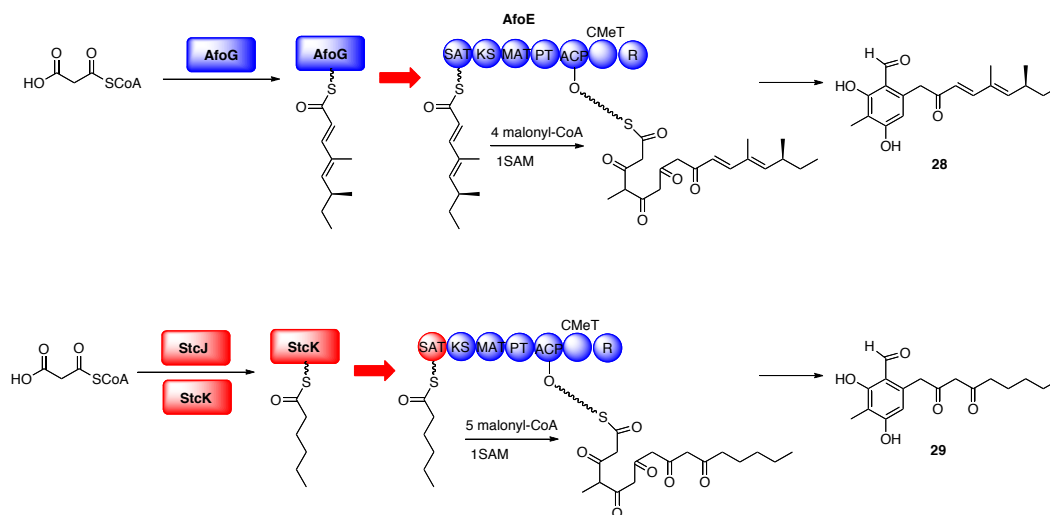


Figure 2-12 Production of unnatural polyketide **29** by swapping the SAT domain.

2.2.3 Conclusions

In collaboration with Professor Yi Tang and co-workers, the biosynthesis of DHZ, an advanced precursor of a kinase inhibitor hypothemycin, was reconstituted *in vitro*. Our collaborators successfully expressed and purified Hpm8 and Hpm3 from BJ5464-NpgA, and I synthesized compounds **8** and **27** for biosynthetic studies. In addition, I was able to crystallize DHZ to unambiguously assign its stereochemistry, which is unexpected from the biosynthetic mechanism. Detailed study of stereochemical control of Hpm8 will be discussed in the next section.

Hpm8 is catalytically active as a stand-alone enzyme as shown by production of **6**, **7** and **8** as shunt products when malonyl-CoA and NADPH are supplied. In contrast, Hpm3 cannot initiate the biosynthesis as a stand-alone

enzyme using malonyl-CoA as a starter unit. However, Hpm3 can utilize a small molecule, **27**, as a starter unit to initiate the DHZ biosynthesis. This result also verifies the distribution of labor between the HR-NR PKS hybrid: Hpm8 is responsible for the construction of a reduced hexaketide; while Hpm3 is in charge of synthesizing the aromatic portion. In addition, kinetic studies suggest that the synthesis of the hexaketide by Hpm8 is the rate-limiting step during DHZ biosynthesis *in vitro*.

The function of Hpm3 SAT was probed by the point mutation of its active site Ser121. The inability of Hpm3-SAT⁰ to produce **5** by collaboration with Hpm8 suggests the SAT domain is essential for the communication between Hpm8 and Hpm3. In addition, the specificity of the SAT domain was studied. Either pairing Hpm8 with PKS13, or with Hpm3 containing PKS13 SAT domain does not produce RAL products, suggesting that SAT-mediated interactions are highly specific.

2.3 Hpm8 KR domain stereospecificity*

2.3.1 Introduction

In the crystal structure of DHZ (**5**), both of the C6' and C10' positions have *S*-stereochemistry.⁴¹ This suggests that the KR domain of Hpm8 reduces the β -keto groups of diketide and tetraketide with different stereospecificity during the biosynthesis of DHZ (**Figure 2-13**). When discussing the stereochemical control of the KR domain, the DL-system is more efficient and convenient because the stereochemistry is independent of the substituents introduced by the next round of chain elongation. The stereochemistry of C6' and C10' can be assigned as D and L respectively as shown in **Figure 2-13**. A single KR domain capable of switching its stereochemical control based the structures of substrates is intriguing. Thus this prompted us to investigate the unprecedented KR domain programming.

* This is a collaborative project with the Tang group. I was responsible for synthesis and characterizations of intermediates and products (except compounds **30**, **30D**, and **30L**), whereas our collaborators, Professor Yi Tang and co-workers, were in charge of protein expression and purification, as well as biological assay.

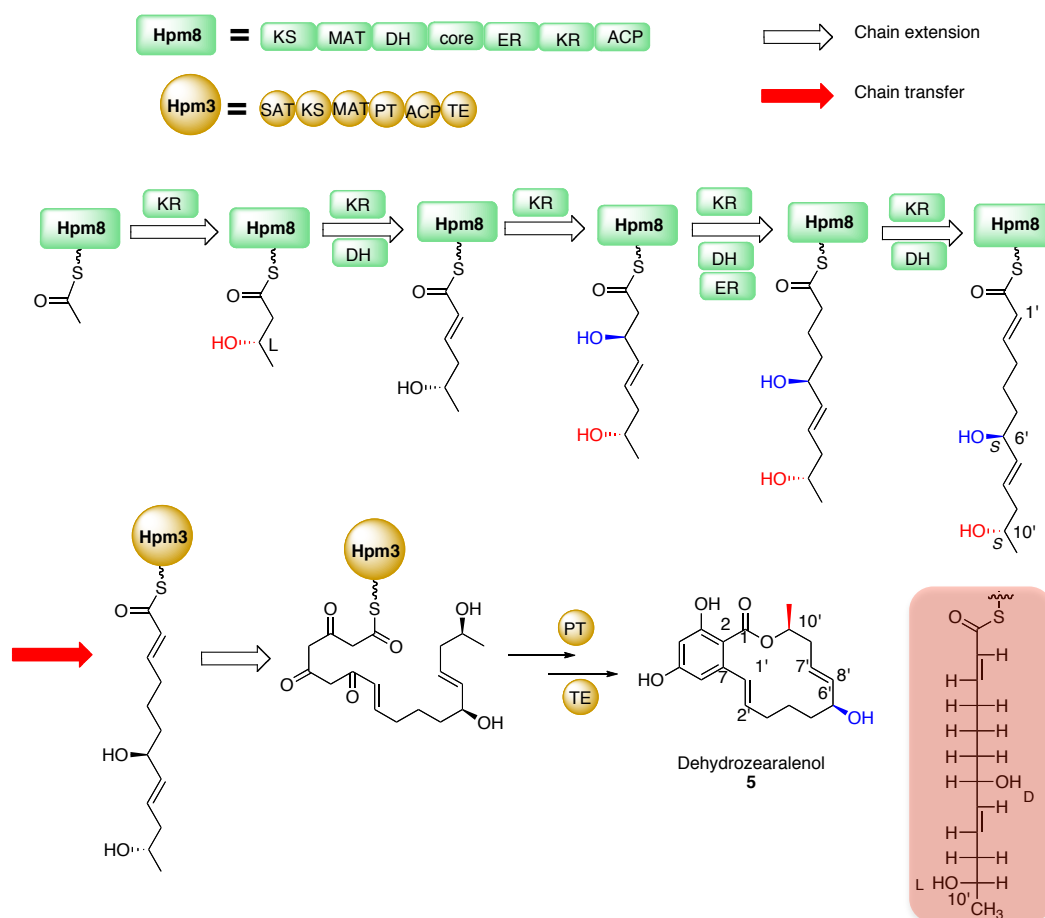


Figure 2-13 KR domain of Hpm8 reduces the β -keto groups of the diketide and tetraketide with different stereospecificity during the biosynthesis of DHZ. The structure in the red box is the Newman projection of the hexaketide intermediate.

Unlike the iterative PKS KR domain, the stereospecificity of the modular PKS KR domain is well studied.^{31, 33, 34, 90-97} The geometry of the modular KR active site fixes the position of the β -keto group of intermediates relative to NADPH; therefore a single stereochemistry can be generated through stereospecific attack of the hydride from NADPH. Because the modular KR domains are only used once, they can be programmed differently to introduce different stereochemistries at different positions within the PKS products. Both

biochemical and structural studies have revealed some conserved amino acid residues or sequence motifs involved in directing the substrate binding for stereocontrol.^{90, 92, 95} A conserved Trp located between the catalytic Ser and Tyr orientates the β -keto group for a *re* face attack to generate L-configured hydroxyl (A-type KR);^{90, 94, 96} while a *si* face attack is facilitated by a signature Leu-Asp-Asp patch to form D-configured hydroxyl (B-type KR).^{33, 92, 97}

However, the aforementioned model cannot be applied to Hpm8 KR, because it is used iteratively. Stereochemical control of the KR domain should be substrate-controlled. Different substrates in the KR active site can adopt different conformations, thus leading to different stereochemistries. The structural differences of the diketide and tetraketide intermediate are likely to determine substrate conformations in the active site. The differences between the diketide and tetraketide intermediates are as follows: (1) chain length; (2) the additional hydroxyl group on the tetraketide; and (3) the double bond on the tetraketide.

To determine which factors are involved in the stereochemical control of the KR domain, we synthesized a series of ketide intermediates or analogs as SNAC thioesters and assayed them in the presence of Hpm8 and NADPH (**Figure 2-14**). In addition, β -hydroxyl-SNAC thioesters in both L and D-configuration were also synthesized as authentic standards.

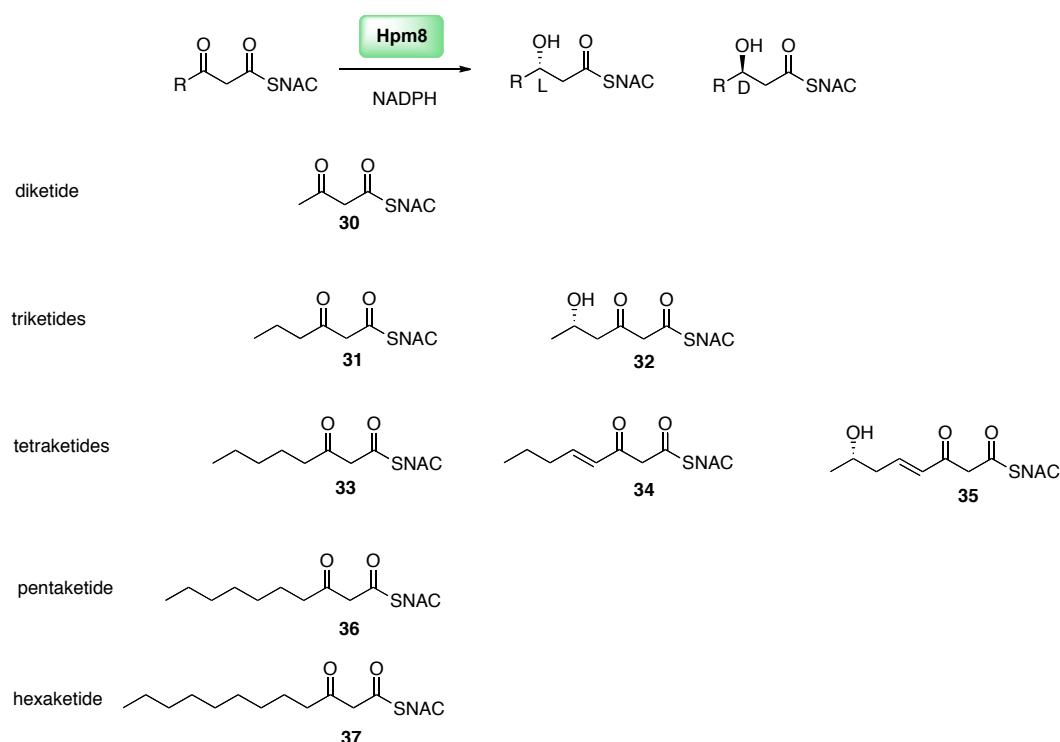


Figure 2-14 β -keto SNAC thioesters used to probe stereochemical control of the Hpm8 KR domain.

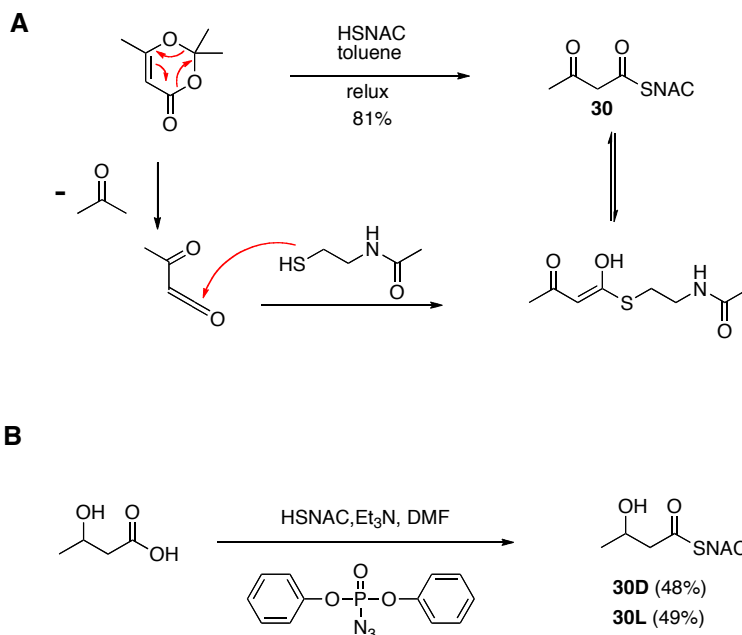
2.3.2 Results and discussion

2.3.2.1 Synthesis of SNAC thioesters

2.3.2.1.1 Synthesis of diketides 30, 30D and 30L

The synthesis of the diketides was performed in the Tang group. Diketide **30** was prepared in one step from 2,2,6-trimethyl-1,3-dioxin-4-one and HSNAC. Compound 2,2,6-trimethyl-1,3-dioxin-4-one decomposed into a ketene⁹⁸ intermediate upon refluxing in toluene, which was subsequently attacked by the nucleophilic thiol to form **30** in its enol form, which underwent rapid tautomerization into its keto form. The two corresponding β -hydroxyl diketides

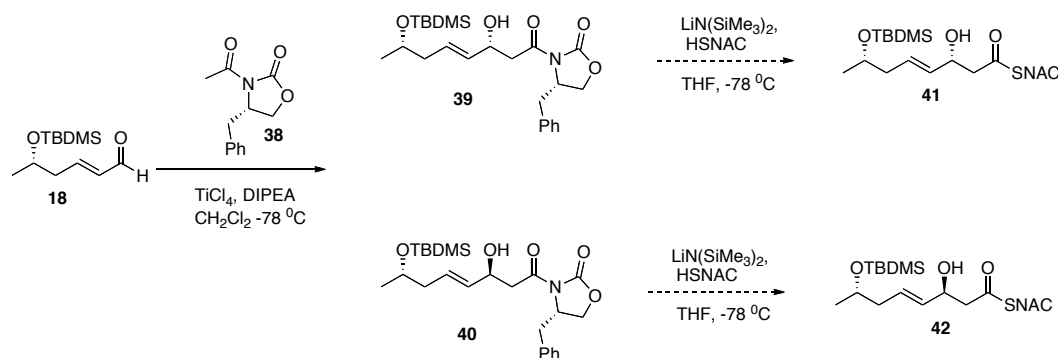
were synthesized from 3-(*R*)-hydroxybutyric acid and 3-(*S*)-hydroxybutyric acid. The two free acids condensed with HSNAC in the presence of diphenylphosphoryl azide and Et₃N to afford **30D** and **30L**, respectively (**Scheme 2-3**).



Scheme 2-2 Synthesis of diketides (A) **30** and (B) **30D** and **30L**.

2.3.2.1.2 Synthesis of tetraketides **35**, **35D** and **35L**

Tetraketides **35D** and **35L** were originally envisioned to be synthesized from an aldol reaction employing Evans' auxiliary chemistry (**Scheme 2-4**). Aldehyde **18** reacted with acetylated Evans' auxiliary **38** to form two diastereomers **39** and **40** in a 2:3 ratio.



Scheme 2-3 Original synthetic routes toward synthesis of **30D** and **30L**.

Unlike the α -substituted enolate of Evans' auxiliary, the stereochemical control of aldol reactions of acetylated Evans' auxiliary is known to be problematic.⁹⁹ But it is not obvious why an α -unsubstituted enolate is not as stereoselective as the α -substituent counterpart in our case. The stereochemical control of Evans' auxiliary chemistry has been rationalized by the Zimmerman-Traxler model¹⁰⁰ of six-membered chair transition states (TS) (**Figure 2-15A**).^{101,}
¹⁰² Of four TSs, only TS **43** and **44** are plausible due to the aldehyde approach from the opposite side of the benzyl group of the oxazolidone. TS **43** is generally more favorable than TS **44**, because its dipole is minimized by orientating the oxazolidone away from the C-O double bond, leading to the Evans-*syn* configuration in the product (**47**). In addition, the product of TS **44** (**48**) suffers from a steric clash between the benzyl group and the α -substituent (methyl group in this case). In contrast, in the case of the α -unsubstituted aldol reactions, product **54** does not suffer from a steric clash like **48**, and thus forms in a significant amount (**Figure 2-15B**). However, the dipole maximization renders TS **50** slightly less favored than TS **49**.

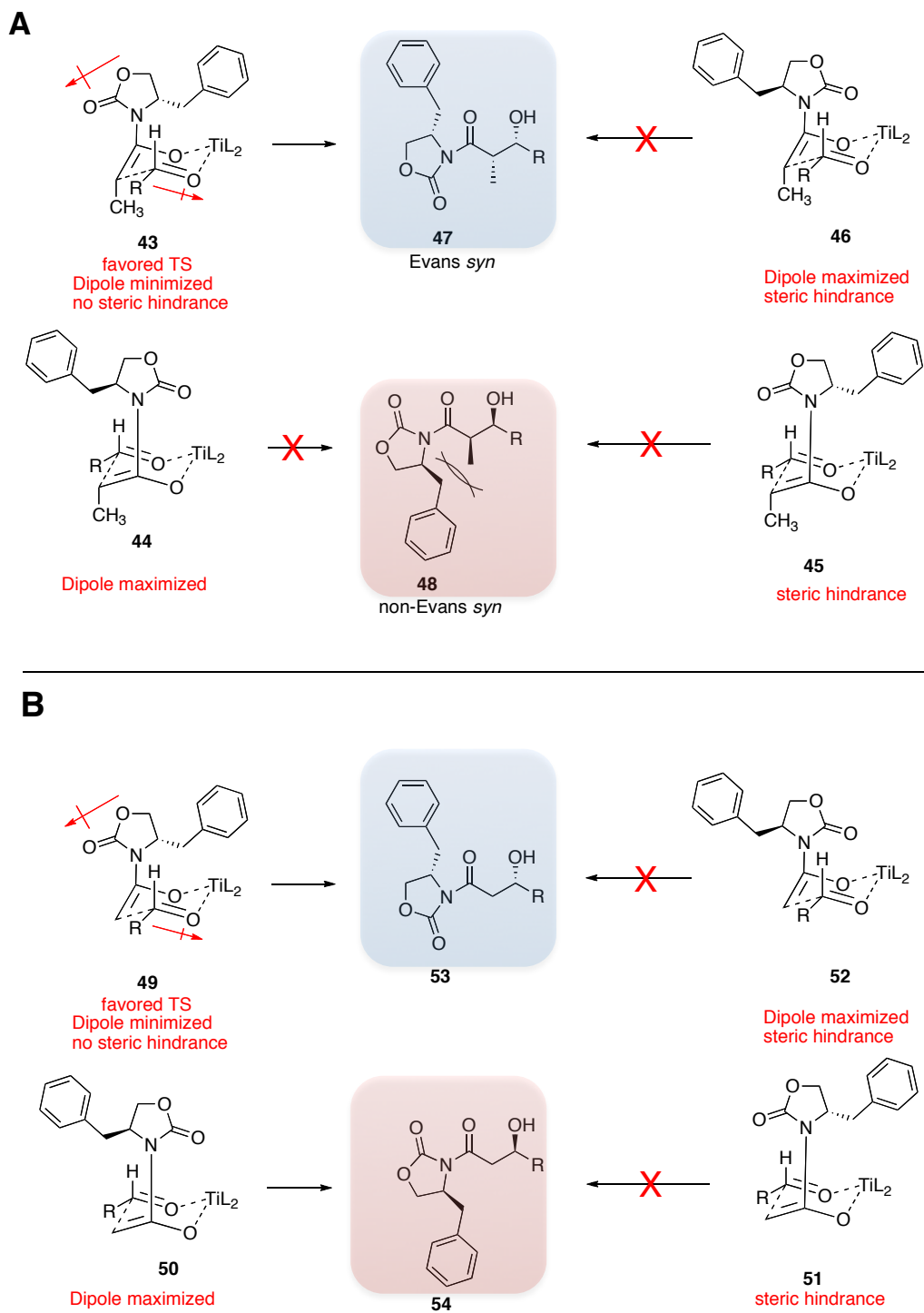
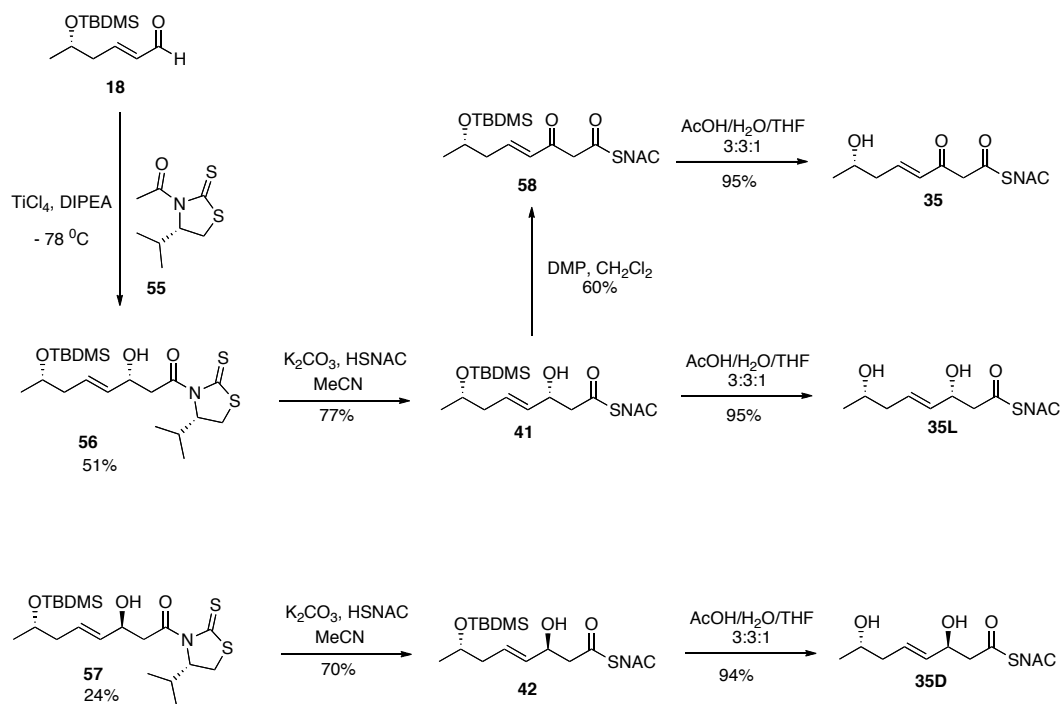


Figure 2-15 Possible transition states of aldol reactions containing: (A) α -substituted enolate; and (B) α -unsubstituted enolate.

Although **39** and **40** were formed as a mixture (**Scheme 2-4**), they could be separated by flash chromatography. This turned out to be an advantage in the synthesis of **35D** and **35L**, because both precursors could be obtained in one reaction. However, direct displacement of Evans' auxiliary with HSNAC in the presence of $\text{LiN}(\text{SiMe}_3)_2$ yielded a complex mixture.¹⁰³ An attempt to convert **39** and **40** to free acids, and then couple with HSNAC was not promising due to low yields.

Crimmins' auxiliary (thiazolidinethione, originally known as the Fujita-Nago auxiliary¹⁰⁴) stands out as an excellent leaving group.¹⁰⁵⁻¹⁰⁷ The sulfur atom is larger than the oxygen atom, so the negative charge developed from the SNAC displacements is better stabilized for Crimmins' auxiliary than that of Evan's auxiliary. Indeed, products **56** and **57**, formed from the aldol reaction between the acetylated Crimmins' auxiliary **55** and aldehyde **18**, were easily displaced by HSNAC using K_2CO_3 as a base to form **41** and **42**, respectively (**Scheme 2-5**). In addition, Crimmins' auxiliary chemistry provides an additional advantage. The bright yellow color of the acylated Crimmins' auxiliary simplifies detection during purification via flash chromatography. Also, the displacement reactions with HSNAC can be monitored by the disappearance of the yellow color, which usually finishes in less than an hour. The desired products **35D** and **35L** were formed by deprotection of **41** and **42**, respectively. Compound **35** was synthesized from **41** by oxidation of the hydroxyl group with Dess-Martin periodinane (DMP), followed by deprotection of TBDMS with $\text{AcOH}/\text{H}_2\text{O}/\text{THF}$ (3:3:1).



Scheme 2-4 Synthesis of tetraketides **35**, **35D** and **35L**.

It is found that the stereoselectivity of the aldol reactions with Crimmins' auxiliary is opposite to that of Evans' auxiliary. The result can be explained by the favored TS **60** (**Figure 2-16**). Although the dipole is not minimized in TS **60**, the additional chelation between the thiocarbonyl and titanium makes it more stable, thus leading to the formation of **64** as a major product.

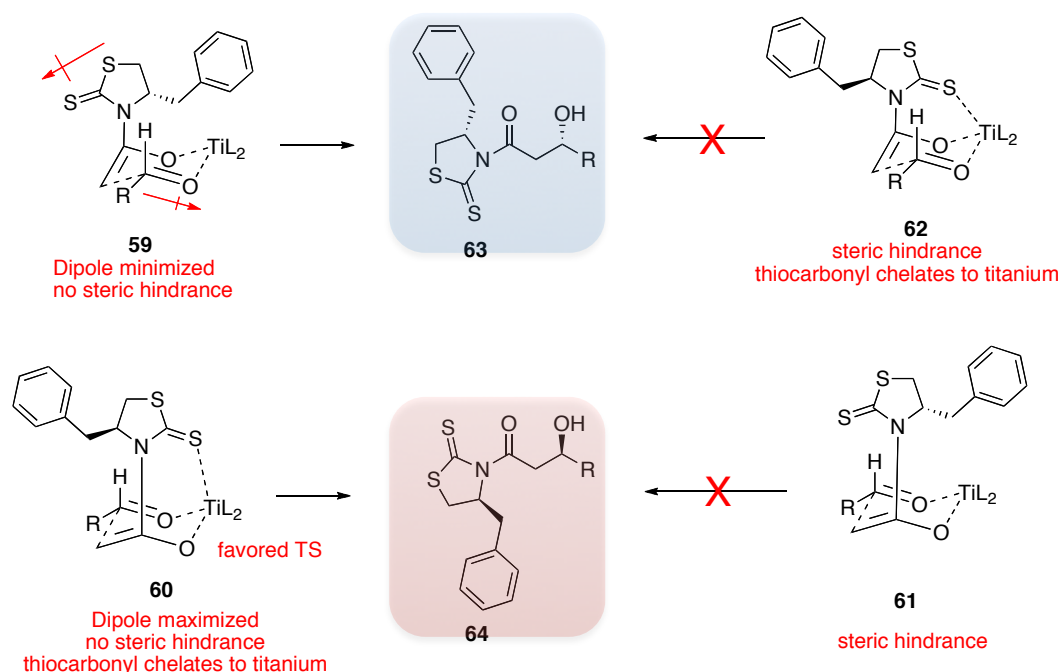
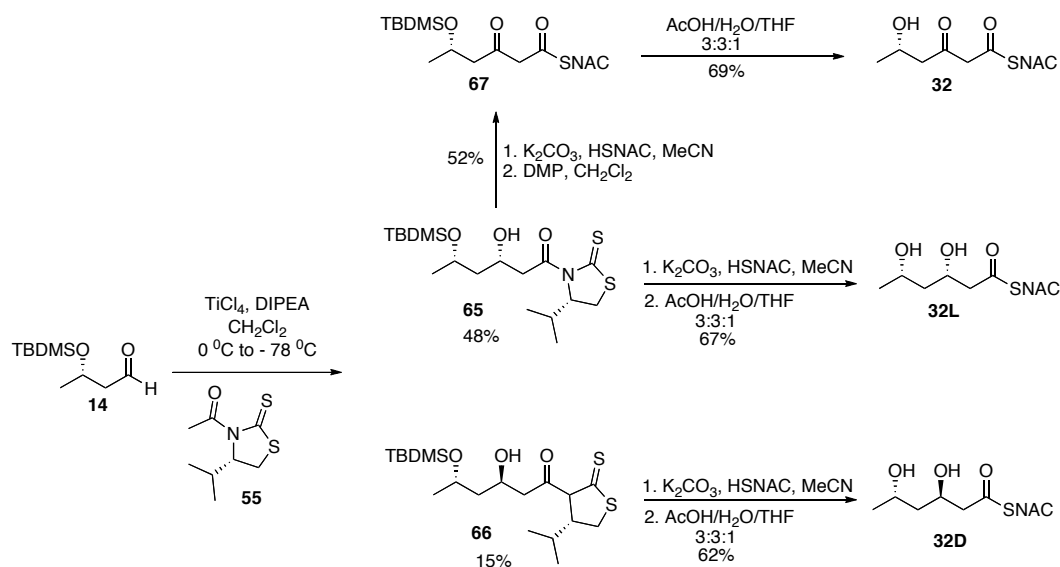


Figure 2-16 Transition states of Crimmins' auxiliary promoted aldol reaction.

2.3.2.1.3 Syntheses of triketides **32**, **32D** and **32L**.

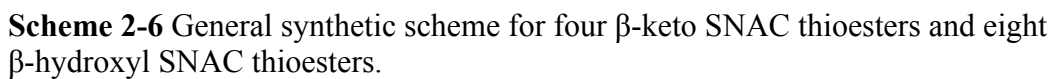
The method used to prepare **35** was employed with some modifications to synthesize triketide **32** (Scheme 2-6). Aldehyde **14** underwent an aldol reaction with **55** to furnish **65** and **66**, which were separated by flash chromatography. The auxiliary portion of **65** was displaced with HSNAC in the presence of K_2CO_3 , and the resulting product was directly treated with AcOH/H₂O/THF (3:3:1) to afford **32L**. The **32D** was synthesized similarly from **66**. In addition, displacement of **65** with HSNAC in the presence of K_2CO_3 , followed by DMP oxidation, provided **67**. Compound **67** was deprotected with AcOH/H₂O/THF (3:3:1) to furnish triketide **32**.

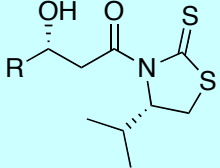
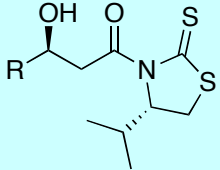
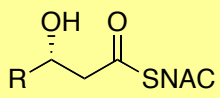


Scheme 2-5 Syntheses of triketides **32**, **32D** and **32L**.

2.3.2.1.4 Synthesis of triketides **31**, **31D** and **31L**, tetraketides **33**, **33D** and **33L**, **34**, **34D** and **34L**, and pentaketides **36**, **36D** and **36L**.

The synthesis is shown in **Scheme 2-7**. The starting materials, propionaldehyde, hexanal, (*E*)-hex-2-enal and octanal, each underwent aldol reactions with **55** to form four pairs of diastereomers. The diastereomers were separated and then treated with K_2CO_3 and HSNAC to afford the eight β -hydroxyl SNAC thioesters (**Table 2-1**). Then β -hydroxyl SNAC thioesters, **31L**, **33L**, **34L** and **36L** were oxidized with DMP to yield **31**, **33**, **34** and **36**, respectively. The yields for the syntheses are summarized in **Table 2-1**.

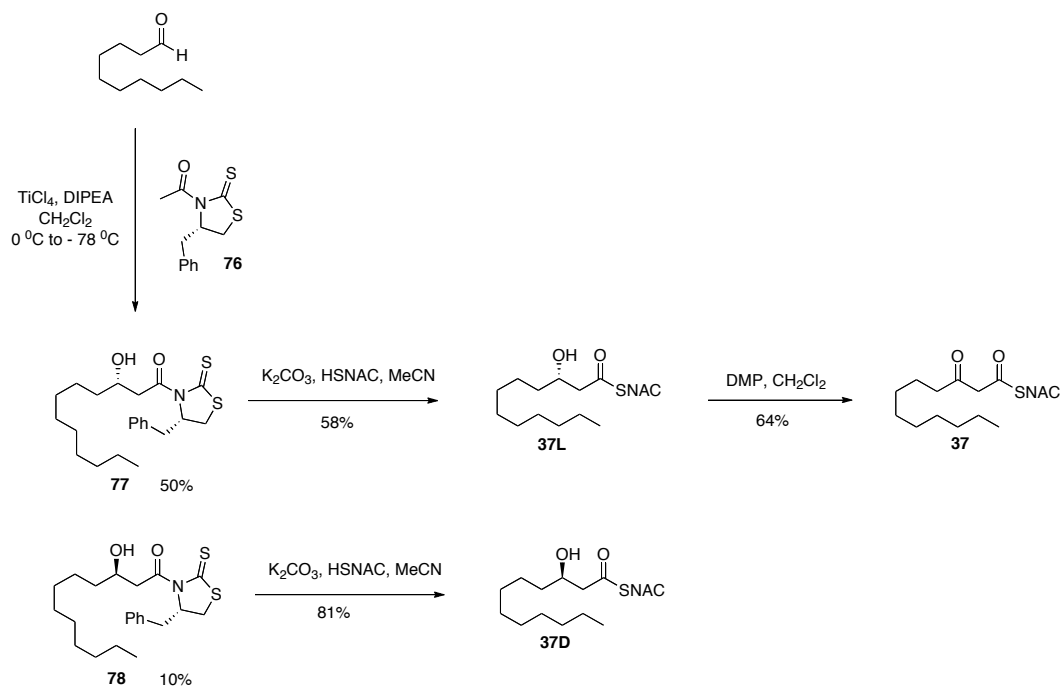


	Triketides 31, 31D and 31L	Tetraketides 33, 33D and 33L	Tetraketides 34, 34D and 34L	Pentaketides 36, 36D and 36L
	<p>68</p> <p>45%</p>	<p>70</p> <p>50%</p>	<p>72</p> <p>50%</p>	<p>74</p> <p>49%</p>
	<p>69</p> <p>18%</p>	<p>71</p> <p>23%</p>	<p>73</p> <p>14%</p>	<p>75</p> <p>33%</p>
	<p>31L</p> <p>67%</p>	<p>33L</p> <p>66%</p>	<p>34L</p> <p>61%</p>	<p>36L</p> <p>69%</p>

	31D 66%	33D 80%	34D 74%	36D 65%
	31 27%	33 46%	34 60%	36 30%

2.3.2.1.5 Synthesis of hexaketides **37**, **37D** and **37L**

Auxiliary **55** was changed to **76** for the synthesis of **37**, **37D** and **37L** (Scheme 2-8). An aldol reaction between decanal and **76** in the presence of TiCl_4 and DIPEA yielded diastereomers **77** and **78**, which were converted to **37L** and **37D**, respectively, by treatment with K_2CO_3 and HSNAC. Compound **37** was synthesized from **37L** by DMP oxidation of the β -hydroxyl group.



Scheme 2-7 Synthesis of hexaketides **37**, **37D** and **37L**.

In summary, a group of β -hydroxyl and β -keto SNAC thioesters were synthesized using Crimmins' auxiliary chemistry. The yields of the aldol reactions range from 60% to 82%, and the ratios of the resulting diastereomers are from 1.5 to 5. The auxiliary is smoothly displaced by HSNAC in the presence of K_2CO_3 , in 58% to 81% yield. The HSNAC-displaced products could be oxidized by DMP to afford the β -keto SNAC thioesters (yields from 24% to 64%).

2.3.2.2 Stereospecificity of Hpm8 KR domain at diketide and tetraketide stages

The *in vitro* assays were performed in the Tang group. When Hpm8 is incubated with diketide **30** in the presence of NADPH, L-hydroxyl thioester **30L** is formed as a major product, together with a small amount (9%) of its enantiomer **30D**, as detected by chiral HPLC. Stereochemical control of the reduction of **30** *in vitro* is consistent with the stereospecificity of the KR domain at the diketide stages, suggesting the stereoselectivity of KR domain can be reproduced under the assay condition. Because the product is reduced in its SNAC form, a possible mechanism of the ketoreduction of **30** could be proposed (**Figure 2-17**). The SNAC moiety, which mimics the Ppant arm attached to the ACP domain, could direct the diketide into the active site of the KR domain, where a stereoselective reduction occurs to yield **30L** as a major product. On the other hand, it is also possible that **30** is first primed on the ACP domain by transthioesterification and then transferred to the KR active site for a stereoselective reduction. Cane and co-workers demonstrated that recombinant DEBS KR domains can reduce diketide SNAC thioesters stereoselectively without the involvement of the ACP

domains.^{31, 108} Therefore, the first mechanism is more reasonable. Nevertheless, recombinant DEBS KR2, KR5 and KR6 display reduced stereoselectivity towards **30** as compared to the β -keto diketide anchored on ACP.¹⁰⁸ The erosion in stereoselectivity of KR toward SNAC mimics indicates that ACP might be involved in orientating the diketide substrate properly in the KR active site. Because the Hpm8 KR domain also displays a relaxed stereoselectivity toward the same diketide (**30**), direct reduction of the SNAC-tethered diketide in the KR active site is more plausible. The formation of a small amount of **30D** could be rationalized by an improper orientation of the SNAC-tethered diketide in the Hpm8 KR active site during *in vitro* reduction.

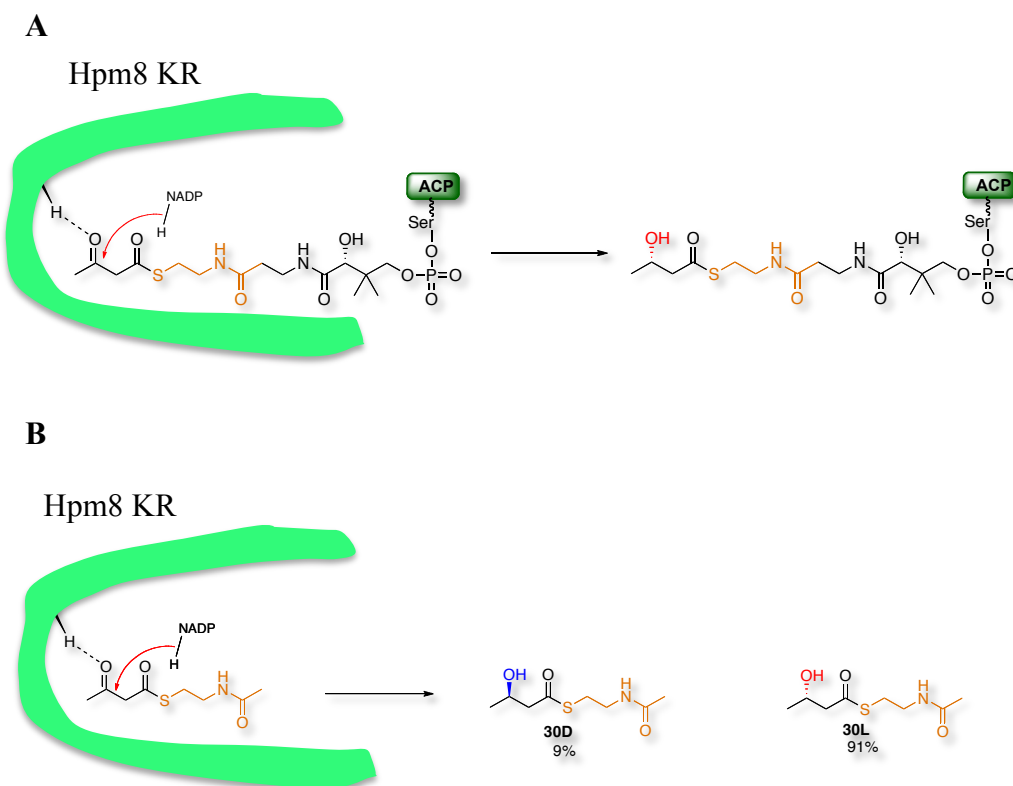


Figure 2-17 (A) *In vivo* ketoreduction of **30** tethered to ACP; and (B) *in vitro* reduction of **30** tethered to SNAC by the Hpm8 KR domain.

Hpm8 KR exclusively generates D-configured products (**33D**, **34D** and **35D**) when tetraketides **33**, **34** and **35** are supplied (**Figure 2-18**). For the natural substrate **35**, the D-configuration of product (**35D**) matches with that of the intermediate formed in the third round extension. Hpm8 KR reduces natural substrate analogs **33** and **34** with the same facial selectivity, suggesting that the terminal hydroxyl group and the alkene may not play any role in the stereospecificity of Hpm8 KR.

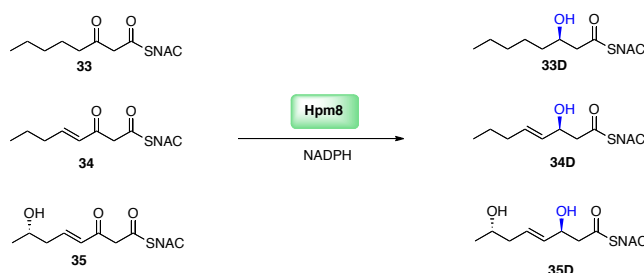


Figure 2-18 The stereospecificity of Hpm8 KR at the tetraketide stage.

2.3.2.3 Probing stereospecificity of Hpm8 KR at other ketide stages

Unlike the diketide and tetraketide stages, the stereospecificity of Hpm8 KR domain at triketide, pentaketide and hexaketide stages are not revealed in the PKS product DHZ. To probe the stereochemistry of the triketide intermediate during DHZ biosynthesis, triketides **31** and **32** are individually tested in *in vitro* assays containing Hpm8 and NADPH (**Figure 2-19**). Chiral HPLC comparisons with D and L β -hydroxyl standards suggest that both triketides **31** and **32** are stereospecifically reduced to the D-configured products by the KR domain. So it is reasonable to assume that the functional groups on the carbon skeleton do not affect the stereochemistry of the resulting β -hydroxyl groups. Therefore,

pentaketide and hexaketide with aliphatic chains were solely used to probe the stereochemical course of Hpm8 KR during the pentaketide and hexaketide stages. D-Configured products (**36D** and **37D**) are formed exclusively when **36** and **37** are incubated individually with Hpm8 and NADPH, clearly showing that Hpm8 KR displays a substrate chain length-tuning stereospecificity. The KR domain reduces diketides to L-configured hydroxyls; but it reduces all other ketides to D-configured hydroxyls during the biosynthesis of the reduce portion of DHZ.

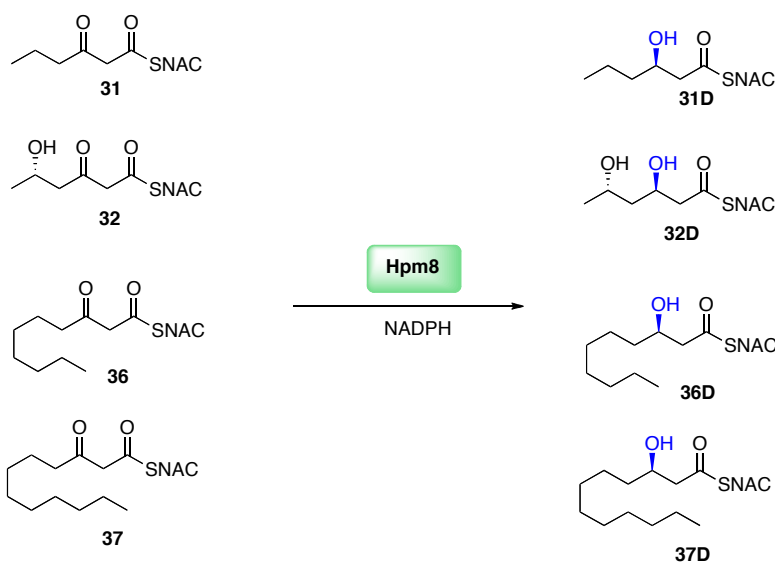
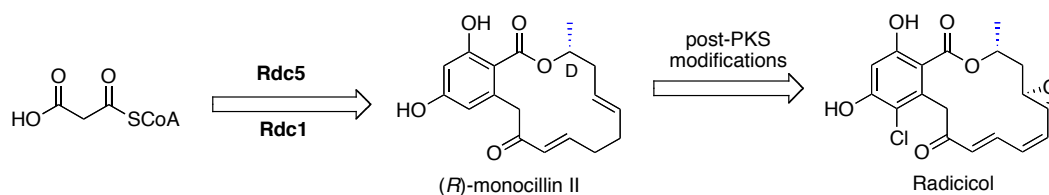


Figure 2-19 The stereospecificity of the Hpm8 KR domain at the triketide, pentaketide and tetraketide stages.

2.3.2.4 Domain swaps between Hpm8 KR and Rdc5 KR

Rdc5 (HRPKS) and Rdc1 (NRPKS) are responsible for the biosynthesis of (*R*)-monocillin II, a precursor toward radicicol (**Scheme 2-9**).^{39, 40, 109} In contrast to DHZ, C10' of (*R*)-monocillin II is D-configured. Sequence alignment between Rdc5 and Hpm8 suggests that the two KR domains share a 66% amino acids identity. By comparisons to DEBS KR1, the catalytic triad in Hpm8 is identified

as Lys2088, Ser2113 and Tyr2126. Mutants Hpm8_Lys²⁰⁸⁸Asp, Hpm8_Ser²¹¹³Ala and Hpm8_Tyr²¹²⁶Ala lost their ability to cooperate with Hpm3 to product DHZ (Figure 2-20).



Scheme 2-8 General scheme of biosynthesis of (*R*)-monocillin II, a precursor toward radicicol.

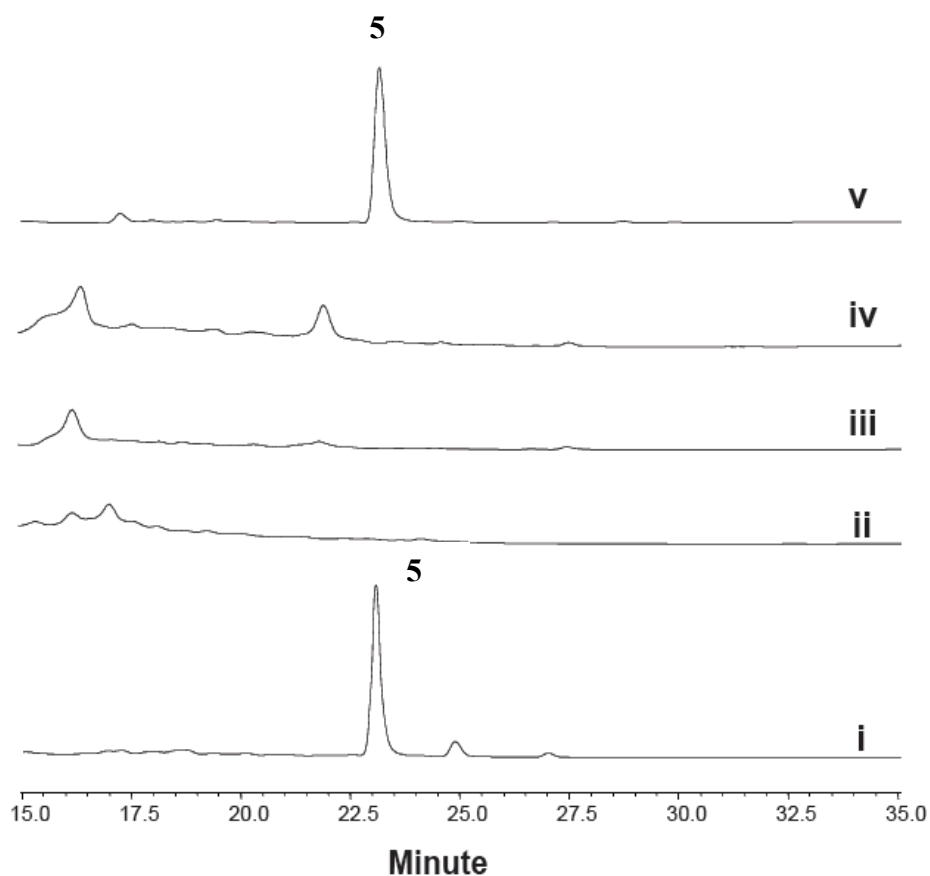


Figure 2-20 The HPLC traces of the *in vivo* metabolites profiles from the *S. cerevisiae* co-transformants expressing Hpm3 and (i) Hpm8 (ii) Hpm8_Lys²⁰⁸⁸Asp, (iii) Hpm8_Ser²¹¹³Ala, (iv) Hpm8_Tyr²¹²⁶Ala or (v) Hpm8_Tyr²¹¹⁸Phe. The chromatograms above are obtained by monitoring at 320 nm. Mutations of Lys²⁰⁸⁸, Ser²¹¹³ and Tyr²¹²⁶ abolish the activities of Hpm8.

Type I modular PKS KRs can be divided into two groups in general: (1) A-type KRs possess a conserved Trp residue to guide the Ppant arm of ACP in the active site of the KR domain to produce L-OH;^{90, 94, 96} and (2) B-type KRs produce D-OH, and share a conserved Leu-Asp-Asp motif.^{33, 92, 97} However, these fingerprints can not be applied to either Hpm8 KR or Rdc5 KR. Hpm8 KR and Rdc5 KR both have aromatic residues (Tyr2118 in Hpm8, Phe2143 in Rdc5),

analogous to the Trp residue of A-type KRs. In addition, the signature motif Leu-Asp-Asp is replaced with a conserved Leu-Arg-Asp motif in both Hpm8 KR and Rdc5. The key differences between Hpm8 KR and Rdc5 KR are the aromatic residues in the fingerprints derived from modular KRs: Tyr2118 in Hpm8 and Phe2143 in Rdc5. However, a point mutation Tyr2118Phe in Hpm8 does not alternate the stereochemistry on the C10' of DHZ (**Figure 2-20**), suggesting that additional regions are involved in the stereochemical control of Hpm8 KR.

To map the crucial region for the stereospecificity of the KR domain, homology modeling of Hpm8 and Rdc5 was performed by using the online server HHpred (<http://toolkit.tuebingen.mpg.de>). The overall structures of both Hpm8 KR and Rdc5 KR show a Rossmann fold^{110, 111} with two $\beta\alpha\beta\alpha\beta$ motifs that are connected by α_3 (**Figure 2-21**). The $\beta_1\alpha_1\beta_2\alpha_2\beta_3$ stretch is involved in NADPH binding, while the $\beta_4\alpha_4\beta_5\alpha_{5/6}\beta_6$ motif harbors the catalytic residues and the putative active site. To map the secondary structural element that contributes to the stereospecificity differences between the two KR domains, a series of Hpm8 mutants (**Figure 2-21C**) containing chimeric KR sequences from Rdc5 were constructed in the Tang group based on the modeled structures. Hpm8B1 contains the whole catalytic part of Rdc5 KR domain. Hpm8B2 covers most of the Rossmann fold and contains Rdc5 sequences from the loop between β_2 and α_2 to the loop between β_6 and α_7 . Hpm8B3 contains the α_7 to α_9 region from Rdc5 KR. Hpm8B4 to Hpm8B9 contains smaller portion that are swapped with Rdc5 KR compared to Hpm8B2. Except Hpm8B1, Hpm8B3 and Hpm8B6, all other chimeric enzymes are solubly expressed.

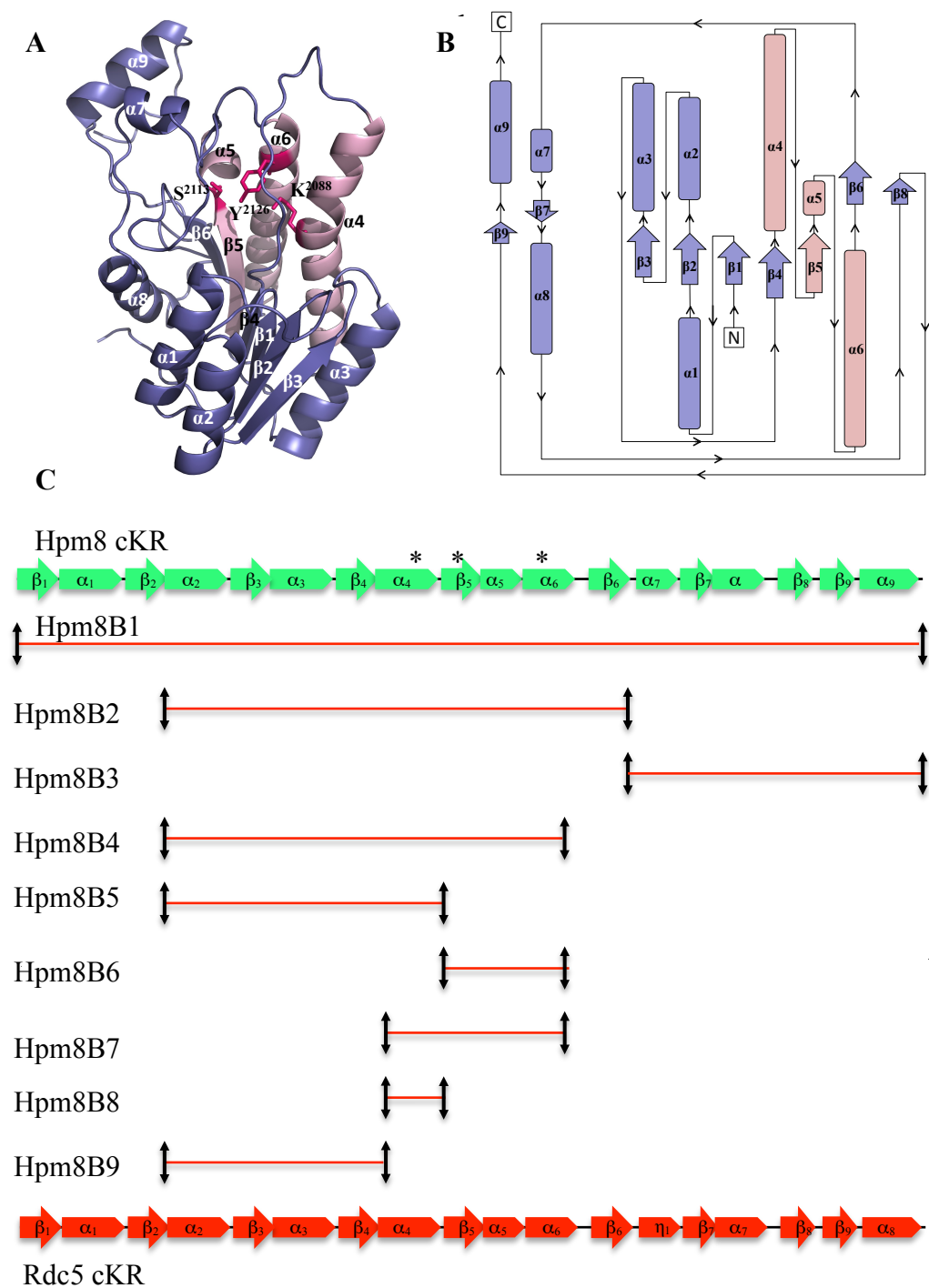


Figure 2-21 (A) Cartoon view of the homology model of Hpm8_cKR. The catalytic residues Ser²¹¹³, Lys²⁰⁸⁸ and Tyr²¹²⁶ are shown as sticks in red. (B) The topology diagram of the model structure of Hpm8_cKR. The $\alpha_4\beta_5\alpha_5\alpha_6$ motif is highlighted in salmon. (C) Illustration of the swapping regions between

Hpm8_cKR and Rdc5_cKR in different chimeric HRPKSs. In the schematic chimeric enzymes, the backbone is based on Hpm8. The substituting regions derived from Rdc5 are displayed in red lines. * indicates the positions of the three catalytic residues.

2.3.2.5 Stereospecificity of chimeric Hpm8 toward β -keto SNAC thioesters

The enzymatic assays were performed in the Tang group. The stereospecificity of the KR domain is successfully inverted in Hpm8B2. A D-configured diketide is produced by the reduction of **30** using Hpm8B2, indicating that swapping of α_2 to β_6 region of Hpm8 KR could alter its stereoselectivity. Similarly, a small amount of **30L** (5%) is also observed, possibly because of lost fidelity of SNAC compared to the entire ACP domain when the substrate interacts with the KR domain. To further narrow down the determining region, Hpm8B4, lacking the β_6 of Rdc5 KR compared to Hpm8B2, was incubated with **30**. A similar product profile was obtained, suggesting β_6 is not essential for the stereospecificity of the KR domain. However, elimination of $\beta_5\alpha_5\alpha_6$ in Hpm8B5 switches the stereospecificity of the KR domain back: **30L** is produced when **30** is incubated with Hpm8B5, suggesting that the $\beta_5\alpha_5\alpha_6$ motif, where Ser2113 and Tyr2126 are located, is crucial for stereochemical control of the KR domain. Unfortunately, the $\beta_5\alpha_5\alpha_6$ -swapped Hpm8B6 is not solubly expressed. Hpm8B7, which includes α_4 in addition to the $\beta_5\alpha_5\alpha_6$ motif, is expressed but the KR activity is very weak. Despite this, Hpm8B7 does produce expected **30D** as a major product (70%), suggesting that the minimal swapped region capable of inverting the diketide stereospecificity is $\alpha_4\beta_5\alpha_5\alpha_6$. To test if α_4 is involved in the

stereoselectivity, an α_4 -swapped Hpm8B8 was incubated with **30**, and the L-configured hydroxyl group was formed as a major product. In addition, the involvement of $\beta_2\alpha_2\beta_3\alpha_3\beta_4$, where the NADPH binding site is located, is excluded because Hpm8B9 produced **30L** as a major product. Although α_4 and $\beta_2\alpha_2\beta_3\alpha_3\beta_4$ do not determine the stereospecificity of Hpm8 KR, they may be involved in the stabilization of the $\beta_5\alpha_5\alpha_6$ motif because swapping only $\beta_5\alpha_5\alpha_6$ leads to the insolubly expression of Hpm8B6, and swapping only $\alpha_4\beta_5\alpha_5\alpha_6$ results in the low activity of Hpm8B7.

The chimeric megasynthases were further assayed for ketoreduction of tetraketide **35**, and all of them reduce the tetraketide stereospecifically to **35D**. Furthermore, Hpm8B4 reduces all other β -keto SNAC thioesters to their D-configured products. These results suggest swaps do not affect the stereospecificity of Hpm8 KR at other ketide stages except the diketide.

2.3.2.6 Activities of chimeric Hpm8 and Hpm3 *in vivo*

The *in vivo* enzymatic activities of chimeric Hpm8 were probed by co-expression with Hpm3 in BJ5464-NpgA. As expected from the *in vitro* stereoselectivity, Hpm8B5, Hpm8B8 and Hpm8B9 give the same product profile as the wild type. However, Hpm8B2, Hpm8B4 and Hpm8B7 form a new compound **79** together with about an equal amount of DHZ. The product titer of Hpm8B7 is lower than with other chimeric Hpm8 enzymes, which is in agreement with its weak activity *in vitro*.

2.3.2.6.1 Identity of 79

Because Hpm8B2, Hpm8B4 and Hpm8B7 produce a D-configured diketide *in vitro*, they could possibly produce an epimer of DHZ together with Hpm3 (**Figure 2-22**) *in vivo*. Indeed, the NMR spectrum of the new product **79** is similar to that of DHZ (**Table 2-2**), and the UV and MS spectra of the two compounds are same.

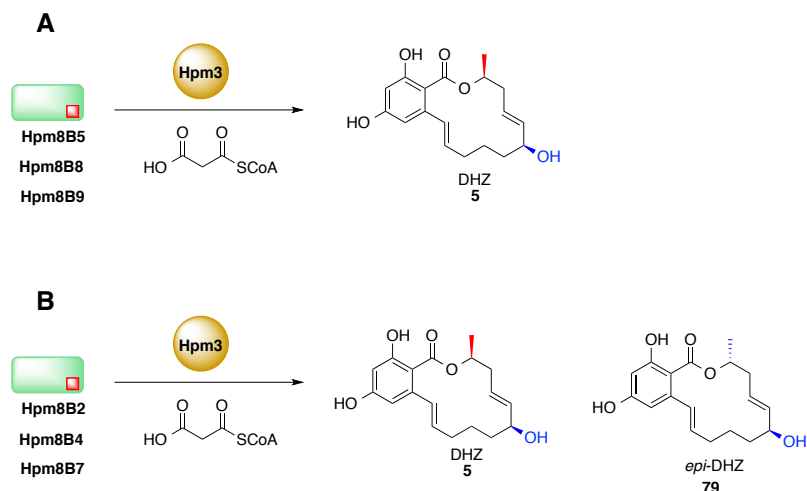


Figure 2-22 (A) Production of DHZ by Hpm8B5, Hpm8B8 and Hpm8B9; and (B) Production of *epi*-DHZ and DHZ by Hpm8B2, Hpm8B4 and Hpm8B7.

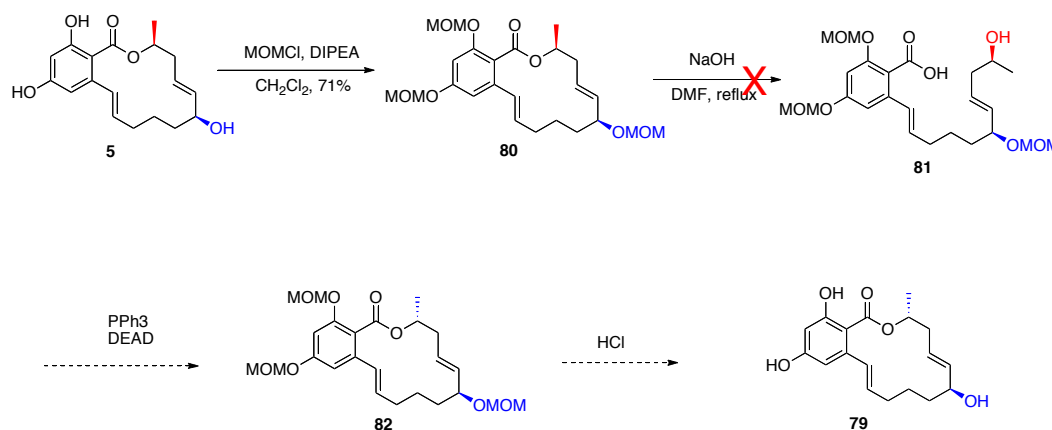
Table 2-2 NMR data^a comparison between **79** and **5**.

No.	¹³ C δ (ppm)	¹ H δ (ppm) (m, area, J _{HH} (Hz))	No.	¹³ C δ (ppm)	¹ H δ (ppm) (m, area, J _{HH} (Hz))
1	171.0	-	1	172.4	-
2	103.4	-	2	106.5	-
3	162.0	-	3	163.0	-
4	101.5	6.44 (d, 1H, 2.4)	4	102.5	6.40 (d, 1H, 3)
5	164.1	-	5	164.3	-
6	106.2	6.19 (d, 1H, 2.4)	6	107.6	6.20 (d, 1H, 3)
7	142.7	-	7	143.6	-

1'	129.4	7.09 (d, 1H, 15.8)		131.5	6.94 (d, 1H, 15.8)
2'	131.4	6.06 (dt, 1H, 15.8, 5.4)		133.3	5.94 (dt, 1H, 15.8, 6.28)
3'	29.3	2.33-2.39 (m, 2H) 2.15 (m, 1H)		31.6	2.14-2.28 (m, 2H)
4'	22.4	1.61-1.66 (m, 2H)		22.6	1.74-1.84 (m, 2H)
5'	34.2	1.49-1.54 (m, 1H) 1.67-1.73 (m, 1H)		34.7	1.52-1.71 (m, 2H)
6'	72.9	3.95 (m, 1H)		72.8	4.23 (m, 1H)
7'	136.8	5.52-5.49 (m, 1H)		137.5	5.59-5.72 (m, 2H)
8'	125.1	5.80 (m, 2H)		126.6	5.59-5.72 (m, 2H)
9'	36.5	2.42-2.44 (m, 1H) 2.50-2.56 (m, 1H)		38.8	2.53 (dt, 1H, 15.8, 4.2)
10'	71.2	5.44-5.48 (m, 1H)		73.2	5.30 (m, 1H)
11'	17.2	1.39 (d, 3H, 6.5)		19.8	1.37 (d, 3H, 6.5)

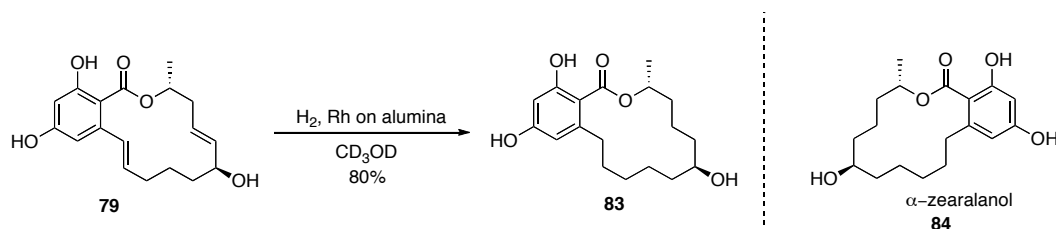
^a Spectra were obtained at 500 MHz for proton and 120 MHz for carbon and were recorded in methanol-*d*₄.

To conclusively confirm the stereochemistry of **79**, an attempt to convert DHZ to **79** was envisioned as shown in **Scheme 2-10**. Hydrolysis of MOM protected DHZ (**80**) could provide the free acid and hydroxyl groups (**81**), which are set up for a Mitsunobu reaction to invert the stereochemistry on C10'. However, the resorcylic ester group is very stable, and even NaOH in refluxing DMF failed to open the macrolactone of **80**.



Scheme 2-9 Attempts to synthesize **79** from **5** via a Mitsunobu reaction.

An alternative route was designed to confirm the stereochemistry of **79** (Scheme 2-11). Hydrogenation of **79** in the presence of Rh on alumina formed **83**, which should be an enantiomer of well characterized (6'*R*, 10*S*')- α -zearalanol (**84**). Indeed, they possess an identical NMR spectrum, while showing inverted circular dichroism spectra (Figure 2-23). Therefore, the stereochemistry of **79** is established as 6'*S* and 10'*R*.



Scheme 2-10 Synthesis of **83**, an enantiomer of α -zearalanol.

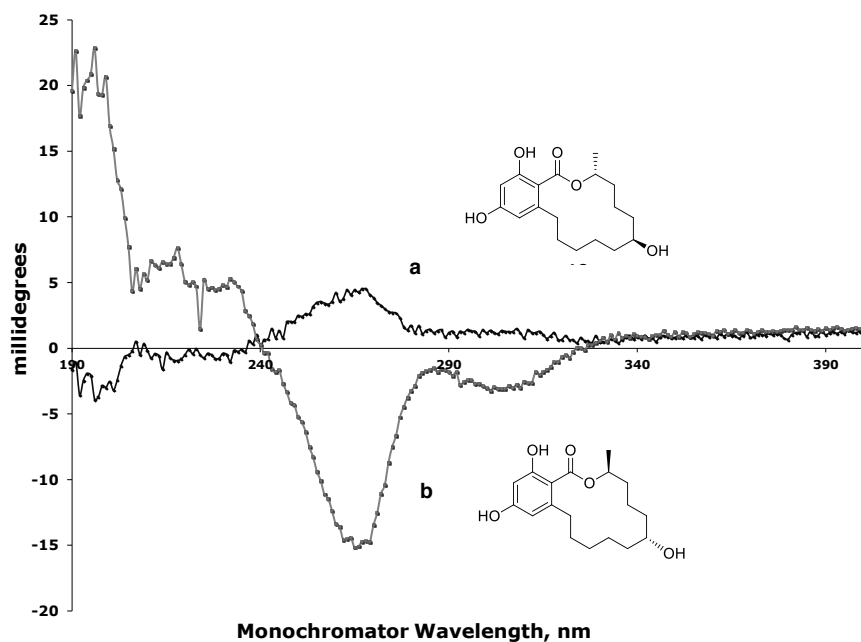
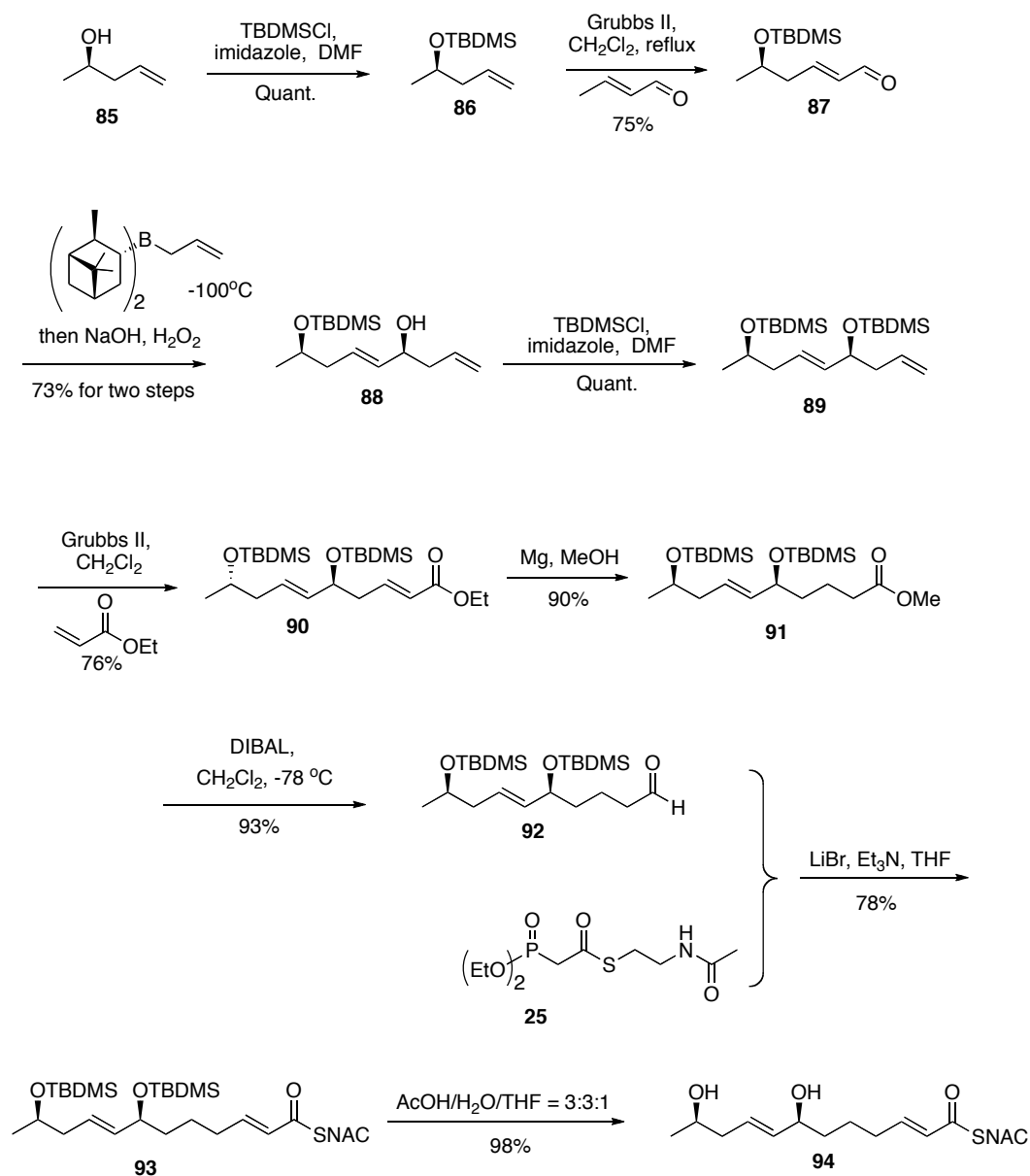


Figure 2-23 CD spectra of **83** (line a) and **84** (line b).

2.3.2.6.2 Probing epimerization activity of Hpm3

To further exclude the epimerization activity of Hpm3, an epimer of hexaketide **27**, compound **94**, was synthesized from (*R*)-pent-4-en-2-ol (**Scheme 2-12**), analogous to the synthesis of **27** (**Scheme 2-2**). As expected, *epi*-DHZ (**79**) is produced as a single product when **94** is incubated with Hpm3 and malonyl-CoA, indicating that Hpm3 does not show epimerization activity. Furthermore, the yield of *epi*-DHZ is comparable with that of DHZ when **27** is supplied to Hpm3, suggesting that Hpm3 does not discriminate against the D-configured hydroxyl group. The formation of **79** also suggests that Hpm3 TE displays a relaxed substrate specificity. In contrast, the DEBS TE domain involved in erythromycin biosynthesis is specific toward the stereochemistry of the terminal hydroxyl group. It only macrocyclizes a substrate with *R*-configured hydroxyl group, whereas it hydrolyzes substrates with terminal *S*-configured hydroxyl groups to the free acids.¹¹²



Scheme 2-11 Synthesis of **94**.

2.3.2.6.3 Rational for production of *epi*-DHZ by Hpm8B2, Hpm8B4 or

Hpm8B7

Although Hpm8B2, Hpm8B4, and Hpm8B7 reduce diketide **30** to mainly **30D** *in vitro*, together with Hpm3 they produce *epi*-DHZ and DHZ in comparable

levels *in vivo*. Hpm8 should be responsible for these strange *in vivo* results because Hpm3 does not show discrimination against the D-hydroxyl group when **94** is supplied. Thus, the similar yields of *epi*-DHZ and DHZ could be explained by the preference of the L-hydroxyl group diketide by Hpm8: although the L-configured diketide intermediate is formed much slower than the D-configured diketide, L-diketide has a much higher turn-over rate toward the hexaketide intermediate because its L-hydroxyl group is natural for the subsequent enzymatic assembly in Hpm8.

2.3.3 Conclusions

An unusual degree of programming of HRPKS Hpm8 was uncovered, in which a single ketoreductase domain shows substrate-dependent stereospecificity. Specificity was determined by synthesis of a series of β -keto SNAC thioesters (eight) and β -hydroxyl SNAC thioesters (sixteen), followed by assays with Hpm8 in the presence of NADPH. Hpm8 reduces diketide **30** to its L-configured β -hydroxyl SNAC thioester (**30L**). However, Hpm8 reduces all other synthesized ketides, including two triketides, three tetraketides, one pentaketide and one hexaketide to the D-configured hydroxyl SNAC thioesters. These results suggest that functional groups attached to the carbon chain do not affect the stereospecificity of Hpm8 KR, and that the chain length of polyketide intermediates solely dictates the stereospecificity of Hpm8 KR.

In addition, sequence swaps between Hpm8 KR and Rdc5 KR were performed. These chimeric enzymes were individually incubated with the diketide **30**. Hpm8B2, Hpm8B4, and Hpm8B7 displays altered stereoselectivity toward

diketide **30**. Co-expression of the chimeric enzymes, Hpm8B2, Hpm8B4 or Hpm8B7, with Hpm3 in BJ5464-NpgA also leads to production of **79**, an epimer of DHZ, together with a nearly equal amount of DHZ. The stereochemistry of **79** (6'*S*, 10'*R*) was confirmed by comparing the NMR, mass and CD spectra with α -zearelanol, after hydrogenation of two double bonds of **79**. Hpm8B7 only contains the $\alpha_4\beta_5\alpha_5\alpha_6$ region from Rdc5 and is able to alter the stereoselectivity of the KR domain, thus suggesting that $\alpha_4\beta_5\alpha_5\alpha_6$ is the minimal requirement for stereochemical control of the KR domain. However, Hpm8B8, containing only α_4 from Rdc5 KR, is unable to disturb the stereoselectivity of the KR domain, suggesting that α_4 is not essential for stereochemical control. On the other hand, α_4 , together with another region ($\beta_2\alpha_2\beta_3\alpha_3\beta_4$), may be involved in the stabilization of the $\beta_5\alpha_5\alpha_6$ motif because swapping only $\beta_5\alpha_5\alpha_6$ leads to the insoluble expression of Hpm8B6, while only $\alpha_4\beta_5\alpha_5\alpha_6$ -swapped Hpm8B7 possesses significant lower activity both *in vitro* and *in vivo* compared with Hpm8B2 and Hpm8B4.

Finally, the epimerization activity of Hpm3 was evaluated. Compound **94**, an epimer of natural intermediate **27**, was chemically synthesized and supplied to Hpm3 together with malonyl-CoA. HPLC analysis of the organic extract shows *epi*-DHZ (**79**) is produced and the yield of *epi*-DHZ (**79**) is comparable to that of DHZ when **27** is fed. This result suggests that Hpm3 does not have epimerization activity, and it does not show discrimination against the D-hydroxyl group. In contrast, Hpm8 may discriminate against the unnaturally D-configured hydroxyl group because Hpm8B2, Hpm8B4, Hpm8B7 produce about equal amounts of *epi*-

DHZ and DHZ together with Hpm3, although they all reduce diketide **30** to **30D** as a predominant product.

The detailed mechanism of this substrate-dependent stereospecificity of Hpm8 KR is still not clear. The β -keto group of the diketide intermediate may adopt a different conformation from all other ketides in the KR domain active site; therefore, a different stereochemistry is generated even though NADPH attacks the keto groups from the same direction. Crystal structures of Hpm8 KR would be desirable to further decipher the complex programming rules.

2.4 Investigation of HRPKS functions using partially assembled intermediates *

2.4.1 Introduction

Although great advancements have been achieved in the field of polyketide biosynthesis,^{49, 60, 113} the cryptic programming rules of HRPKS are still unresolved because they are enigmatically embedded in the amino acid sequences.²³ However, the veil of HRPKS has been slightly lifted by recent work in the Cox group.⁵¹ Their domain swap data suggested that the KR domain is involved in both chain length and C-methylation control, in addition to its native function, the iterative ketoreductions. Moreover, as discussed in the previous section, a new level of programming complexity of the Hpm8 KR domain has been uncovered. Our results suggest that the Hpm8 KR domain displays a substrate chain length-tuning stereospecificity during ketoreductions.⁵⁵

Nevertheless, a key requirement for these advancements is the structural determination of the intermediates involved in the polyketide biosynthesis. Various approaches have been developed to facilitate the determination of intermediates, such as using non-hydrolyzable CoA analogs to trap intermediates in conjugation with mass spectrometry for some modular bacterial PKS systems;¹¹⁴⁻¹¹⁸ and direct FT-ICR-MS for examining potential intermediates

* This is a collaborative project with the Tang group. I was responsible for synthesis and characterizations of intermediates and products, whereas our collaborators, Professor Yi Tang and co-workers, were in charge of protein expression and purification, as well as biological assay.

loaded on the PKS.^{30,31} These methods rely heavily on mass spectrometry to detect the intermediates, despite its intrinsic disadvantages such as being unable to determine the stereochemistry of intermediates and analysis of possible isomers. An alternative approach pioneered by Cane, Hutchinson, and co-workers employs *S*-*N*-acetylcysteamine (SNAC) thioesters of partially assembled precursors to probe the mechanism of modular bacterial PKS systems.^{84, 119-122} PKS domain inactivation or elimination of entire modules followed by addition of putative intermediate SNAC thioesters allowed production of natural polyketides or their analogs in a cell-free system.^{123, 124} However, it is challenging to apply this advanced precursor feeding approach to iterative PKS systems because domain inactivation abolishes production of polyketides, since iterative PKSs only consist of a single set of domains. In addition, this approach usually fails with whole or disrupted fungal cells due to catabolism of the precursors, except in some isolated cases.¹²⁵⁻¹³⁰ Therefore, new approaches are required to probe fungal PKS functions using partially assembled intermediates, which could aid deciphering the programming rules of these complex machineries.

During the biosynthesis of hypothemycin, an iterative HRPKS (Hpm8) cooperates with an iterative NRPKS (Hpm3) to synthesize the first PKS product, DHZ (**5**).^{39, 41} Hpm8 first assembles a reduced hexaketide intermediate, which is then transferred downstream to Hpm3 with the assistance of the SAT domain. Hpm3 extends the nascent hexaketide to a nonaketide, which undergoes regioselective cyclization and macrolactonization to afford DHZ. Although the general functions of the two PKSs have been investigated, it remains unclear how

Hpm8 controls the oxidation levels of the intermediates en route to the hexaketide intermediate using its processing domains (KR, DH and ER). To probe the programming rules of HRPKSs, confirmation of the structures of enzyme-bound intermediates and the way they interact with their enzyme would be desirable.

Therefore, we envisioned to incorporate partly assembled precursors into a HRPKS, such as Hpm8. The subsequent analysis of incorporation products would provide valuable information about the interactions between substrates and PKSs. On the basis of the generally accepted mechanisms for polyketide biosynthesis,¹ we proposed that fourteen ACP-tethered intermediates are en route to the hexaketide that is eventually transferred to Hpm3 for further elaborations (**Figure 2-24**). Among these fourteen compounds, four are classified as ready precursors because they have the correct functionality to proceed to the next round of chain elongation in the KS active site. The other ten putative intermediates are unready precursors because they must first undergo reductive modifications by KR, DH or ER prior to chain extensions.

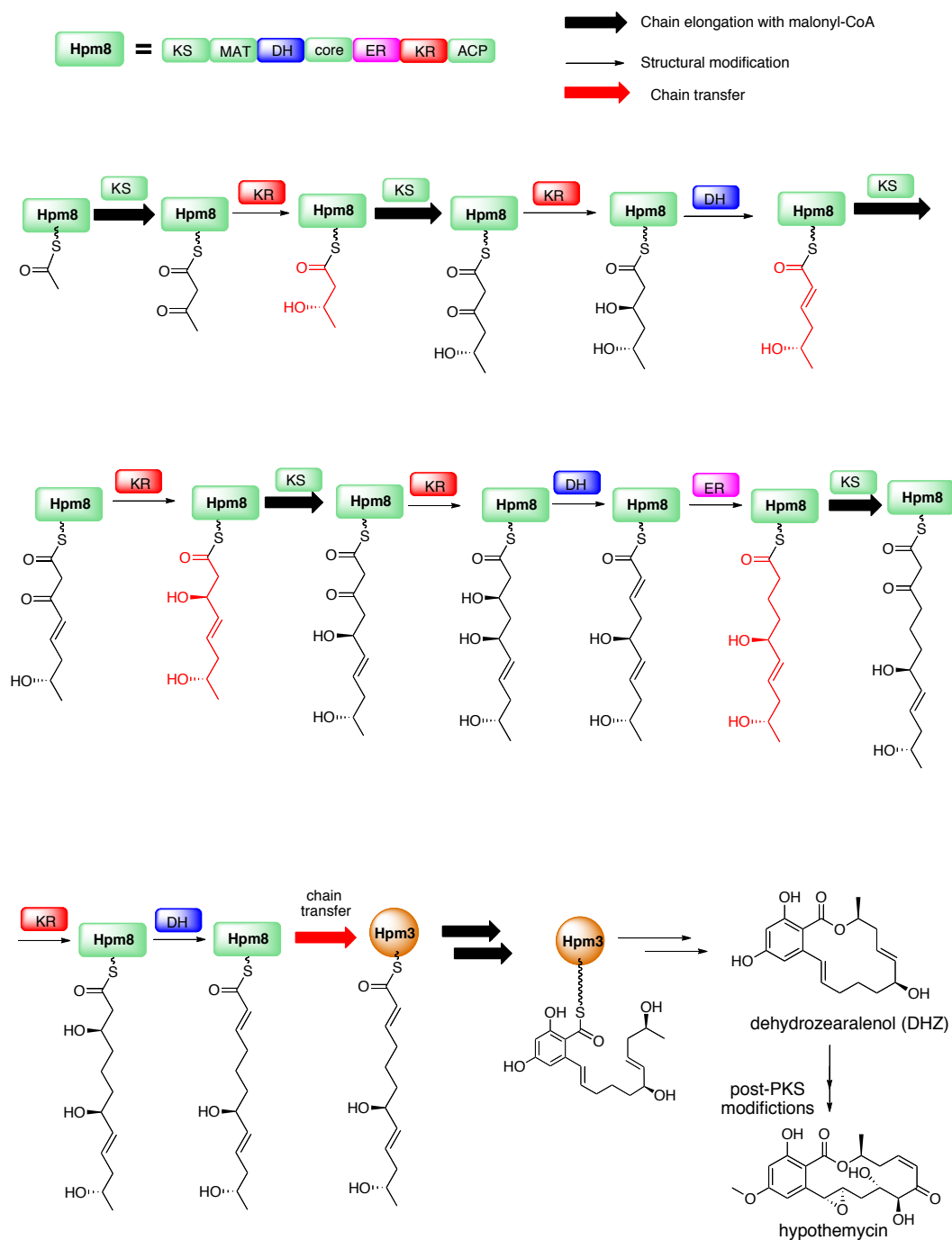


Figure 2-24 The fourteen intermediates en route to the hexaketide intermediate transferred to Hpm3 for production of DHZ. The four red structures are ready precursors, and the ten black structures between the acetyl unit and the hexaketide are unready precursors.

We planned to chemically synthesize all the postulated ready precursors (**96**, **99**, **101** and **103**) and several unready precursors (**95**, **98**, **100** and **102**) as ^{13}C -labeled SNAC thioesters (**Figure 2-25A**), and determine whether these compounds could prime onto Hpm8 to give the corresponding enzyme-bounded intermediates. If the enzyme bounded intermediates could be generated, Hpm8 should be able to further extend them to a ^{13}C -labeled hexaketide intermediate, which could be ultimately converted to ^{13}C -labeled DHZ by partnered Hpm3. We selected unready precursors **95**, **98**, **100** and **102** because they cover the scope of possible oxidation states at the β -positions. The D-configuration of the β -hydroxyl of unready precursor **98** is based on the stereospecificity of the Hpm8 KR domain during the triketide state.⁵⁵ However, unready precursor **98** has not been conclusively proven to be an intermediate during the triketide state, so an L-hydroxyl triketide (**97**) was also synthesized. To test the substrate specificity of Hpm8 and Hpm3, unnatural precursors **30D**, **104** and **105** were synthesized to assess if they could be transformed to DHZ analogs (*epi*-DHZ, β -zearalenol) (**Figure 2-25B**).

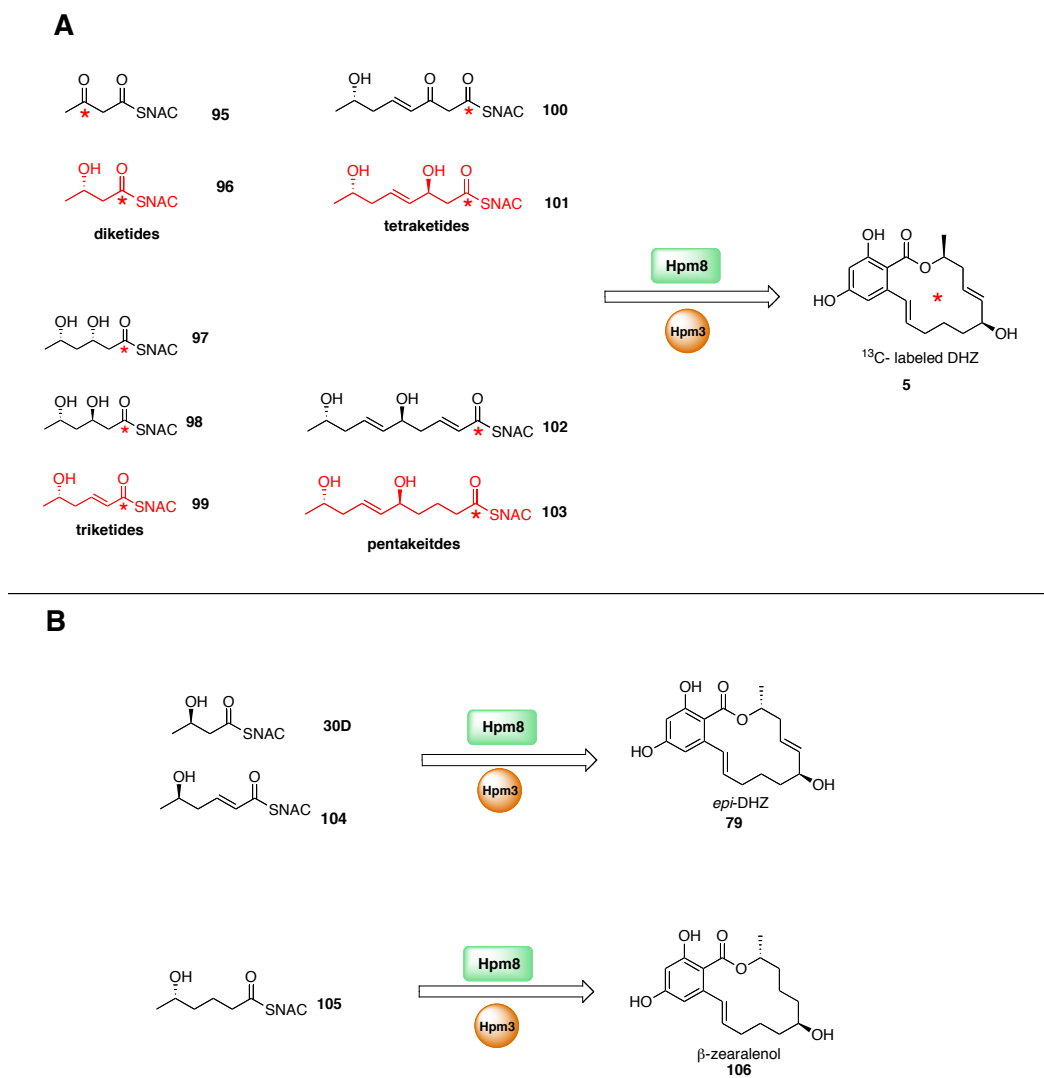


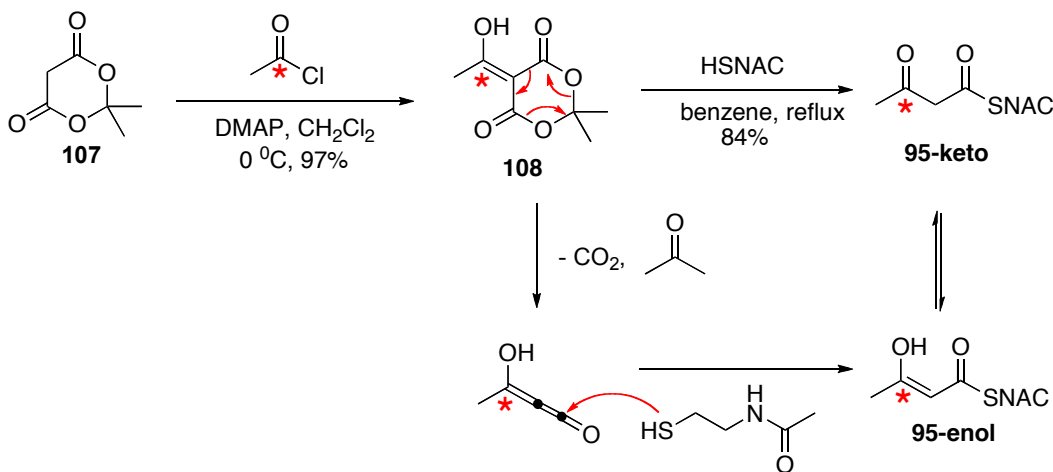
Figure 2-25 Feeding experiments involving advanced precursors or analogs. (A) incorporation of ¹³C labeled precursors; the red structures are ready precursors; and (B) incorporation of precursor analogs.

2.4.2 Results and discussion

2.4.2.1 Synthesis of SNAC thioesters

2.4.2.1.1 Synthesis of ^{13}C -labeled diketide **95**

The synthesis of **95** is shown in **Scheme 2-13**. Meldrum's acid (**107**) condensed with [$1\text{-}^{13}\text{C}$]acetyl chloride in the presence of DMAP to afford **108**. Compound **108** decomposed upon refluxing in benzene to a transient ketene intermediate, 131 which was rapidly scavenged by the nucleophilic *N*-acetylcysteamine (HSNAC) to furnish **95** as a mixture of keto and enol forms (4.5:1)

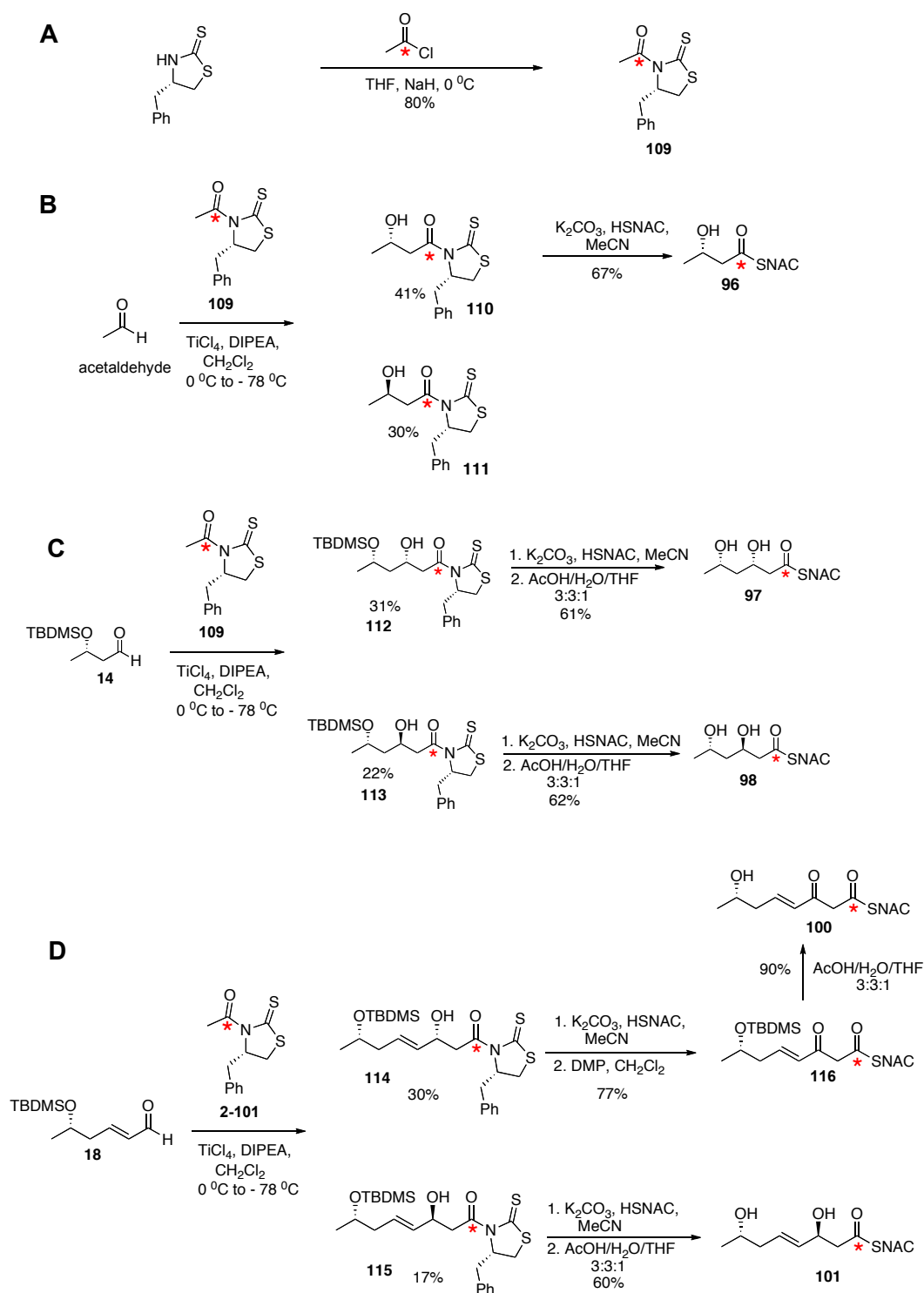


Scheme 2-12 Synthesis of ^{13}C -labeled diketide **95**.

2.4.2.1.2 Synthesis of ^{13}C -labeled diketide **96**, triketides **97** and **98**, and tetraketides **100** and **101**

These syntheses employed aldol reactions with [$1\text{-}^{13}\text{C}$]acetylated Crimmins' auxiliary **109** (**Scheme 2-14**). Acetaldehyde, **144** and **18** were

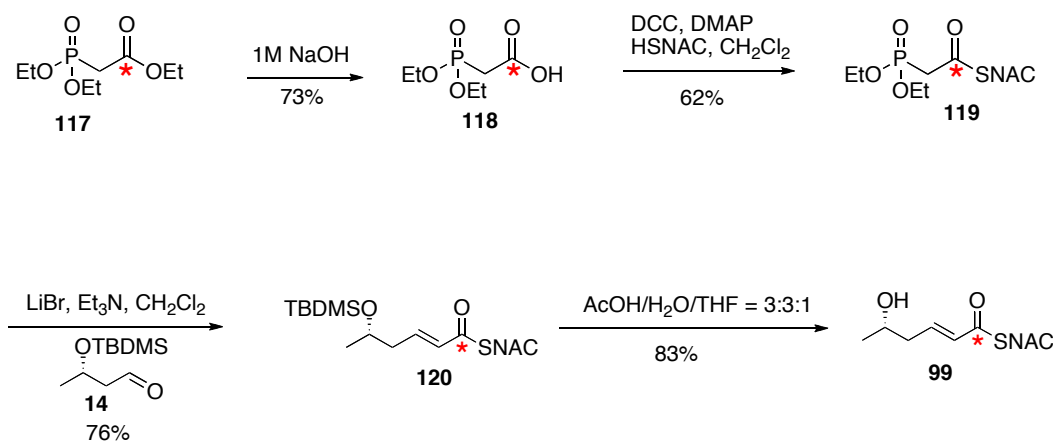
individually transformed to a pair of diastereomers (**110** & **111**, **112** & **113** and **114** & **115**, respectively) via aldol reactions. Displacement of Crimmins' auxiliary with HSNAC in the presence of K_2CO_3 generated **96**, **97**, **98** and **101** from **110**, **112**, **113** and **115**, respectively. The β -keto tetraketide **100** was synthesized from **114** by first displacing the auxiliary with HSNAC, followed by oxidation of the β -hydroxyl with DMP, and deprotection of the TBDMS group with AcOH/H₂O/THF.



Scheme 2-13 Synthesis of (A) **109**, (B) diketide **96**, (C) triketides **97** and **98**, and (D) tetraketides **100** and **101**.

2.4.2.1.3 Synthesis of ^{13}C -labeled triketide **99**

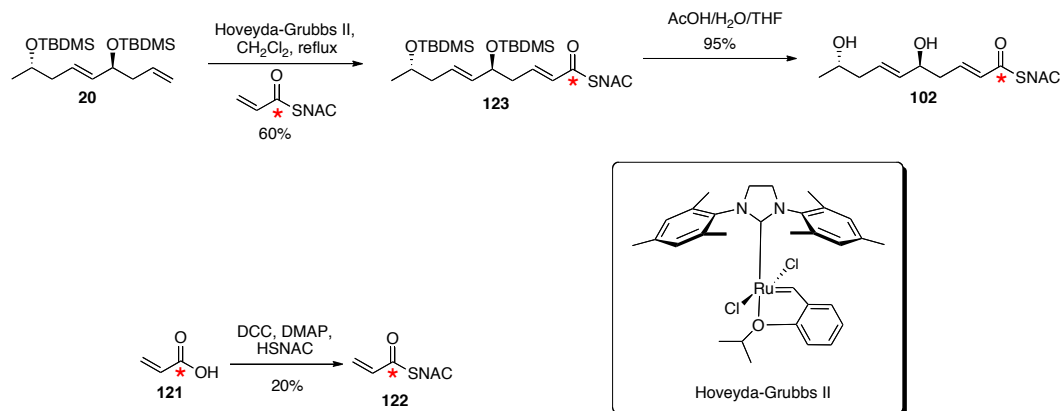
The synthesis of **99** is shown in **Scheme 2-15**. Commercially available ^{13}C -labeled **117** was hydrolyzed with 1 M NaOH to afford free acid **118**, which was condensed with HSNAC in the presence of DCC and DMAP to yield **119**. Compound **119** underwent a HEW reaction under Masamune-Roush conditions (LiBr , Et_3N)⁸⁵ with **14** to provide **120**, and then the TBDMS group was removed to furnish the desired triketide **99**.



Scheme 2-14 Synthesis of ^{13}C -labeled triketide **99**.

2.4.2.1.4 Synthesis of ^{13}C -labeled pentaketide **102**

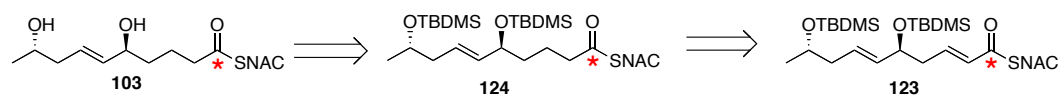
The synthesis of **102** is shown in **Scheme 2-16**. Compound **20** underwent regioselective cross-metathesis with ^{13}C -labeled **122** to afford **123**, which was subsequently converted to the desired pentaketide **102** by removal of the TBDMS groups. ^{13}C -Labeled **122** was prepared from a coupling reaction between [1- ^{13}C]acrylic acid (**121**) and HSNAC in the presence of DCC and DMAP.



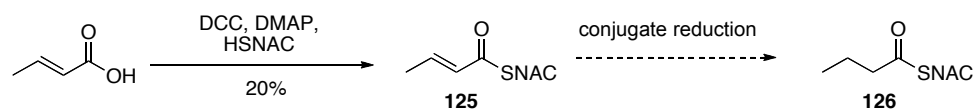
Scheme 2-15 Synthesis of ^{13}C -labeled pentaketide **102**.

2.4.2.1.5 Synthesis of ^{13}C -labeled pentaketide **103**

Pentaketide **103** was envisioned to be synthesized from **123** by a regioselective reduction of the conjugated double bond (**Scheme 2-17**). However, there was no reported methodology for this transformation during the course of this study. So we decided to investigate the reduction of conjugated SNAC thioesters using **125** as a model system (**Scheme 2-18**). Compound **125** was synthesized from HSNAC and (*E*)-but-2-enoic acid by a coupling reaction using DCC and DMAP.



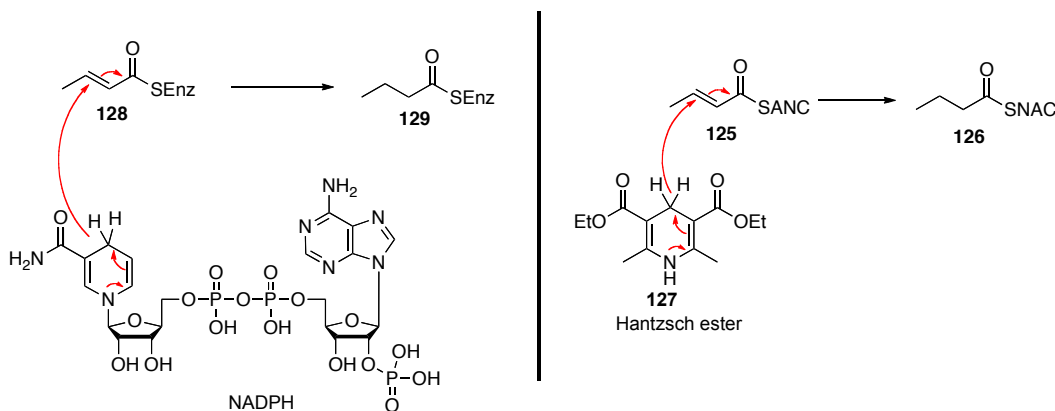
Scheme 2-16 Retrosynthesis of pentaketide **103**.



Scheme 2-17 Synthesis of **125**.

2.4.2.1.5.1 Conjugate reduction of **125** with Hantzsch esters

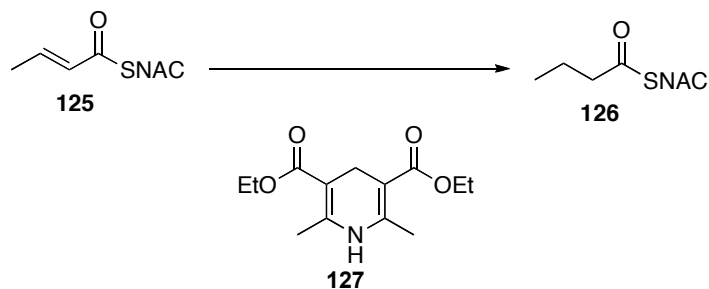
Because nature uses NADPH to reduce the conjugated double bond of thioesters, it was envisioned that Hantzsch ester (**127**), an NADPH mimic, could possibly reduce a double bond in a similar fashion (**Scheme 2-19**). In addition, **127** has been used as a hydride source for reducing imine derivatives,¹³² conjugated ketones and aldehydes.¹³³



Scheme 2-18 Conjugate reduction by NADPH and Hantzsch ester.

The direct reduction of **125** in the presence of **127** by refluxing in toluene was not successful. Additions of Lewis acids to coordinate with the carbonyl group improved the transformation, as shown in **Table 2-3**. The best conversation (determined by NMR analysis of the reaction mixtures) from **125** to **126** was achieved using silica gel (SiO_2) as a Lewis acid. This condition has been shown to promote the conjugate reduction of α,β -unsaturated ketones and aldehydes with **127**.¹³³ However, the transformation is not promising since only 77% of **125** is converted to **126** in the presence of SiO_2 after refluxing in toluene for 24 h, and **125** and **126** cannot be readily separated by flash chromatography.

Table 2-3 Conditions employed for conjugate reduction of **125** to **126** with Hantzsch ester.



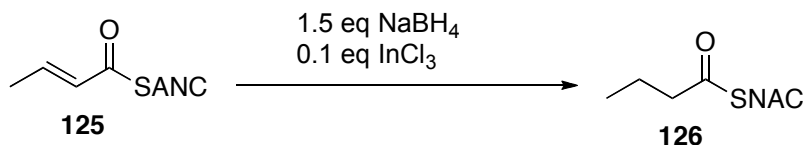
Additives (Solvent, temperature, time)	Conversion
None (PhMe, reflux, 24 h)	0
TiCl ₄ (THF, 23 °C, 24 h)	0
MgBr ₂ ·EtO ₂ (CH ₃ Cl, 23 °C, 48 h)	20%
MgBr ₂ ·EtO ₂ (CH ₃ Cl ₃ , reflux, 72 h)	50%
MgBr ₂ ·EtO ₂ (PhMe, reflux, 24 h)	56%
SiO ₂ (PhMe, 80 °C, 24 h)	30%
SiO ₂ (PhMe, 120 °C, 24 h)	77%
ZnO (PhMe, 120 °C, 24 h)	0%
AcOH (PhMe, 120 °C, 3 h)	0%
AlCl ₃ (PhMe, 120 °C, 1 h)	23%

2.4.2.1.5.2 Conjugated reduction of **125** with NaBH₄ and InCl₃

Ranu *et al.* reported that NaBH₄ and a catalytic amount of InCl₃ could selectively reduce the α,β -double bond of $\alpha,\beta,\gamma,\delta$ -unsaturated diaryl ketones, dicarboxylic esters, cyanoesters and dicyano compounds.¹³⁴ When α,β -unsaturated SNAC thioester **125** is treated with NaBH₄-InCl₃ in CH₃CN for 12 h,

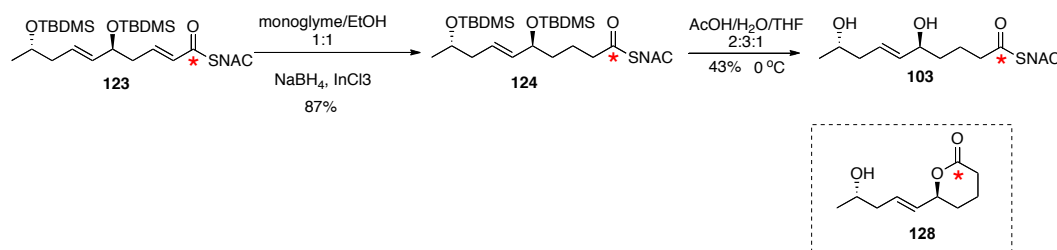
product **126** is formed in 30% conversion (determined by NMR). Changing the solvent to DMF improves overall conversion to 100% after 12 h. However, the reaction is not clean, and the product peaks are weak in the NMR spectrum. The conversion drops to 60% when the reaction is done in diglyme for 12 h. The reduction of **125** was then performed in a mixture of diglyme/EtOH. After 12 h, the NMR spectrum of the reaction mixture shows that **125** is completely consumed. The reaction is clean with only several solvent peaks present in the NMR spectrum in addition to that of **125**. However, diglyme is hard to remove due to its high boiling point. So the diglyme was substituted with monoglyme. After 1.5 h, the reduction of **125** with NaBH₄-InCl₃ in a 1:1 (V/V) mixture of monoglyme and EtOH is finished. The NMR analysis of the reaction mixture suggests that it consists predominantly of the desired product **126**.

Table 2-4 Conditions employed for conjugated reduction of **125** to **126** with NaBH₄-InCl₃.



Conditions (temperature, time)	Conversion
CH ₃ CN (23 °C, 12 h)	30%
DMF (23 °C, 12 h)	100%
Diglyme (23 °C, 12 h)	60%
Diglyme/EtOH (1:1) (23 °C, 12 h)	100%
Monoglyme/EtOH (1:1) (23 °C, 1 h)	100%

After the successful reduction of module substrate **125**, the NaBH₄-InCl₃ promoted conjugate reduction was tried on **123**. Compound **123** is selectively reduced to **124** in 3 h with 87% isolated yield without the need to purify via flash chromatography. However, it should be noted that the prolonged reaction time is detrimental to the product. Increasing the reaction time to 12 h, the NMR analysis of the crude reaction mixture suggests that side products start to arise (not isolated). Deprotection of the TBDMS group of **124** was not straightforward because of its high tendency to form a six-membered side product **128** (not isolated, **Scheme 2-20**). The deprotection of **124** was done under a milder condition, AcOH/H₂O/THF (2:3:1) at 0 °C, to furnish the desired product **103**.

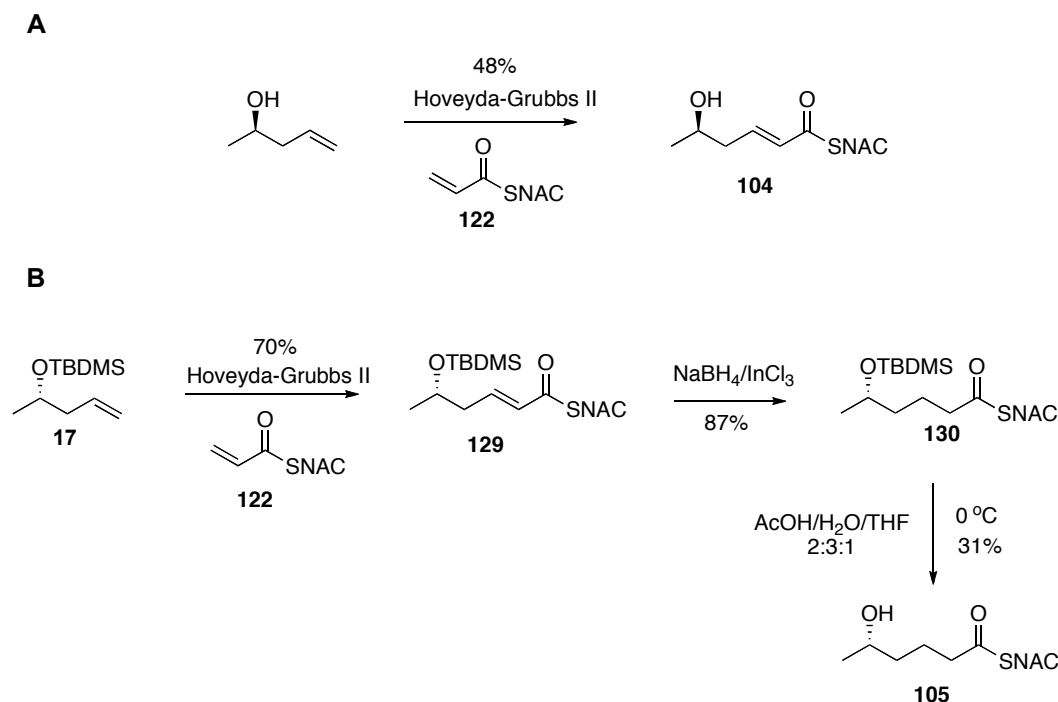


Scheme 2-19 Synthesis of ¹³C-labeled pentaketide **103**.

2.4.2.1.6 Synthesis of unnatural triketides **104** and **105**

Triketide **104** was synthesized by cross metathesis between **122** (unlabeled) and (*R*)-pent-4-en-2-ol using Hoveyda-Grubbs II catalyst (**Scheme 2-21A**). The synthesis of **105** is shown in **Scheme 2-21B**. Alkene **17** reacted with **122** in the presence of Hoveyda-Grubbs II catalyst to furnish **129**, the double bond of which was then reduced by NaBH₄-InCl₃ to afford **130**. Similar to the synthesis

of **103**, a mild condition (2:3:1 AcOH/H₂O/THF, 0 °C) was used to remove the TBDMS group of **130** to yield **105**.



Scheme 2-20 Synthesis of unnatural precursors (A) **104** and (B) **105**.

2.4.2.2 Incorporation of ¹³C-labeled partially assembled precursors

Without domain inactivation, incorporation of ¹³C-labeled substrates into iterative PKSs is difficult, because iterative PKSs can self-prime unlabeled malonyl-CoA to form a large amount of background unlabeled PKS products. This hampers the detection of ¹³C-labeled PKS products. To minimize the amount of unlabeled DHZ that could be formed by initial self-loading of unlabeled malonyl-CoA, the incorporation of a ¹³C-labeled precursor was done using a pre-loading assay (**Figure 2-26**) consisting of (1) incubation of Hpm8 (10 μM) with a

large excess of labeled substrate (e.g., **99**) (0.2 mM) for 15 min. This allows the labeled substrate to preload to Hpm8; (2) addition of 10 μ M Hpm3, 4 mM NADPH, and 0.4 mM malonyl-CoA, incubated for 1 h; and (3) subsequent addition of 0.4 mM malonyl-CoA at 1 h intervals (nine times) and addition of 0.2 mM labeled substrate every 2 h. Then the reaction was quenched with EtOAc with 1% AcOH, and the organic extract is analyzed by LC-MS.

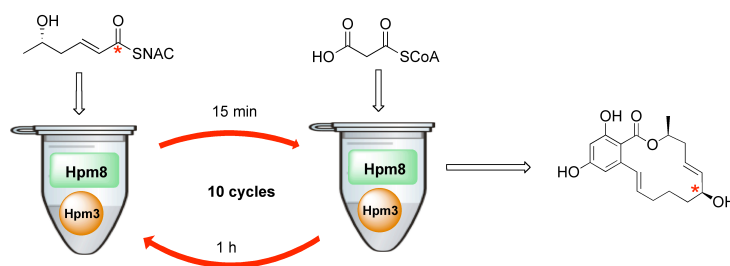


Figure 2-26 Incorporation of ^{13}C -labeled precursors in a pre-loading assay.

2.4.2.2.1 Incorporation of triketide **99**

The first substrate tested is ready triketide **99**, which is labeled with ^{13}C at the carbonyl position proposed to become C6' in DHZ. Analysis of the organic extract of the **99** incorporation assay suggests that a new compound is generated with identical LC and UV profiles to DHZ (**Figure 2-27**). This compound displays a major peak in the mass spectrum at m/z 318 ($[\text{M}-\text{H}]^-$) (**Figure 2-27**), implying that it consists predominantly of a singly ^{13}C -labeled DHZ. The incorporation ratio is calculated to be 78% on the basis of this mass spectrum.

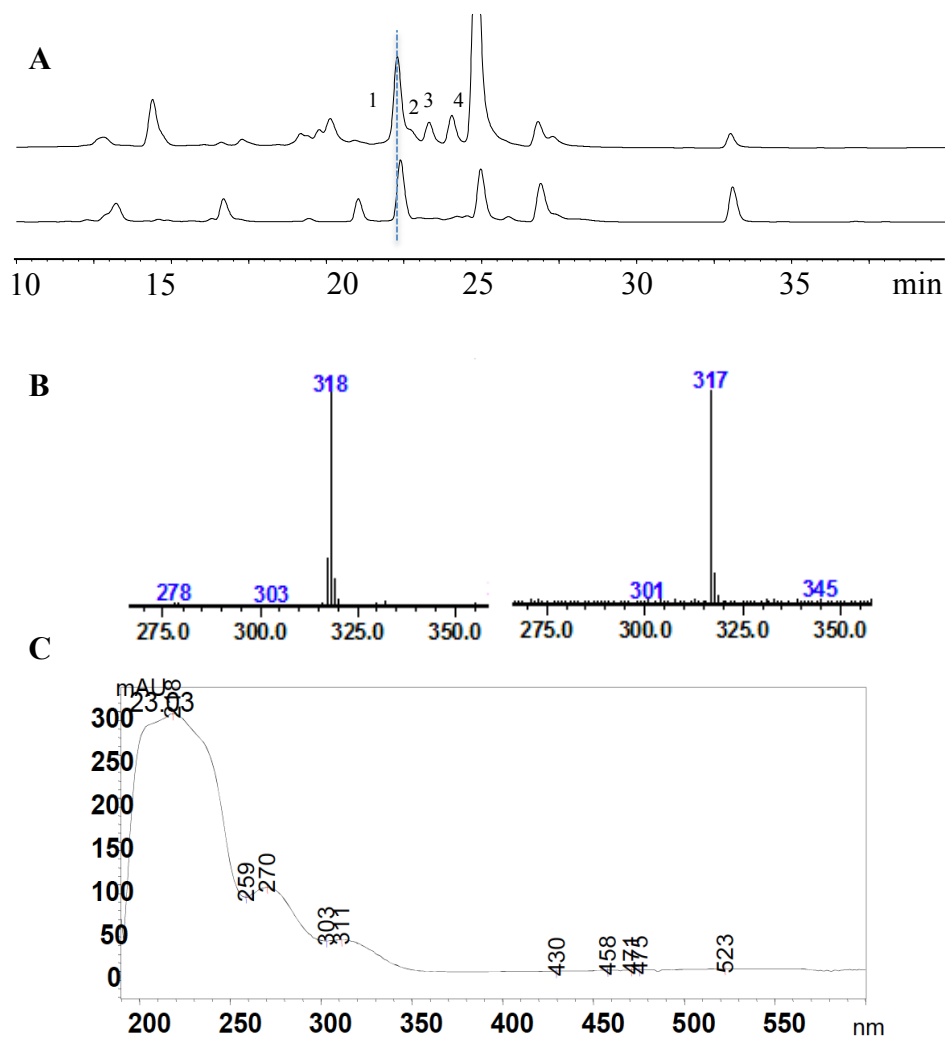


Figure 2-27 LC-MS of the triketide **99** assay. (A) LC trace of triketide **99** assay (top); LC trace of control assay without substrate addition (bottom); (B) MS spectrum of peak 1 of triketide **99** assay (left); MS spectrum of peak 1 of control assay (right); (B) UV spectrum of peak 1 from triketide **99**.

In addition to DHZ, three new compounds are also observed in the triketide assay by LC-MS, with mass peaks at 316, 435 and 437 m/z (peaks 2, 3, and 4, respectively, in **Figure 2-27A**). The structures are predicted to be ^{13}C -labeled compounds as shown in **Figure 2-28** because they display altered isotopic patterns in the mass spectra while showing typical UV spectra for a resorcyate core.

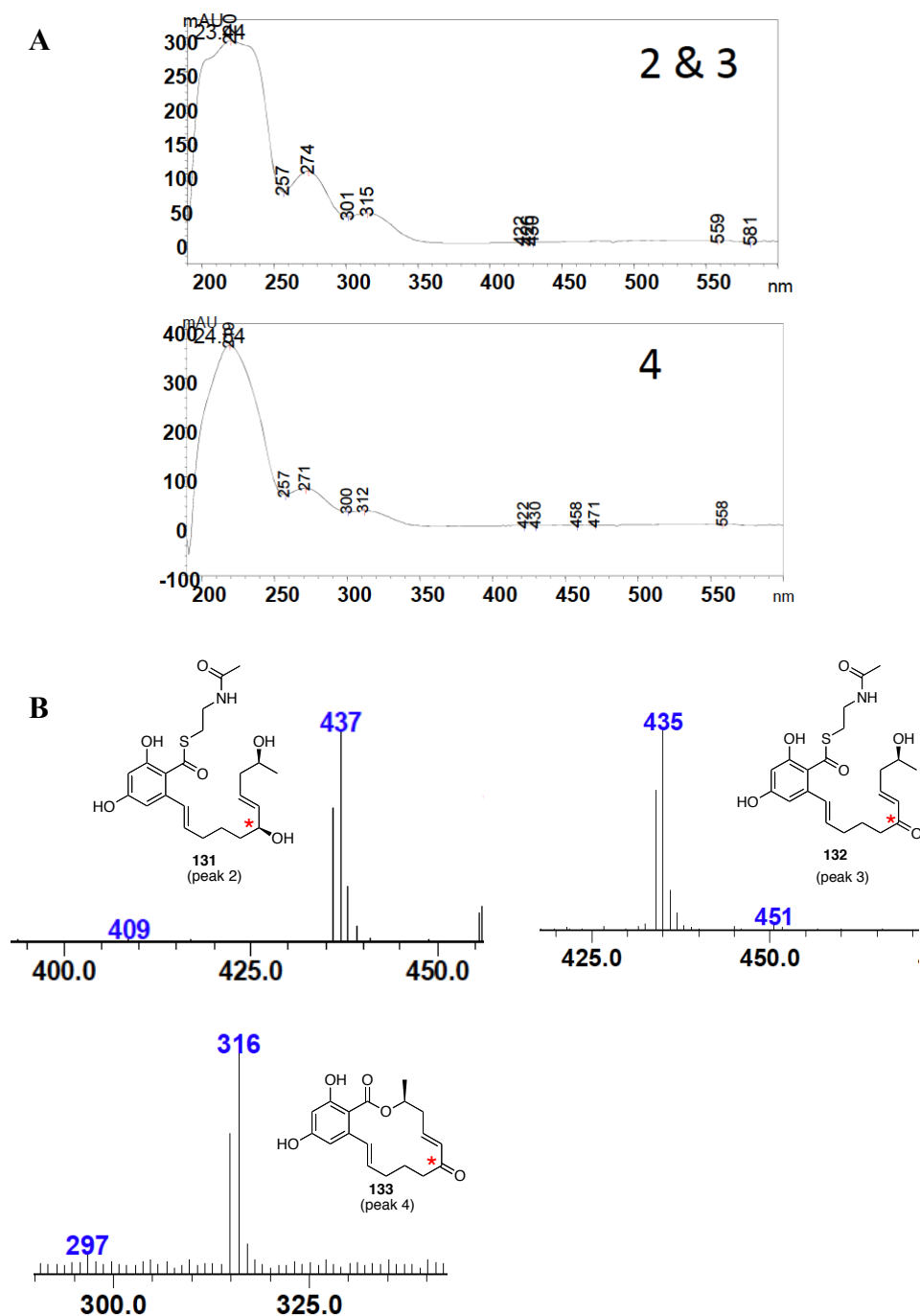
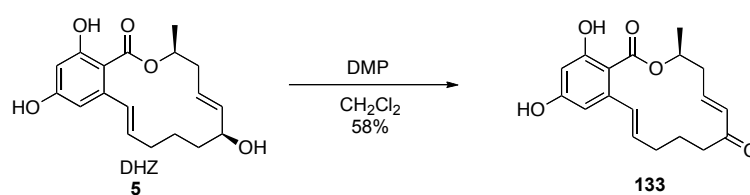


Figure 2-28 UV and MS spectra of **131**, **132** and **133**. (A) UV spectra of **131** and **132** (top); UV spectra of **133** (bottom). (B) MS spectra of **131**, **132** and **133** and their proposed structures.

The compound from peak 4 was identified as **133**, by compared to a synthetic standard, formed by oxidation of DHZ with DMP (**Scheme 2-22**).

However, compounds **131** and **132** were not conclusively identified. The formation of **133** suggests that a tetraketide, formed by one round extension of ^{13}C -labeled triketide **99**, skips the ketoreduction step, and directly proceeds to the next round of chain elongation. Compound **133** is not produced in the control experiment (no labeled substrate addition), suggesting that an exogenous substrate might be able to slightly alter the programming of Hpm8.



Scheme 2-21 Synthesis of **133** from DHZ.

Although the identity of ^{13}C -labeled DHZ was confirmed by LC-MS, the location of the ^{13}C enrichment was not firmly established. Therefore the *in vitro* pre-loading assay containing Hpm8, Hpm3, NADPH, malonyl-CoA and substrate **99** was repeated many times to eventually afford approximately 20 μg of ^{13}C -labeled DHZ (based on UV absorbance), after intensive HPLC purifications. The ^{13}C spectrum displays only a single resonance at 72.8 ppm, corresponding to the C6' position of DHZ (**Figure 2-29**). This demonstrates that C6' of DHZ is indeed ^{13}C -enriched, consistent with its origin from the ^{13}C -labeled carbonyl group of **99**. These data illustrate that **99** can prime on Hpm8, possibly on the KS domain by transthioesterification,¹³⁵ and hijack the biosynthetic pathway of DHZ to produce a ^{13}C -labeled counterpart. To the best of our knowledge, this represents the first

example of incorporation of a labeled advanced intermediate by a purified iterative HRPKS.

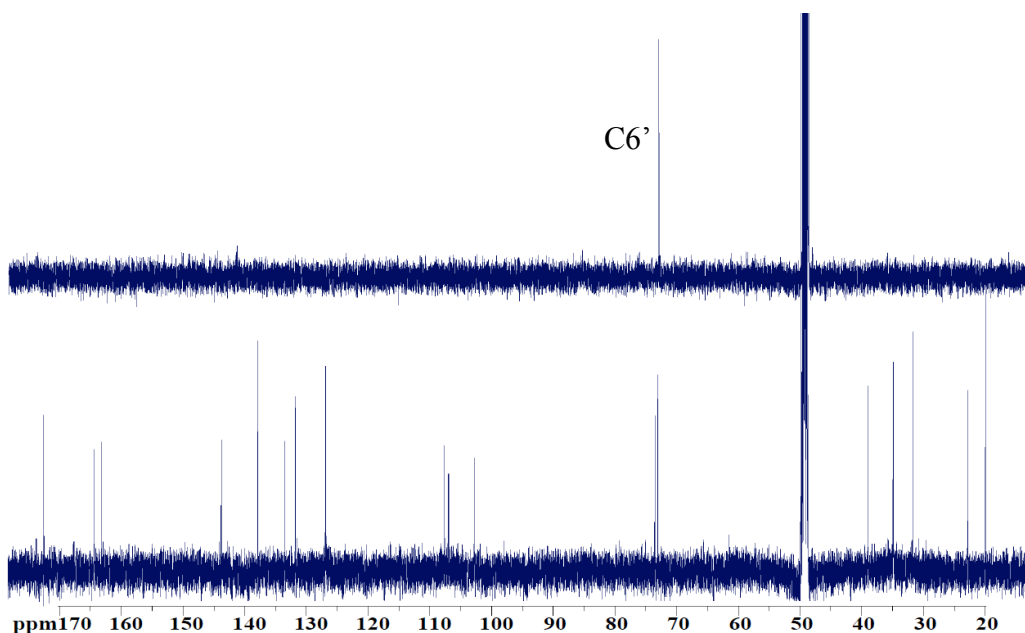


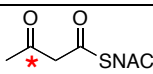
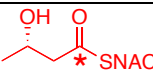
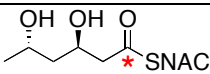
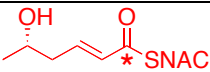
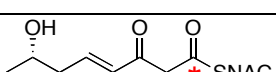
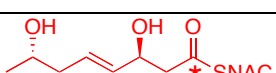
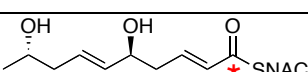
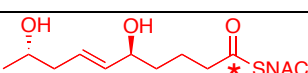
Figure 2-29 ^{13}C NMR spectrum of ^{13}C -labeled DHZ (upper) and DHZ standard (bottom).

2.4.2.2.2 Incorporation of other ^{13}C -labeled ketide intermediates

The incorporation of other putative intermediates is shown in **Table 2-5**: diketides **95** & **96**, triketide **98**, tetraketides **100** & **101**, and pentaketides **102** & **103**. Ready precursors **96**, **101** and **103** are incorporated efficiently, with ^{13}C enrichments of 37, 27, and 39%, respectively, based on the mass spectra. The relative yield of the resorcylic acid lactone (RAL), determined by comparison with the control assays where no precursor is added, ranges from 1.0 to 2.6 based on UV absorbance. Interestingly, the more advanced the precursor, the more DHZ is produced. This could be because the advanced precursors require fewer additional elaborations from Hpm8. Thus the hexaketide is generated faster,

which leads to higher total RAL yield. Alternatively, more advanced precursors might also prime faster onto the cysteine thiol of the KS domain, thus resulting in a higher turn-over rate.

Table 2-5 Incorporation of partially assembled precursors.

Compound number	¹³ C-labeled Precursors ^{a,b}	¹³ C Enrichment	Relative RAL yield
	None	None	1.0
95		41%	0.4
96		37%	1.0
98		15%	0.6
99		78%	1.0
100		19%	0.4
101		27%	2.0
102		8%	0.9
103		39%	2.6

^a * indicates the location of the ¹³C label. ^b structures of ready precursor are shown in red.

In contrast, with the exception of diketide **95**, conversions of unready precursors **95**, **98**, **100** and **102** yield relatively low ¹³C enrichments of DHZ (41, 15, 19, and 8%, respectively) and poor relative RAL production (0.4, 0.6, 0.4 and

0.9, respectively). For example, unready precursors **98** and **102** are incorporated about 5-fold less than their corresponding ready counterparts **99** and **103**. Therefore, the Hpm8 machinery clearly prefers precursor analogs that are structurally comparable to the correctly tailored intermediates ready for the next round of chain extension. The differences between the incorporation efficiencies obtained in the ready and unready precursor feeding experiments provide insights into the mechanism of the Hpm8 enzymes. Carbon chains of the ready precursors are correctly functionalized, so they can easily prime on the KS domain, and serve as the starting material for the next round of chain elongation. For incorporation of the unready precursors, several alternative mechanisms could be considered. One possibility is that the unready precursors load directly on the ACP domain by transthioesterification and are then further converted into the ready forms in the active sites of KR, DH and ER, in a normal fashion. However, the ACP Ppant thiol is normally already loaded with malonyl-CoA by the MAT domain. Competition for the vacant ACP Ppant thiol is likely to be very inefficient. An alternative path would involve loading the unready precursors on the active site thiol of the KS domain with subsequent transthioesterification to the ACP domain, followed by modification into the ready precursors. This KS to ACP transfer of incompletely tailored fragments does not occur naturally, so this process may occur slowly, if at all. The most likely pathway is direct action of the processing domains (KR, DH, or ER) on the unready SNAC thioesters, generating the correct functionalized ready precursors for the next round chain elongation. As discussed in the previous section, unready SNAC thioesters such as **95** and

100 can be effectively reduced to ready precursors **96** and **101**, respectively, by Hpm8 in the presence of NADPH. The KR domain can recognize the SNAC moiety, which mimics the P_{pant} arm attached to the ACP domain, and this recognition can direct the acyl chain to the active site of the KR domain for ketoreduction. This analogous concept may apply to the direct transformation of **98** to **99** by the DH domain or of **102** to **103** by the ER domain; The DH domain has been shown to be inefficient at utilizing SNAC precursors,¹³⁶ which may account for the significantly lower incorporation of **98**.

The differences in the ¹³C enrichments and relative RAL yields may also disclose the interactions between substrates and Hpm8. As discussed above, ready precursors, such as **96**, can easily prime on the KS domain because KS treats it as a starting material (**Figure 2-30A**). The KS domain may be programmed to have special motifs to recognize these ready precursors. On the other hand, KS “sees” **95** and **100** as its Claisen condensation products (**Figure 2-30B**). The KS domain may also be able to expel the products out of its catalytic cavity. However, in this pre-loading assay, a large excess of precursor, for example **95**, is added. Therefore **95** might be able to interfere with the KS native activities, which includes the formation of a **95**-like intermediate. With the KS activity disturbed, less DHZ is formed. As discussed before, **95** could also be directed to the active site of KR for ketoreduction to afford the ready precursor **96**. Nascent ¹³C-labeled **96** could easily prime on the KS domain to initiate the biosynthesis of ¹³C-labeled DHZ. Because production of ¹³C-DHZ bypasses the inhibited β-keto diketide stage, the ¹³C-enrichment is raised despite the fact that the absolute yield of ¹³C-labeled

DHZ ($41\% \times 0.4 = 0.16$) is dropped dramatically compared to that of the ready precursor **96** assay ($37\% \times 1.0 = 0.37$). Finally, for unready precursors **98** and **102**, the KS domain may not encounter them in its active site before they are correctly modified (**Figure 2-29C**). Therefore, high concentrations of **98** and **102** may not hinder KS activities as dramatically as **95** and **100**.

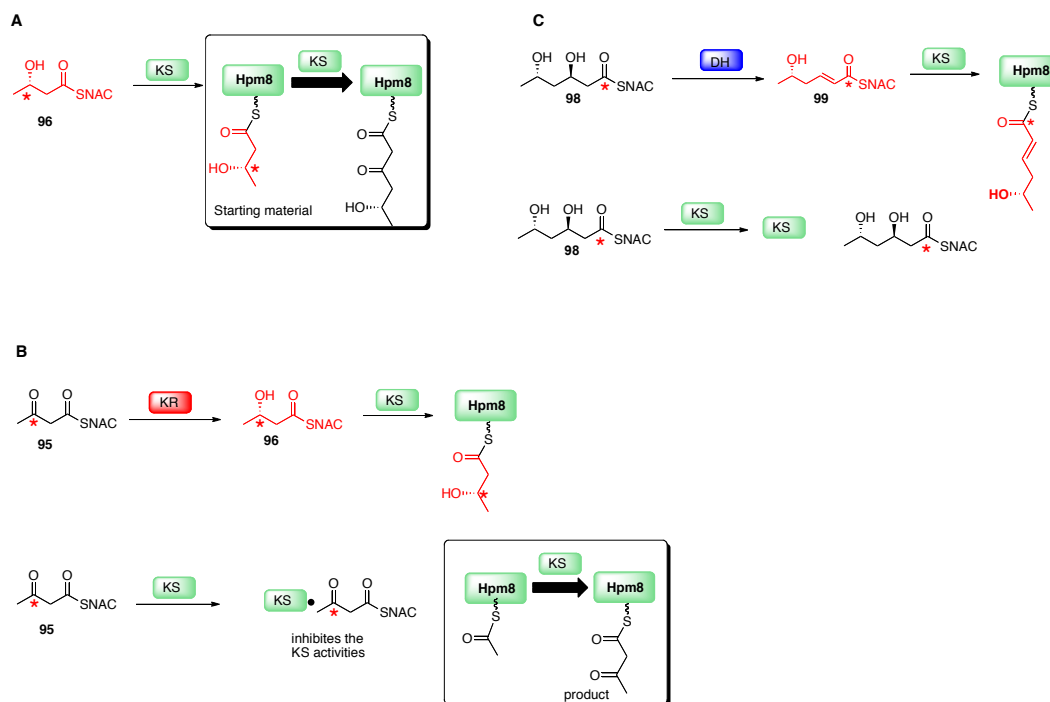


Figure 2-30 Three type of interactions between substrates and Hpm8. (A) ready precursor; (B) β -keto unready precursor; and (C) other unready precursor.

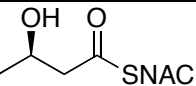
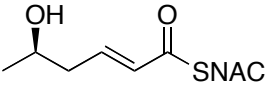
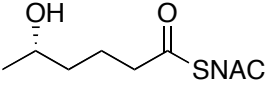
2.4.2.3 Incorporation of unnatural precursors **97**, **30D**, **104**, and **105**

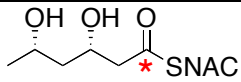
Incorporation of ^{13}C -labeled **97** is not successful, which is expected because its diastereomer **98** with a D-hydroxyl group is predicted to be an intermediate during the triketide stage based on Hpm8 KR stereospecificity.⁵⁵ This indicates that the L-hydroxyl group is not a good substrate for the DH active site, which is consistent with results for other PKS and FAS systems.¹³⁷ More

importantly, this result suggests incorporation of ^{13}C -labeled precursors is a valid approach to determine the true intermediates with correct stereochemistry involved in the fungal polyketide biosynthesis.

Compounds **30D** and **104** are successfully incorporated by Hpm8 and Hpm3 to afford an epimer of DHZ (**79**). The incorporation efficiency is lower, which is consistent with the observation in the previous section that Hpm8 shows discrimination toward the D-hydroxyl group.⁵⁵ Compound **105**, which represents an over-reduced precursor, is similarly incorporated by this system to generate β -zearalenol. The absolute yield of β -zearalenol ($30\% \times 2.0 = 0.60$) from triketide **105** is higher than that of *epi*-DHZ ($25\% \times 1.5 = 0.37$) from triketide **104**, but slightly lower than that of ^{13}C -labeled DHZ ($78\% \times 1.0 = 0.78$) from natural triketide **99**. This suggests that Hpm8 could effectively distinguish the change of the hydrophilic group, but could not easily detect the alteration of a double bond to a single bond.

Table 2-6 Incorporation of partially assembled precursors analogs.

Compound Number	Unnatural Analog	DHZ Analog Production ^a	Relative RAL yield ^b
	None	None	1.0
30D		24%	1.3
104		25%	1.5
105		30%	2.0

97		0%	0.4
-----------	---	----	-----

^a Production is the amount of DHZ analogue formed, expressed as a percentage of the total RAL production. ^b The relative RAL yields include DHZ and DHZ analogs.

2.4.3 Conclusions

In this section, we developed an assay for probing the functions of iterative PKSs using ¹³C-labeled partially assembled precursors. Eight ¹³C-labeled precursors were chemically synthesized and incorporated into DHZ using purified Hpm8 and Hpm3. To confirm the location of the predicted ¹³C label in DHZ, about 20 µg ¹³C-labeled DHZ was isolated from the triketide **99** assay. ¹³C NMR analysis of ¹³C-labeled DHZ shows a single resonance corresponding to the C6' of DHZ, which firmly establishes the ¹³C label in DHZ, and also validates this approach as a method to determine putative intermediates in fungal polyketide biosynthesis.

The ready precursors are easily recognized and taken up by Hpm8 to produce ¹³C labeled DHZ with relatively high ¹³C-enrichments and RAL yields. In contrast, the unready precursors give relatively low enrichments and yields. These results indicate that these substrates interact with megasynthases differently. The ready precursors, which are the starting materials for KS, straightforwardly prime on the KS domain to initiate the biosynthesis of DHZ. However, the unready precursors possibly have to be reduced first to ready precursors prior being taken by the KS domain. Unready precursors **95** and **100** have to be reduced by KR, whereas unready precursors **98** and **102** have to be tailored by DH and ER, respectively. Unready precursors **95** and **100** closely

resemble the β -keto products formed in the KS domain, thus inhibiting DHZ biosynthesis. Unready precursors **98** and **102** show significantly lower incorporation ratios, indicating that the DH and ER domains may not effectively reduce SNAC-tethered thioesters.

In addition, the unnatural precursors (**30D**, **97**, **104** and **105**) were also tested to probe the substrate tolerance of Hpm8. Scrambling the stereochemistry of the distal hydroxyl group of putative diketides and triketides results in a lower yield of DHZ analogs, while elimination of the double bond of a triketide does not dramatically reduce a DHZ analog production. Incorrectly configured hydroxyl groups at the β -position are detrimental to DHZ production, suggesting that Hpm8 DH is highly specific toward the L-hydroxyl precursors during the *syn* elimination to generate an *E*-double bond. In summary, our findings not only further support the processive nature of polyketide biosynthesis but also provide a basis for precursor-directed biosynthesis to generate novel polyketides with improved biological profiles.

Chapter 3: Biosynthetic Studies of Radicol*

3.1 Introduction of radicol

Radicol (**134**, **Figure 3-1**) belongs to a family of compounds, called resorcylic acid lactones (RALs),¹³⁸ which also includes hypothemycin and zearalenone. Radicol was first isolated from the fungus *Monocillium nordinii* in 1953 and named “monorden”, but the chemical structure was not assigned.¹³⁹ The same compound was independently isolated by Mirrington *et al.*¹⁴⁰ from *Nectria radicola* in 1964, and it was termed “radicol” with the structural connectivity correctly proposed. Later, the stereochemistry of radicol was unambiguously confirmed by chemical synthesis¹⁴¹ and X-ray crystallography.¹⁴²

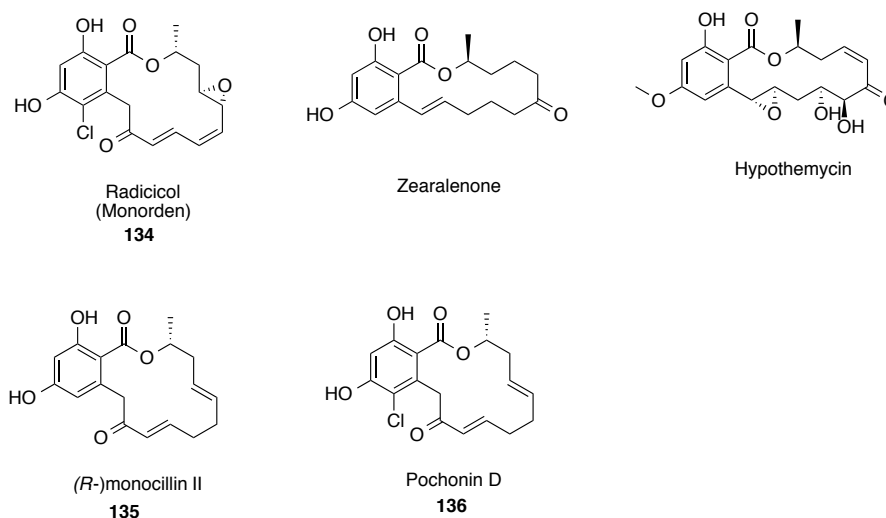


Figure 3-1 Resorcylic acid lactones (RALs): radicol, zearalenone, and hypothemycin, (R)-monocillin II, Pochonin D.

* A version of this chapter has been published. Zhou, H.; Qiao, K.; Gao, Z.; Vederas, J. C.; Tang, Y. *J. Biol. Chem.* **2010**, *285*, 41412-41421.

Radicicol was originally identified as an anti-fungal agent but did not attract much attention.^{139, 140, 142} The importance of radicicol increased with the discovery of its potent inhibitory activity ($IC_{50} = 20$ nM) against the heat shock protein 90 (Hsp90).^{143, 144} Hsp90 is a molecular chaperone associated with the maturation of a wide range of oncogenic proteins,¹⁴⁵ and therefore became an attractive target in anticancer-drug research. Radicicol acts as a competitive inhibitor by occupying the ATP-binding site of Hsp90, as shown in the co-crystal structure of radicicol and Hsp90.¹⁴⁶ Although radicicol features a reactive epoxide and conjugated dienone (Michael acceptor), it does not covalently interact with the ATP-binding site of Hsp90. In contrast, hypothemycin blocks the activity of kinases by covalently binding the ATP-binding sites.^{80, 81}

The two reactive moieties of radicicol do impede its activities *in vivo*.^{147, 148} The metabolic instability of the epoxide and conjugated dieneone renders radicicol an unsuitable drug candidate. However, radicicol analogs derived from chemical synthesis have shown potential to overcome these limitations.¹⁴⁹ The C2' oxime derivatives of (*R*)-monocillin II (**135**) and pochonin D (**136**), from a chemical library screening, display enhanced *in vivo* activity.^{149, 150} A phosphate prodrug strategy (inactive precursors, which can be converted to active pharmacological agents in the body) has been developed to further enhance oral bioavailability.¹⁵¹ These encouraging results suggest that the radicicol scaffold remains attractive toward the development of Hsp90 inhibitors, and this prompted us to examine the biosynthesis of radicicol in detail.

The gene cluster of radicicol has been identified in two producing fungi,

Pochonia chlamydosporia and *Chaetomium chiversii*.^{39, 109} A pair of iterative highly reducing PKS (HRPKS) and nonreducing PKS (NRPKS) is essential for production of radicicol. There are five genes in the *rad* gene cluster in *P.chlamydosporia* (**Figure 135**). Genes *rdc1* and *rdc5* are predicted to encode a pair of PKSs; while the *rdc2* and *rdc4* gene products are responsible for post-PKS modifications. Rdc3 is predicted to be a transporter that belongs to the major facilitator superfamily (MFS).

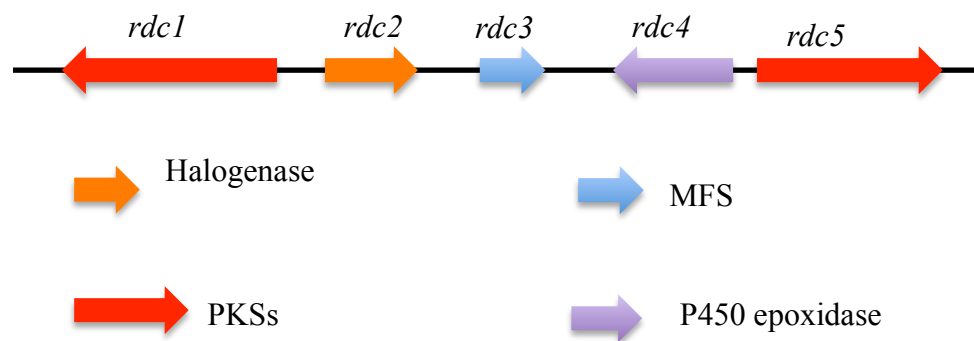


Figure 3-2 The gene cluster of radicicol in *Pochonia chlamydosporia*.

The domain architectures of the two *P. chlamydosporia* PKSs are shown in **Figure 3-3**. The HRPKS, Rdc5, has the same set of domains as Hpm8: KS, MAT, DH, core, ER, KR, and ACP.³⁹ The “core” domain, located between the DH and ER domains, consists of a non-functional structural KR pseudo-domain and an inactive C-methyltransferase pseudo-domain (CMeT), which is similar to Hpm8. Analogous to Hpm3, Rdc1 possesses the SAT, KS, MAT, PT, ACP, and TE domains.



Figure 3-3 Domain architectures of Rdc5 and Rdc1. KS: ketosynthase; MAT: malonyl-CoA:acyltransferase; ACP: acyl carrier protein; KR: ketoreductase; DH: dehydratase; ER: enoyl reductase; SAT: starter unit:ACP transacylase; PT: product template; TE: thioesterase.

Rdc5 is proposed to synthesize the reduced portion of radicicol by KS-catalyzed iterative condensations and processing domains (KR, DH, and ER)-directed sequential β -position reductions (**Figure 3-4**). With the assistance of the SAT domain, the reduced portion is then transferred downstream to Rdc1, where it is further elongated to a nonaketide without any reduction at the β -positions. The nascent nonaketide enters the active site of the PT domain, where it is cyclized to a resorcyate core. Lastly, the C-terminal TE domain cyclizes the polyketide chain to release an RAL intermediate, which is further decorated by post-PKS modifications (Rdc2 and Rdc4) to furnish radicicol.

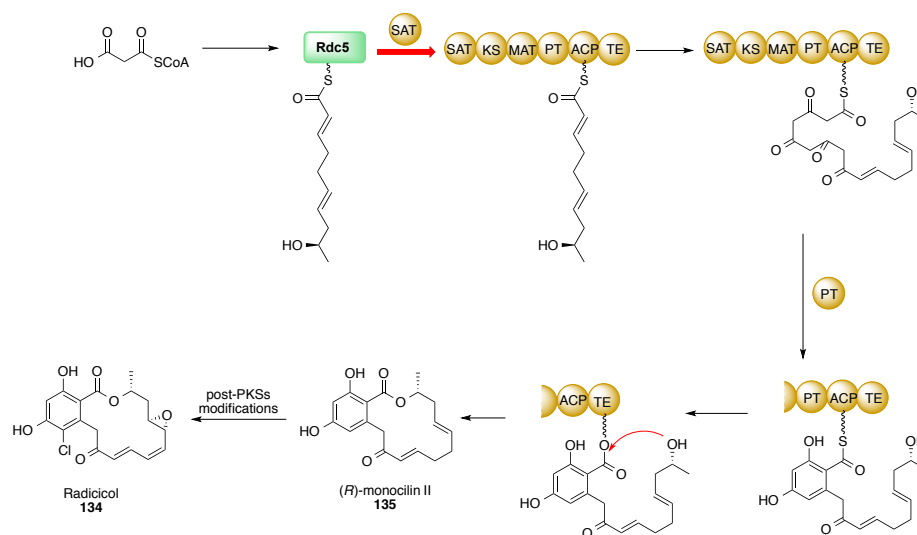


Figure 3-4 Proposed biosynthesis of radicicol (**134**).

3.2 Results and discussion*

3.2.1 Expressions of Rdc5 and Rdc1 and their activities

Although the *rdc* gene cluster has been identified in two different fungal hosts,^{39, 109} the biochemical characterization of key iterative PKSs has not been performed, and the earliest RAL intermediate has not been conclusively identified. To gain further insights into radicicol biosynthesis, our collaborators successfully expressed and purified Rdc1 and Rdc5 from the heterologous host *S. cerevisiae* BJ5464-NpgA. BJ5464-NpgA is a genetically modified strain housing a phosphopantetheinyl transferases gene *npgA*, which enables the heterologous expression of phosphopantetheinylated PKSs.^{82, 83}

* This is a collaborative project with the Tang group. I was responsible for synthesis and characterizations of intermediates and products, whereas our collaborators, Professor Yi Tang and co-workers, were in charge of protein expression and purification, as well as biological assay.

When purified Rdc5 and Rdc1 are incubated with 2 mM malonyl-CoA and NADPH, a major compound **135** is produced with identical UV and LC-MS profiles to that of (*R*)-monocillin II (**Figure 3-5**, trace iii), which has been isolated from other radicicol-producing strains.^{109, 152, 153} To conclusively identify this PKS product, two plasmids harboring *rdc1* and *rdc5* with different auxotrophic selection markers (*TRP1* and *URA3*) were co-transformed into *S. cerevisiae* BJ5464-NpgA. The co-expression strain produces the PKS product **135** with a titer of 15 mg/liter. The NMR spectrum of **135** is indistinguishable from that of (*R*)-monocillin II.

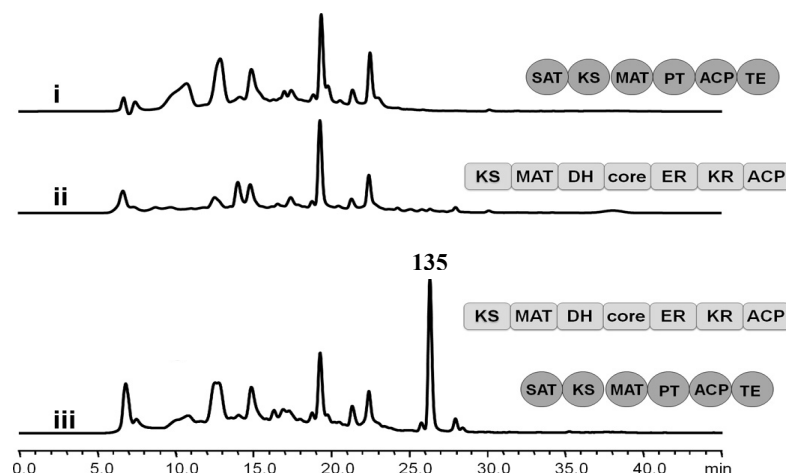
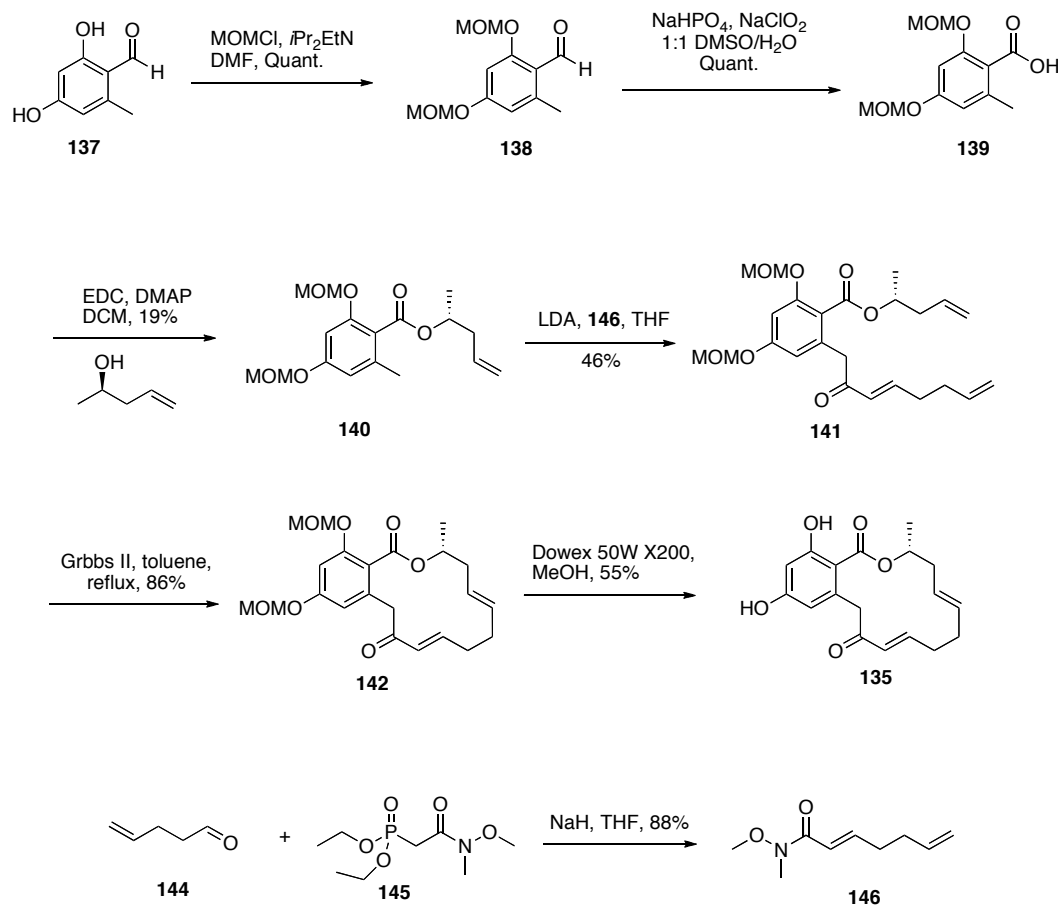


Figure 3-5 *In vivo* reconstitution of biosynthesis of **135**. LC-MS profiles of organic extract from trace i) BJ5464-NpgA expressing Rdc1; trace ii) BJ5464-NpgA/ pKJ61 expressing Rdc5; trace iii) BJ5464-NpgA co-expressing Rdc5 and Rdc1.

To verify the *R*-stereochemistry of **135**, an authentic standard was chemically synthesized as shown in **Scheme 3-1** using a literature procedure with slight modifications.¹⁵⁴ Protection of **137** with chloromethyl methyl ether

(MOMCl) in the presence of *i*Pr₂EtN afforded aldehyde **138**, which was immediately oxidized to carboxylic acid **139** via a Pinnick oxidation. EDC- and DMAP-catalyzed coupling reaction between **139** and (*R*)-pent-4-en-2-ol furnished **140**, which was treated with fresh-made LDA before the displacement of Weinreb amide **146** to yield **141**. Compound **146** was a product of the HWE reaction between **144** and **145** using NaH as a base. Ring-closure metathesis using Grubbs II catalyst successfully produced, after MOM deprotection, the authentic standard (*R*)-monocillin II (**135**). The UV pattern, retention time on chiral column, and NMR data of **135** are identical to that of (*R*)-monocillin II from the *in vitro* and *in vivo* assay.



Scheme 3-1 Synthesis of (*R*)-monocillin II (**135**).

The *in vitro* biosynthesis of **135** by purified Rdc1 and Rdc5 indicated that (*R*)-monocillin II is the first RAL compound in the *rdc* pathway and is the product directly offloaded from Rdc1 as shown in **Figure 3-6**. Interestingly, a saturated bond at C5'-C6' is found in **135**, suggesting that the ER domain in Rdc5 indeed functions during the third round chain elongation, and the *cis*-double bond in radicicol is probably introduced by post-PKS modifications. This hypothesis is consistent with the genetic studies with *Chaetomium chiversii*, which suggested that C7'-C8' epoxidation and C5' hydroxylation may be catalyzed by a single P450 RdcP (Rdc4 homology).¹⁰⁹ In contrast, the *cis*-double bond of hypothemycin is isomerized from the *trans*-double bond introduced by Hpm8.^{39, 41} This isomerization is catalyzed by the glutathione *S*-transferase, encoded by *hpm2* in the *hpm* gene cluster, in the presence of glutathione.³⁹ It is interesting that nature could generate *cis*-double bonds with different mechanisms, and that they are usually facilitated by post-PKS modifications. There are only a few isolated cases where *cis*-double bonds are directly generated by the PKS DH domains.^{137, 155}

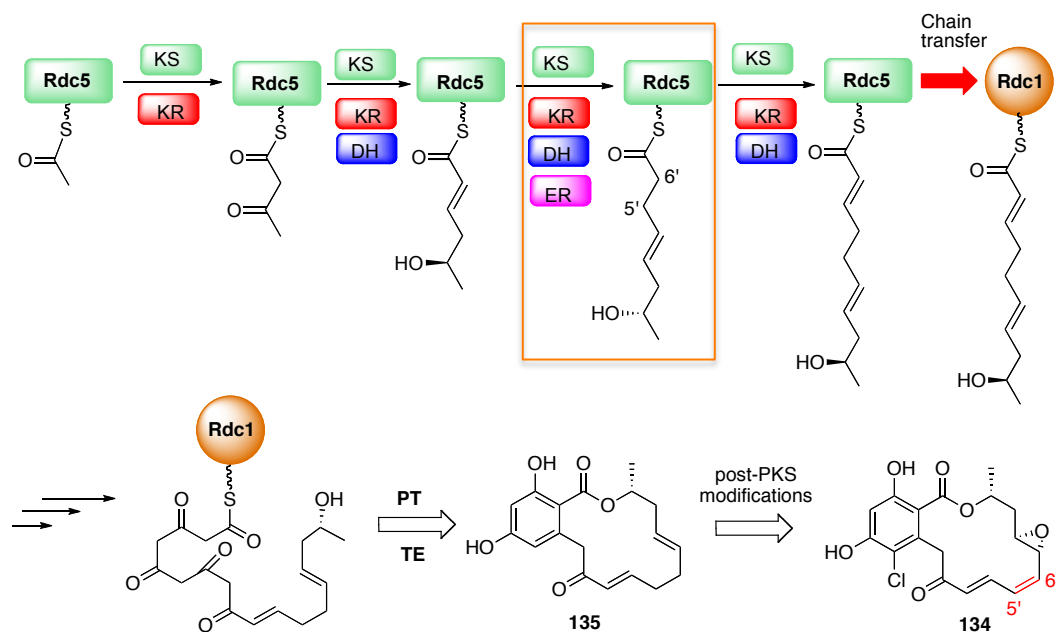


Figure 3-6 Origin of the C5'-C6' *cis*-double bond. Rdc5 generates a single bond at C5'-C6'. The *cis*-double bond of C5'-C6' is introduced by post-PKS modifications.

3.2.2 Polyketide chain length control of Rdc5 and Rdc1

3.2.2.1 6+3 combination and 5+4 combination

In contrast to modular PKSs, iterative PKSs employ complex programming rules to control the oxidation level, stereochemistry, and chain length of intermediates. The mechanisms behind these programming rules are still mysterious. Although gene sequence alignments can provide limited information about PKSs programming,^{23, 51, 137} bioinformatics are currently far from predicting the chain length control of iterative PKSs. In the case of radicicol, Rdc5 could synthesize a hexaketide intermediate (**Figure 3-7A**) and transfer it downstream to Rdc1 with the assistance of the SAT domain for three additional chain elongations (6+3 combination). This distribution of ketides between the pair of PKSs is

identical to that of some other RALs, such as hypothemycin and zearalenone.^{41, 88,}
¹⁵⁶ Alternatively, Rdc5 could generate a pentaketide (**Figure 3-7B**), which could then be extended four times (5+4 combination) by Rdc1. Both the 6+3 and 5+4 combinations provide the same nonaketide for further modifications.

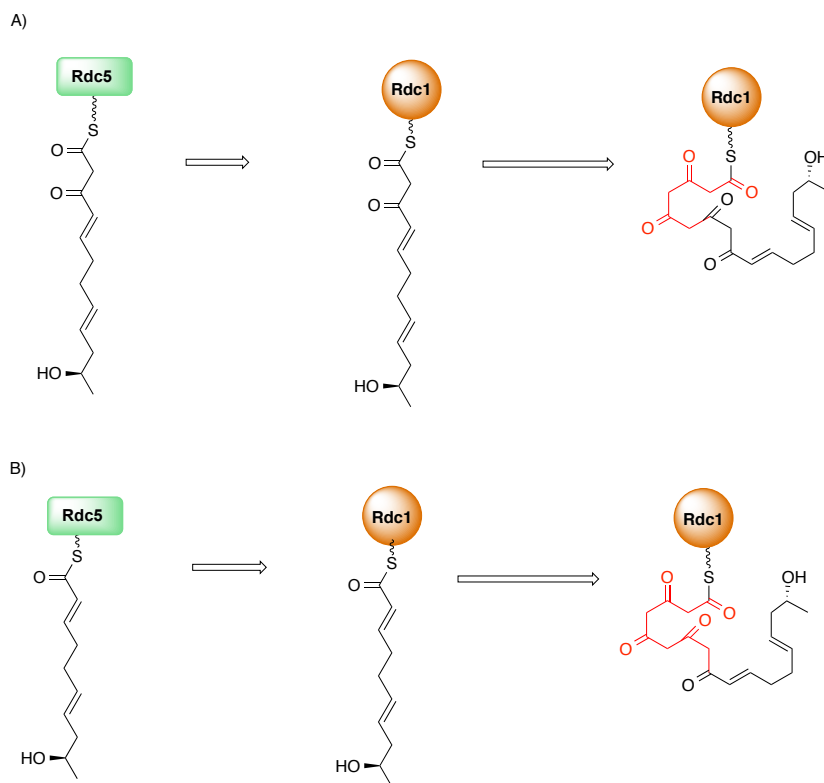


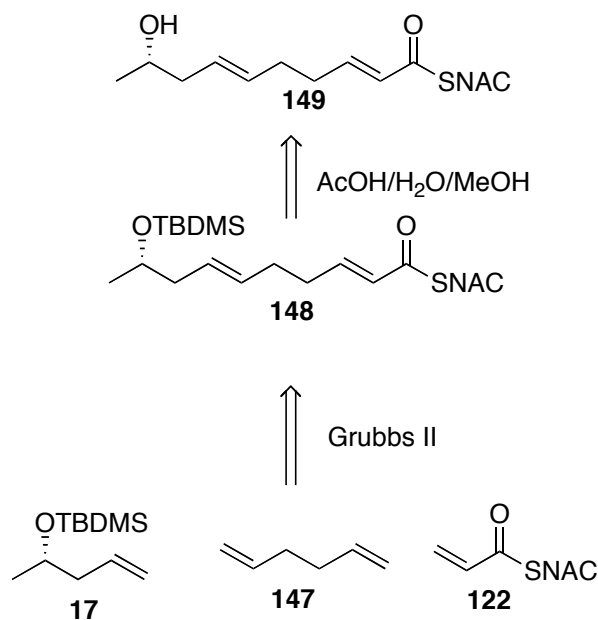
Figure 3-7 Distribution of labor between Rdc5 and Rdc1. (A) 6+3 combination; and (B) 5+4 combination. Ketide units added by Rdc1 are shown in red.

One method to distinguish these two pathways is an advanced precursor feeding experiment. Some NRPKSs can accept putative biosynthetic intermediates in their SNAC forms as starter units and extend them to fully assembled PKS products.^{41, 88} For example, Hpm3 can accept the hexaketide-SNAC thioester (**27**) and extend it to DHZ.⁴¹ Analogously, supplying Rdc1 with

the hexaketide or pentaketide intermediates (**Figure 3-7**) in their SNAC forms and monitoring the formation of (*R*)-monocillin II could test the true biosynthetic intermediate of radicicol biosynthesis. If the pentaketide is indeed the starter unit for Rdc1, (*R*)-monocillin II should be produced. If the *rdc* pathway utilizes the alternative combination (6+3), feeding Rdc1 with the pentaketide will either generate no product, because the KS domain does not accept the shorter starter unit, or an unnatural 12-membered RAL compound, because only three additional iterations would be conducted.

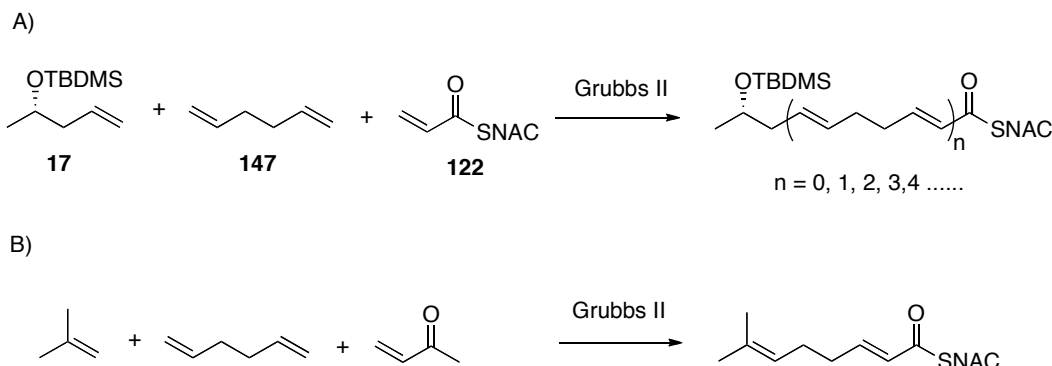
3.2.2.2 Synthesis of pentaketide SNAC thioester **149**

The retrosynthesis of pentaketide SNAC thioester **149** is shown in **Scheme 3-2**. TBDMS protected **149** could in theory be obtained from three-component cross metathesis with **17**, **147** and **122**. Deprotection of the TBDMS group could quickly furnish **149** in only 2 steps.



Scheme 3-2 Retrosynthesis of pentaketide **149**.

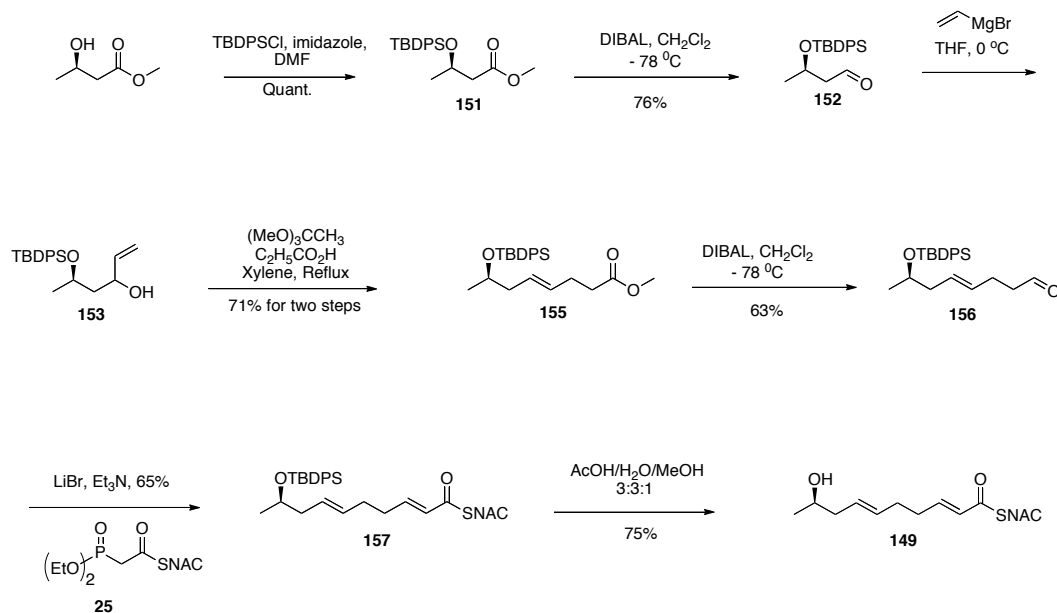
Indeed, the formation of **148** in the three-component cross metathesis reaction was detected by mass spectra. However, multiple rounds of cross metathesis occurred and generated a series of complex compounds differing in the number of hexadiene units (**Scheme 3-3A**). A sequential addition strategy was attempted, but did not alter the results. Grubbs and co-workers have demonstrated the possibility of three-component cross metathesis with isobutylene, **147**, and methyl vinyl ketone (**Scheme 3-3B**).¹⁵⁷ Isobutylene is a type III olefin and reacts with methyl vinyl ketone at a much slower rate, leading to almost a single product in the three-component cross metathesis. However, **17** and **147** are both type I olefins and both react with **122** rapidly, and thus polymerization occurred.



Scheme 3-3 Three-component cross metathesis.

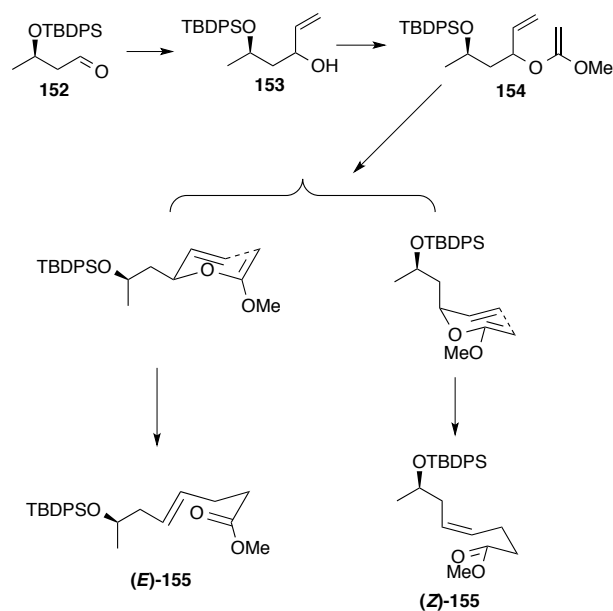
The literature precedent of compound **155**¹⁵⁸ inspired an alternative synthesis of **149** (**Scheme 3-4**). Known aldehyde **152** was obtained in 2 steps from methyl (*R*)-3-hydroxybutanoate. Treatment of **152** with vinylmagnesium bromide generated intermediate **153** (not isolated), which subsequently reacted trimethyl orthoacetate in the presence of a catalytic amount of propionic acid to

furnish known methyl ester **155** via a Johnson-Claisen rearrangement.¹⁵⁹ Reduction of methyl ester **155** with DIBAL afforded aldehyde **156**, which underwent the HWE reaction with **25** in the presence of LiBr and Et₃N to give **157**. The required compound **149** was obtained after deprotection of the TBDMS group of **157**.



Scheme 3-4 An alternative synthesis of pentaketide **149**.

A key step in the synthesis of **149** is the Johnson-Claisen rearrangement. Aldehyde **152** is attacked by vinylmagnesium bromide to form **153**. The newly formed allylic alcohol condenses with trimethyl orthoacetate to provide precursor **154** for the Johnson-Claisen rearrangement. The *E* configuration of the rearrangement product is dictated by the chair conformation of the transition-state with the bulky side chain at the equatorial position (**Scheme 3-5**).



Scheme 3-5 Mechanism of the Johnson-Claisen rearrangement.

3.2.2.3 Incorporation of **149**

The *in vitro* assay was performed by incubating purified Rdc1 with starter unit **149** and 2 mM malonyl-CoA. LC-MS analysis suggests that (*R*)-monocillin II (**135**) is produced in the *in vitro* assay. To further demonstrate the precursor-directed biosynthesis of **135** *in vivo*, **149** was supplemented to the Rdc1-expression yeast culture (3-day old) at a concentration of 100 mg/liter. After one additional day of culturing, production of **135** was observed in the organic extracts (**Figure 3-8A, trace iii**). Therefore Rdc1 is able to precisely elongate the acyl chain of **149** four times to afford a nonaketide backbone both *in vitro* and *in vivo*. This result suggests the 5+4 pathway shown in **Figure 3-7B** as the most likely mechanism for the biosynthesis of **135**.

The biosynthesis of **135** by Rdc1 alone in the presence of **149** both *in vitro* and *in vivo* also demonstrates that the synthetic starter unit could replace the

HRPKS functions in the tandem iterative PKS system, which was also observed in hypothemycin and zearalenone biosynthetic studies.^{41, 88, 156} Moreover, the programming feature of radicicol PKSs is apparently different from the 6+3 combination employed by zearalenone and hypothemycin biosynthesis.^{41, 88, 156} Why and how the PKSs employ different distributions of labor between PKSs is still unclear.

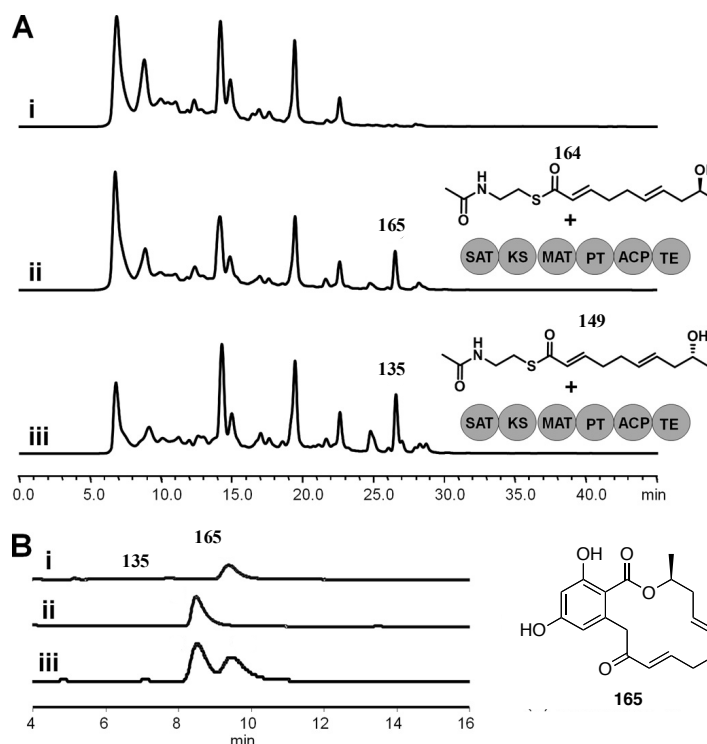


Figure 3-8 Precursor-directed feeding using SNAC substrates. **A)** LC-MS profiles of organic extracts from strain harboring Rdc1 and trace i without substrate feeding; *trace ii*, supplementation with the pentaketide SNAC **164**; *trace iii*, supplementation with the pentaketide SNAC **149**. **B)** Chiral HPLC separation of the enantiomers **135** and **165** on a Lux 3 μ m cellulose-1 column (Phenomenex): *trace i*, **165**; *trace ii*, **135**; *trace iii*, co-injection of a mixture of **165** and **135**. All traces are monitored at 300 nm.

3.2.3 Functions of the Rdc1 TE domain

3.2.3.1 Knock-out of the TE domain of Rdc5

The TE domain is hypothesized to offload (*R*)-monocillin II (**135**) by macrolactonization using the terminal hydroxyl group of the nascent polyketide chain to attack the TE bound carboxyl ester (**Figure 3-4**). To verify the function of the Rdc5 TE domain, the active site Ser1889 of the catalytic triad was mutated by the Tang group to Ala to afford the Rdc1-S1889A mutant. This mutant was expressed and purified from BJ5464-NpgA. When Rdc1-S1889A was incubated with pentaketide SNAC thioester **149** and malonyl-CoA, production of **135** was completely abolished. Instead, a new compound **158** with an identical mass as that of **135** was detected. Interestingly, compound **158** was also present in the culture extract of BJ5464-NpgA harboring Rdc1-S1889A and Rdc5, but with much lower titer than that of **135** (>100 fold less) in BJ5464-NpgA harboring Rdc1 and Rdc5. The UV spectrum of **158** does not display the characteristic peaks observed from RAL-type compounds. The spectrum is more complex and similar to isocoumarin compounds SMA76b and SMA76c (**Figure 3-9B**) produced by PKS4 from *Gibberella fujikuroi*.⁶²

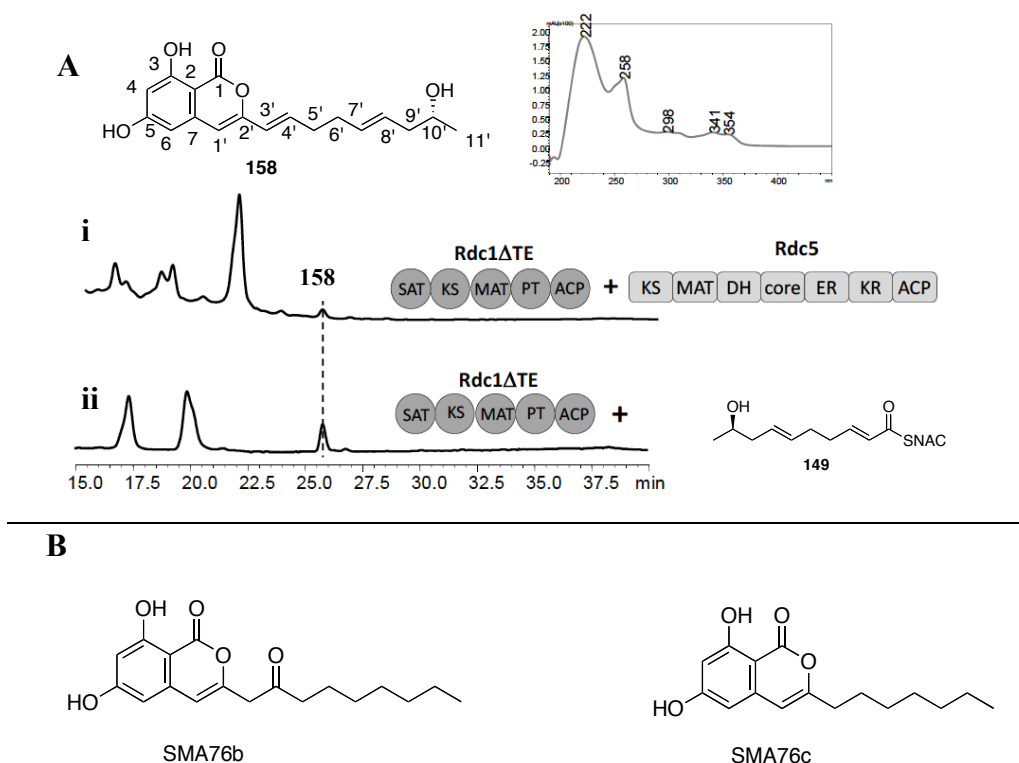
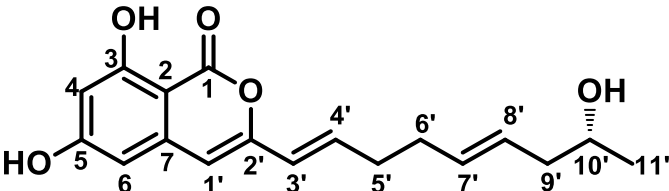


Figure 3-9 Reconstitution of Rdc1-S1889A *in vivo* and *in vitro*. (A) HPLC analysis (300 nm) of polyketides synthesized by (i) expressing Rdc1-S1889A and Rdc5 *in vivo* and (ii) incubating Rdc1-S1889A with compound **149** *in vitro*. (B) UV spectrum and compound structure of **158**. (B) Structures of isocoumarin compounds SMA76b and SMA76c.

The yeast culture harboring Rdc-S1889A and Rdc5 was scaled up to obtain enough **158** for NMR analysis (Table 3-1). Compared to the NMR spectrum of **135**, the chemical shifts of C1' and C2' in **158** shift downfield (48.9 to 105.5 Hz) and upfield (196.4 to 152.9), respectively. These changes in chemical shifts suggests that the C2' group is an enol structure, which is consistent with isocoumarin compounds. In addition, the upfield shift of C10' (72.9 to 67.5 Hz) and its associated hydrogen (5.23 to 3.71 Hz) indicates that the C10' hydroxyl group is not a part of an ester group, and this is in agreement with the proposed structure shown in Figure 3-9.

Table 3-1 NMR assignment of **158**^a

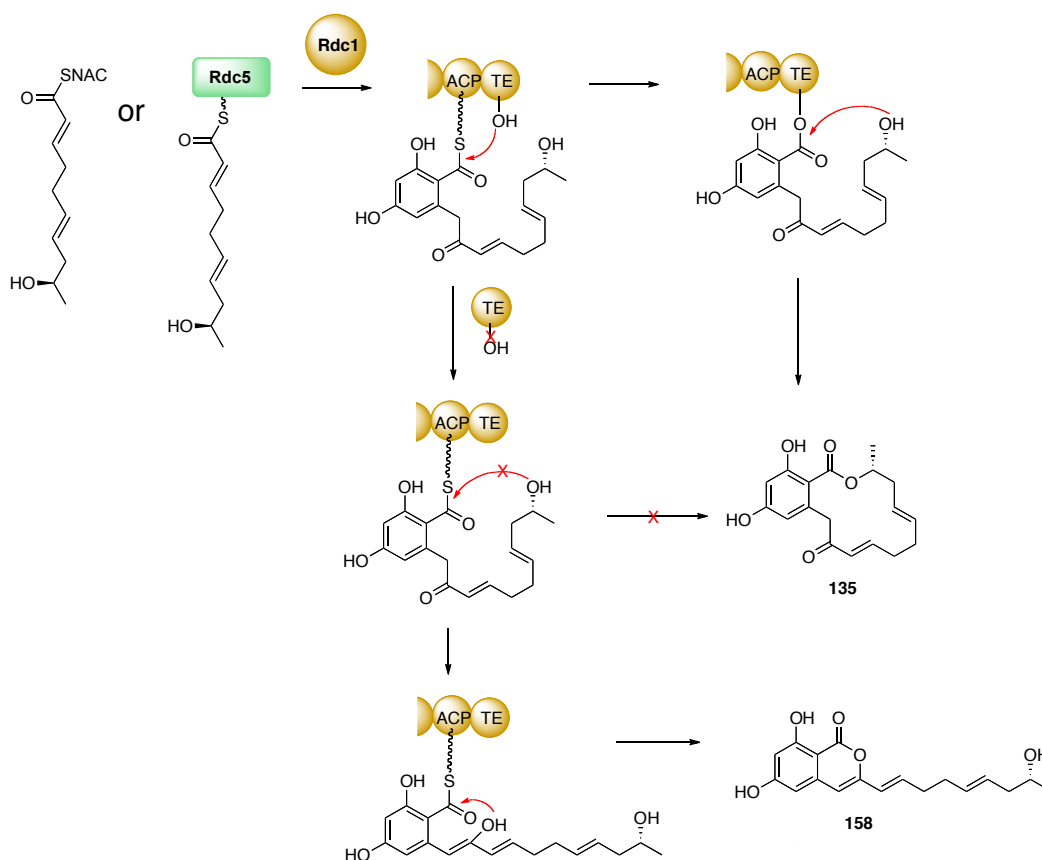
			
No.	¹³ C δ (ppm)	¹ H δ (ppm) (m, area, <i>J</i> _{HH} (Hz))	HMBC
1	166.2	-	
2	99.8	-	
3	164.4	-	
4	102.5	6.46 (d, 1H, 2.11)	C5, C2
5	166.4	-	
6	104.1	6.38 (d, 1H, 2.10)	C5, C2, C4
7	129.1	-	
1'	105.5	6.45 (s 1H)	C2', C3'
2'	152.9		
3'	123.1	6.19 (dt, 1H, 15.6, 1.42)	C2', C5'
4'	136.5	6.63 (dt, 1H, 15.6, 7.09)	C2', C5'
5'	33.3	2.30-2.34 (m, 2H)	C3', C4', C6'
6'	32.6	2.18-2.23 (m, 2H)	C7', C5'
7'	128.9	5.46-5.58 (m, 1H)	C6', C9'
8'	131.9	5.46-5.58 (m, 1H)	C6', C9'
9'	43.4	2.12-2.17 (m, 2H)	C10', C8'
10'	67.5	3.71 (s, 1H, 6.1 Hz)	
11'	23.2	1.08 (d, 3H, 6.2)	C9', C10'

^a Spectra were obtained at 600 MHz for proton and 125 MHz for carbon and were recorded in CD₃COCD₃.

To verify the involvement of the Rdc1 TE domain in the production of **158**, a truncated Rdc1 without the TE domain was constructed, expressed and purified in the same heterologous host by the Tang group. Both the *in vitro* assay of Rdc1ΔTE supplemented with pentaketide **149** and the *in vivo* assay of Rdc1ΔTE co-expressed with Rdc5 produce compound **158**, but abolish the

production of **135**. These results clearly demonstrate the TE domain is essential for the biosynthesis of **135**, but is not involved in the production of **158**.

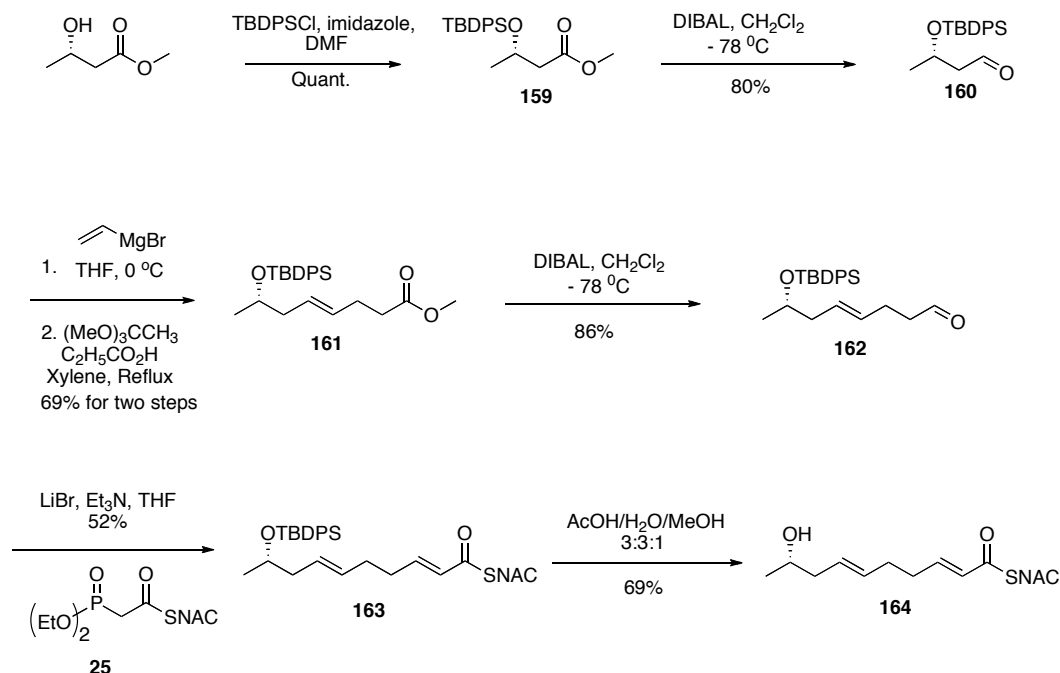
Therefore, the formation of **135** and **158** can be rationalized as follows (**Scheme 3-6**): pentaketide **149** is extended four rounds by Rdc1 to a nonaketide, which undergoes regioselective cyclization to generate the resorcylic core. This intermediate is transferred to the TE domain active site Ser1889, where macrolactonization releases the intermediate as (*R*)-monocillin II (**135**). With the active site Ser1889 of TE mutated to Ala, the nonaketide can no longer be transferred to the TE domain. In order to discharge the nonaketide off the enzyme, the C2' keto group is enolized to generate a relatively nucleophilic hydroxyl group, which attacks the thioester tethered to the ACP domain to release isocoumarin **158**. The inability of the C10' hydroxyl group to attack the ACP-tethered thioester suggests that the acyl chain has to be folded in a certain conformation by the TE domain to overcome the reaction entropy.



Scheme 3-6 Mechanisms of formation of **135** and **158**.

3.2.3.2 Probing the stereoselectivity of the TE domain

The stereochemistry of the C10' *R*-OH is generated by the KR domain during the first round of chain elongation. This terminal hydroxyl group of radicicol is stereochemically opposite to that of hypothemycin or zearalenone. Although Rdc5 is programmed to generate the *R*-stereochemistry exclusively, it is still unknown if Rdc1 TE is stereoselective towards the terminal (*R*)-hydroxyl group during the macrolactonization. To probe the stereoselectivity of the TE domain towards the pentaketide intermediate, compound **164** (the enantiomer of **149**) was chemically synthesized (**Scheme 3-7**), analogous to the synthesis of **149**.



Scheme 3-7 Synthesis of **164**.

When **164** is added to the Rdc1-expressing BJ5464-NpgA culture, a new compound **165** emerges. This compound is indistinguishable from **135** in terms of NMR, retention time on a C18 reverse phase HPLC column, UV absorbance, and mass spectrum. However, compound **165** could be clearly separated from **135** when co-injected onto a chiral HPLC column as shown in **Figure 3-8B**. In addition, the circular dichroism spectra of **135** and **165** are mirror images of each other (**Figure 3-10**). Together, these data indicate that compound **165** is an enantiomer of **135**, consistent with the fact that an enantiomer of the natural starter unit was supplied.

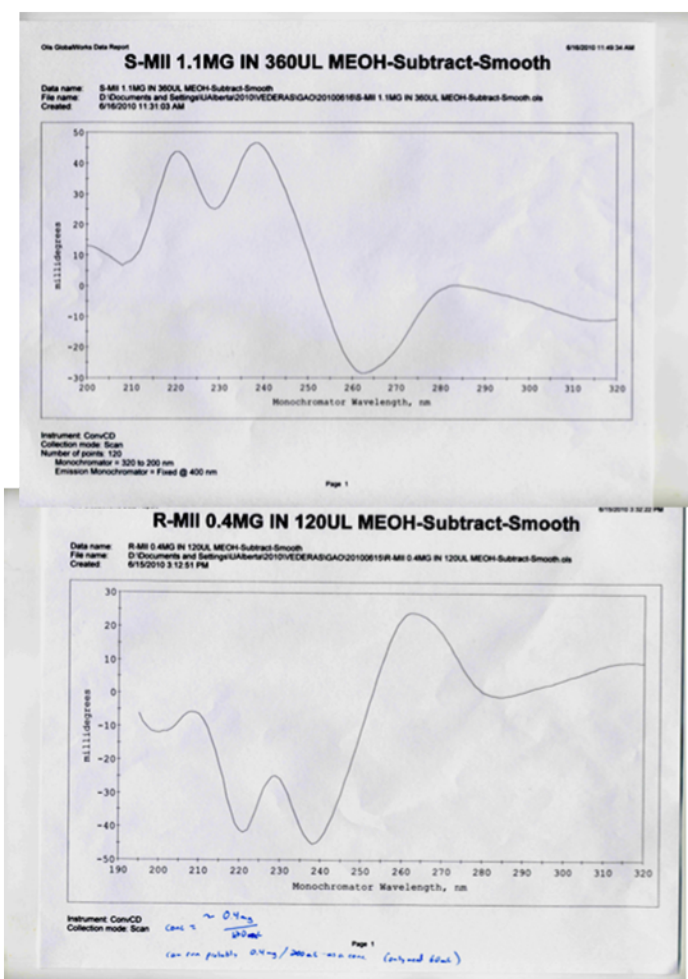


Figure 3-10 Circular dichroism (CD) spectra of (*S*)-monocillin II (**165**, upper) and (*R*)-monocillin II (**135**, bottom)

The titer of **165** from the *in vivo* and *in vitro* precursor-feeding assay is comparable with that of **135**, apparently indicating that the TE domain is insensitive to the stereoconfiguration of the terminal hydroxyl group during macrolactonization. It is possible that the linear portion of the nonaketide is flexible enough to allow the hydroxyl in either configuration to be deprotonated by a general base (histidine), thereby generating both *S*- and *R*-configured RAL compounds with equal efficiency. In addition, the similar level of production of **165** and **135** also indicates that the KS and PT domains of Rdc1 are not specific to

the chirality of the terminal hydroxyl group either. This result is consistent with the relaxed stereoselectivity of Hpm3 and suggests that relaxed substrate specificity at distal sites may be a common feature of this type of PKS, which provides an opportunity for the precursor-directed biosynthesis of natural product analogs.

3.2.4 Function of Rdc2

3.2.4.1 Rdc2 transforms (*R*)-monocillin II to pochonin D

The chlorine atom of radicicol is essential for its inhibitory effect on Hsp90.¹⁵⁰ The chlorine-less version of radicicol, monocillin, shows significantly lower activity towards Hsp90. Moreover, the chlorinated version of (*R*)-monocillin II, pochonin D (**136**), shows a potent inhibitory effect ($IC_{50} = 80$ nM) on the Hsp90, whereas (*R*)-monocillin II, is more than 600 fold less inhibitory.¹⁵⁰ Crystal structures show that the chlorine atom occupies a hydrophobic pocket in the ATP-binding site of Hsp90,¹⁴⁶ which enhances the affinity of radicicol toward Hsp90. Removing the chlorine induces a conformational change detrimental to its binding in the ATP-binding site.¹⁵⁰

These observations evoked an interest in the function of Rdc2, which is proposed to introduce the chlorine atom of radicicol. A knockout mutant of the Rdc2 homolog (RadH) in *C. chiversii* resulted in formation of monocillin, the nonhalogenated version of radicicol.¹⁰⁹ BLAST searches indicated that Rdc2 houses a pfam04820 (tryptophan) halogenase conserved domain and displays sequence homology to several FAD-dependent halogenases. To verify the

function of Rdc2, our collaborators constructed a yeast expression plasmid containing a *LEU2* selection marker. When the BJ5464-NpgA host is transformed with three expression plasmids separately encoding Rdc1, Rdc2, and Rdc5, a major RAL product is isolated (14.3 mg/L). Although a small amount of **135** is obtained, the titer was less than 5% of the overall RAL pool at the end of 4 days of continuous culturing. The mass, UV, and NMR spectra indicate that the compound is the chlorinated version of (*R*)-monocillin II, pochonin D. Therefore, these data suggest that the function of Rdc2 is a chlorinase.

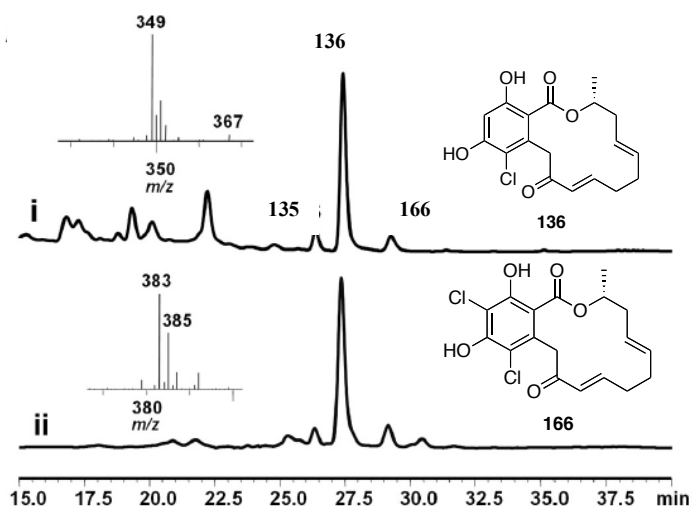


Figure 3-11 LC-MS profiles for production of chlorinated RALs from the following: trace i, BJ5464-NpgA expressing Rdc5, Rdc1, and Rdc2; trace ii, *in vitro* assay of 50 μ M Rdc2 incubated with 1 mM **135**, 100 μ M FAD, 2 mM NADPH, 50 mM NaCl, and 10 μ M SsuE (flavin reductase). *Inset* in trace i shows observed $[M-H]^-$ MS spectrum of **136**, and *inset* in trace ii shows the observed $[M-H]^-$ MS spectrum of **166**.

In vitro conversion of **135** to **136** was also tested. cDNA of *rdc2* was inserted into an *E. coli* pET24a expression vector. Rdc2 was then purified from *E.*

coli containing the Rdc2-expression plasmid. Almost complete conversion of **135** to **136** was observed when **135** was incubated with Rdc2, NADPH, and *E. coli* SsuE used as a flavin reductase accessory enzyme. Another compound **166** is also detected by LC-MS, and appears to be the dichlorinated version of **135**. However it is produced at a low yield.

3.2.4.2 Substrate specificity of Rdc2

RALs share structural similarity in the resorcyate core, so Rdc2 may be capable of chlorinating other RALs. Indeed, Rdc2 successfully chlorinates dehydrozearalenol (**167**) in the presence of SsuE, and NADPH *in vitro*. To characterize the chlorinated dehydrozearalenol, Rdc2, Hpm8, and Hpm3 expression plasmids are co-transformed into BJ5464-NpgA, and the resulting yeast produce **167** at a titer of 9 mg/L. NMR analysis of **167** indicates the compound is 6-chloro-7,8-dehydrozearalenol. The relatively relaxed substrate specificity of Rdc2 suggests its potential utility in combinatorial biosynthesis.

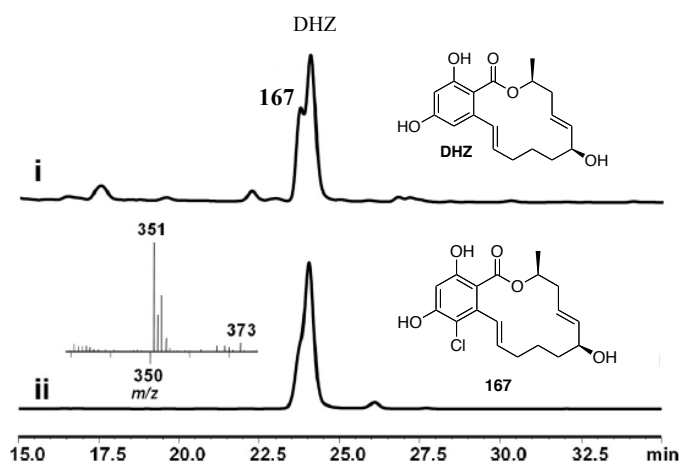
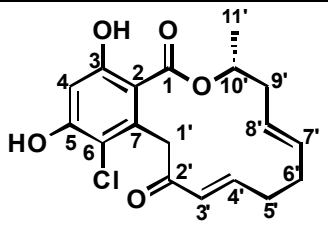


Figure 3-12 LC-MS profiles for production of **167** from the following: trace i, BJ5464-NpgA expressing Hpm8, Hpm3, and Rdc2; trace ii, *in vitro* assay of 50

μ M Rdc2 incubated with 1 mM DHZ, 100 μ M FAD, 2 mM NADPH, 50 mM NaCl, and 10 μ M SsuE. *Inset* in trace ii shows observed $[M - H]^-$ MS spectrum of **167**.

Table 3-2 NMR assignment of **167**^a

			
No.	¹³ C δ (ppm)	¹ H δ (ppm) (m, area, J_{HH} (Hz))	HMBC
1	170.7	-	
2	108.3	-	
3	163.6	-	
4	103.8	6.62 (s, 1H)	C2, C3, C5, C6
5	158.9	-	
6	116.2	-	
7	138.0	-	
1'	46.3	4.14 (d, 1H, 17.5) 4.36 (d, 1H, 17.5)	C2, C6, C7, C2'
2'	195.3		
3'	131.0	5.85 (d, 1H, 15.5)	C2'
4'	147.4	6.69-6.73 (m, 1H)	C2', C5', C6'
5'	31.9	2.17-2.34 (m, 2H)	C3', C4', C6', C7'
6'	31.9	2.17-2.34 (m, 2H)	C5'
7'	127.7	5.34-5.36 (m, 1H)	C5', C6', C8', C9'
8'	133.0	5.25-5.31 (m, 1H)	C6'
9'	37.3	2.26-2.29 (m, 1H) 2.59-2.64 (m, 1H)	C7', C8', C10', C11'
10'	73.4	5.40-5.45 (m, 1H)	C1, C9'
11'	18.2	1.32 (d, 3H, 6.6)	C9', C10'

^a Spectra were obtained at 500 MHz for proton and 125 MHz for carbon and were recorded in CD₃COCD₃.

3.3 Conclusions

In this study, together with our collaborators (Professors Yi Tang and co-workers), we fully reconstituted the enzymatic activities of Rdc5 and Rdc1, and showed that (*R*)-monocillin II (**135**) is the first PKS product during radicicol biosynthesis. Analogous with the biosynthesis of other RALs, production of **135** requires a pair of iterative PKSs, a HRPKS (Rdc5) and a NRPKS (Rdc1). Using pentaketide SNAC **149** for precursor-directed biosynthesis, we demonstrated that the “5+4” distribution of effort between Rdc5 and Rdc1 is a highly plausible mechanism of assembling **135**. This 5+4 combination is different from the distribution of labor between the HRPKS and NRPKS employed in the biosynthesis of hypothemycin, which is a 6+3 combination. Further investigations into the mechanisms governing chain length control of Rdc5 and Hpm8, possibly by domain swaps, should contribute to our understanding of type I iterative PKS programming.

In addition, the function of the TE domain was also investigated in this study. The Rdc1 TE domain is involved in the biosynthesis of **135** as demonstrated by the knock-out strain of the TE domain abolishing production of **135**. The TE domain also displays relaxed substrate specificity toward the terminal hydroxyl group of the pentaketide intermediate. Supplying **164**, an enantiomer of the natural pentaketide, to Rdc1 forms an enantiomer of **135**, (*S*)-monocillin II. This result demonstrates the potential utility of this type of NRPKSs as a biosynthetic factory for the production of natural product analogs.

Finally, Rdc2 is a flavin-dependent halogenase in the biosynthesis of radicicol. Rdc2 also displays broad substrate specificity, and is able to chlorinate DHZ both *in vivo* and *in vitro*. Therefore, Rdc2 could potentially be developed as a biosynthetic tool to chlorinate late-stage RALs, a transformation that is otherwise quite challenging synthetically.

Chapter 4: Biosynthetic studies of dehydrocurvularin

4.1 Introduction

4.1.1 Introduction to curvularins and their biological activities

Curvularins (**Figure 4-1**) are a family of macrolide phytotoxins produced by fungi *Alternaria*, *Nectria*, *Curvularia*, *Penicillium*, *Aspergillus* and *Eupenicillium*.¹⁶⁰⁻¹⁶⁸ Curvularin was first discovered by Musgrave from the culture filtrate of *Curvularia* in 1956,¹⁶⁰ and the structure was elucidated in the same group by chemical degradation. The structures of curvularin and dehydrocurvularin (DHC, **168**) were confirmed by X-ray crystallography.^{169, 170}

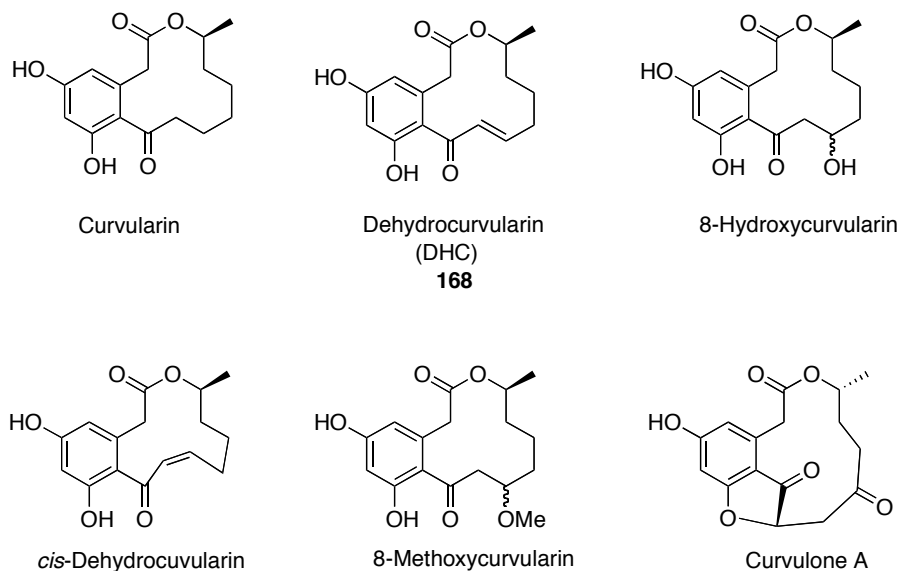
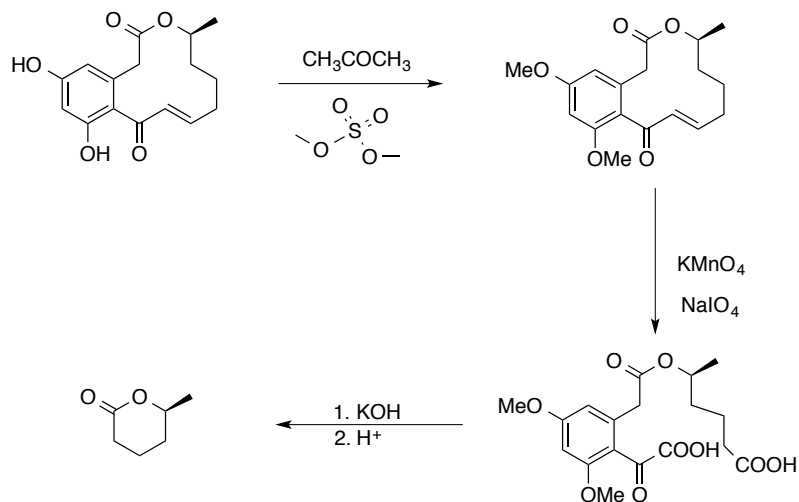


Figure 4-1 Curvularin-type natural products.

The stereochemistry of dehydrocurvularin has been established by chemical degradation (**Scheme 4-1**).¹⁷¹ The treatment of dimethyl protected dehydrocurvularin with potassium permanganate and sodium periodate furnished the known¹⁷² (*S*)- δ -caprolactone, after hydrolysis. Thus the stereochemistry of dehydrocurvularin was established to be *S*.



Scheme 4-1 Degradation of DHC to confirm the stereochemistry.

The curvularin family exhibits a variety of biological activities. Originally, they were identified as antibacterial and antifungal agents acting as a defense mechanism. Curvularins recently have been rediscovered as promising anti-inflammatory agents¹⁷³⁻¹⁷⁶ and broad-spectrum inhibitors of cancer cells.¹⁷⁷⁻¹⁸⁰

1. Anti-inflammatory agents: Yao *et al.*¹⁷³ screened 1000 mycelial fungal extracts, and discovered that curvularin inhibits the expression of cytokine-induced inducible nitric-oxide synthase (iNOS), an enzyme that plays a pivotal role in proinflammatory immune processes. Continued efforts¹⁷⁶ by the same group suggested that curvularin is capable of reducing proinflammatory gene

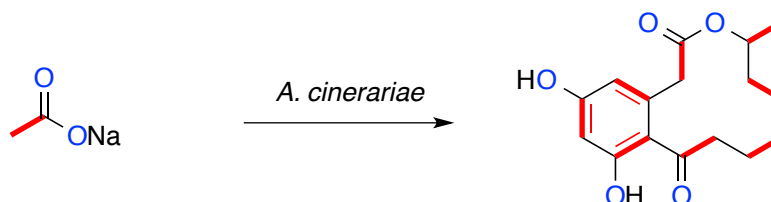
expression in a mouse model, and that this effect could be translated to a human cell model. In addition, their data indicated that curvularin exhibits no major side effects on mice. Further development of curvularin as a new therapeutic could provide a treatment for chronic inflammatory diseases.

2. Anti-cancer therapeutics: He *et al.* have evaluated the cytotoxicities of dehydrocurvularin, 8-hydroxycurvularin, and 8-methoxycurvularin.¹⁸⁰ They found that these curvularins display potent cytotoxicity against four cancer cell lines (NCI-H460, MCF-7, SF-268 and MIA Pa Ca-2), with IC₅₀ values ranking from 0.9 to 4.1 μ M. Further mechanistic studies¹⁷⁸ implied that dehydrocurvularin induces the heat shock response, a conserved mechanism used by eukaryotic cells to maintain protein homeostasis. In addition, curvularin and dehydrocurvularin exert inhibitory effects on the TGF- β signaling pathway, which is overexpressed during tumor progression.¹⁷⁷ Therefore, curvularins are attractive anticancer candidates with combinatorial anticancer effects, and may be developed as the next generation of therapeutics for cancer treatments.

4.1.2 Previous biosynthetic studies of dehydrocurvularin

Considerable efforts have been invested in the biosynthesis of curvularin compounds. As early as 1959, Birch *et al.*¹⁸¹ showed that curvularin is derived from a head to tail condensation of eight acetic acid units by incorporation of [1-¹⁴C]acetic acid. With advanced NMR technology, our group¹⁷¹ was able to apply stable-isotope labeling methodology toward the mechanistic studies of dehydrocurvularin formation. A series of incorporation experiments, namely, incorporation of sodium [1-¹³C]-, [2-¹³C]-, [1, 2-¹³C₂]-, [1-¹³C, ²H₃]-, [2-¹³C, ²H₃]-

, and [1-¹³C, 2-¹⁸O₃]acetates into the dehydrocurvularin producing strain *Alternaria cinerariae* ATCC 11784, were conducted.¹⁷¹ These experiments not only led to the unambiguous NMR assignments of dehydrocurvularin, but also confirmed the origin of all constituent atoms (**Scheme 4-2**).



Scheme 4-2 Intact incorporation of acetate units into DHC in *A. cinerariae*.

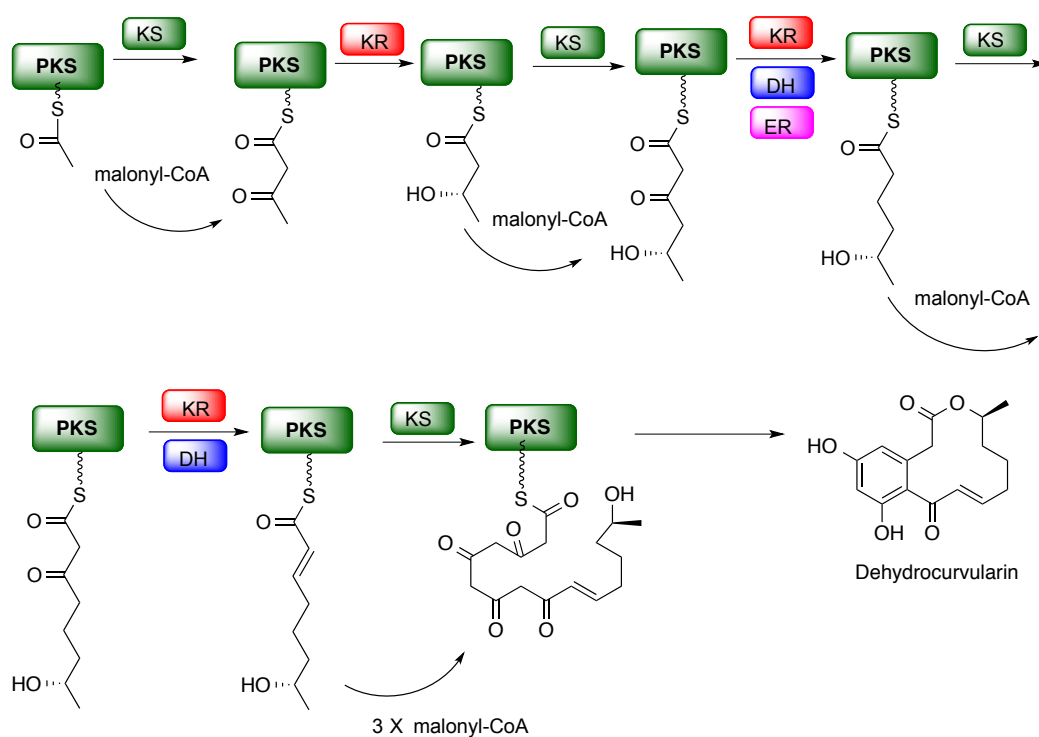
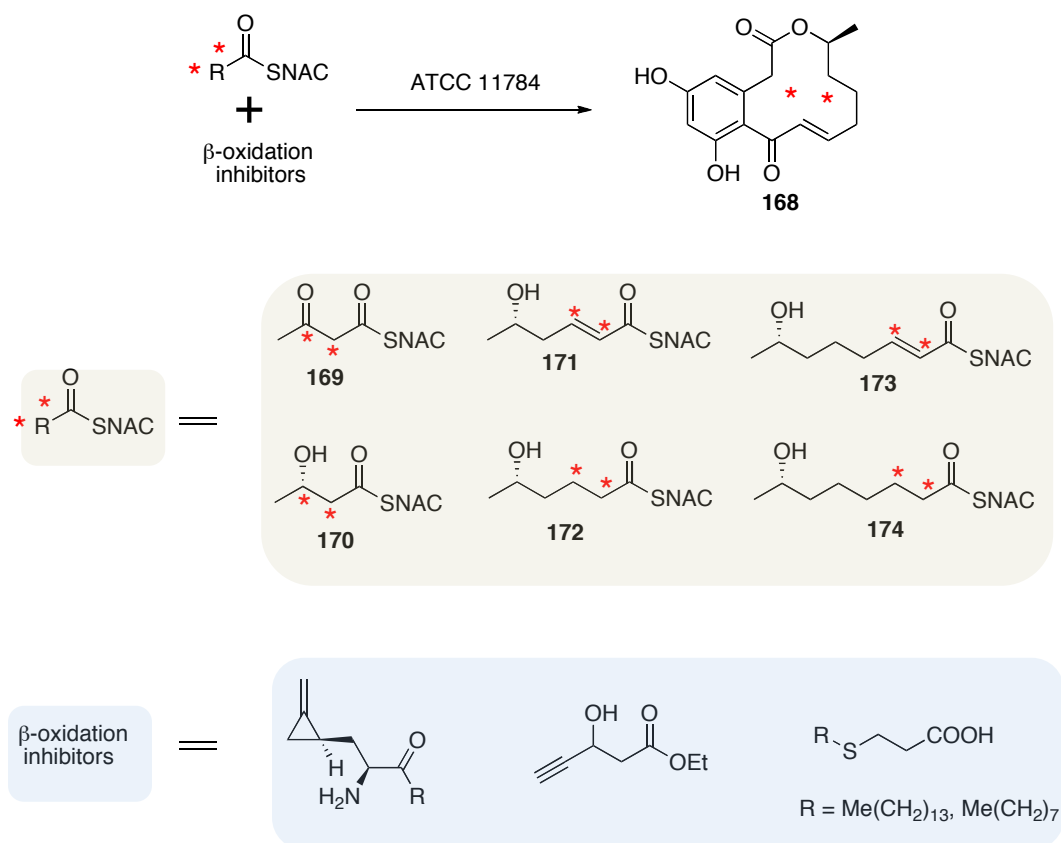


Figure 4-2 Proposed biosynthesis of dehydrocurvularin.

Based on the proposed biosynthesis of DHC (**Figure 4-3**), a set of ¹³C-labelled partially assembled precursors **169-173** were supplied to a culture of *A.*

cinerariae for incorporation of ^{13}C label into DHC (**Scheme 4-2**).^{125, 129} With the assistance of β -oxidation inhibitors, most of the partially assembled precursors were incorporated (**Table 4-1**) as determined by ^{13}C NMR and MS, except for triketides **171** and **172**. The successful incorporation of the partially assembled precursors supported the processive nature of polyketide synthase, in which the modifications of the β -position of the intermediates tethered to the ACP domain are completed before the next chain elongation.



Scheme 4-3 Incorporation of partially assembled precursors into dehydrocurvularin.

Table 4-1 Incorporation ratio of ¹³C-labeled partially assembled precursors.

Precursors	Diketide		Triketide		Tetraketide	
	169	170	171	172	173	174
Incorporation	22%	14%	None	None	70%	None

The exceptionally high incorporation ratio of **173** suggested the tetraketide might be the intermediate transferred to the downstream enzyme for further elaborations, analogous to hypothemycin and radicicol biosynthesis.^{40, 41} Indeed, DHC was produced when the tetraketide SNAC thioester was supplied to AtCuRS2 (**Figure 4-3A**), the NRPKS responsible for DHC production in *Aspergillus terreus*.¹⁸² Attempts to convert the reduced version of tetraketide, **174**, into curvularin in *A. cinerariae* was not successful, and this is consistent with the recent finding that **174** was transformed into **175** instead in *A. terreus* (**Figure 4-3B**).¹⁸²

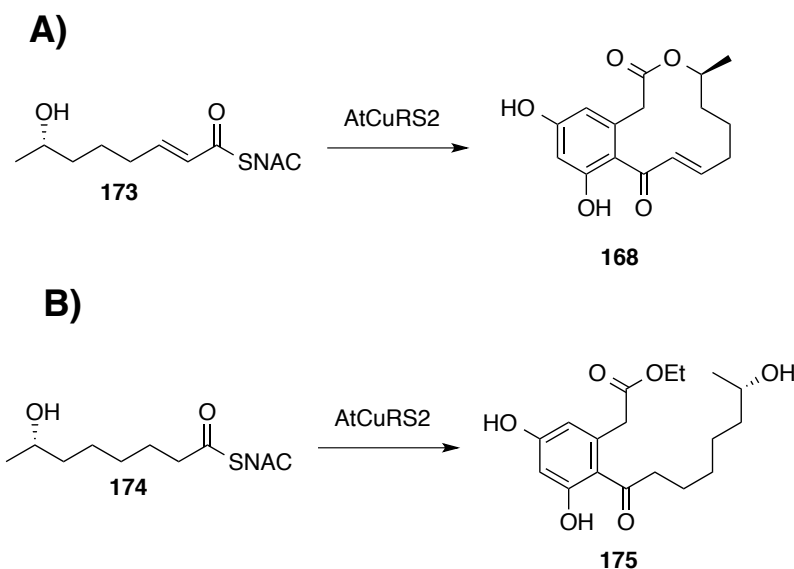


Figure 4-3 A) Production of DHC when supplying AtCuRS2 with L-5. B) Production of **175** when supplying AtCuRS2 with **174**.

4.1.3 Project Goals

Although progress has been made in the biosynthetic studies of dehydrocurvularin, there are still unresolved problems. The gene or gene clusters accounting for the production of DHC have not been identified in *A. cinerariae*. Uncovering the gene cluster and characterizing the specific PKSs responsible for DHC production *in vitro* and *in vivo* will advance our understanding of the mechanisms of the genetic factory, and could potentially guide us toward production of DHC analogues with improved biological activities. DHC bears a 12-membered dihydroxyphenylacetic acid lactone (DAL) moiety, in contrast to its congeners hypothemycin and radicicol, which feature a 14-membered resorcylic acid lactone (RAL). The differences are the result of distinct cyclization mechanisms catalyzed by the product template (PT) domains. C2-C7 cyclization yields RAL-type compounds such dehydrozearalenol; while C3-C8 cyclization

produces DAL-type compounds such as dehydrocurvularin (**Figure 4-4**). Insight into the structural details governing the cyclization mechanisms may allow us to design unique chemical structures.

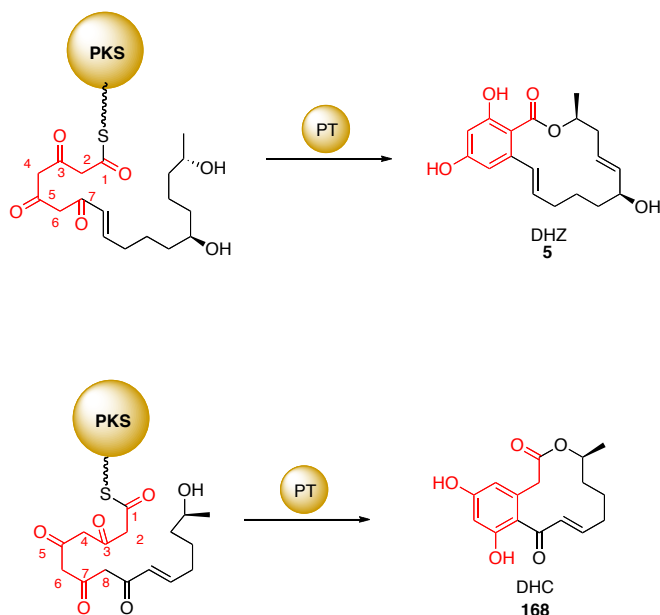


Figure 4-4 Distinct cyclization mechanisms during the formation of **5** and **168**. C2-C7 cyclization yields RALs, while C3-C8 cyclization yields DALs.

4.2 Results and discussion

4.2.1 Gene cluster for dehydrocurvularin

At the beginning of this study, genomic sequences of DHC producing strains were not available. In order to localize the gene cluster of DHC in *A. cinerariae* ATCC 11784, Dr. Sandra Marcus and Dr. Jesse Li in our group employed a degenerate PCR primers approach. The structural similarities between DHC and the RALs zearalenone, hypothemycin and radicicol (**Figure 4-5**), suggested that their biosynthesis might also be similar. A pair of degenerate PCR

primers was designed based on the sequence of the conserved KS domain of ZEA2 gene from *Gibberella zeae*.^{156, 183} This pair of primers was used to amplify the KS region of a PKS from *A. cinerariae* using its cDNA as a template. The amplified DNA was sequenced and new primers were designed based on the newly obtained sequences. These primers were used to amplify the KS domain from the genomic DNA of *A. cinerariae*, generating a DNA probe. A fosmid library of fragments of *A. cinerariae* genomic DNA was generated, which was hybridized with the DNA probe. Positive clones were sequenced by primer walking to reveal two PKS genes, a HRPKA and a NRPKS. In addition, the nucleotide sequences also revealed some other genes related to DHC biosynthesis.

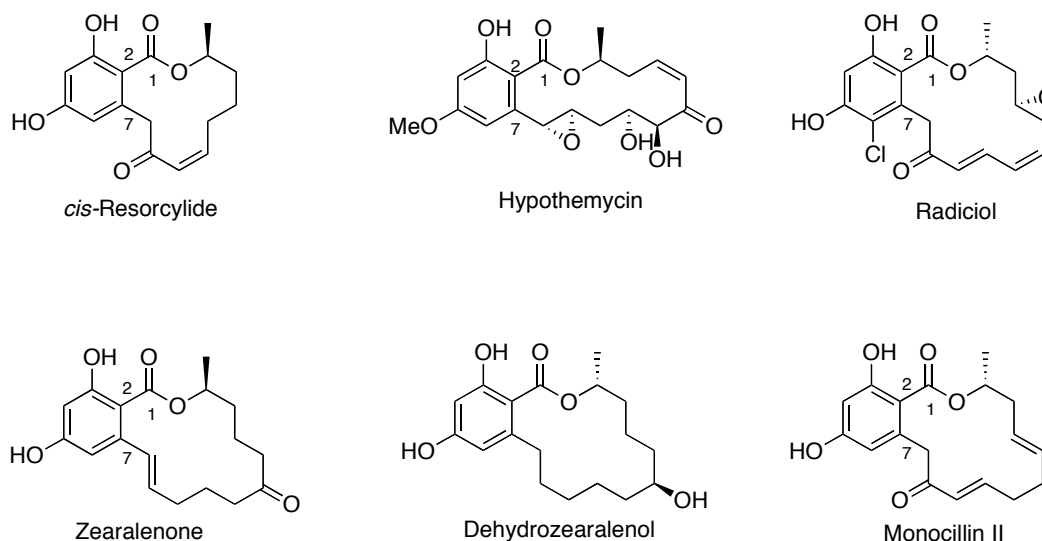


Figure 4-5 RAL-type compounds: *cis*-resorcyllide, hypothemycin, radicol, zearalenone, dehydrozearalenol and monocillin II.

With the rapid advancement of next generation sequencing, the cost for whole genome sequencing has been reduced dramatically, from tens of thousands

of dollars to less than three thousand dollars for fungi genomes, which falls into an affordable range for a single research group. To reduce the tedious and laborious sequencing work, we submitted the genome of *A. cinerariae* (ATCC 11784) for Illumina Sequencing (Ambry Genetics). Genomic sequences of 34 Mb located on 908 contigs were obtained.

The genomic sequence was annotated by antiSMASH (Antibiotics & Secondary Metabolite Analysis Shell, <http://antismash.secondarymetabolites.org/>), which is a recognized server for the identification, annotation and analysis of secondary metabolite biosynthesis gene clusters.^{184, 185} A total of 39 secondary metabolite genes were revealed in the genome of *A. cinerariae*, 8 of which are for type I iterative PKSs. Only one gene cluster, located on contig 59, closely resembles the gene clusters of hypothemycin and radicicol. Not surprisingly, it is the same gene cluster found by the degenerate PCR primer approach. This cluster of gene was virtually spliced by the HMM-based gene structure prediction program “Softberry” (<http://linux1.softberry.com/berry.phtml>), and the resulting genes were BLAST individually (<http://blast.ncbi.nlm.nih.gov/>). Five genes potentially related to the DHC biosynthesis were identified (**Figure 4-6**). Dhc1 is a 477 a.a. protein identified as a putative PKS-NRPS hybrid. A phosphopantetheine binding site and a thioester reductase-like domain are detected. Dhc2 (581 a.a.) belongs to the MFS (Major Facilitator Superfamily), which facilitates the transportation of molecules across membranes. Dhc4 (764 a.a.) is a typical transcriptional factor that contains Zn₂Cys₆ binuclear DNA-binding site. Dhc3 (2389 a.a.), a HRPKS,

shares 60%, 59% and 55% identity with Hpm8, PKS4 and RADS1 (HRPKS for radicicol biosynthesis in *Chaetomium chiversii*), respectively; while the NRPKS, Dhc5 (2079 a.a.), shares 54%, 53% and 53% identity with Hpm3, PKS13 and RADS2 (NRPKS for radicicol biosynthesis in *Chaetomium chiversii*), respectively.

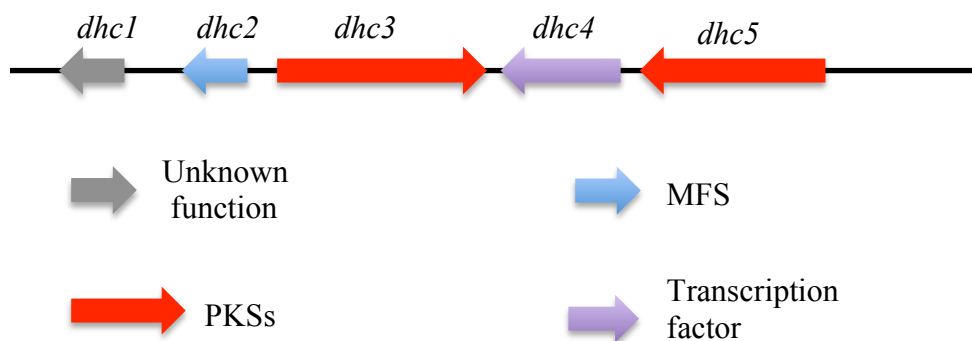


Figure 4-6 Gene cluster of dehydrocurvularin biosynthesis.

This cluster of genes encodes proteins that share great structural similarity with those encoded by a subsequently identified DHC gene cluster from *A. terreus*.¹⁸² Dhc2 and AtCurE are both efflux pumps and the sequence identity is 80%. Dhc4 displays the same transcriptional regulatory property as AtCurR and they share 55% sequence identity. The HR-NR PKS pair of Dhc3 and Dhc5 share 75% and 77% sequence identity with AtCurS1 and AtCurS2, respectively. No homologous gene was found in the *A. terreus* locus for Dhc1.

Surprisingly, the DHC genes from *A. cinerariae* exhibit even greater similarity with a set of orphan genes in *Pyrenophora tritici-repentis*. Dhc3 shares 88% sequence identity with a HRPKS (GenBank accession number EDU47225)

from *P. tritici-repentis*, and Dhc5 possesses 88% sequence identity with a NRPKS (GenBank accession number EDU47223) from *P. tritici-repentis*. In addition, the transporter Dhc2 and the transcriptional factor Dhc4 also have counterparts in *P. tritici-repentis*, GliA (92% sequence identity) and the C6 zinc finger domain containing protein (83% sequence identity). However, no Dhc1-like protein was found in the available genome sequence of *P. tritici-repentis*. The close homology suggests they might produce the same or a similar compounds. Indeed, *cis*-resorcyllide (**Figure 4-5**), a structural isomer of DHC, has been isolated from *P. tritici-repentis*. *cis*-Resorcyllide is derived from the same polyketide origin (both from 8 acetate units, with the same reductive modifications) as dehydrocurvularin, but the C2-C7 cyclization (**Figure 4-4**) renders it into the RAL family. It is unknown if this gene cluster is responsible for the production of *cis*-resorcyllide. Recent findings in Molnar's group¹⁸⁶ suggested three conserved residues (Phe¹⁴⁵⁵, Tyr¹⁵⁷⁶, and Trp¹⁵⁸⁴) in the PT domain of AtCurS2 control the DAL-type cyclization; while three conserved residues (Tyr¹⁴⁷⁸, Phe¹⁶⁰¹, and Trp¹⁶⁰⁹) in RADS2 lead intermediates to the RAL-type cyclization. Replacing the residues in AtCurS2 with their counterparts (Phe¹⁴⁵⁵ to Tyr¹⁴⁵⁵, Tyr¹⁵⁷⁶ to Phe¹⁵⁷⁶, and Trp¹⁵⁸⁴ to Leu¹⁵⁸⁴) produced a RAL-type of compound (**Figure 4-7B**). But the sequence of the PT domain in the putative conidial yellow pigment PKS also features these 3 residues (Phe¹⁴⁵⁵, Tyr¹⁵⁷⁶, and Trp¹⁵⁸⁴), which is inconsistent with the RAL folding of *cis*-resorcyllide. It is possible that this gene cluster is responsible for the biosynthesis of DHC instead of *cis*-resorcyllide, and *cis*-resorcyllide might be a product of unidentified gene

cluster. This question may well be worth further investigation by heterologous reconstitution of the HR-NR pair of PKSs.

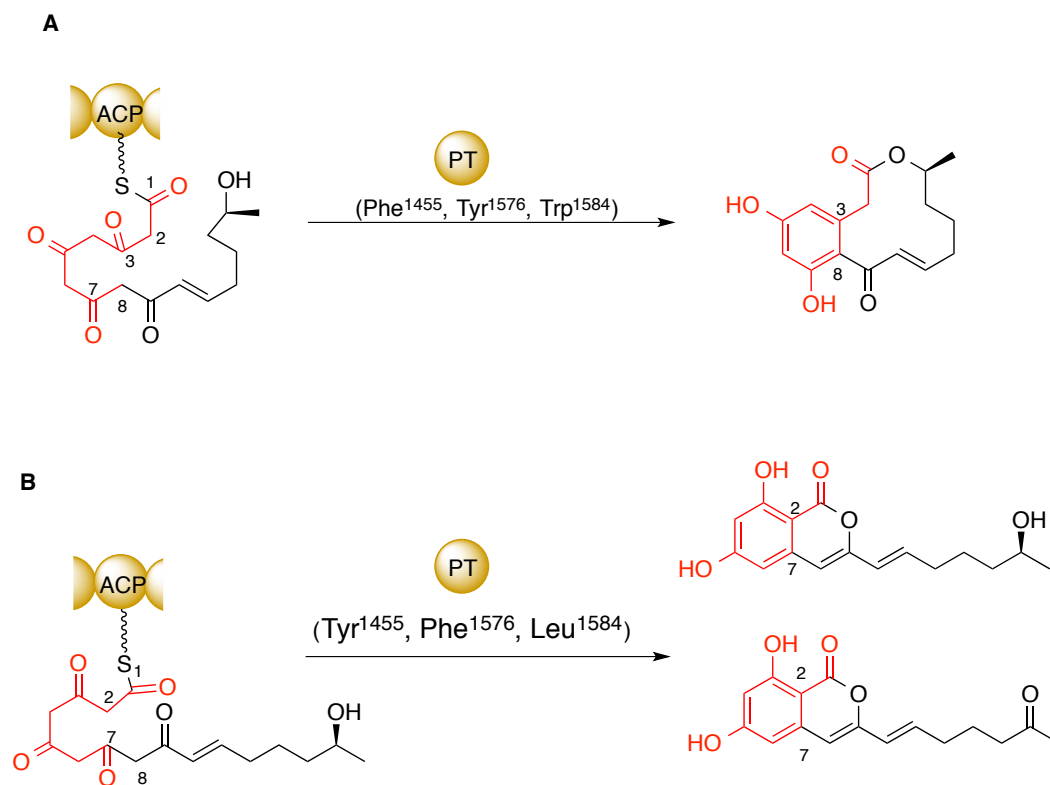


Figure 4-7 (A). Three conserved residues (Phe¹⁴⁵⁵, Tyr¹⁵⁷⁶, and Trp¹⁵⁸⁴) promote DAL-type cyclization. (B). Mutations of the three residues to Tyr¹⁴⁵⁵, Phe¹⁵⁷⁶, and Leu¹⁵⁸⁴ lead to RAL-type cyclization.

4.2.2 Proposed biosynthesis of dehydrocurvularin.

Dhc3 displays the typical domain architecture of a fungal HRPKS, KS-MAT-DH-core-ER-KR-ACP. The core domain consists of a structural KR pseudo-domain and an inactive CMeT pseudo-domain, analogous to Hpm8. Dhc5 consists of 6 domains, SAT, KS, MAT, PT, ACP and TE, which is a standard

arrangement for a fungal NRPKS. Recently advancements in RAL biosynthesis^{40, 41} prompted us to propose an improved biosynthetic pathway for DHC (**Figure 4-8**). Dhc3 synthesizes a tetraketide tethered to the ACP domain. With the assistance of the SAT domain, the tetraketide is transferred downstream to Dhc5. Dhc5 catalyzes another four rounds of chain elongation to generate an octaketide. The four adjacent keto groups of the octaketide undergo a Dieckmann condensation to furnish a resorcyate moiety, which is immediately transferred to the TE domain, where a macrolactonization reaction releases DHC from the enzyme.

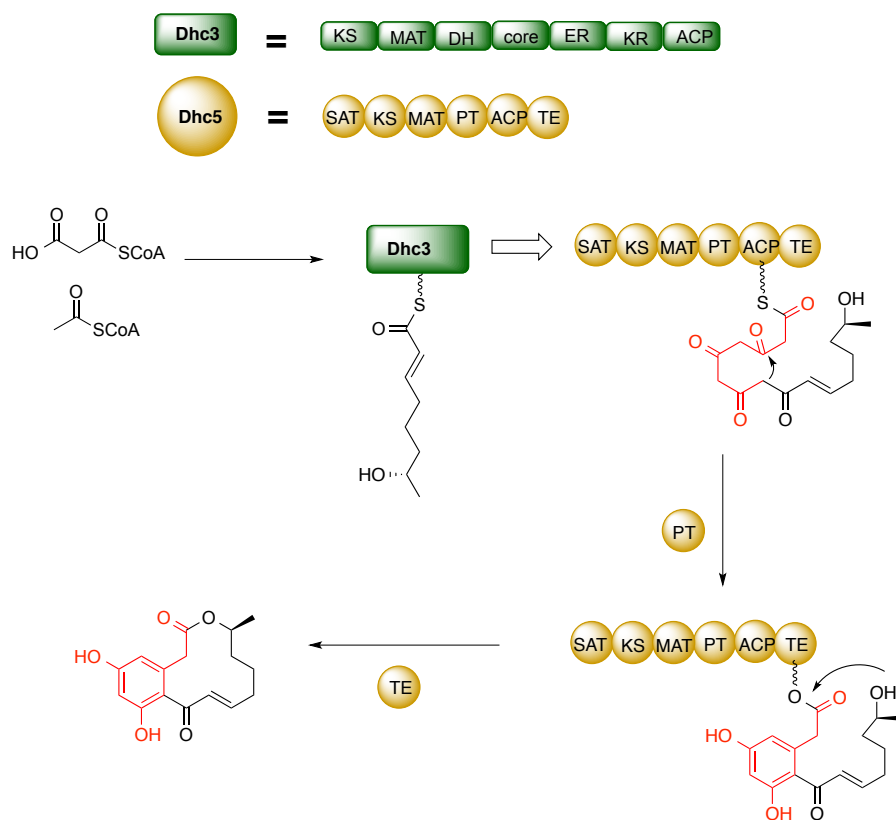


Figure 4-8 Proposed biosynthetic pathway for DHC.

4.2.3 Plasmid construction

4.2.3.1 Plasmids constructed (Collaboration with Mr. Gareth Lambkin)

One significant difference between prokaryotes and eukaryotes is that the genes in eukaryotes are interrupted by introns, which renders the manipulation of eukaryotic gene more challenging. Introns in the gene structures can be removed either by splicing the exons together by overlap-extension PCR,¹⁸⁷ or by recovering cDNA from the mRNA using a reverse transcriptase.

To obtain cDNA of the *A. cinerariae* ATCC 11784, total RNA was isolated from the *A. cinerariae* by Dr. Sandra Marcus. RT-PCR with SuperScript II Reverse Transcriptase using the total RNA as a template generated cDNA. The resulting cDNA was used as a template, from which to amplify the PKS genes (Figure 4-9).

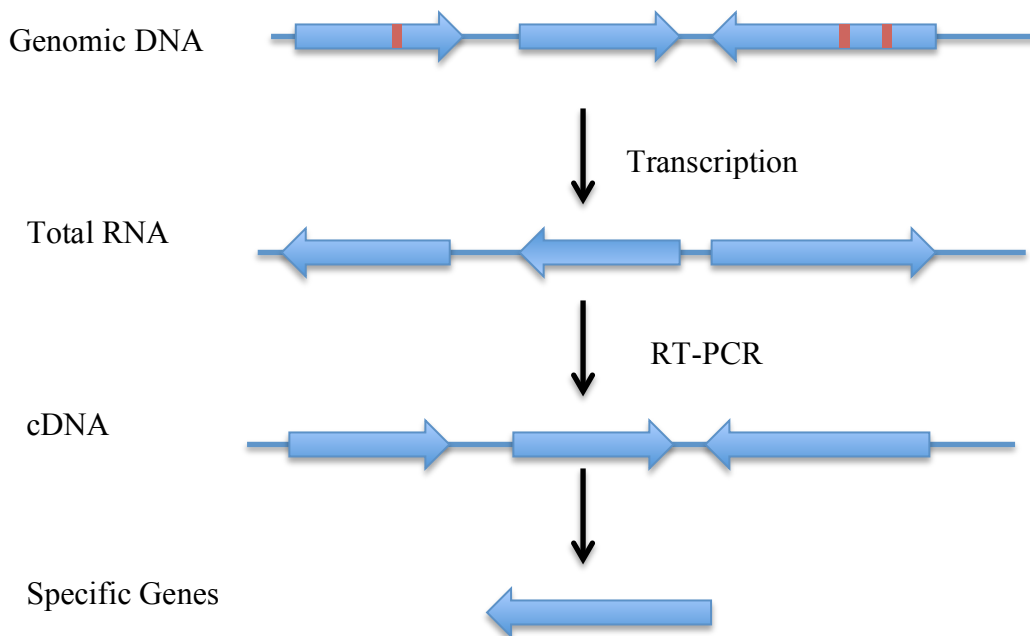


Figure 4-9 Synthesis of the first strain of cDNA. Red boxes represent introns.

Two 2 μ -based yeast-*E. coli* shuttle vectors, pKOS518-120A and pXK30, (from the Tang Lab) (**Figure 4-10**) were employed for the expression of PKSs. pKOS518-120A harbors the *hpm3* gene, and contains the *TRP1* auxotrophic marker and *NdeI*-*EcoRI* restriction endonuclease sites. pXK30 harbors the *lnks* (*lovastatin nonaketide synthetase*) gene and contains the *URA3* auxotrophic marker and *NdeI*-*PmlI* restriction endonuclease sites. Two expression vectors with different auxotrophic markers were employed in this study because the *TRP1* and *URA3* markers allow co-transformation of two plasmids containing *dhc3* and *dhc5* into BJ5464-NpgA.

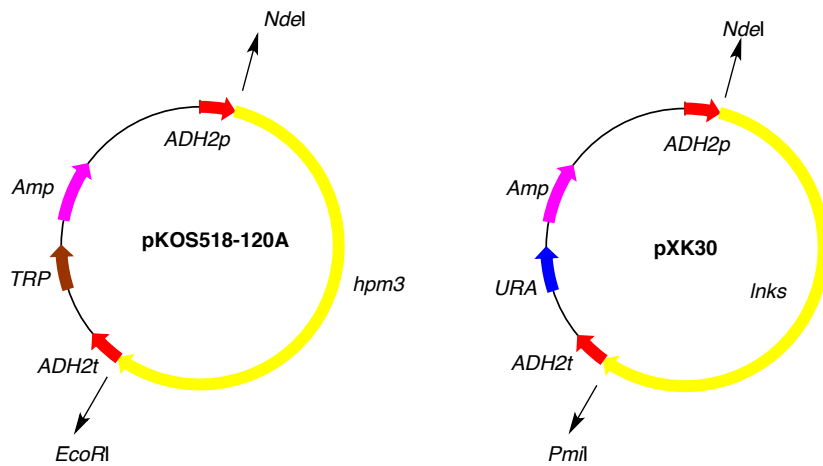


Figure 4-10 pXK30 and pKOS518-120A plasmids. Amp is the ampicillin resistance gene. ADH2p is the ADH2 promoter sequences. ADH2t is the ADH2 terminator sequences.

The native yeast ADH2 promoter is found upstream of the structural gene. The ADH2 promoter expression behaves in a glucose dependent manner: when glucose is present in the medium, the promoter is tightly repressed; upon the depletion of glucose, attachment of an alcohol dehydrogenase regulator protein (Adr1)¹⁸⁸⁻¹⁹⁰ onto the upstream activation site of the ADH2 promoter derepresses

the promoter and initiates the transcription.¹⁹¹ The advantage of this promoter is that no external inducer is required.

The transformation-associated recombination (TAR) method was used to construct expression plasmids.¹⁹² TAR is a very powerful tool used to assemble a large gene, as demonstrated by the chemical synthesis of the 582970 bp *Mycoplasma genitalium* genome by Gibson *et al.*¹⁹³ TAR requires that both ends of an insert gene carry about 35 bp of homologous sequences to a linearized vector. Co-transformation of the insert gene and the linearized vector into *S. cerevisiae* will yield circular plasmids containing the genes of interest (**Figure 4-11**).

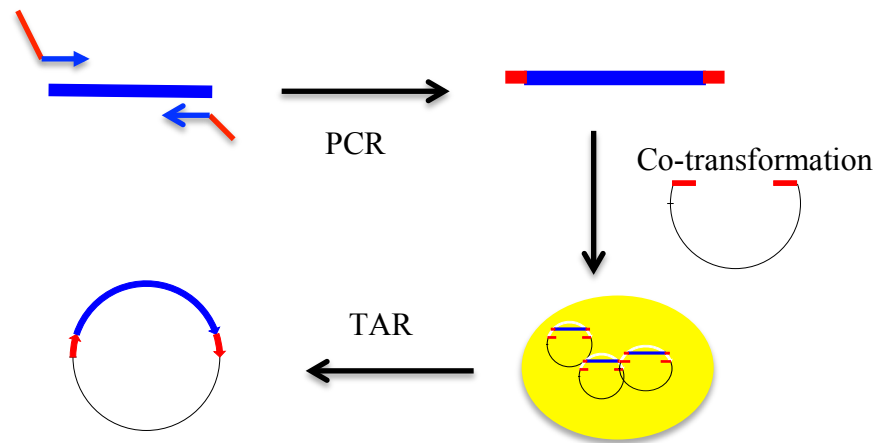


Figure 4-11 Construction of an expression plasmid by TAR in *S. cerevisiae*.

More recently, in the current work we amplified *dhc3* and *dhc5* with primer pairs containing a 35 bp overlap with the ADH2 promoter and terminator sequences of 2 μ -based yeast-*E. coli* shuttle vectors (pXK30 and pKOS518-120A). In addition, the 6 \times His tag encoding sequence was also introduced into the inserts

(at the C-terminus of the protein sequence) by PCR. However, only *dhc5* with extra homologous sequences on both ends was successfully generated. Amplification of *dhc3* formed a smear of products, as detected by gel electrophoresis. So a two-part strategy was used to subclone *dhc3* (**Figure 4-12**). In the first part, *dhc3-1*, the forward primer contains about 35 bp sequence of the ADH2 promoter; while the reverse primer is a primer for the middle of the *dhc3* sequence. In the second part, *dhc3-2*, the forward primer is a standard primer for the middle of the *dhc3* sequence, and the reverse primer contains 35 bp of the ADH2 terminator. The downstream end of the *dhc3-1* was designed to have more than 35 bp sequence overlap with the upstream end of *dhc3-2*. The resulting PCR products, *dhc3-1* combined with *dhc3-2*, and *dhc5*, were co-transformed with linearized pKOS518-120A (digested with *NdeI-EcoRI*) and pXK30 (*NdeI-PmlI*), respectively, into *S. cerevisiae* BJ5464-NpgA (**Figure 4-12**). TAR in the BJ5464-NpgA strain yielded two expression plasmids pGR-1 and pGR-2 harboring *dhc3* and *dhc5* respectively.

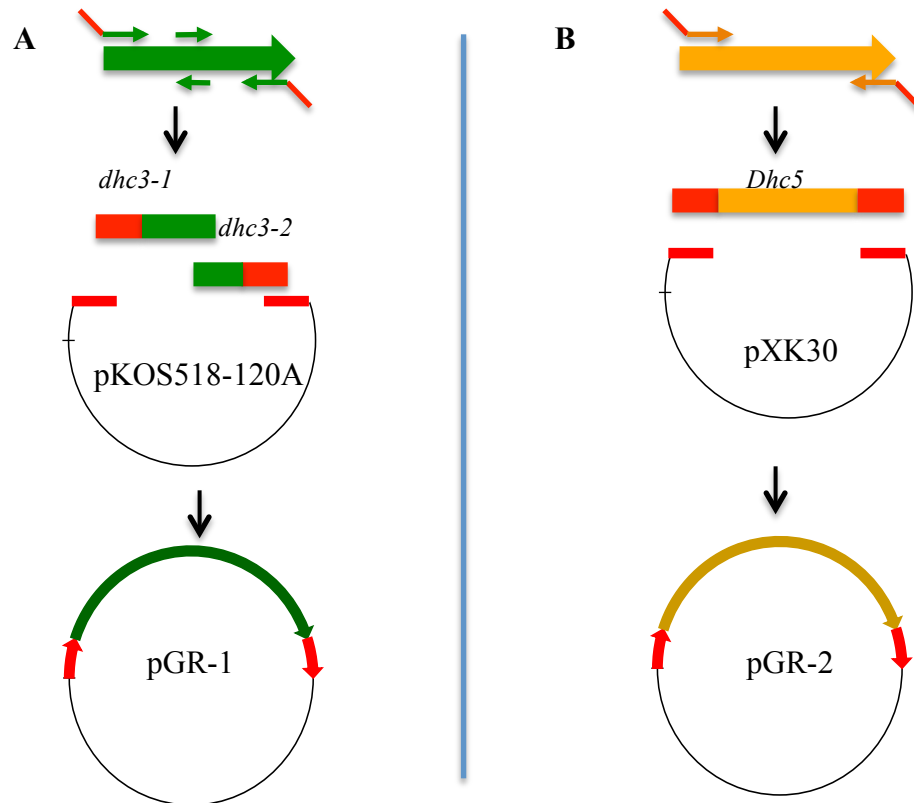


Figure 4-12 A) Construction of Dhc3 expression plasmid from *dhc3-1*, *dhc3-2* and linearized pKOS518-120A. B) Construction of the Dhc5 expression plasmid from *dhc5* and linearized pXK30.

Unfortunately, only Dhc3 was successfully expressed and purified from BJ5464-NpgA (**Figure 4-13**). Expression of Dhc5 cannot be detected by Coomassie blue stain or by Western blot. Co-transformation of pGR-1 and pGR-2 into BJ5464-NpgA did not produce DHC, suggesting the pGR-2 plasmid was not functional. Further investigation of the inserted sequences revealed that there are about 20 non-silent mutations in both genes, possibly introduced by the reverse transcriptase. Although these mutations did not occur in or near the active sites

based primary sequences, they might still responsible for the unsuccessful expression of Dhc5 and production of DHC.

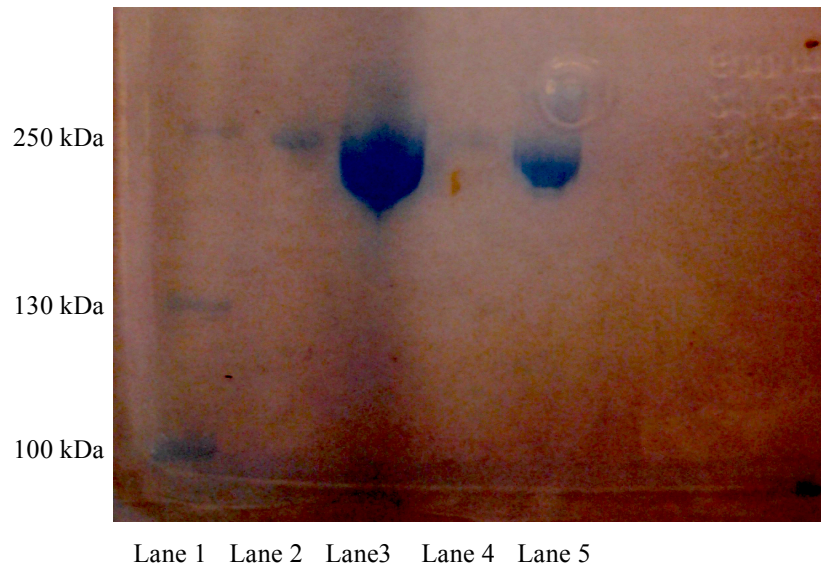


Figure 4-13 6% SDS-PAGE gel of proteins purified from *S. cerevisiae* BJ5464-NpgA containing *hpm3* and *dhc3* after Ni-NTA chromatography. Lane 1: Protein Marker. Lane 2: Dhc3 elution. Lane 3: concentrated Dhc3. Lane 4: Hpm3 elution. Lane 5: concentrated Hpm3.

4.2.3.2 Plasmid construction

The mutations in pGR-1 and pGR-2 indicated that either the cDNA used as the PCR template contain mutations or the PCR created mutations. New cDNA from *A. cinerariae* was generated. First, total RNA was isolated from 7 days culture of *A. cinerariae* with an RNeasy Plant Mini Kit (Qiagen). In order to avoid mutations in the cDNA, the more accurate AccuScript HighFidelity 1st Strand cDNA Synthesis Kit (Agilent) was employed to construct the cDNA library from the total RNA with the poly(T) primer provided by the kit. Gene

specific primers were then used to amplify *dhc3* and *dhc5* individually, in order to construct Dhc3 and Dhc5 expression plasmids.

4.2.3.2.1 Dhc3 plasmid construction

Attempts to amplify of *dhc3* with about 35 bp of complementary sequences with the ADH2 promoter and terminator resulted in no PCR products. Changing the PCR conditions (annealing temperatures, template concentrations) did not alter the result. So an alternative route was employed (**Figure 4-14**). Instead of attaching complementary sequences onto the insert, homologous sequences were introduced to the vector. Linearization of pGR-1 by PCR, followed by TAR in *S. cerevisiae* with *dhc3* generated plasmid pGzzB116. Replication of pGzzB116 in *E. coli* DH5 α and subsequent sequence analysis showed nine mutations in the *dhc3* insert. These mutations again could be copied from the cDNA template. However, the PCR product derived from cDNA, showed no mutations in the half readable sequences of *dhc3* (only half of the sequence was recovered because the concentration of the PCR product is low). The batch of DH5 α that was used might have introduced these mutations during replication. Changing to a fresh batch of DH5 α (Invitrogen), together with changing from Platinum *Taq* HIFI DNA Polymerase to the more faithful *Pfu*Ultra II Fusion HS DNA polymerase for amplification of *dhc3*, generated two constructs with many fewer mutations: one with 1 mutation, and one with 2 silent mutations (pGzzB221).

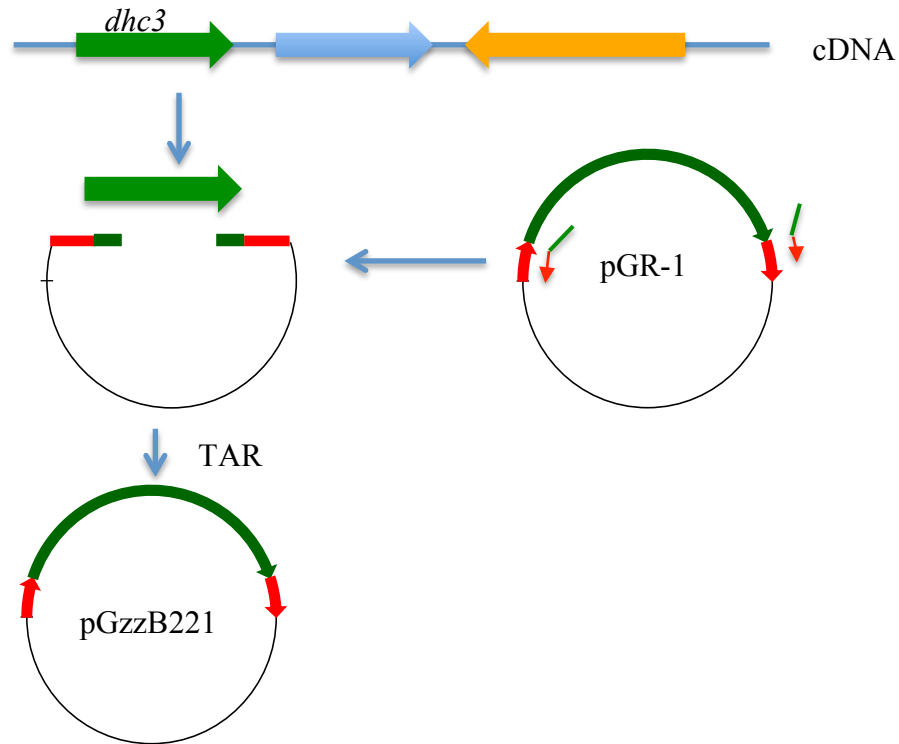


Figure 4-14 An alternative way to construct Dhc3 expression plasmid.

4.2.3.2.2 Dhc5 plasmid construction

Similar to *dhc3*, amplification with a pair of long primers (35 bp) did not provide the desired *dhc5*. Because the introns of *dhc5* are all located within the first 3000 bp, two parts, *dhc5-1* and *dhc5-2*, were designed. To decrease the possibility of mutations, *dhc5-1* was amplified from cDNA to remove the introns, while the remaining 4000 bp were obtained from amplification of genomic DNA (**Figure 4-15**). This approach generated four plasmids with two, three, three and six mutations respectively. These results suggest the genomic DNA might not be a good choice. Encouraged by the result of Dhc3 construct, *dhc5* was amplified from cDNA using *PfuUltra* II Fusion HS DNA polymerase. Amplicon *dhc5* was

co-transformed with linearized pGR-2 to BJ5464-NpgA to furnish two constructs: one having one mutation, and the other one (pGZZB237-8) not having any mutation.

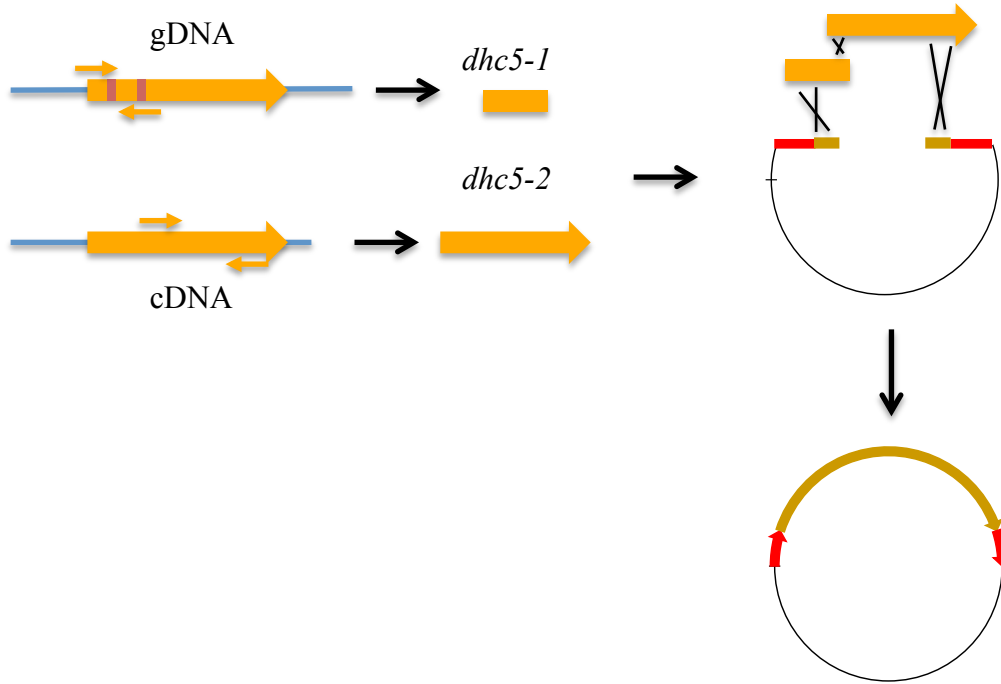


Figure 4-15 Construction of Dhc5 expression plasmid from gDNA and cDNA.

Surprisingly, expression of Dhc5 by transformation of BJ5464-NpgA with pGzzB237-8 was not successful. Carefully examining the sequences suggested that one A is missing in the poly(A) part of the ADH2 promoter, which might account for the unsuccessful expression of Dhc5. DNA polymerase might have introduced this mutation during the linearization of pXK30 using PCR. To fix this problem, the *dhc5* with about 35 bp overlap with ADH2 promoter was amplified from pGzzB237-8. Digest the pXK30 plasmid and subsequent TAR with *dhc5* generated two constructs pGzzB255 (one mutation), pGzzB257 (no mutation). Dhc5 could be expressed from both plasmids in BJ5464-NpgA (**Figure 4-16**).

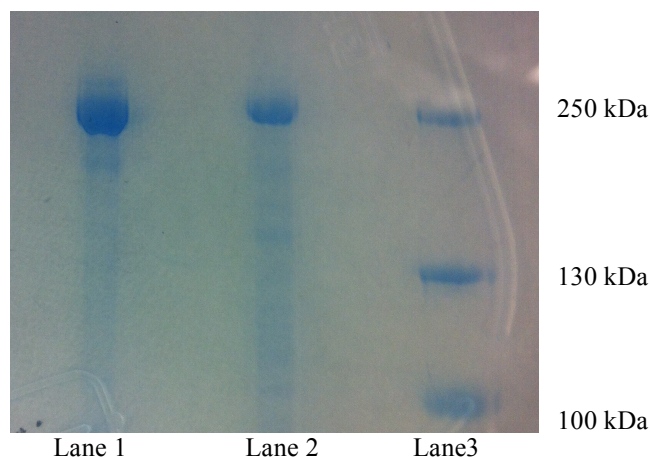


Figure 4-16 6% SDS-PAGE gel of proteins purified from *S. cerevisiae* BJ5464-NpgA containing *dhc5* after Ni-NTA chromatography. Lane 1: concentrated Dhc5 (no mutation). Lane 2: Concentrated Dhc5 (1 mutation). Lane 3: Protein Marker.

4.2.4 Attempts toward reconstitution of the biosynthesis of DHC

To test whether Dhc3 and Dhc5 are responsible for production of DHC, plasmids pGzzB221 and pGzzB257 harboring the *dhc3* and *dhc5* genes were co-transformed into BJ5464-NpgA. Culturing the resulting yeast for 3 days did not produce any detectable amount of DHC. This was unexpected because it was certain that both Dhc3 and Dhc5 enzymes are present in the culture, because both enzymes can be expressed individually (**Figure 4-16** and **Figure 4-17**). During the course of this study, a pair of HRPKS and NRPKS from *A. terreus*, AtCurR1 and AtCurR2, was discovered to produce DHC in BJ5464-NpgA. Therefore, Dhc3 and Dhc5, analogous to AtCurR1 and AtCurR2, should be able to produce DHC in BJ5464-NpgA. To rule out the possibility that the 6xHis tag may interfere with the interaction between Dhc3 and Dhc5, a version of Dhc5 without 6xHis tag, pGzzB255-ΔHis was constructed. However, co-expression of pGzzB221 and

pGzzB255-ΔHis did not produce DHC, suggesting the 6xHis tag might not be the problem.

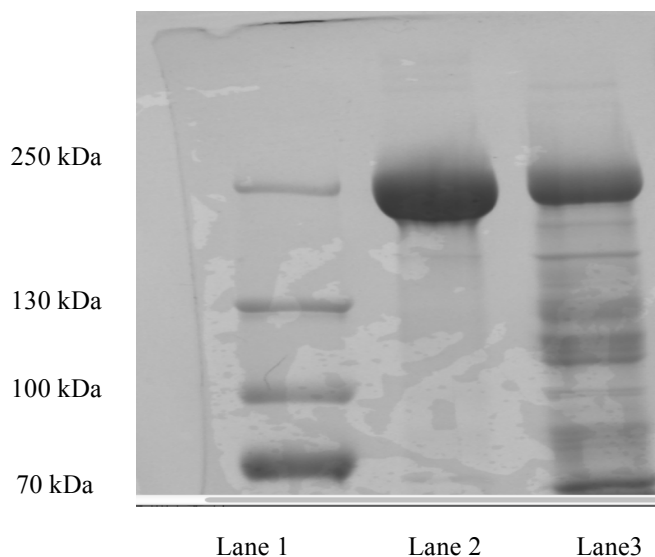
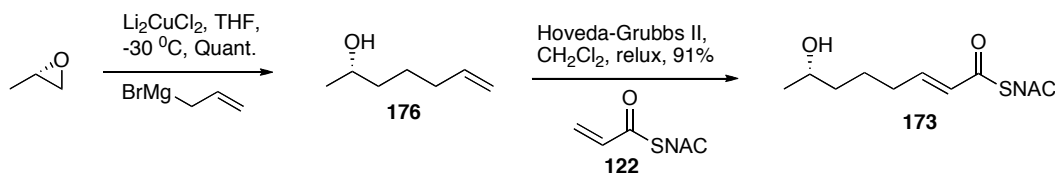


Figure 4-17 6% SDS-PAGE gel of proteins purified from *S. cerevisiae* BJ5464-NpgA containing *hpm3* and *dhc3* after Ni-NTA chromatography. Lane 1: Protein Marker. Lane 2: concentrated Hpm3. Lane 3: concentrated Dhc3.

Another way to test the biosynthesis of DHC is to test if the NRPKS (Dhc5) can accept the proposed tetraketide and extended it to DHC. So the tetraketide in its SNAC form was synthesized (**Scheme 4-4**). The commercially available (*S*)-propylene oxide was treated with allylmagnesium bromide in the presences of Li_2CuCl_2 to generate **176**. Cross metathesis between **176** and **122** furnished the desired tetraketide **173** in two steps.



Scheme 4-4 Synthesis of tetraketide **173**.

Adding **173** (100 mg/L) to BJ5464-NpgA cultures harboring the Dhc5 expression plasmid did not yield any detectable amount of DHC. This reminds us of the problem of lovastatin biosynthesis. Co-expression of LovB and LovC in BJ5464-NpgA did not furnish the desired product dihydromonacolin L, an advanced precursor of lovastatin biosynthesis. However, production of dihydromonacolin L could be restored by the addition of exogenous TE enzymes. Recently, Yi Tang and co-workers¹⁹⁴ demonstrated a cryptic thioesterase, LovG, is responsible for the offloading of dihydromonacolin L. This finding prompted us to look for a *trans*-acting thioesterase in the *A. cinerariae* genome. Blasting the LovG sequence against the ATCC1174 genome did yield some hits but nothing close to the DHC locus. Ma *et al.*⁵⁴ suggested a small amount of dihydromonacolin L could be removed from LovB by a base treatment. However, KOH treatment of Dhc5 after supplied with **173** and malonyl-CoA did not yield DHC as detected by LC-MS.

4.3 Conclusions

The genome of *A. cinerariae* ATCC 11784 was sequenced and a putative gene cluster of DHC was identified. The gene cluster encodes five genes, two of which are putative iterative PKSs. Dhc3 is a putative HRPKS, displaying great sequence similarity to Hpm8; and Dhc5 is a putative NRPKS, showing similarity to Hpm3.

Expression plasmids harboring *dhc3* and *dhc5* were successfully constructed. Transformation of BJ5464-NpgA using plasmids harboring *dhc3* and

dhc5 individually yielded Dhc3 and Dhc5 enzymes, respectively, after Ni-NTA chromatography purification. Reconstitution of DHC production *in vivo* in BJ5464-NpgA was not successful, despite the fact that both PKSs can be expressed in the heterologous system. Putative biosynthetic intermediate **173** was synthesized to test the biosynthesis of DHC *in vivo*. However, DHC was not produced when **173** was added to the Dhc5 expression culture.

The following are two possible reasons for the unsuccessful production of DHC in BJ5464-NpgA.

1) The gene cluster of DHC is mis-identified. This is unlikely because genomic annotation and blast searches all suggest that this pair of HRPKS and NRPKS is a very possible candidate for DHC production. In addition, AntiSMASH analysis of genomic sequence indicates that only this cluster of genes shows significant homology with those for hypothemycin, radicicol and zearalenone. Furthermore, this gene cluster shows great sequence identity to the gene cluster of DHC from *A. terreus*. All these data indicate that this is the right gene cluster for DHC in *A. cineraria*. However, further efforts are needed to demonstrate the functions of Dhc3 and Dhc5. One possible way is the RNA silencing approach.¹⁹⁵ It has been found short interfering RNAs could trigger the silencing of gene expression. Therefore, gene specific RNAs can be designed and transformed to *A. cineraria* ATCC 11784 to test whether the production of DHC could be suppressed. Alternatively, knock-out of *dhc3* and *dhc5* in *A. cineraria* ATCC 11784 could also probe the functions of DHC3 and DHC5.

2) Other cryptic genes are involved in production of DHC. Dhc1, which is located at the beginning of the DHC gene cluster, is similar to a PKS-NRPKS hybrid containing PP and NADPH binding sites. It is unclear as to the function of Dhc1, and it may play a crucial role in the biosynthesis of DHC. In addition, no Dhc1-like protein is present in *A. terreus*. Therefore, *A. cinerariae* may utilize different mechanisms for the biosynthesis of DHC, in contrast to *A. terreus*, where a pair of HRPKS and NRPKS is sufficient to produce DHC in BJ5464-NpgA. To verify the function of Dhc1, the *dhc1* gene can be cloned and inserted into an expression plasmid, which can be co-transformed with expression plasmids encoding DHC3 and DHC5 into BJ5464-NpgA to check for the production of DHC.

In summary, to gain an understanding of the programming rules of fungal iterative PKSs, we and our collaborators investigated the biosynthesis of three natural products, hypothemycin, radicicol and dehydrocurvularin. (1) We found that a pair of HRPKS and NRPKS is employed to produce the first PKS products during the biosynthesis of hypothemycin and radicicol. In addition, our data suggest the two NRPKSs (Hpm3 and Rdc5) display relaxed substrate specificity. HRPKS Hpm8 also exhibits decent substrate specificity. Hpm8 could accept substrate analogues to produce *epi*-DHZ and β -zearalenol. Moreover, a chlorinase, Rdc2, shows relaxed substrate specificity as it could effectively produces chlorinated-DHZ. Therefore, iterative PKSs and their post-PKS enzymes could be potentially employed in the combinatorial biosynthesis to generate polyketide analogues, where traditional medicinal chemistry encounters

significant challenges because of the complex structures of polyketides. (2) By incubating the Hpm8 KR domain with a series of β -keto SNAC thioesters, we found that the KR domain displays a substrate-tuning stereospecificity: the chain length of the substrates solely dictates the stereospecificity. This result suggests that substrate-enzyme interactions in iterative PKSs are more dynamic than that of modular PKSs, where all the active sites are pre-fixed for specific actions. Our finding is an important step toward fully deciphering the cryptic programming of fungal PKSs. (3) Next-generation genomic sequencing plays an increasing role in the current biosynthetic studies. Genomic sequencing plus the ready available bioinformatics tools vastly reduce the time and cost of biosynthetic studies of natural products. By sequencing *A. cineraria* genome, we identify a putative gene cluster for DHC production. The two putative PKSs (DHC3 and DHC5) were successfully expressed and purified from *S. cerevisiae* strain BJ5464-NpgA. Moreover, genomic sequencing also uncovered many other putative PKS gene clusters. Expression of these gene clusters in heterologous hosts could potential produce more structurally diverse polyketides.

Chapter 5: Experimental

5.1 General synthetic procedures

5.1.1 Reagents, solvents, and purifications

All reactions involving air or moisture sensitive reactants were conducted under a positive pressure of dry argon. All solvents and chemicals were reagent grade and used as supplied unless otherwise stated. ^{13}C labeled acetyl chloride and acrylic acid were purchased from *Cambridge Isotope Laboratories*. All other chemical reagents were purchased from *Sigma-Aldrich Chemical Company*, *Alfa Aesar*, *Tokyo Chemical Industry*. For anhydrous reactions, solvents were dried according to the procedures detailed in Perrin and Armarego.¹⁹⁶ Tetrahydrofuran and diethyl ether were distilled over sodium and benzophenone under an atmosphere of dry argon. Acetonitrile, dichloromethane, methanol, pyridine, and triethylamine were distilled over calcium hydride. Deionized water was obtained from a Milli-Q reagent water system (Millipore Co., Milford, MA). Unless otherwise specified, solutions of NH_4Cl , NaHCO_3 , HCl , NaOH , KOH , $\text{Na}_2\text{S}_2\text{O}_3$, and LiOH refer to aqueous solutions. Brine refers to a saturated solution of NaCl . Removal of solvent was performed under reduced pressure, below 40 °C, using a Büchi rotary evaporator. All reactions and fractions from column chromatography were monitored by thin layer chromatography (TLC). Analytical TLC was done on glass plates (5 × 1.5 cm) precoated (0.25 mm) with silica gel (normal SiO_2 , Merck 60 F₂₅₄). Compounds were visualized by exposure to UV light and by dipping the plates in 1% $\text{Ce}(\text{SO}_4)_2 \cdot 4\text{H}_2\text{O}$ 2.5% $(\text{NH}_4)_2\text{MoO}_7 \cdot 4\text{H}_2\text{O}$ in 10%

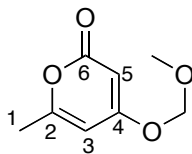
H₂SO₄ followed by heating on a hot plate. Flash chromatography was performed on silica gel (EM Science, 60Å, 230-400 mesh).

5.1.2 Compound characterization

Nuclear magnetic resonance (NMR) spectra were obtained on Varian Inova 400, Varian Mercury 400, Varian Inova 500 MHz, Varian 500 (equipped with cryo-probe) or 600 MHz spectrometers. ¹H NMR chemical shifts are reported in parts per million (ppm) using the residual proton resonance of solvents as reference: CDCl₃ δ 7.26, CD₂Cl₂ δ 5.32, and CD₃OD δ 3.30. ¹³C NMR chemical shifts are reported relative to CDCl₃ δ 77.0, CD₂Cl₂ δ 53.8, and CD₃OD δ 49.0. Infrared spectra (IR) were recorded on a Nicolet Magna 750 or a 20SX FT-IR spectrometer. Film Cast refers to the evaporation of a solution on a NaCl plate. Mass spectra were recorded on a Kratos IMS-50 (high resolution, electron impact ionization (EI)), and a ZabSpec IsoMass VG (high resolution, electrospray (ES)). Optical rotations were measured on Perkin Elmer 241 polarimeter with a microcell (10 cm, 1 mL) at 23 °C.

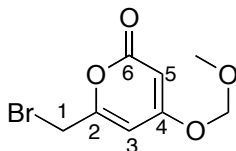
5.2 Synthesis and characterization of compounds

4-(Methoxymethoxy)-6-methyl-2H-pyran-2-one (9)



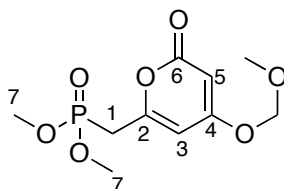
The known compound¹⁹⁷ was prepared as follows. To a stirred solution of 4-hydroxy-6-methyl-2H-pyran-2-one (2.00 g, 15.8 mmol) in 35 mL DCM was added 2.43 mL (45.0 mmol) *i*Pr₂EtN at 0 °C under Ar. After stirring for 10 min at 0 °C, 1.32 mL (17.4 mmol) methoxymethyl chloride (MOMCl) was added and the reaction was warmed up to 25 °C. After stirring for 12 h, the reaction was diluted with Et₂O (100 mL) and washed with NH₄Cl (100 mL), brine (100 mL) and then dried over Na₂SO₄. The solvent was removed *in vacuo* and the residue was purified using flash column chromatography (1:1 EtOAc/hexanes) to give the product (2.18 g, 81%) as a white solid. IR (CH₂Cl₂, cast film) 3091, 2961, 2923, 2835, 1710, 1648, 1567cm⁻¹; ¹H NMR (500 MHz, CDCl₃): δ 5.81 (m, 1H, H-3), 5.57 (dd, 1H, *J* = 2.2, 04 Hz, H-5), 5.13 (s, 2H, OCH₂O), 3.45 (s, 3H, OCH₃), 2.20 (dd, *J* = 0.9, 0.5 Hz, 3H). ¹³C NMR (125 MHz, CDCl₃) δ 168.7, 164.6, 162.6, 100.1, 94.2, 90.2, 56.9, 19.9; HRMS (ES) calculated for C₈H₁₀O₄Na, 193.0471; found 193.0469 [M+Na]⁺.

6-(Bromomethyl)-4-(methoxymethoxy)-2-pyrone (10)



The known compound¹⁹⁷ was prepared as follows. To a stirred solution of **9** (1.50 g, 6.02 mmol) in 75 mL CCl₄ was added AIBN (300 mg, 1.76 mmol) and NBS (1.15 g, 19.4 mmol) under Ar. The reaction mixture was stirred at 80 °C with reflux for 12 h. The precipitate in the mixture was filtered and the solvent was removed *in vacuo*. The residue was then purified using flash column chromatography (1:2 EtOAc/ hexanes) to yield the product (1.20 g, 55%) as a light orange solid. IR (CH₂Cl₂, film cast) 3096, 3038, 2966, 2834, 1728, 1650, 1483; ¹H NMR (300 MHz, CDCl₃): δ 6.10 (d, 1H, *J* = 2.1 Hz, H-3), 5.62 (d, 1H, *J* = 2.2 Hz, H-5), 5.12 (s, 2H, OCH₂O), 4.08 (s, 2H, H-1), 3.41 (s, OCH₃); ¹³CNMR (125 MHz, CDCl₃): δ 167.8, 163.2, 159.0, 102.2, 94.5, 92.5, 57.1, 26.6; HRMS (ES) calculated for C₈H₉BrO₄Na, 270.9576; found 270.9576 [M+Na]⁺.

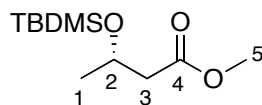
Dimethyl (4-(methoxymethoxy)-2-oxo-2H-pyran-6-yl) methylphosphonate (11)



The known compound¹⁹⁷ was prepared as follows. Trimethyl phosphite (1.00 mL, 8.42 mmol) was added to **9** (400 mg, 1.37 mmol) (neat). The reaction mixture was

stirred under reflux at 60 °C for 24 h. The residual phosphite was removed under reduced pressure and the resulting residue was purified using flash column chromatography (100:3 EtOAc/ MeOH) to afford the product (430 mg, 96%) as a light yellow oil. IR (CH₃Cl film cast) 3094, 2958, 2852, 1718, 1647, 1564 cm⁻¹; ¹H NMR (500 MHz, CDCl₃): δ 6.04 (dd, 1H, *J* = 3.8, 2.2 Hz, H-3), 5.65 (t, 1H, *J* = 2.0 Hz, H-5), 5.15 (s, 2H, OCH₂O), 3.81 (d, 6H, *J*_{1H-31P} = 11.1 Hz, H-7), 3.47 (s, 3H, OCH₃), 3.05 (d, 2H, *J*_{1H-31P} = 22.0 Hz, H-1). ¹³CNMR (125 MHz, CDCl₃): δ 168.3 (d, *J*_{1C-31P} = 3.2 Hz), 163.7 (d, *J*_{1C-31P} = 1.0 Hz), 156.2 (d, *J*_{1C-31P} = 9.5 Hz), 102.5 (d, *J*_{1C-31P} = 8.2 Hz), 94.4, 91.3 (d, *J*_{1C-31P} = 2.6 Hz), 57.1, 53.3 (d, *J*_{1C-31P} = 6.6 Hz), 31.4 (d, *J*_{1C-31P} = 139.8 Hz). HRMS (ES) calculated for C₁₀H₁₅PO₇Na, 301.0447; found 301.0448 [M+Na]⁺.

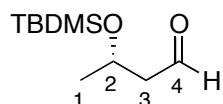
(S)-methyl 3-(*tert*-butyldimethylsilyloxy)butanoate (14)



The known compound¹⁹⁸ was prepared according to literature procedure. To a stirred solution of (*S*)-methyl 3-hydroxybutanoate (1.18 g, 10.2 mmol) in 5 mL dry DMF was sequentially added *tert*-butyldimethylsilyl chloride (1.93 g, 12.5 mmol) and imidazole (1.03 g, 15.0 mmol). The solution was stirred for 12 h at 25 °C and then poured into hexanes (100 mL). The layers were separated and the organic layer was washed with H₂O (3 × 100 mL), brine (50 mL), dried over Na₂SO₄ and concentrated *in vacuo* to give the product as a colorless oil (2.40 g, quant.). IR (CHCl₃, film cast) 2956, 2897, 2857, 1757 cm⁻¹; ¹H NMR (300 MHz,

CDCl₃) δ 4.29-4.21 (m, 1H), 3.64 (s, 3H, H-5), 2.46 (dd, 1H, J = 14.5, 7.6 Hz, H-3), 2.35 (dd, 1H, J = 14.5, 5.3 Hz, H-3), 1.17 (d, 3H, J = 6.1 Hz, H-1), 0.88 (s, 9H, Si-C(CH₃)₃), 0.04 (s, 3H, SiCH₃), 0.02 (s, 3H, SiCH₃); ¹³C NMR (125 MHz, CDCl₃) δ 172.1, 65.8, 51.4, 44.7, 25.7, 23.9, 17.9, -4.5, -5.1; [α]_D²⁵ = -22.1 (c = 1.50, CHCl₃).

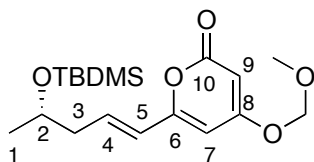
(S)-3-(tert-butyldimethylsilyloxy)butanal (15)



The known compound¹⁹⁹ was prepared according to literature procedure. To a stirred solution of **14** (2.32 g, 10.4 mmol) in 10 mL CH₂Cl₂ was added DIBAL (1.0 M in CH₂Cl₂, 11.0 mL, 11.0 mmol) over 15 min at -78 °C. The reaction mixture was stirred for 1.5 h at -78 °C, and then 4 mL MeOH was added to quench the excess DIBAL. The solution was diluted with Et₂O, and 20 mL of saturated aqueous potassium sodium tartrate was added. The mixture was stirred until 2 clear layers had formed. The 2 layers were separated and the organic layer was washed with brine (20 mL) and then dried over Na₂SO₄. The solvent was removed *in vacuo* and then purified using flash column chromatography (1:15 Et₂O /hexanes) to give the product (1.22 g, 60%) as a colorless oil. IR (CHCl₃, cast film) 2957, 2930, 2888, 2858, 2720, 1730 cm⁻¹; ¹H NMR (300 MHz, CDCl₃) δ 9.79 (dd, 1H, J = 2.8, 2.1 Hz, H-4), 4.29-4.21 (m, 1H, H-1), 2.54 (ddd, 1H, J = 15.7, 7.0, 2.8 Hz, H-3), 2.46 (dd, 1H, J = 15.7, 4.9, 2.1 Hz, H-3), 1.23 (d, 3H, J = 6.2 Hz, H-1), 0.86 (s, 9H, Si-C(CH₃)₃), 0.07 (s, 3H, SiCH₃), 0.06 (s, 3H, SiCH₃);

^{13}C NMR (125 MHz, CDCl_3) δ 202.2, 64.6, 53.0, 25.8, 24.2, 18.0, -4.4, -5.0;
 $[\alpha]_{\text{D}}^{25} = 13.0$ ($c = 1.50$, CHCl_3).

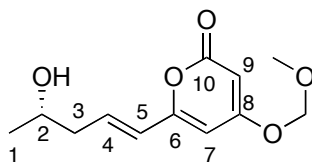
(*S, E*)-6-(4-(*tert*-Butyldimethylsilyloxy)pent-1-enyl)-4-(methoxymethoxy)-2*H*-pyran-2-one (12)



To a stirred solution of **11** (0.40 g, 1.43 mmol) in 7 mL dry THF was added 0.60 mL *n*-BuLi solution (2.5 M in THF, 1.50 mmol) at $-78\text{ }^{\circ}\text{C}$. After 30 min, aldehyde **15** (0.32 g, 1.58 mmol) was added, and the reaction mixture was warmed to $25\text{ }^{\circ}\text{C}$ over 12 h. The solvent was removed *in vacuo* and then purified using flash column chromatography (1:8 EtOAc/ hexanes) to give the product as its 3:1 *E/Z* mixture. The mixture was treated with I_2 (0.03 g, 0.01 mmol) in 10 mL CHCl_3 for 48 h. The solution was washed with saturated $\text{Na}_2\text{S}_2\text{O}_3$ (10 mL), H_2O (10 mL), brine (10 mL), and then dried over Na_2SO_4 . The solvent was removed *in vacuo* to give the product (0.34 g, 67%) as its *E* isomer (a colorless oil). IR (CHCl_3 , film cast) 3100, 2956, 2897, 2857, 1726, 1658, 1617 cm^{-1} ; ^1H NMR (300 MHz, CDCl_3) δ 6.67 (dt, 1H, $J = 15.5, 7.7$ Hz, H-4), 5.95 (dt, 1H, $J = 15.5, 1.3$ Hz, H-5), 5.82 (d, 1H, $J = 2.1$ Hz, H-7), 5.65 (d, 1H, $J = 2.1$ Hz, H-9), 5.18 (s, 2H, OCH_2OCH_3), 3.92 (sextet, 1H, $J = 6.1$ Hz, H-2), 3.49 (s, 3H, OCH_2OCH_3), 2.34 (m, 2H, H-3), 1.16 (d, 3H, $J = 6.2$ Hz, H-1), 0.88 (s, 9H, $\text{Si-C}(\text{CH}_3)_3$), 0.05 (s, 3H, SiCH_3), 0.04 (s, 3H, SiCH_3); ^{13}C NMR (125 MHz, CDCl_3) δ 168.6, 163.9, 159.0,

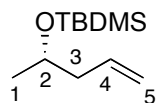
136.6, 123.5, 99.5, 94.3, 91.5, 67.9, 56.9, 43.1 (C-3), 25.8, 23.7, 18.1, -4.53; $[\alpha]_{\text{D}}^{25}$ = 23.64 (c = 0.45, CHCl_3); HRMS (ES) calculated for $\text{C}_{18}\text{H}_{31}\text{O}_5\text{Si}$, 355.1935; found 355.1941 $[\text{M}+\text{H}]^+$.

(*S*, *E*)-4-Hydroxy-6-(4-hydroxypent-1-enyl)-2*H*-pyran-2-one (8)



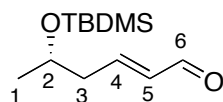
To a stirred solution of compound **12** (32.0 mg, 0.14 mmol) in 10 mL dry CH_2Cl_2 was added 1.00 mL (8.10 mmol) $\text{BF}_3 \cdot \text{Et}_2\text{O}$ at 0 °C. After stirring for 15 min at 0 °C, 10 mL of pH = 7.0 phosphate buffer solution was added to quench the reaction. The mixture was extracted with EtOAc (3×10 mL) and the combined organic layers were washed with brine (20 mL), and then dried over Na_2SO_4 . The solvent was removed *in vacuo* and then purified using flash column chromatography (10:1 EtOAc/MeOH) to give the product (5.00 mg, 18%) as a white solid. IR (MeOH, cast film) 3344, 3082, 2970, 2930, 1690, 1614, 1560, 1507 cm^{-1} ; ^1H NMR (600 MHz, CD_3OD) δ 6.65 (dt, 1H, J = 15.5, 7.7 Hz, H-4), 6.15 (dt, 1H, J = 15.5, 1.3 Hz, H-5), 5.97 (d, 1H, J = 2.1 Hz, H-7), 5.32 (d, 1H, J = 2.1 Hz, H-9), 3.85 (sextet, 1H, J = 6.1 Hz, H-2), 2.36 (m, 2H, H-3), 1.18 (d, 3H, J = 6.2 Hz, H-1); ^{13}C NMR (125 MHz, CD_3OD) δ 167.9, 160.8, 136.9, 124.9, 102.5, 67.9, 43.3, 23.2; $[\alpha]_{\text{D}}^{25}$ = 17.00 (c = 0.20, MeOH); HRMS (ES) calculated for $\text{C}_{10}\text{H}_{11}\text{O}_4$, 195.0663; found 195.0665 $[\text{M}-\text{H}]^-$.

(*S*)-*tert*-Butyldimethyl(pent-4-en-2-yloxy)silane (17)



The known compound²⁰⁰ was prepared according to literature procedure. To a stirred solution of (*S*)-pent-4-en-2-ol (2.00 g, 23.2 mmol) in 10 mL dry DMF was sequentially added *tert*-butyldimethylsilyl chloride (4.30 g, 28.0 mmol) and imidazole (2.40 g, 34.8 mmol). The solution was stirred for 12 h at 25 °C and then poured into hexanes (100 mL). The layers were separated and the organic layer was washed with H₂O (3 × 100 mL), brine (50 mL), dried over Na₂SO₄ and concentrated *in vacuo* to give the product as a colorless oil (4.60 g, quant.). IR (CHCl₃, cast film) 2957, 2930, 2897, 2858, 1472 cm⁻¹; ¹H NMR (400 MHz, CDCl₃) δ 5.81 (ddt, 1H, *J* = 17.2, 10.2, 7.1 Hz, H-4), 5.06-5.00 (m, 2H, H-5), 3.84 (sextet, 1H, *J* = 6.1 Hz, H-2), 2.22-2.15 (m, 2H, H-3), 1.13 (d, 3H, *J* = 6.1 Hz, H-1), 0.90 (s, 9H, Si-C(CH₃)₃), 0.05 (s, 3H, SiCH₃), 0.04 (s, 3H, SiCH₃); ¹³C NMR (100 MHz, CDCl₃) δ 135.6, 116.5, 68.4, 44.3, 25.8, 23.4, -4.55, -4.74; [α]_D²⁵ = 4.65 (c = 1.5, CHCl₃).

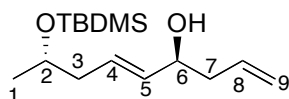
(*S, E*)-5-(*tert*-Butyldimethylsilyloxy)hex-2-enal (18)



The known compound²⁰¹ was prepared as follows. To a stirred solution of **17** (4.60 g, 23.0 mmol) in 100 mL dry CH₂Cl₂ was sequentially added Grubbs II catalyst (0.41 g, 28.0 mmol) and 12.0 mL of crotonaldehyde (138 mmol). The

solution was heated to reflux for 4 h. The solvent was removed under vacuum, and the residue was purified by column chromatography using 1:15 EtOAc/hexanes as eluent to afford the product as a colorless oil (4.00 g, 76%). IR (CHCl₃, cast film) 2957, 2930, 2887, 2858, 2808, 2725, 1697, 1472 cm⁻¹; ¹H NMR (300 MHz, CDCl₃) δ 9.48 (d, 1H, *J* = 7.9 Hz, H-6), 6.84 (dt, 1H, *J* = 15.6, 7.4 Hz, H-4), 6.14-6.06 (m, 1H, H-5), 3.97 (sextet, 1H, *J* = 6.1 Hz, H-2), 2.45-2.40 (m, 2H, H-3), 1.12 (d, 3H, *J* = 6.1 Hz, H-1), 0.85 (s, 9H, Si-C(CH₃)₃), 0.03 (s, 3H, SiCH₃), 0.01 (s, 3H, SiCH₃); ¹³C NMR (100 MHz, CDCl₃) δ 193.7, 155.2, 134.7, 67.3, 42.7, 25.7, 23.7, 18.0, -4.5, -4.9; [α]_D²⁵ = - 5.08 (c = 1.48, CHCl₃); HRMS (ES) *m/z* calculated for C₁₂H₂₄SiO₂Na 251.1438 found 251.1438 [M+Na]⁺.

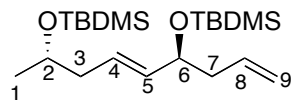
(4*S*, 8*S*, *E*)-8-(*tert*-Butyldimethylsilyloxy)nona-1,5-dien-4-ol (19**)**



A flask under Ar containing 40 mL of dry ether and 0.46 g (2.00 mmol) of **18** was cooled to -100 °C. In another flask, under Ar, containing 2.40 mL (2.40 mmol) of (-)-Ipc₂B(allyl)borane (1M in pentane) was cooled to -78 °C. The solution of (-)-Ipc₂B(allyl)borane was then added to the solution of **18** and allowed to stir at -100 °C for 1 h. The mixture was then treated with 0.88 mL (2.60 mmol) of 3M NaOH and 0.88 mL 30% H₂O₂ and allowed to warm to room temperature where it was stirred for 12 h. The aqueous layer was extracted with ether (3×10 mL) and the combined organic layers were washed with 10 mL water, 10 mL brine, and dried

over Na₂SO₄. This was concentrated under vacuum. The residue was purified by a silica gel column eluted with 10% Et₂O/hexanes to afford the product as a colorless oil (0.39 g, 72%). IR (CHCl₃, cast film) 3343, 3077, 2957, 2929, 2897, 2858, 1472, 1466 cm⁻¹; ¹H NMR (500 MHz, CDCl₃) δ 5.82 (m, 1H, H-8), 5.68 (m, 1H, H-4), 5.52 (ddt, 1H, *J* = 15.6, 6.7, 1.3 Hz, H-5), 5.14 (m, 2H, H-9), 4.13 (m, 1H, H-6), 3.85 (sextet, 1H, *J* = 6.0 Hz, H-2), 2.30 – 2.15 (m, 4H, H-3, H-7), 1.13 (d, 3H, *J* = 6.1 Hz, H-1), 0.88 (s, 9H, Si-C(CH₃)₃), 0.05 (s, 3H, SiCH₃), 0.04 (s, 3H, SiCH₃); ¹³C NMR (125 MHz, CDCl₃) δ 134.4, 134.2, 128.6, 118.1, 71.7, 68.4, 42.6, 41.9, 25.9, 23.4, 18.2, -4.5, -4.8; [α]_D²⁵ = -4.23 (c = 0.43, CHCl₃); HRMS (ES) *m/z* calculated for C₁₅H₃₀SiO₂Na 293.1907 found 293.1913 [M+Na]⁺.

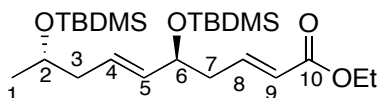
(5*S*, 9*S*, *E*)-5-Allyl-2, 2, 3, 3, 9, 11, 11, 12, 12-nonamethyl-4, 10-dioxo-3, 11-disilatridec-6-ene (20)



To a stirred solution of **19** (1.60 g, 5.93 mmol) in 10 mL dry DMF was sequentially added *tert*-butyldimethylsilyl chloride (1.13 g, 7.41 mmol) and imidazole (607 mg, 8.89 mmol). The solution was stirred for 12 h at 25 °C and then poured into hexanes (100 mL). The layers were separated and the organic layer was washed with H₂O (3 × 100 mL), brine (50 mL), dried over Na₂SO₄ and concentrated *in vacuo* to give the product as a colorless oil (2.27 g, quant.). IR (CHCl₃, cast film) 3077, 2957, 2930, 2897, 2858, 1472, 1463, 1257 cm⁻¹; ¹H

NMR (400 MHz, CDCl₃) δ 5.80 (m, 1H, H-8), 5.55 (m, 1H, H-4), 5.45 (ddt, 1H, J = 15.4, 6.2, 1.1 Hz, H-5), 5.05 (m, 2H, H-9), 4.10 (m, 1H), 3.80 (sextet, 1H, J = 6.0 Hz, H-2), 2.27–2.11 (m, 4H, H-3, H-7), 1.10 (d, 3H, J = 6.1 Hz, H-1), 0.88 (s, 18H, Si-C(CH₃)₃), 0.06 (s, 6H, SiCH₃), 0.05 (s, 3H, SiCH₃), 0.03 (s, 3H, SiCH₃); ¹³C NMR (125 MHz, CDCl₃) δ 135.3, 135.2, 126.7, 116.6, 73.2, 68.6, 43.1, 42.6, 25.9, 25.8, 23.3, 18.2, 18.1, -4.3, -4.4, -4.7, -4.7; $[\alpha]_D^{25}$ = -0.18 (c = 1.75, CHCl₃); HRMS (ES) m/z calculated for C₂₁H₄₄Si₂O₂Na 407.2772, found 407.2778 [M+Na]⁺.

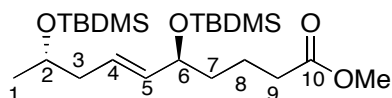
(2E, 5S, 6E, 9S)-Ethyl 5,9-bis(*tert*-butyldimethylsilyloxy) deca-2,6-dienoate (21)



To a stirred solution of **20** (108 mg, 0.28 mmol) in 5 mL dry CH₂Cl₂ was sequentially added Grubbs II catalyst (9.00 mg, 10.6 μ mol) and 0.16 mL of ethyl acrylate (1.50 mmol). The solution was stirred at 25 °C for 12 h. The solvent was removed under vacuum, and the residue was purified by column chromatography on silica gel using a 1:50 Et₂O/hexanes eluent to afford the product as a colorless oil (98.0 mg, 76%). IR (CHCl₃, cast film) 2957, 2930, 2897, 2858, 1725, 1657, 1472, 1463 cm⁻¹; ¹H NMR (400 MHz, CDCl₃) δ 6.94 (dt, 1H, J = 15.5, 7.7 Hz, H-8), 5.82 (dt, 1H, J = 15.7, 1.3 Hz, H-9), 5.60 (m, 1H, H-4), 5.45 (ddt, 1H, J = 15.4, 6.5, 1.2 Hz, H-5), 4.18 (m, 3H, H-6, OCH₂CH₃), 3.82 (sextet, 1H, J = 6.0 Hz, H-2), 2.38–2.12 (m, 4H, H-3, H-7), 1.28 (t, 3H, J = 7.1 Hz, OCH₂CH₃) 1.10

(d, 3H, $J = 6.2$ Hz, H-1), 0.89 (s, 9H, Si-C(CH₃)₃), 0.88 (s, 9H, Si-C(CH₃)₃), 0.05 (s, 6H, SiCH₃), 0.04 (s, 3H, SiCH₃), 0.02 (s, 3H, SiCH₃); ¹³C NMR (100 MHz, CDCl₃) δ 166.6, 145.9, 134.9, 127.7, 123.6, 72.7, 68.7, 60.1, 42.8, 41.7, 26.1, 26.0, 23.6, 18.2, 18.1, 14.4, -4.3, -4.5, -4.7, -4.8; $[\alpha]_D^{25} = -0.49$ (c = 1.63, CHCl₃); HRMS (ES) m/z calculated for C₂₄H₄₈Si₂O₄Na 479.2983, found 479.2984 [M+Na]⁺.

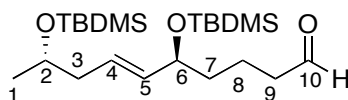
(5*S*, 9*S*, *E*)-Methyl 5,9-bis(*tert*-butyldimethylsilyloxy)dec-6-enoate (22**)**



To a stirred solution of **21** (117 mg, 0.26 mmol) in 5 mL dry MeOH was added magnesium metal (62.4 mg, 2.57 mmol). The solution was heated to reflux for 10 min and then stirred at 25 °C for 12 h. The MeOH was removed under vacuum, and then 10 mL of 1 M citric acid was added to the solution. The aqueous layer was extracted with ether (3×10 mL). The combined organic layers were washed with 10 mL water, 10 mL brine, and dried over Na₂SO₄. This was concentrated under vacuum. The residue was purified by column chromatography on silica gel using a 1:50 Et₂O /hexanes as eluent to afford the product as a colorless oil (83.3 mg, 73%). IR (CHCl₃, cast film) 2957, 2930, 2897, 2858, 1725, 1657, 1472, 1463 cm⁻¹; ¹H NMR (500 MHz, CDCl₃) δ 5.55 (m, 1H, H-4), 5.40 (ddt, 1H, $J = 15.4$, 6.5, 1.2 Hz, H-5), 4.08 (dt, 1H, $J = 6.5$, 6.3 Hz, H-6), 3.82 (sextet, 1H, $J = 6.0$ Hz, H-2), 3.67 (s, 3H, OCH₃), 2.31 (t, 2H, $J = 7.5$ Hz, H-9), 2.15 (m, 2H, H-3), 1.65-1.45 (m, 4H, H-7, H-8), 1.11 (d, 3H, $J = 6.2$ Hz, H-1), 0.89 (s, 9H, Si-C(CH₃)₃),

0.88 (s, 9H, Si-C(CH₃)₃), 0.05 (s, 6H, SiCH₃), 0.04 (s, 3H, SiCH₃), 0.02 (s, 3H, SiCH₃); ¹³C NMR (125 MHz, CDCl₃) δ 174.1, 135.4, 126.8, 73.1, 68.5, 51.4, 42.6, 37.8, 34.1, 26.0, 25.9, 23.4, 20.8, 18.2, 18.1, -4.7, -4.7, -4.8; [α]_D²⁵ = -0.72 (c = 0.47, CHCl₃); HRMS (ES) *m/z* calculated for C₂₃H₄₈Si₂O₄Na 467.2983, found 467.2988 [M+Na]⁺.

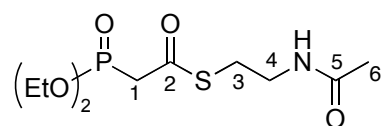
(5*S*, 9*S*, *E*)-5, 9-bis(*tert*-Butyldimethylsilyloxy)dec-6-enal (23**)**



To a stirred solution of **22** (90.0 mg, 0.20 mmol) in 10 mL CH₂Cl₂ was added DIBAL (1.0 M in CH₂Cl₂, 0.30 mL, 0.30 mmol) over 15 min at -78 °C. The reaction mixture was stirred for 1.5 h at -78 °C, and then 4 mL MeOH was added to quench the excess DIBAL. The solution was diluted with Et₂O, and 20 mL of saturated aqueous potassium sodium tartrate was added. The mixture was stirred until 2 clear layers had formed. The 2 layers were separated and the organic layer was washed with brine (20 mL) and then dried over Na₂SO₄. The solvent was removed *in vacuo* and then purified using flash column chromatography (1:50 Et₂O /hexanes) to give the product (61.0 mg, 73%) as a colorless oil. IR (CHCl₃, cast film) 2956, 2930, 2897, 2858, 2710, 1743, 1473, 1255 cm⁻¹; ¹H NMR (600 MHz, CDCl₃) δ 9.76 (t, 1H, *J* = 1.8 Hz, H-10), 5.55 (m, 1H, H-4), 5.45 (ddt, 1H, *J* = 15.4, 6.5, 1.2 Hz, H-5), 4.08 (m, 1H, H-6), 3.82 (sextet, 1H, *J* = 6.0 Hz, H-2), 2.42 (td, 2H, *J* = 7.3, 1.8 Hz, H-9), 2.16 (m, 2H, H-3), 1.70-1.45 (m, 4H, H-7, H-8), 1.11 (d, 3H, *J* = 6.2 Hz, H-1), 0.89 (s, 18H, Si-C(CH₃)₃), 0.06 (s, 3H, SiCH₃),

0.05 (s, 3H, SiCH₃) 0.04 (s, 3H, SiCH₃), 0.02 (s, 3H, SiCH₃) ; ¹³C NMR (125 MHz, CDCl₃) δ 202.6, 135.2, 126.7, 73.1, 68.5, 43.8, 42.6, 37.7, 25.9, 25.8, 23.4, 18.1, 17.9, -4.2, -4.5, -4.7, -4.8; [α]_D²⁵ = 3.02 (c = 0.54, CHCl₃); HRMS (ES) *m/z* calculated for C₂₂H₄₆Si₂O₃Na 437.2878, found 437.2879 [M+Na]⁺.

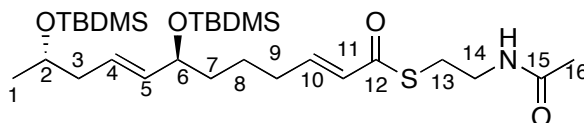
***S*-2-Acetamidoethyl 2-(diethoxyphosphoryl)ethanethioate (25)**



The known compound²⁰² was prepared as follows. To a stirred solution of 2-(diethoxyphosphoryl)acetic acid (196 mg, 1.00 mmol) in 5 mL CH₂Cl₂ was added DMAP (12.2 mg, 0.10 mmol) at 0 °C. Then DCC (226 mg, 1.10 mmol) and *N*-acetylcysteamine (131 mg, 1.10 mmol) were added to the solution sequentially. The mixture was stirred at 0 °C for 30 min, then warmed to 25 °C and stirred for a further 12 h. The solvent was removed *in vacuo* and then 10 mL 1:1 EtOAc/Et₂O was added. The precipitated DCU was removed by filtration; the filtrate was concentrated and then purified using flash column chromatography (10:1 EtOAc/MeOH) to give the product (110 mg, 37%) as a white solid. IR (CHCl₃, cast film) 3287, 2982, 2916, 1676, 1551, 1474, 1249 cm⁻¹; ¹H NMR (400 MHz, CDCl₃) δ 6.18 (s, 1H, NH), 4.2 (m, 4H, OCH₂CH₃), 3.47 (dt, 2H, *J* = 6.2, 6.2 Hz, H-4), 3.25 (d, 2H, *J*_{HP} = 21.3 Hz, H-1), 3.10 (t, 2H, *J* = 6.3 Hz, H-3), 1.90 (s, 3H, H-6), 1.36 (t, 6H, *J* = 7.1 Hz, OCH₂CH₃); ¹³C NMR (125 MHz, CDCl₃) δ 190.6 (d, *J*_{CP} = 6.7 Hz), 170.5, 63.0 (d, *J*_{CP} = 6.2 Hz), 43.5 (d, *J*_{CP} = 131.1 Hz), 39.1,

29.5, 23.1, 16.3 (d, $J_{CP} = 6.2$ Hz); HRMS (ES) m/z calculated for $C_{10}H_{20}PSNO_5Na$ 320.0692, found 320.0693 $[M+Na]^+$.

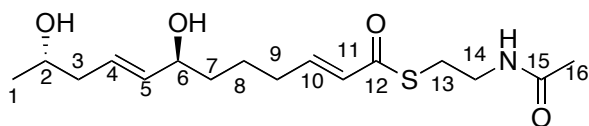
(2*E*, 7*S*, 8*E*, 11*S*)-*S*-2-Acetamidoethyl 7,11-bis(*tert*-butyldimethylsilyloxy) dodeca-2,8-dienethioate (26)



To a stirred solution of LiBr (26.0 mg, 0.31 mmol) in 0.5 mL dry THF was added **25** (36.8 mg, 0.12 mmol). The solution was stirred for 10 min at 25 °C followed by addition of Et₃N (0.05 mL, 0.37 mmol) in 0.5 mL THF. The solution was stirred for another 10 min, and then **23** (26.0 mg, 62.0 μmol) in 0.5 mL dry THF was added. The solution was stirred at 25 °C for 12 h. The solvent was removed *in vacuo* and then purified using flash column chromatography (2:1 EtOAc/hexanes) to give the product (21.0 mg, 60%) as a colorless oil. IR (CHCl₃, cast film) 2955, 2929, 2896, 2857, 1660, 1633, 1551, 1472, 1289 cm⁻¹; ¹H NMR (500 MHz, CDCl₃) δ 6.92 (dt, 1H, $J = 15.5, 7.0$ Hz, H-10), 6.13 (dt, 1H, $J = 15.5, 1.5$ Hz, H-11), 5.86(s, 1H, NH), 5.54 (m, 1H, H-4), 5.40 (ddt, 1H, $J = 15.4, 6.5, 1.2$ Hz, H-5), 4.06 (dt, 1H, $J = 5.8, 5.8$ Hz, H-6), 3.82 (sextet, 1H, $J = 6.0$ Hz, H-2), 3.47 (dt, 2H, $J = 6.2, 6.2$ Hz, H-14), 3.10 (t, 2H, $J = 6.3$ Hz, H-13), 2.25-2.10 (m, 4H, H-3, H-9), 1.97 (s, 3H, H-16), 1.4-1.6(m, 4H, H-7, H-8), 1.10 (d, 3H, $J = 6.0$ Hz, H-1), 0.88 (s, 18H, Si-C(CH₃)₃), 0.05 (s, 3H, SiCH₃), 0.05 (s, 3H, SiCH₃), 0.04 (s, 3H, SiCH₃), 0.02 (s, 3H, SiCH₃); ¹³C NMR (100 MHz, CDCl₃) δ 190.4, 170.2, 146.5, 135.4, 128.3, 126.8, 73.1, 68.6, 42.6, 39.8, 37.8, 32.2, 28.2, 25.9,

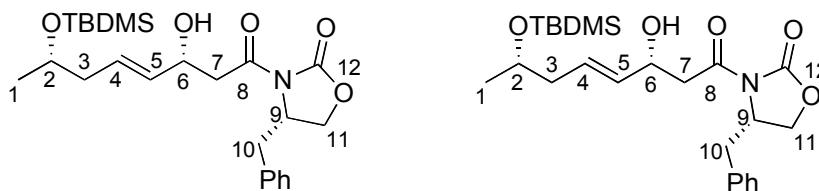
25.8, 23.6, 23.4, 23.2, 18.2, 18.1, -4.2, -4.5, -4.7, -4.8; $[\alpha]_D^{25} = 3.89$ ($c = 0.18$, CHCl_3); HRMS (ES) m/z calculated for $\text{C}_{28}\text{H}_{55}\text{NSi}_2\text{O}_4\text{SNa}$ 580.3283, found 580.3281 $[\text{M}+\text{Na}]^+$.

(2E, 7S, 8E, 11S)-S-2-Acetamidoethyl 7,11-dihydroxydodeca-2,8-dienethioate
(27)



To a stirred solution of **26** (20.0 mg, 0.04 mmol) was added 2 mL of $\text{AcOH}/\text{H}_2\text{O}/\text{THF}$ as a 3:3:1 solution. Then the solution was stirred at 45 °C for 12 h. The solvent was removed *in vacuo* and the residue was purified using flash column chromatography (10:1 EtOAc/MeOH) to give the product (9.00 mg, 60%) as a colorless oil. IR (CHCl_3 , cast film) 3093, 3088, 2964, 2930, 2864, 1660, 1632, 1555, 1435, 1291 cm^{-1} ; ^1H NMR (500 MHz, CDCl_3) δ 6.92 (dt, 1H, $J = 15.5, 7.0$ Hz, H-10), 6.13 (dt, 1H, $J = 15.5, 1.5$ Hz, H-11), 5.92 (s, 1H, NH), 5.68 (m, 1H, H-4), 5.57 (ddt, 1H, $J = 15.4, 6.5, 1.2$ Hz, H-5), 4.10 (dt, 1H, $J = 5.8, 5.8$ Hz, H-6), 3.85 (sextet, 1H, $J = 6.0$ Hz, H-2), 3.45 (dt, 2H, $J = 6.2, 6.2$ Hz, H-14), 3.09 (t, 2H, $J = 6.3$ Hz, H-13), 2.27-2.15 (m, 4H, H-3, H-9), 1.95 (s, 3H, H-16), 1.77 (s, 2H, OH), 1.45-1.64 (m, 4H, H-7, H-8), 1.10 (d, 3H, $J = 6.0$ Hz, H-1); ^{13}C NMR (125 MHz, CDCl_3) δ 190.3, 170.3, 146.1, 136.2, 128.6, 127.8, 72.4, 67.2, 41.9, 39.8, 36.6, 32.0, 28.3, 23.8, 23.2, 23.0; $[\alpha]_D^{25} = 12.74$ ($c = 0.35$, CHCl_3); HRMS (ES) m/z calculated for $\text{C}_{16}\text{H}_{27}\text{NSO}_4\text{Na}$ 352.1553 found 352.1550 $[\text{M}+\text{Na}]^+$.

(*S*)-4-benzyl-3-((3*R*,7*S*,*E*)-7-(*tert*-butyldimethylsilyloxy)-3-hydroxyoct-4-enoyl)oxazolidin-2-one (39) and (*S*)-4-benzyl-3-((3*S*,7*S*,*E*)-7-(*tert*-butyldimethylsilyloxy)-3-hydroxyoct-4-enoyl)oxazolidin-2-one (40)



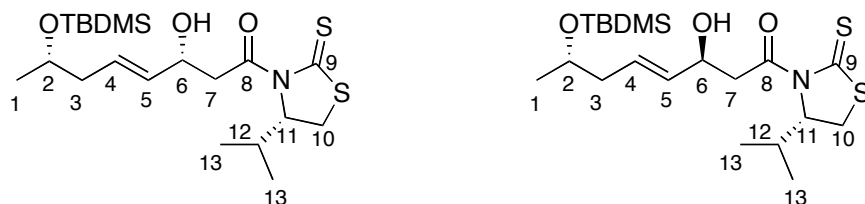
To a stirred solution of (*S*)-3-acetyl-4-benzyloxazolidin-2-one (458 mg, 2.10 mmol) in dry CH₂Cl₂ (20 mL) was added TiCl₄ (1.0 M solution in CH₂Cl₂, 4.20 mL, 4.20 mmol) at -78 °C under Ar. The reaction mixture was stirred for 10 min. DIPEA was added to the reaction mixture, which was then stirred for 1 h at -78 °C. A solution of aldehyde **18** (530 mg, 2.32 mmol) in CH₂Cl₂ (2 mL) was added to the reaction mixture, which was then stirred for 5 h at -78 °C. The reaction was quenched with 10 mL saturated ammonium chloride. The layers were separated and the aqueous layer was extracted with EtOAc (3 x 10 mL). The combined organic layers were washed with brine (20 mL) and dried over Na₂SO₄. The solvent was removed *in vacuo* and the residue was purified using flash column chromatography (1:6 EtOAc/hexanes) to give two diastereomers **39** (171 mg, 16% yield) and **40** (264 mg, 26% yield) as colorless oils.

39: IR (CHCl₃, cast film) 3503, 2956, 2928, 2856, 1785, 1699 cm⁻¹; ¹H NMR (500 MHz, CDCl₃) δ 7.35-7.26 (m, 3H, Ph-H), 7.21-7.20 (m, 2H, Ph-H), 5.79-5.76 (m, 1H, H-4), 5.59 (dd, 1H, *J* = 15.5, 6.3 Hz, H-5), 4.69-4.67 (m, 2H, H-6, H-9), 4.23-4.16 (m, 2H, H-11), 3.84 (sextet, 1H, *J* = 6.1 Hz, H-2), 3.30 (dd, 1H, *J* = 13.4, 3.4

Hz, H-10), 3.18-3.15 (m, 2H, H-7), 2.79 (dd, 1H, $J = 13.4, 9.6$ Hz, H-10), 2.18 (m, 2H, H-3), 1.12 (d, 3H, $J = 6.1$ Hz, H-1), 0.89 (s, 9H, Si-C(CH₃)₃), 0.06 (s, 6H, SiCH₃); ¹³C NMR (100 MHz, CDCl₃) δ 172.0, 153.4, 135.1, 132.7, 129.4, 129.2, 129.0, 127.4, 68.6, 68.4, 66.3, 55.1, 42.7, 42.6, 37.9, 25.9, 23.5, 18.1, -4.50, -4.66; $[\alpha]_D^{25} = 111.46$ (c = 0.23, CHCl₃); HRMS (ES) m/z calculated for C₂₄H₃₇NSiO₅Na 470.2333 found 470.2338 [M+Na]⁺.

40: IR (CHCl₃, cast film) 3503, 2956, 2928, 2856, 1785, 1699 cm⁻¹; ¹H NMR (500 MHz, CDCl₃) δ 7.35-7.26 (m, 3H, Ph-H), 7.21-7.20 (m, 2H, Ph-H), 5.76 (ddd, 1H, $J = 14.9, 7.7, 1.1$ Hz, H-4), 5.62-5.57 (m, 1H, H-5), 4.71-4.68 (m, 1H, H-9), 4.61 (m, 1H, H-6), 4.23-4.16 (m, 2H, H-11), 3.84 (sextet, 1H, $J = 6.1$ Hz, H-2), 3.28 (dd, 1H, $J = 13.5, 3.4$ Hz, H-10), 3.22 (dd, 1H, $J = 17.2, 8.9$ Hz, H-7), 3.12 (dd, 1H, $J = 17.2, 3.3$ Hz, H-7), 2.80 (dd, 1H, $J = 13.5, 9.4$ Hz, H-10), 2.20-2.15 (m, 2H, H-3), 1.12 (d, 3H, $J = 6.1$ Hz, H-1), 0.88 (s, 9H, Si-C(CH₃)₃), 0.05 (s, 6H, SiCH₃); ¹³C NMR (100 MHz, CDCl₃) δ 172.2, 153.4, 135.0, 132.7, 129.4, 129.2, 129.0, 127.4, 68.7, 68.3, 66.3, 55.1, 42.7, 42.5, 37.8, 25.9, 23.5, 18.1, -4.50, -4.66; $[\alpha]_D^{25} = 8.31$ (c = 0.65, CHCl₃); HRMS (ES) m/z calculated for C₂₄H₃₇NSiO₅Na 470.2333 found 470.2340 [M+Na]⁺.

(3*R*, 7*S*, *E*)-7-(*tert*-Butyldimethylsilyloxy)-3-hydroxy-1-((*S*)-4-isopropyl-2-thioxothiazolidin-3-yl)oct-4-en-1-one (56) and (3*S*, 7*S*, *E*)-7-(*tert*-Butyldimethylsilyloxy)-3-hydroxy-1-((*S*)-4-isopropyl-2-thioxothiazolidin-3-yl)oct-4-en-1-one (57)

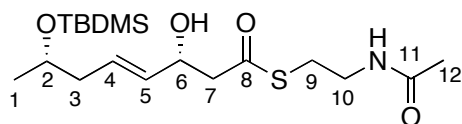


To a stirred solution of (*S*)-4-isopropyl-*N*-acetyl-1, 3-thiazolidine-2-thione (193 mg, 0.95 mmol) in dry CH₂Cl₂ (10 mL) was added TiCl₄ (1.0 M solution in CH₂Cl₂, 1.05 mL, 1.05 mmol) at 0 °C under Ar. The reaction mixture was stirred for 5 min and then cooled to -78 °C. A solution of DIPEA (148 mg, 1.14 mmol) in CH₂Cl₂ (2 mL) was added. The reaction mixture was stirred at -78 °C for 2 h. A solution of aldehyde **18** (195 mg, 0.86 mmol) in CH₂Cl₂ (2 mL) was added to the reaction mixture, which was then stirred for 15 min at -78 °C. The reaction was quenched with 10 mL saturated ammonium chloride. The layers were separated and the aqueous layer was extracted with EtOAc (3 x 10 mL). The combined organic layers were washed with brine (20 mL) and dried over Na₂SO₄. The solvent was removed *in vacuo* and the residue was purified using flash column chromatography (1:6 EtOAc/hexanes) to give two diastereomers **56** (190 mg, 51% yield) and **57** (90.0 mg, 24% yield.) as yellow oils.

56: 190 mg, yellow oil, 51% yield. IR (CHCl₃, cast film) 3452, 2959, 2928, 2894, 2856, 1695, 1471 cm⁻¹; ¹H NMR (500 MHz, CDCl₃) δ 5.74 (m, 1H, H-5), 5.55 (ddt, 1H, *J* = 15.5, 6.2, 1.1 Hz, H-5), 5.15 (ddd, 1H, *J* = 7.51, 6.6, 0.9 Hz, H-11), 4.64 (m, 1H, H-6), 3.83 (sextet, 1H, *J* = 6.0 Hz, H-2), 3.55 (dd, 1H, *J* = 17.6, 2.9 Hz, H-7), 3.51 (dd, 1H, *J* = 11.5, 7.9 Hz, H-10), 3.30 (dd, 1H, *J* = 17.6, 9.0 Hz, H-7), 3.05 (dd, 1H, *J* = 11.5, 1.0 Hz, H-10), 2.38 (m, 1H, H-3), 2.17 (m, 2H, H-3, H-12), 1.11 (d, 3H, *J* = 6.0 Hz, H-1), 1.06 (d, 3H, *J* = 6.8 Hz, H-13), 0.98 (d, 3H, *J* = 6.9 Hz, H-13), 0.88 (s, 9H, Si-C(CH₃)₃), 0.05 (s, 6H, SiCH₃); ¹³C NMR (125 MHz, CDCl₃) 202.8, 172.5, 132.6, 129.1, 71.4, 68.7, 68.3, 45.4, 42.6, 30.8, 30.6, 25.8, 23.5, 19.1, 18.1, 17.8, -4.49, -4.64; $[\alpha]_D^{25} = 253$ (c = 0.690, CHCl₃); HRMS (ES) *m/z* calculated for C₂₀H₃₇NS₂O₃SiNa 454.1876, found 454.1878 [M+Na]⁺.

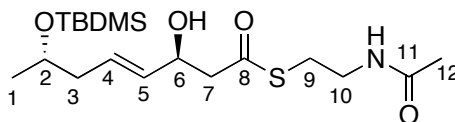
57: 90.0 mg, yellow oil, 24% yield. IR (CHCl₃, cast film) 3449, 2928, 2894, 2856, 1695, 1471 cm⁻¹; ¹H NMR (500 MHz, CDCl₃) δ 5.76 (m, 1H, H-5), 5.58 (ddt, 1H, *J* = 15.5, 6.1, 1.3 Hz, H-5), 5.20 (ddd, 1H, *J* = 7.6, 6.2, 1.1 Hz, H-11), 4.56 (m, 1H, H-6), 3.86 (sextet, 1H, *J* = 6.0 Hz, H-2), 3.65 (dd, 1H, *J* = 17.3, 9.0 Hz, H-7), 3.54 (dd, 1H, *J* = 11.5, 7.9 Hz, H-10), 3.38 (dd, 1H, *J* = 17.3, 3.2 Hz, H-7), 3.05 (dd, 1H, *J* = 11.5, 1.2 Hz, H-10), 2.38 (m, 1H, H-3), 2.17 (m, 2H, H-3, H-12), 1.18 (d, 3H, *J* = 6.0 Hz, H-1), 1.05 (d, 3H, *J* = 6.8 Hz, H-13), 1.00 (d, 3H, *J* = 6.9 Hz, H-13), 0.88 (s, 9H, Si-C(CH₃)₃), 0.087 (s, 6H, SiCH₃); ¹³C NMR (125 MHz, CDCl₃) 203.0, 173.0, 132.7, 129.1, 71.4, 69.1, 68.4, 45.2, 42.6, 30.8, 30.6, 25.9, 23.5, 19.1, 18.2, 17.8, -4.4, -4.6; $[\alpha]_D^{25} = 197$ (c = 0.290, CHCl₃); HRMS (ES) *m/z* calculated for C₂₀H₃₇NS₂O₃SiNa 454.1876, found 454.1882 [M+Na]⁺.

(3*R*, 7*S*, *E*)-*S*-2-Acetamidoethyl 7-(*tert*-butyldimethylsilyloxy)-3-hydroxyoct-4-enethioate (41)



To a stirred solution of **56** (284 mg, 0.659 mmol) in 5 mL MeCN was added K_2CO_3 (350 mg, 2.30 mmol) and *N*-acetylcysteamine (152 mg, 0.791 mmol). The reaction mixture was stirred until the yellow color disappeared. The reaction was quenched with 5 mL saturated ammonium chloride. The layers were separated and the aqueous layer was extracted with EtOAc (3 x 10 mL). The combined organic layers were washed with brine (20 mL) and dried over Na_2SO_4 . The solvent was removed *in vacuo* and the residue was purified using flash column chromatography (EtOAc) to give the product (196 mg, 77% yield) as a white solid. IR ($CHCl_3$, cast film) 3290, 2956, 2929, 2897, 2857, 1689, 1657 cm^{-1} ; 1H NMR (500 MHz, $CDCl_3$) δ 5.80 (s, 1H, NH), 5.73 (m, 1H, H-4), 5.50 (ddt, 1H, J = 15.5, 6.5, 1.2 Hz, H-5), 4.56 (m, 1H, H-6), 3.82 (sextet, 1H, J = 6.0 Hz, H-2), 3.45 (m, 2H, H-10), 3.04 (m, 2H, H-9), 2.78 (m, 2H, H-7), 2.48 (s, 1H, OH), 2.15 (m, 2H, H-3), 1.97 (s, 3H, H-12), 1.10 (d, 3H, J = 6.0 Hz, H-1), 0.88 (s, 9H, Si- $C(CH_3)_3$), 0.036 (s, 3H, SiCH $_3$), 0.032 (s, 3H, SiCH $_3$); ^{13}C NMR (125 MHz, $CDCl_3$) 198.2, 170.7, 132.7, 129.1, 69.4, 68.2, 51.1, 42.4, 39.1, 28.7, 25.8, 23.3, 23.0, 18.0, -4.6, -4.8; $[\alpha]_D^{25}$ = 10.3 (c = 0.130, $CHCl_3$); HRMS (ES) m/z calculated for $C_{18}H_{35}NSO_4SiNa$ 412.1948, found 412.1944 $[M+Na]^+$.

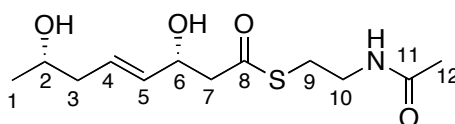
(3*S*, 7*S*, *E*)-*S*-2-Acetamidoethyl 7-(*tert*-butyldimethylsilyloxy)-3-hydroxyoct-4-enethioate (42)



Compound **42** was synthesized from **57** according to the procedure used to prepare **41**.

42: 37.0 mg, white solid, 70% yield. IR (CHCl₃, cast film) 3298, 2956, 2929, 2895, 2856, 1686, 1657 cm⁻¹; ¹H NMR (500 MHz, CDCl₃) δ 5.95 (s, 1H, NH), 5.73 (m, 1H, H-4), 5.50 (ddt, 1H, *J* = 15.4, 6.4, 1.2 Hz, H-5), 4.54 (m, 1H, H-6), 3.82 (sextet, 1H, *J* = 6.0 Hz, H-2), 3.45 (m, 2H, H-10), 3.04 (m, 2H, H-9), 2.76 (m, 2H, H-7), 2.71 (s, 1H, OH), 2.15 (m, 2H, H-3), 1.95 (s, 3H, H-12), 1.09 (d, 3H, *J* = 6.24 Hz, H-1), 0.88 (s, 9H, Si-C(CH₃)₃), 0.026 (s, 3H, SiCH₃), 0.021 (s, 3H, SiCH₃); ¹³C NMR (125 MHz, CDCl₃) 198.7, 170.5, 132.5, 129.5, 69.5, 68.2, 51.0, 42.5, 39.3, 28.8, 25.9, 23.5, 23.2, 18.2, -4.5, -4.7; [α]_D²⁵ = -3.67 (c = 0.180, CHCl₃); HRMS (ES) *m/z* calculated for C₁₈H₃₅NSO₄SiNa 412.1948, found 412.1949 [M+Na]⁺.

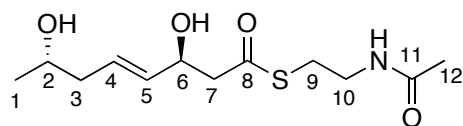
(3*R*, 7*S*, *E*)-*S*-2-Acetamidoethyl 3,7-dihydroxyoct-4-enethioate (35L)



To a flask containing **41** (9.00 mg, 0.023 mmol) was added 2 mL of a 3:3:1 solution of AcOH/H₂O/THF. The resulting solution was stirred at 25 °C for 12 h. The solvent was removed *in vacuo* and the residue was purified using flash

column chromatography (EtOAc) to give the product (6.00 mg, 95% yield) as a white solid. IR (CHCl₃, cast film) 3300, 3094, 2965, 2919, 1687, 1658, 1555 cm⁻¹; ¹H NMR (500 MHz, CDCl₃) δ 6.03 (s, 1H, NH), 5.76 (m, 1H, H-4), 5.60 (ddt, 1H, *J* = 15.5, 6.0, 1.2 Hz, H-5), 4.57 (m, 1H, H-6), 3.82 (m, 1H, H-2), 3.44 (q, 2H, *J* = 6.2 Hz, H-10), 3.04 (td, 2H, *J* = 6.0, 1.93, H-9), 2.87 (s, 1H, OH), 2.81 (m, 2H, H-7), 2.30-2.10 (m, 2H, H-3), 1.97 (s, 3H, H-12), 1.20 (d, 3H, *J* = 6.14 Hz, H-1); ¹³C NMR (125 MHz, CDCl₃) 198.6, 170.6, 134.0, 128.5, 69.4, 67.0, 50.9, 42.0, 39.2, 29.1, 23.2, 23.0; [α]_D²⁵ = 12.1 (c = 0.140, CHCl₃); HRMS (ES) *m/z* calculated for C₁₂H₂₁NSO₄Na 298.1082, found 298.1083 [M+Na]⁺.

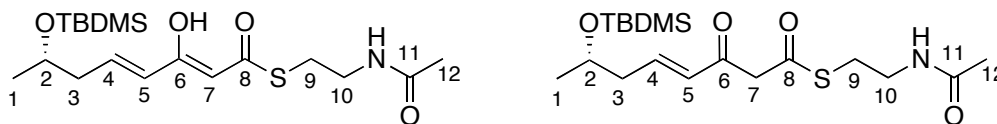
(3*S*, 7*S*, *E*)-*S*-2-Acetamidoethyl 3,7-dihydroxyoct-4-enethioate (35D)



Compound **35D** was synthesized from **42** according to the procedure used to prepare **35L**.

35D: 8.00 mg, white solid, 94% yield. IR (CHCl₃, cast film) 3296, 3094, 2967, 2925, 1687, 1658, 1555 cm⁻¹; ¹H NMR (500 MHz, CDCl₃) δ 6.00 (s, 1H, NH), 5.76 (m, 1H, H-4), 5.60 (ddt, 1H, *J* = 15.5, 6.3, 1.1 Hz, H-5), 4.58 (m, 1H, H-6), 3.82 (m, 1H, H-2), 3.44 (m, 2H, H-10), 3.04 (m, 2H, H-9), 2.87 (s, 1H, OH), 2.82 (m, 2H, H-7), 2.30-2.10 (m, 2H, H-3), 1.97 (s, 3H, H-12), 1.20 (d, 3H, *J* = 6.2 Hz, H-1); ¹³C NMR (125 MHz, CDCl₃) 198.5, 170.6, 134.1, 128.7, 69.6, 67.0, 51.0, 42.0, 39.2, 29.1, 23.2, 23.0; [α]_D²⁵ = 31.3 (c = 0.310, CHCl₃); HRMS (ES) *m/z* calculated for C₁₂H₂₁NSO₄Na 298.1082, found 298.1083 [M+Na]⁺.

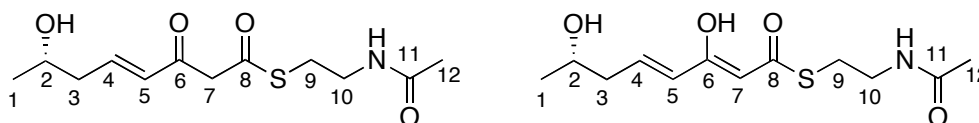
(*S*, *E*)-*S*-2-Acetamidoethyl 7-(*tert*-Butyldimethylsilyloxy)-3-oxooct-4-enethioate and (*S*, 4*E*)-*S*-2-Acetamidoethyl 7-(*tert*-butyldimethylsilyloxy)-3-hydroxyocta-2, 4-dienethioate (58)



To a stirred solution of **41** (36.0 mg, 0.092 mmol) in 5 mL CH₂Cl₂ was added Dess-Martin periodinane (47 mg, 0.110 mmol). The resulting solution was stirred at 25 °C for 2 h. The reaction was quenched by addition of 5 mL of 1:1 10% Na₂S₂O₃ : saturated aqueous NaHCO₃. The layers were separated and the aqueous layer was extracted with EtOAc (3 x 10 mL). The combined organic layers were washed with brine (20 mL) and dried over Na₂SO₄. The solvent was removed *in vacuo* and the residue was purified using flash column chromatography (EtOAc) to give the product (21.00 mg, 60% yield, keto:enol = 3:2) as a white solid. IR (CHCl₃, cast film) 3287, 3079, 2956, 2930, 2857, 1724, 1656, 1623, 1553 cm⁻¹; ¹H NMR (500 MHz, CDCl₃) δ 5.90 (s, 1H, NH), 5.49 (s, 0.4H, enol-H-5), 4.30 (m, 0.6H, keto-H-2), 4.18 (m, 0.4H, enol-H-2), 3.78 (d, 0.6H, *J* = 15.5 Hz, keto-H-5), 3.72 (d, 0.6H, *J* = 15.5 Hz, keto-H-5), 3.48 (m, 2H, H-8), 3.09 (m, 2H, H-7), 2.70 (dd, 0.6H, *J* = 15.1, 7.2 Hz, keto-H-3), 2.53 (dd, 0.6H, *J* = 15.1, 4.6 Hz, keto-H-3), 2.24 (d, 0.8H, *J* = 6.2 Hz, enol-H-3), 1.98 (s, 1.8H, keto-H-10), 1.97 (s, 1.2H, enol-H-10), 1.19 (m, 3H, H-1), 0.88 – 0.89 (m, 9H, Si-C(CH₃)₃), 0.11 – 0.00 (m, 6H, SiCH₃); ¹³C NMR (125 MHz, CDCl₃) 201.4, 194.3, 192.2, 174.4, 170.5, 170.3, 101.3, 66.1, 65.4, 58.6, 52.6, 45.4, 39.9, 39.2, 29.1, 27.7, 25.8, 25.7,

24.1, 23.9, 23.2, 23.1, 18.0, 17.9, -4.5, -4.6, -4.9, -5.1; HRMS (ES) m/z calculated for $C_{16}H_{32}NSO_4SiNa$ 384.1635, found 385.1635 $[M+Na]^+$.

(*S, E*)-*S*-2-Acetamidoethyl 7-hydroxy-3-oxooct-4-enethioate and (*S, 4E*)-*S*-2-Acetamidoethyl 3,7-dihydroxyocta-2, 4-dienethioate (35**)**



Compound **35** was synthesized from **58** according to the procedure used to prepare **35L**.

35: 18.0 mg, white solid, 95% yield, keto:enol = 2:3. IR ($CHCl_3$, cast film) 3296, 3086, 2969, 2930, 1657, 1583 cm^{-1} ; 1H NMR (500 MHz, $CDCl_3$) δ 6.95 (dt, 0.4H, $J = 15.9, 7.3$ Hz, keto-H-4), 6.78 (dt, 0.6H, $J = 15.2, 7.5$ Hz, enol-H-4), 6.22 (dt, 0.4H, $J = 15.9, 1.3$ Hz, keto-H-5), 6.04 (s, 0.4H, \underline{NH}), 5.99 (s, 0.6H, \underline{NH}), 5.82 (d, 0.6H, $J = 15.5$ Hz, enol-H-5), 5.46 (s, 0.6H, enol-H-7), 3.95 (m, 1H, H-2), 3.86 (s, 0.8H, keto-H-7), 3.48 (m, 2H, H-10), 3.09 (m, 2H, H-9), 2.40 (m, 2H, H-3), 1.97 (s, 1.8H, enol-H-12), 1.97 (s, 1.2H, keto-H-12), 1.25 (d, 1.2H, $J = 6.2$ Hz, keto-H-1), 1.23 (d, 1.8H, $J = 6.2$ Hz, enol-H-1); ^{13}C NMR (125 MHz, $CDCl_3$) 194.8, 192.6, 191.5, 170.6, 170.5, 167.3, 147.1, 139.6, 131.8, 126.6, 100.3, 67.1, 66.8, 55.1, 42.6, 42.3, 40.0, 39.2, 29.5, 28.1, 23.6, 23.4, 23.4, 23.3; HRMS (ES) m/z calculated for $C_{12}H_{19}NSO_4Na$ 269.0927, found 269.0929 $[M+Na]^+$.

(3*S*, 5*S*)-5-(*tert*-butyldimethylsilyloxy)-3-hydroxy-1-((*S*)-4-isopropyl-2-thioxothiazolidin-3-yl)hexan-1-one (65) and (3*R*, 5*S*)-5-(*tert*-butyldimethylsilyloxy)-3-hydroxy-1-((*S*)-4-isopropyl-2-thioxothiazolidin-3-yl)hexan-1-one (66)



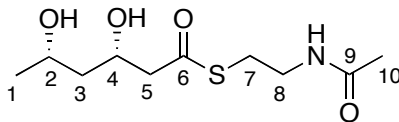
To a stirred solution of (*S*)-4-isopropyl-*N*-acetyl-1, 3-thiazolidine-2-thione (380 mg, 1.87 mmol) in dry CH₂Cl₂ (10 mL) was added TiCl₄ (1.0 M solution in CH₂Cl₂, 2.05 mL, 2.05 mmol) at 0 °C under Ar. The reaction mixture was stirred for 5 min and then cooled to -78 °C. A solution of DIPEA (291 mg, 2.24 mmol) in CH₂Cl₂ (2 mL) was added. The reaction mixture was stirred at -78 °C for 2 h. A solution of aldehyde **15** (333 mg, 1.65 mmol) in CH₂Cl₂ (2 mL) was added to the reaction mixture, which was then stirred for 15 min at -78 °C. The reaction was quenched with 10 mL saturated ammonium chloride. The layers were separated and the aqueous layer was extracted with EtOAc (3 x 10 mL). The combined organic layers were washed with brine (20 mL) and dried over Na₂SO₄. The solvent was removed *in vacuo* and the residue was purified using flash column chromatography (1:6 EtOAc/hexanes) to give two diastereomers **65** (320 mg, 48% yield) and **66** (100 mg, 15% yield) as yellow oils.

65: IR (CHCl₃, cast film) 3497, 2959, 2930, 2895, 2856, 1695, 1471 cm⁻¹; ¹H NMR (500 MHz, CDCl₃) δ 5.16 (ddd, 1H, *J* = 7.8, 6.3, 1.1 Hz, H-9), 4.30 (m, 1H,

H-4), 4.07 (m, 1H, H-2), 3.56-3.50 (m, 2H, H-5, H-8), 3.44 (s, 1H, OH), 3.25 (dd, 1H, $J = 17.5, 8.6$ Hz, H-5), 3.00 (dd, 1H, $J = 11.5, 1.0$ Hz, H-8), 2.35 (ABX₆, 1H, $J = 6.8$ Hz, H-10), 1.57-1.75 (m, 2H, H-3), 1.19 (d, 3H, $J = 6.0$ Hz, H-1), 1.05 (d, 3H, $J = 6.8$ Hz, H-11), 0.98 (d, 3H, $J = 6.9$ Hz, H-11), 0.88 (s, 9H, Si-C(CH₃)₃), 0.087 (s, 3H, SiCH₃), 0.082 (s, 3H, SiCH₃); ¹³C NMR (125 MHz, CDCl₃) 202.9, 174.4, 71.5, 68.4, 67.0, 45.7, 45.4, 30.9, 30.6, 25.8, 24.2, 19.1, 17.9, 17.8, -4.0, -4.8; $[\alpha]_D^{25} = 262$ (c = 0.420, CHCl₃); HRMS (ES) m/z calculated for C₁₈H₃₅NS₂O₃SiNa 428.1720, found 428.1718 [M+Na]⁺.

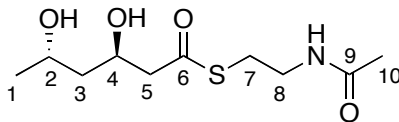
66: IR (CHCl₃, cast film) 3490, 2959, 2930, 2897, 2856, 1695, 1471 cm⁻¹; ¹H NMR (500 MHz, CDCl₃) δ 5.18 (ddd, 1H, $J = 7.5, 6.1, 1.2$ Hz, H-9), 4.33 (m, 1H, H-4), 4.15 (m, 1H, H-2), 3.54-3.44 (m, 3H, H-5, H-8, OH), 3.32 (dd, 1H, $J = 17.4, 3.39$ Hz, H-5), 3.00 (dd, 1H, $J = 11.5, 1.2$ Hz, H-8), 2.35 (ABX₆, 1H, $J = 6.8$ Hz, H-10), 1.50-1.70 (m, 2H, H-3), 1.19 (d, 3H, $J = 6.1$ Hz, H-1), 1.05 (d, 3H, $J = 6.7$ Hz, H-11), 0.98 (d, 3H, $J = 6.9$ Hz, H-11), 0.88 (s, 9H, Si-C(CH₃)₃), 0.087 (s, 3H, SiCH₃), 0.082 (s, 3H, SiCH₃); ¹³C NMR (125 MHz, CDCl₃) 202.9, 173.2, 71.4, 66.1, 65.1, 46.1, 45.1, 30.8, 30.4, 25.9, 23.7, 19.1, 18.0, 17.7, -4.4, -4.9; $[\alpha]_D^{25} = 146$ (c = 0.820, CHCl₃); HRMS (ES) m/z calculated for C₁₈H₃₅NS₂O₃SiNa 428.1720, found 428.1717 [M+Na]⁺.

(3*S*, 5*S*)-*S*-2-acetamidoethyl 3,5-dihydroxyhexanethioate (32L)



To a stirred solution of **65** (70.0 mg, 0.173 mmol) in 5 mL MeCN was added K₂CO₃ (91.0 mg, 0.605 mmol) and *N*-acetylcysteamine (HSNAC) (39.8 mg, 0.207 mmol). The reaction mixture was stirred until the yellow color disappeared (about 30 min). The reaction was quenched with 5 mL saturated ammonium chloride. The layers were separated and the aqueous layer was extracted with EtOAc (3 x 10 mL). The combined organic layers were washed with brine (20 mL) and dried over Na₂SO₄. The solvent was removed *in vacuo*. The residue was dissolved in 5 mL of a solution of 3:3:1 AcOH/H₂O/THF. The resulting solution was stirred at 25 °C for 12 h. The solvent was removed *in vacuo* and the residue was purified using flash column chromatography (9:1 EtOAc/MeOH) to give the product (28.0 mg, 67% yield) as a white solid. IR (CHCl₃, cast film) 3300, 3093, 2967, 2931, 1686, 1657, 1554 cm⁻¹; ¹H NMR (500 MHz, CDCl₃) δ 6.13 (s, 1H, NH), 4.41 (m, 1H, H-4), 4.15 (m, 1H, H-2), 3.70 (s, 1H, OH), 3.45 (m, 2H, H-8), 3.32 (m, 2H, H-7), 2.71 (dd, 1H, *J* = 15.0, 8.2 Hz, H-5), 2.69 (dd, 1H, *J* = 15.1, 3.6, Hz, H-5), 1.95 (s, 3H, H-10), 1.58 (m, 2H, H-3), 1.19 (d, 3H, *J* = 6.2 Hz, H-1); ¹³C NMR (125 MHz, CDCl₃) 198.6, 170.7, 69.5, 68.3, 51.6, 44.0, 39.1, 28.9, 23.9, 23.2; [α]_D²⁵ = 24.6 (c = 0.460, CHCl₃); HRMS (ES) *m/z* calculated for C₁₀H₁₉NSO₄Na 272.0927, found 272.0928 [M+Na]⁺.

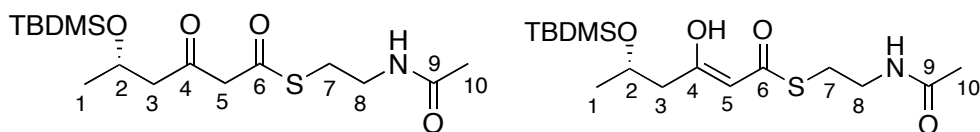
(3*R*, 5*S*)-*S*-2-acetamidoethyl 3, 5-dihydroxyhexanethioate (32D)



Compound **32D** was synthesized from **66** by the same method for synthesizing **32L**.

32D: 19.0 mg, white solid, 62% yield. IR (CHCl₃, cast film) 3302, 3093, 2965, 2931, 1686, 1658, 1555, cm⁻¹; ¹H NMR (500 MHz, CDCl₃) δ 6.10 (s, 1H, NH), 4.40 (m, 1H, H-4), 4.13 (m, 1H, H-2), 3.70 (s, 1H, OH), 3.45 (m, 2H, H-8), 3.32 (m, 2H, H-7), 2.86 (s, 1H, OH), 2.80 (dd, 1H, *J*=15.1, 8.8 Hz, H-5), 2.70 (dd, 1H, *J*=15.1, 3.7 Hz, H-5), 1.96 (s, 3H, H-10), 1.62 (m, 2H, H-3), 1.23 (d, 3H, *J*=6.3 Hz, H-1); ¹³C NMR (125 MHz, CDCl₃) 199.1, 170.8, 66.4, 64.9, 51.2, 43.8, 39.2, 28.9, 23.6, 23.2; [α]_D²⁵ = -5.42 (c = 0.550, CHCl₃); HRMS (ES) *m/z* calculated for C₁₀H₁₉NSO₄Na 272.0927, found 272.0928 [M+Na]⁺.

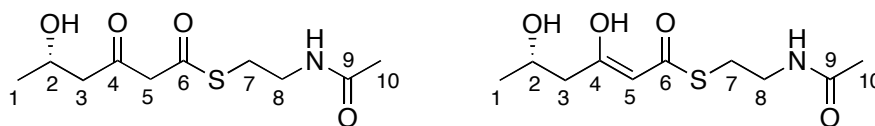
(*S*)-*S*-2-Acetamidoethyl 5-(*tert*-butyldimethylsilyloxy)-3-oxohexanethioate and (*S*)-*S*-2-Acetamidoethyl 5-(*tert*-butyldimethylsilyloxy)-3-hydroxyhex-2-enethioate (67)



To a stirred solution of **65** (114 mg, 0.282 mmol) in 15 mL MeCN was added K₂CO₃ (150 mg, 0.987 mmol) and *N*-acetylcysteamine (59.6 mg, 0.310 mmol). The reaction mixture was stirred until the yellow color disappeared. The reaction

was quenched with 5 mL saturated ammonium chloride. The layers were separated and the aqueous layer was extracted with EtOAc (3 x 10 mL). The combined organic layers were washed with brine (20 mL) and dried over Na₂SO₄. The solvent was removed *in vacuo*. To the resulting residue was added 10 mL CH₂Cl₂ and Dess-Martin periodinane (179 mg, 0.423 mmol). The resulting solution was stirred at 25 °C for 2 h. The reaction was quenched by addition of 10 mL of 1:1 10% Na₂S₂O₃:saturated aqueous NaHCO₃. The layers were separated and the aqueous layer was extracted with EtOAc (3 x 10 mL). The combined organic layers were washed with brine (20 mL) and dried over Na₂SO₄. The solvent was removed *in vacuo* and the residue was purified using flash column chromatography (EtOAc) to give the product (58.0 mg, 52% yield, keto:enol = 2:3) as a colorless oil. IR (CHCl₃, cast film) 3287, 3079, 2956, 2930, 2857, 1724, 1656, 1623, 1553 cm⁻¹; ¹H NMR (500 MHz, CDCl₃) δ 5.90 (s, 1H, NH), 5.49 (s, 0.4H, enol-H-5), 4.30 (m, 0.6H, keto-H-2), 4.18 (m, 0.4H, enol-H-2), 3.78 (d, 0.6H, *J* = 15.5 Hz, keto-H-5), 3.72 (d, 0.6H, *J* = 15.5 Hz, keto-H-5), 3.48 (m, 2H, H-8), 3.09 (m, 2H, H-7), 2.70 (dd, 0.6H, *J* = 15.1, 7.2 Hz, keto-H-3), 2.53 (dd, 0.6H, *J* = 15.1, 4.6 Hz, keto-H-3), 2.24 (d, 0.8H, *J* = 6.2 Hz, enol-H-3), 1.98 (s, 1.8H, keto-H-10), 1.97 (s, 1.2H, enol-H-10), 1.19 (m, 3H, H-1), 0.88-0.89 (m, 9H, Si-C(CH₃)₃), 0.11-0.00 (m, 6H, SiCH₃); ¹³C NMR (125 MHz, CDCl₃) 201.4, 194.3, 192.2, 174.4, 170.5, 170.3, 101.3, 66.1, 65.4, 58.6, 52.6, 45.4, 39.9, 39.2, 29.1, 27.7, 25.8, 25.7, 24.1, 23.9, 23.2, 23.1, 18.0, 17.9, -4.5, -4.6, -4.9, -5.1; HRMS (ES) *m/z* calculated for C₁₆H₃₁NSO₄SiNa 384.1635, found 385.1635 [M+Na]⁺.

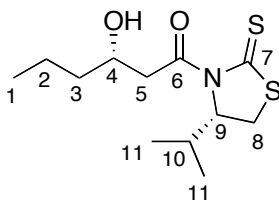
(S)-S-2-Acetamidoethyl 5-hydroxy-3-oxohexanethioate and (S)-S-2-Acetamidoethyl 3,5-dihydroxyhex-2-enethioate (32)



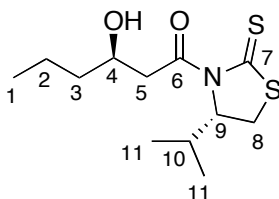
To a flask containing **67** (48.0 mg, 0.133 mmol) was added 5 mL of a 3:3:1 solution of AcOH/H₂O/THF. The resulting solution was stirred at 25 °C for 12 h. The solvent was removed *in vacuo* and the residue was purified using flash column chromatography (EtOAc) to give the product (22.0 mg, yield 69%, keto:enol = 3:1) as a white solid. IR (CHCl₃, cast film) 3298, 3086, 2969, 2930, 1721, 1657, 1553 cm⁻¹; ¹H NMR (500 MHz, CDCl₃) δ 6.08 (s, 1H, NH), 5.53 (s, 0.25H, enol-H-5), 4.28 (sextet, 0.75H, *J* = 6.3 Hz, keto-H-2), 4.19 (m, 0.25H, enol-H-2), 3.75 (s, 1.5H, keto-H-5), 3.48 (m, 2H, H-8), 3.10 (m, 2H, H-7), 2.70 (d, 1.5H, *J* = 5.9 Hz, keto-H-3), 2.32 (m, 0.5H, enol-H-3), 1.99 (m, 3H, H-10), 1.28 (d, 0.75H, *J* = 6.3 Hz, enol-H-1), 1.25 (d, 2.25H, *J* = 6.3 Hz, keto-H-1); ¹³C NMR (125 MHz, CDCl₃) 202.6, 194.6, 192.1, 174.0, 170.6, 170.4, 100.9, 65.5, 63.8, 57.9, 51.5, 44.3, 39.7, 39.1, 29.4, 27.9, 23.3, 23.2, 23.1, 22.4; HRMS (ES) *m/z* calculated for C₁₀H₁₇NSO₄Na 270.0770, found 270.0770 [M+Na]⁺.

(S)-3-Hydroxy-1-((S)-4-isopropyl-2-thioxothiazolidin-3-yl)hexan-1-one (68) and (R)-3-Hydroxy-1-((S)-4-isopropyl-2-thioxothiazolidin-3-yl)hexan-1-one (69)

Compounds **68** and **69** were synthesized from 1-butanal according to the procedure used to prepare **65** and **66**.



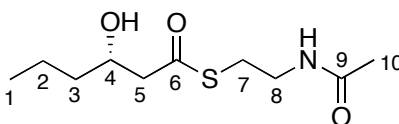
68: 98.0 mg, yellow oil, 45% yield. IR (CHCl₃, cast film) 3447, 2961, 2932, 2873, 1694, 1467 cm⁻¹; ¹H NMR (500 MHz, CDCl₃) δ 5.17 (ddd, 1H, *J* = 7.71, 6.3, 0.9 Hz, H-9), 4.12 (m, 1H, H-4), 3.63 (dd, 1H, *J* = 17.7, 2.3 Hz, H-5), 3.53 (dd, 1H, *J* = 11.5, 7.9 Hz, H-8), 3.12 (dd, 1H, *J* = 17.7, 9.4 Hz, H-5), 3.03 (dd, 1H, *J* = 11.5, 1.0 Hz, H-8), 2.35 (ABX₆, 1H, *J* = 6.7 Hz, H-10), 1.58-1.35 (m, 4H, H-2, H-3), 1.05 (d, 3H, *J* = 6.7 Hz, H-11), 0.98 (d, 3H, *J* = 6.9 Hz, H-11), 0.93 (t, 3H, *J* = 7.1 Hz, H-1); ¹³C NMR (125 MHz, CDCl₃) 203.1, 173.3, 71.4, 67.7, 45.5, 38.5, 30.8, 30.6, 19.1, 18.7, 17.8, 14.0 ; [α]_D²⁵ = 269 (c = 0.480, CHCl₃); HRMS (ES) *m/z* calculated for C₁₂H₂₁NS₂O₂Na 298.0906, found 298.0907 [M+Na]⁺.



69: 40.0 mg, yellow oil, 18% yield. IR (CHCl₃, cast film) 3452, 2961, 2931, 2873, 1697, 1467 cm⁻¹; ¹H NMR (500 MHz, CDCl₃) δ 5.17 (ddd, 1H, *J* = 7.6, 6.4, 1.0 Hz, H-9), 4.03 (m, 1H, H-4), 3.51 (dd, 1H, *J* = 11.6, 7.9 Hz, H-8), 3.43 (dd, 1H, *J* = 17.4, 9.3 Hz, H-5), 3.32 (dd, 1H, *J* = 17.4, 2.6 Hz, H-5), 3.03 (dd, 1H, *J* = 11.6, 1.1 Hz, H-8), 2.35 (ABX₆, 1H, *J* = 6.7 Hz, H-10), 1.58 - 1.33 (m, 4H, H-2, H-3), 1.05 (d, 3H, *J* = 6.8 Hz, H-11), 0.98 (d, 3H, *J* = 6.7 Hz, H-11), 0.92 (t, 3H, *J* = 6.9 Hz, H-1); ¹³C NMR (125 MHz, CDCl₃) 203.1, 173.8, 71.4, 68.2, 45.2, 38.8, 30.8,

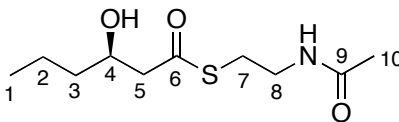
30.6, 19.1, 18.7, 17.8, 14.0; $[\alpha]_D^{25} = 233$ ($c = 0.360$, CHCl_3); HRMS (ES) m/z calculated for $\text{C}_{12}\text{H}_{21}\text{NS}_2\text{O}_2\text{Na}$ 298.0906, found 298.0907 $[\text{M}+\text{Na}]^+$.

(S)-S-2-Acetamidoethyl 3-hydroxyhexanethioate (31L)



To a stirred solution of **68** (56.2 mg, 0.204 mmol) in 5 mL MeCN was added K_2CO_3 (109 mg, 0.715 mmol) and *N*-acetylcysteamine (37.8 mg, 0.196 mmol). The reaction mixture was stirred until the yellow color disappeared. The reaction was quenched with 5 mL saturated ammonium chloride. The layers were separated and the aqueous layer was extracted with EtOAc (3 x 10 mL). The combined organic layers were washed with brine (20 mL) and dried over Na_2SO_4 . The solvent was removed *in vacuo* and the residue was purified using flash column chromatography (EtOAc) to give the product (32.0 mg, 67% yield) as a white solid. IR (CHCl_3 , cast film) 3295, 3085, 2959, 2932, 2873, 1687, 1658, 1553 cm^{-1} ; ^1H NMR (500 MHz, CDCl_3) δ 6.01 (s, 1H, NH), 4.05 (m, 1H, H-4), 3.45 (m, 1H, H-8), 3.03 (m, 2H, H-3), 2.80 (d, 1H, $J = 4.4\text{ Hz}$, OH), 2.73 (dd, 1H, $J = 15.4, 3.5\text{ Hz}$, H-5), 2.67 (dd, 1H, $J = 15.3, 8.6\text{ Hz}$, H-5), 1.96 (s, 3H, H-10), 1.53 - 1.33 (m, 4H, H-2, H-3), 0.92 (t, 3H, $J = 7.1\text{ Hz}$, H-1); ^{13}C NMR (125 MHz, CDCl_3) 199.5, 170.5, 68.5, 51.1, 39.3, 38.9, 28.8, 23.2, 18.6, 13.9; $[\alpha]_D^{25} = 19.1$ ($c = 0.640$, CHCl_3); HRMS (ES) m/z calculated for $\text{C}_{10}\text{H}_{19}\text{NSO}_3\text{Na}$ 256.0978, found 256.0979 $[\text{M}+\text{Na}]^+$.

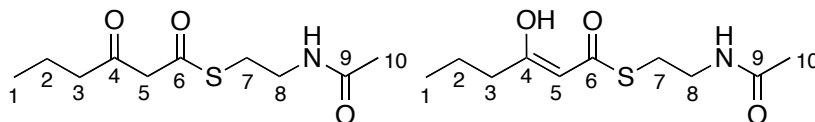
(*R*)-*S*-2-Acetamidoethyl 3-hydroxyhexanethioate (31D)



Compound **31D** was synthesized from **69** by the same method for synthesizing **31L**.

31D: 54.6 mg, white solid, 66% yield. IR (CHCl₃, cast film) 3290, 3082, 2959, 2933, 2873, 1657, 1553 cm⁻¹; ¹H NMR (500 MHz, CDCl₃) δ 6.20 (s, 1H, NH), 4.04 (m, 1H, H-4), 3.43 (m, 1H, H-8), 3.03 (m, 3H, H-3, OH), 2.71 (dd, 1H, *J* = 15.2, 3.5 Hz, H-5), 2.63 (dd, 1H, *J* = 15.0, 7.2 Hz, H-5), 1.93 (s, 3H, H-10), 1.51 - 1.30 (m, 4H, H-2, H-3), 0.90 (t, 3H, *J* = 6.9 Hz, H-1); ¹³C NMR (125 MHz, CDCl₃) 199.3, 170.6, 68.5, 51.2, 39.2, 38.9, 28.8, 23.2, 18.6, 13.9; [α]_D²⁵ = -14.8 (c = 1.10, CHCl₃); HRMS (ES) *m/z* calculated for C₁₀H₁₉NSO₃Na 256.0978, found 256.0978 [M+Na]⁺.

***S*-2-Acetamidoethyl 3-oxohexanethioate and *S*-2-Acetamidoethyl 3-hydroxyhex-2-enethioate (31)**

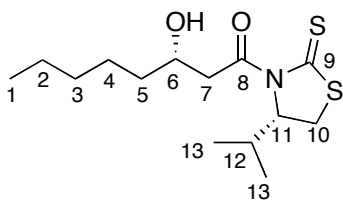


To a stirred solution of **31L** (30.0 mg, 0.129 mmol) in 5 mL CH₂Cl₂ was added Dess-Martin periodinane (79 mg, 0.186 mmol). The resulting solution was stirred at 25 °C for 2 h. The reaction was quenched by addition of 5 mL of 1:1 10% Na₂S₂O₃ : saturated aqueous NaHCO₃. The layers were separated and the aqueous layer was extracted with EtOAc (3 x 10 mL). The combined organic layers were

washed with brine (20 mL) and dried over Na₂SO₄. The solvent was removed *in vacuo* and the residue was purified using flash column chromatography (EtOAc) to give the product (8.00 mg, 27% yield, keto:enol = 3:1) as a white solid. IR (CHCl₃, cast film) 3283, 3103, 2958, 2933, 2876, 1716, 1684, 1637, 1562 cm⁻¹; ¹H NMR (500 MHz, CDCl₃) δ 5.95 (s, 1H, NH), 5.49 (s, 0.25H, enol-H-5), 3.71 (s, 1.5H, keto-H-5), 3.48 (m, 2H, H-8), 3.11 (m, 2H, H-7), 2.53 (t, 1.5H, *J* = 7.2 Hz, keto-H-3), 2.18 (m, 0.5H, enol-H-3), 2.00 (m, 3H, H-10), 1.65 (m, 2H, H-2), 0.94 (m, 3H, H-1); ¹³C NMR (125 MHz, CDCl₃) 202.1, 194.3, 192.4, 177.4, 170.6, 170.4, 99.3, 57.2, 45.3, 39.9, 39.3, 36.8, 29.2, 27.8, 23.3, 23.2, 19.6, 16.9, 13.6, 13.5; HRMS (ES) *m/z* calculated for C₁₀H₁₇NSO₃Na 254.0821, found 254.0821 [M+Na]⁺.

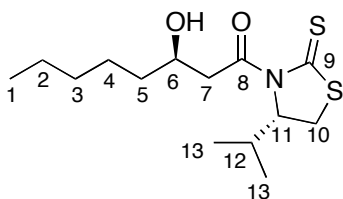
(*S*)-3-Hydroxy-1-((*S*)-4-isopropyl-2-thioxothiazolidin-3-yl)octan-1-one (70)
and (*R*)-3-Hydroxy-1-((*S*)-4-isopropyl-2-thioxothiazolidin-3-yl)octan-1-one (71)

Compounds **70** and **71** were synthesized from 1-hexanal according to the procedure used to prepare **65** and **66**.



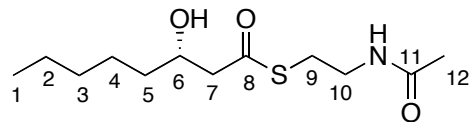
70: 240 mg, yellow oil, 50% yield. IR (CHCl₃, cast film) 3441, 2959, 2930, 2858, 1690, 1466 cm⁻¹; ¹H NMR (500 MHz, CDCl₃) δ 5.18 (ddd, 1H, *J* = 7.43, 6.3, 0.9 Hz, H-11), 4.15 (m, 1H, H-6), 3.66 (dd, 1H, *J* = 17.7, 2.3 Hz, H-7), 3.55 (dd, 1H,

$J = 11.5, 7.9$ Hz, H-10), 3.15 (dd, 1H, $J = 17.7, 9.3$ Hz, H-7), 3.05 (dd, 1H, $J = 11.6, 1.1$ Hz, H-10), 2.79 (s, 1H, OH), 2.38 (ABX₆, 1H, $J = 6.8$ Hz, H-12), 1.62-1.30 (m, 8H, H-2, H-3, H-4, H-5), 1.09 (d, 3H, $J = 6.8$ Hz, H-13), 1.02 (d, 3H, $J = 6.9$ Hz, H-13), 0.86 (t, 3H, $J = 6.8$ Hz, H-1); ¹³C NMR (125 MHz, CDCl₃) 203.1, 173.4, 71.4, 68.1, 45.6, 36.4, 31.8, 30.9, 30.6, 25.2, 22.6, 19.1, 17.9, 14.1; $[\alpha]_D^{25} = 233.76$ ($c = 1.45$, CHCl₃); HRMS (ES) m/z calculated for C₁₄H₂₅NS₂O₂Na 326.1219, found 326.1225 [M+Na]⁺.



71: 110 mg, yellow oil, 23% yield. IR (CHCl₃, cast film) 3450, 2959, 2930, 2858, 1687, 1466 cm⁻¹; ¹H NMR (500 MHz, CDCl₃) δ 5.18 (ddd, 1H, $J = 7.6, 6.3, 1.1$ Hz, H-11), 4.03 (m, 1H, H-6), 3.52 (dd, 1H, $J = 11.6, 7.9$ Hz, H-10), 3.45 (dd, 1H, $J = 17.4, 9.3$ Hz, H-7), 3.32 (dd, 1H, $J = 17.4, 2.6$ Hz, H-7), 3.18 (s, 1H, OH), 3.04 (dd, 1H, $J = 11.6, 1.2$ Hz, H-10), 2.36 (ABX₆, 1H, $J = 6.8$ Hz, H-12), 1.58-1.25 (m, 8H, H-2, H-3, H-4, H-5), 1.07 (d, 3H, $J = 6.8$ Hz, H-13), 0.98 (d, 3H, $J = 6.9$ Hz, H-13), 0.86 (t, 3H, $J = 6.9$ Hz, H-1); ¹³C NMR (125 MHz, CDCl₃) 203.2, 173.9, 71.4, 68.5, 45.2, 36.6, 31.8, 30.8, 30.6, 25.2, 22.6, 19.1, 17.9, 14.1; $[\alpha]_D^{25} = 239.47$ ($c = 0.700$, CHCl₃); HRMS (ES) m/z calculated for C₁₄H₂₅NS₂O₂Na 326.1219, found 326.1225 [M+Na]⁺.

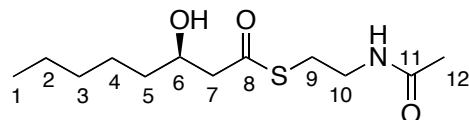
(S)-S-2-Acetamidoethyl 3-hydroxyoctanethioate (33L)



Compound **33L** was synthesized from **70** according to the procedure used to prepare **31L**.

33L: 80.0 mg, white solid, 66% yield. IR (CHCl₃, cast film) 3297, 3086, 2955, 2931, 2859, 1688, 1658, 1553 cm⁻¹; ¹H NMR (500 MHz, CDCl₃) δ 6.18 (s, 1H, NH), 4.02 (m, 1H, H-6), 3.39 (m, 1H, H-10), 3.10 (s, 1H, OH), 3.00 (m, 2H, H-9), 2.68 (dd, 1H, *J* = 15.2, 3.6 Hz, H-7), 2.64 (dd, 1H, *J* = 15.2, 8.1 Hz, H-7), 1.92 (s, 3H, H-12), 1.53-1.23 (m, 8H, H-2, H-3, H-4, H-5), 0.84 (t, 3H, *J* = 6.8 Hz, H-1); ¹³C NMR (125 MHz, CDCl₃) 199.3, 170.7, 68.7, 51.1, 39.2, 36.7, 31.6, 28.7, 25.1, 23.1, 22.5, 13.9; [α]_D²⁵ = 12.31 (*c* = 3.01, CHCl₃); HRMS (ES) *m/z* calculated for C₁₂H₂₃NSO₃Na 284.1291, found 284.1295 [M+Na]⁺.

(R)-S-2-Acetamidoethyl 3-hydroxyoctanethioate (33D)

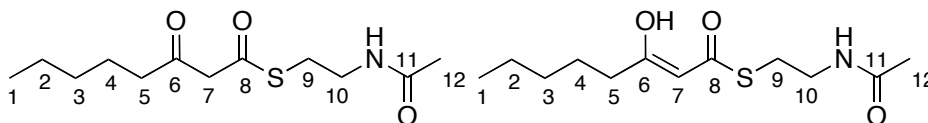


Compound **33D** was synthesized from **71** according to the procedure used to prepare **31L**.

33D: 56.7 mg, white solid, 80% yield. IR (CHCl₃, cast film) 3295, 3084, 2955, 2930, 2859, 1687, 1658, 1552 cm⁻¹; ¹H NMR (500 MHz, CDCl₃) δ 6.18 (s, 1H, NH), 4.03 (m, 1H, H-6), 3.42 (m, 1H, H-10), 3.02 (m, 2H, H-9), 2.95 (s, 1H, OH), 2.72 (dd, 1H, *J* = 15.3, 3.5 Hz, H-7), 2.66 (dd, 1H, *J* = 15.2, 8.5 Hz, H-7), 1.95 (s,

3H, H-12), 1.53-1.23 (m, 8H, H-2, H-3, H-4, H-5), 0.86 (t, 3H, $J = 6.9$ Hz, H-1); ^{13}C NMR (125 MHz, CDCl_3) 199.4, 170.6, 68.8, 51.1, 39.2, 36.8, 31.6, 28.8, 25.1, 23.2, 22.6, 14.0; $[\alpha]_{\text{D}}^{25} = -20.09$ ($c = 0.43$, CHCl_3); HRMS (ES) m/z calculated for $\text{C}_{12}\text{H}_{23}\text{NSO}_3\text{Na}$ 284.1291, found 284.1293 $[\text{M}+\text{Na}]^+$.

***S*-2-acetamidoethyl 3-oxooctanethioate and *S*-2-Acetamidoethyl 3-hydroxyoct-2-enethioate (33)**

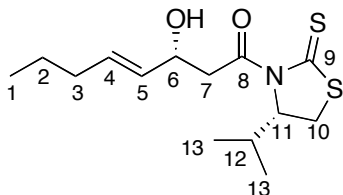


Compound **33** was synthesized from **33L** according to the procedure used to prepare **31**.

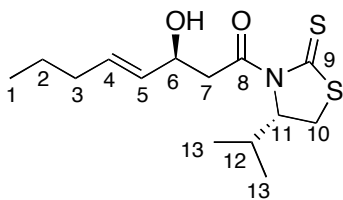
33: 8.2 mg, white solid, 46% yield, keto:enol = 1.85:1. IR (CHCl_3 , cast film) 3283, 3103, 2958, 2952, 2931, 2867, 1717, 1685, 1637, 1563 cm^{-1} ; ^1H NMR (500 MHz, CDCl_3) δ 5.92 (s, 1H, NH), 5.46 (s, 0.35H, enol-H-7), 3.69 (s, 1.3H, keto-H-7), 3.46 (m, 2H, H-10), 3.09 (m, 2H, H-9), 2.52 (t, 1.3H, $J = 7.3$ Hz, keto-H-5), 2.17 (t, 0.7H, $J = 7.6$ Hz, enol-H-5), 1.96 (m, 3H, H-12), 1.59 (m, 2H, H-4), 1.30 (m, 4H, H-2, H-3), 0.89 (m, 3H, H-1); ^{13}C NMR (125 MHz, CDCl_3) 202.3, 194.3, 192.4, 177.7, 170.5, 170.4, 99.1, 57.2, 43.4, 39.9, 39.2, 34.9, 31.3, 31.1, 29.2, 27.8, 25.9, 23.2, 23.1, 23.1, 22.4, 22.3, 13.9, 13.8; HRMS (ES) m/z calculated for $\text{C}_{12}\text{H}_{21}\text{NSO}_3\text{Na}$ 282.1134, found 282.1137 $[\text{M}+\text{Na}]^+$.

(*R*, *E*)-3-Hydroxy-1-((*S*)-4-isopropyl-2-thioxothiazolidin-3-yl)oct-4-en-1-one (72) and (*S*, *E*)-3-Hydroxy-1-((*S*)-4-isopropyl-2-thioxothiazolidin-3-yl)oct-4-en-1-one (73)

Compounds **72** and **73** were synthesized from hex-2-enal according to the procedure used to prepare **65** and **66**.

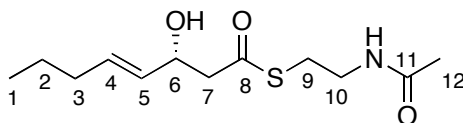


72: 112 mg, yellow oil, 50% yield. IR (CHCl₃, cast film) 3426, 2961, 2929, 2872, 1695, 1465 cm⁻¹; ¹H NMR (500 MHz, CDCl₃) δ 5.75 (m, 1H, H-5), 5.56 (ddt, 1H, *J* = 15.4, 6.4, 1.4 Hz, H-5), 5.17 (ddd, 1H, *J* = 7.43, 6.6, 0.8 Hz, H-11), 4.64 (m, 1H, H-6), 3.63 (dd, 1H, *J* = 17.5, 2.9 Hz, H-7), 3.51 (dd, 1H, *J* = 11.5, 7.9 Hz, H-10), 3.33 (dd, 1H, *J* = 17.6, 8.9 Hz, H-7), 3.05 (dd, 1H, *J* = 11.5, 0.9 Hz, H-10), 2.38 (ABX₆, 1H, *J* = 6.79 Hz, H-12), 2.15 (m, 2H, H-3), 1.43 (sextet, 1H, *J* = 7.43 Hz, H-2), 1.09 (d, 3H, *J* = 6.88 Hz, H-13), 1.01 (d, 3H, *J* = 6.97 Hz, H-13), 0.92 (t, 3H, *J* = 7.42 Hz, H-1); ¹³C NMR (125 MHz, CDCl₃) 202.9, 172.6, 132.5, 130.6, 71.4, 68.8, 45.5, 34.3, 30.8, 30.6, 22.2, 19.1, 17.8, 13.7; [α]_D²⁵ = 293 (*c* = 0.470, CHCl₃); HRMS (ES) *m/z* calculated for C₁₄H₂₃NS₂O₂Na 324.1062, found 324.1063 [M+Na]⁺.



73: 33.0 mg, yellow oil, 14% yield. IR (CHCl₃, cast film) 3427, 2961, 2929, 2872, 1694, 1465cm⁻¹; ¹H NMR (500 MHz, CDCl₃) δ 5.76 (m, 1H, H-5), 5.55 (ddt, 1H, *J* = 15.4, 6.4, 1.3 Hz, H-5), 5.20 (ddd, 1H, *J* = 7.43, 6.3, 1.1 Hz, H-11), 4.56 (m, 1H, H-6), 3.63 (dd, 1H, *J* = 17.3, 9.0 Hz, H-7), 3.53 (dd, 1H, *J* = 11.5, 8.0 Hz, H-10), 3.38 (dd, 1H, *J* = 17.3, 3.2 Hz, H-7), 3.06 (dd, 1H, *J* = 11.5, 1.2 Hz, H-10), 2.38 (ABX₆, 1H, *J* = 6.9 Hz, H-12), 2.15 (m, 2H, H-3), 1.43 (sextet, 1H, *J* = 7.2 Hz, H-2), 1.09 (d, 3H, *J* = 6.8 Hz, H-13), 1.01 (d, 3H, *J* = 6.8 Hz, H-13), 0.93 (t, 3H, *J* = 7.3 Hz, H-1); ¹³C NMR (125 MHz, CDCl₃) 203.1, 173.1, 132.5, 130.7, 71.4, 69.3, 45.3, 34.3, 30.8, 30.6, 22.2, 19.1, 17.8, 13.7; [α]_D²⁵ = 257 (c = 0.500, CHCl₃); HRMS (ES) *m/z* calculated for C₁₄H₂₃NS₂O₂Na 324.1062, found 324.1063 [M+Na]⁺.

(*R,E*)-*S*-2-Acetamidoethyl 3-hydroxyoct-4-enethioate (34D)

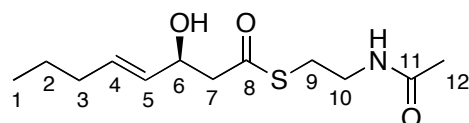


Compound **34D** was synthesized from **72** according to the procedure used to prepare **31L**.

34D: 80.0 mg, yellow oil, 61% yield. IR (CHCl₃, cast film) 3295, 3088, 2958, 2930, 2873, 1687, 1657, 1553 cm⁻¹; ¹H NMR (500 MHz, CDCl₃) δ 6.06 (s, 1H, NH), 5.67 (m, 1H, H-4), 5.45 (m, 1H, H-5), 4.52 (m, 1H, H-6), 3.40 (m, 2H, H-

10), 3.04 (m, 2H, H-9), 2.82 (s, 1H, OH), 2.75 (m, 2H, H-7), 1.97 (m, 2H, H-3), 1.95 (s, 3H, H-12), 1.37 (sextet, 1H, $J = 7.3$ Hz, H-2), 0.87 (t, 3H, $J = 7.4$ Hz, H-1); ^{13}C NMR (125 MHz, CDCl_3) 198.6, 170.6, 132.8, 130.6, 69.6, 51.2, 39.3, 34.2, 28.7, 23.1, 22.1, 13.6; $[\alpha]_{\text{D}}^{25} = 14.3$ ($c = 0.430$, CHCl_3); HRMS (ES) m/z calculated for $\text{C}_{12}\text{H}_{21}\text{NSO}_3\text{Na}$ 282.1134, found 282.1136 $[\text{M}+\text{Na}]^+$.

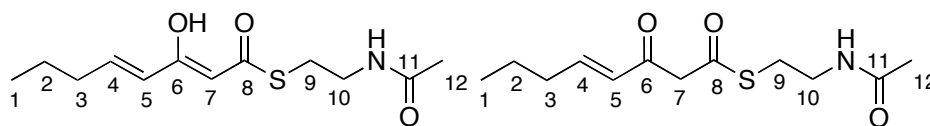
(*S, E*)-*S*-2-Acetamidoethyl 3-hydroxyoct-4-enethioate (34L**)**



Compound **34L** was synthesized from **73** according to the procedure used to prepare **31L**.

34L: 52.0 mg, yellow oil, 74% yield. IR (CHCl_3 , cast film) 3296, 3087, 2958, 2929, 2872, 1687, 1658, 1552 cm^{-1} ; ^1H NMR (500 MHz, CDCl_3) d 6.06 (s, 1H, NH), 5.67 (m, 1H, H-4), 5.45 (m, 1H, H-5), 4.52 (m, 1H, H-6), 3.40 (m, 2H, H-10), 3.04 (m, 2H, H-9), 2.87 (s, 1H, OH), 2.75 (m, 2H, H-7), 1.97 (m, 2H, H-3), 1.95 (s, 3H, H-12), 1.36 (sextet, 1H, $J = 7.5$ Hz, H-2), 0.87 (t, 3H, $J = 7.4$ Hz, H-1); ^{13}C NMR (125 MHz, CDCl_3) 198.6, 170.6, 132.8, 130.6, 69.6, 51.2, 39.3, 34.2, 28.7, 23.1, 22.1, 13.6; $[\alpha]_{\text{D}}^{25} = -11.3$ ($c = 0.390$, CHCl_3); HRMS (ES) m/z calculated for $\text{C}_{12}\text{H}_{21}\text{NSO}_3\text{Na}$ 282.1134, found 282.1136 $[\text{M}+\text{Na}]^+$.

(*E*)-*S*-2-Acetamidoethyl 3-oxooct-4-enethioate and (*4E*)-*S*-2-Acetamidoethyl 3-hydroxyocta-2,4-dienethioate (34)

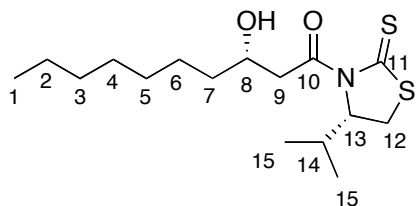


Compound **34** was synthesized from **34D** according to the procedure used to prepare **31**.

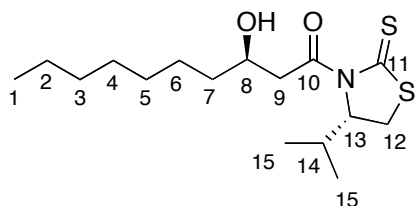
34: 18.0 mg, white solid, 60% yield, keto:enol = 1:5.6. IR (CHCl₃, cast film) 3298, 3078, 2958, 2956, 2918, 2870, 1650, 1597, 1556 cm⁻¹; ¹H NMR (500 MHz, CDCl₃) δ 6.90 (dt, 0.14H, *J* = 15.8, 6.8 Hz, keto-H-4), 6.75 (dt, 0.86H, *J* = 15.4, 7.2 Hz, enol-H-4), 6.15 (dt, 0.14H, *J* = 15.9, 1.5 Hz, keto-H-5), 6.08 (s, 1H, NH), 5.72 (dd, 0.86H, *J* = 15.4, 1.4 Hz, enol-H-5), 5.40 (s, 0.85H, enol-H-7), 3.82 (s, 0.3H, keto-H-7), 3.48 (m, 2H, H-10), 3.09 (m, 2H, H-9), 2.18 (m, 2H, H-3), 1.97 (s, 3H, H-12), 1.46 (m, 2H, H-2), 0.98 (t, 3H, *J* = 6.2 Hz, H-1); ¹³C NMR (125 MHz, CDCl₃) 194.5, 192.6, 191.6, 170.5, 170.4, 167.5, 150.8, 143.9, 129.6, 123.9, 99.7, 54.8, 39.9, 39.2, 34.8, 34.6, 29.2, 27.8, 23.2, 23.1, 21.6, 21.2, 13.7; HRMS (ES) *m/z* calculated for C₁₂H₁₉NSO₃Na 280.0978, found 280.0980 [M+Na]⁺.

(S)-3-Hydroxy-1-((S)-4-isopropyl-2-thioxothiazolidin-3-yl)decan-1-one (74)
and (R)-3-Hydroxy-1-((S)-4-isopropyl-2-thioxothiazolidin-3-yl)decan-1-one (75)

Compounds **74** and **75** were synthesized from octanal according to the procedure used to prepare **65** and **66**.



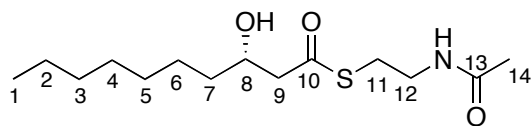
74: 136 mg, yellow oil, 49% yield. IR (CHCl₃, cast film) 3437, 2958, 2927, 2857, 1696, 1467 cm⁻¹; ¹H NMR (500 MHz, CDCl₃) δ 5.15 (ddd, 1H, *J* = 7.6, 6.2, 1.0 Hz, H-13), 4.11 (m, 1H, H-8), 3.61 (dd, 1H, *J* = 17.7, 2.4 Hz, H-9), 3.51 (dd, 1H, *J* = 11.5, 7.8 Hz, H-12), 3.11 (dd, 1H, *J* = 17.7, 9.4 Hz, H-9), 3.02 (dd, 1H, *J* = 11.5, 1.0 Hz, H-12), 2.34 (m, 1H, H-14), 1.58 - 1.1.25 (m, 12H, H-2, H-3, H-4, H-5, H-6, H-7), 1.05 (d, 3H, *J* = 6.7 Hz, H-15), 0.98 (d, 3H, *J* = 6.9 Hz, H-15), 0.85 (d, 3H, *J* = 6.8 Hz, H-1); ¹³C NMR (125 MHz, CDCl₃) 203.0, 173.3, 71.4, 68.0, 45.5, 36.4, 31.8, 30.9, 30.6, 29.5, 29.2, 25.5, 22.6, 19.1, 17.8, 14.1; [α]_D²⁵ = 279 (c = 0.470, CHCl₃); HRMS (ES) *m/z* calculated for C₁₆H₂₉NS₂O₂Na 354.1532, found 354.1532 [M+Na]⁺.



75: 91.3 mg, yellow oil, 33% yield. IR (CHCl₃, cast film) 3448, 2958, 2927, 2855, 1697, 1467 cm⁻¹; ¹H NMR (500 MHz, CDCl₃) δ 5.17 (ddd, 1H, *J* = 7.6, 6.2, 1.1

Hz, H-13), 4.03 (m, 1H, H-8), 3.45 (dd, 1H, $J = 11.5, 7.9$ Hz, H-12), 3.45 (dd, 1H, $J = 17.4, 9.3$ Hz, H-9), 3.32 (dd, 1H, $J = 17.3, 2.6$ Hz, H-9), 3.02 (dd, 1H, $J = 11.5, 1.1$ Hz, H-12), 2.34 (m, 1H, H-14), 1.58-1.25 (m, 12H, H-2, H-3, H-4, H-5, H-6, H-7), 1.05 (d, 3H, $J = 6.8$ Hz, H-15), 0.98 (d, 3H, $J = 6.9$ Hz, H-15), 0.86 (t, 3H, $J = 6.8$ Hz, H-1); ^{13}C NMR (125 MHz, CDCl_3) 203.0, 173.8, 71.3, 68.5, 45.1, 36.6, 31.8, 30.7, 30.6, 29.5, 29.2, 25.4, 22.6, 19.0, 17.8, 14.1; $[\alpha]_{\text{D}}^{25} = 212.47$ (c = 0.470, CHCl_3); HRMS (ES) m/z calculated for $\text{C}_{16}\text{H}_{29}\text{NS}_2\text{O}_2\text{Na}$ 354.1532, found 354.1531 $[\text{M}+\text{Na}]^+$.

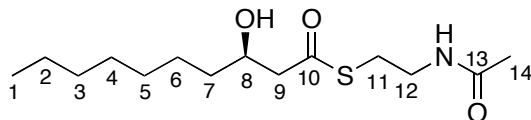
(S)-S-2-Acetamidoethyl 3-hydroxydecanethioate (36L)



Compound **36L** was synthesized from **74** according to the procedure used to prepare **31L**.

36L: 70.0 mg, white solid, 69% yield. IR (CHCl_3 , cast film) 3405, 3313, 2955, 2918, 2851, 1685, 1643, 1546 cm^{-1} ; ^1H NMR (500 MHz, CDCl_3) δ 6.03 (s, 1H, NH), 4.10 (m, 1H, H-8), 3.42 (m, 1H, H-12), 3.03 (m, 2H, H-11), 2.87 (d, 1H, $J = 4.2$ Hz OH), 2.72 (dd, 1H, $J = 15.2, 3.3$ Hz, H-9), 2.66 (dd, 1H, $J = 15.3, 8.6$ Hz, H-9), 1.97 (s, 3H, H-14), 1.53-1.23 (m, 12H, H-2, H-3, H-4, H-5, H-6, H-7), 0.86 (t, 3H, $J = 6.7$ Hz, H-1); ^{13}C NMR (125 MHz, CDCl_3) 199.4, 170.6, 68.8, 51.1, 39.3, 36.8, 31.8, 29.4, 29.2, 28.8, 25.4, 23.2, 22.6, 14.1; $[\alpha]_{\text{D}}^{25} = 14.1$ (c = 1.210, CHCl_3); HRMS (ES) m/z calculated for $\text{C}_{14}\text{H}_{27}\text{NSO}_3\text{Na}$ 312.1604, found 312.1604 $[\text{M}+\text{Na}]^+$.

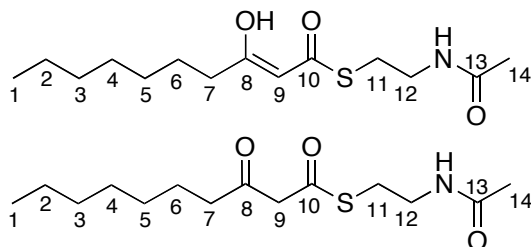
(R)-S-2-Acetamidoethyl 3-hydroxydecanethioate (36D)



Compound **36D** was synthesized from **75** according to the procedure used to prepare **31L**.

36D: 45.0 mg, white solid, 65% yield. IR (CHCl₃, cast film) 3405, 3313, 2955, 2918, 2851, 1685, 1643, 1546 cm⁻¹; ¹H NMR (500 MHz, CDCl₃) δ 6.00 (s, 1H, NH), 4.04 (m, 1H, H-8), 3.43 (m, 1H, H-12), 3.03 (m, 2H, H-11), 2.80 (d, 1H, *J* = 4.1 Hz OH), 2.73 (dd, 1H, *J* = 15.3, 3.4 Hz, H-9), 2.66 (dd, 1H, *J* = 15.3, 8.6 Hz, H-9), 1.97 (s, 3H, H-14), 1.53-1.23 (m, 12H, H-2, H-3, H-4, H-5, H-6, H-7), 0.86 (t, 3H, *J* = 6.8 Hz, H-1); ¹³C NMR (125 MHz, CDCl₃) 199.5, 170.5, 68.8, 51.1, 39.3, 36.8, 31.8, 29.4, 29.2, 28.8, 25.4, 23.2, 22.6, 14.1; [α]_D²⁵ = -14.3 (c = 1.000, CHCl₃); HRMS (ES) *m/z* calculated for C₁₄H₂₇NSO₃Na 312.1604, found 312.1603 [M+Na]⁺.

S-2-Acetamidoethyl 3-oxodecanethioate and S-2-Acetamidoethyl 3-hydroxydec-2-enethioate (36)

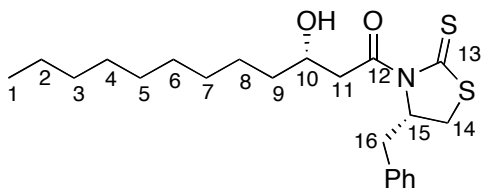


Compound **36** was synthesized from **36L** according to the procedure used to prepare **31**.

36: 15.0 mg, white solid, 30% yield, keto:enol = 1.85:1. IR (CHCl₃, cast film) 3281, 3105, 2949, 2923, 2856, 1717, 1687, 1637, 1563 cm⁻¹; ¹H NMR (500 MHz, CDCl₃) δ 5.95 (s, 1H, NH), 5.45 (s, 0.35H, enol-H-9), 3.69 (s, 1.3H, keto-H-9), 3.46 (m, 2H, H-12), 3.09 (m, 2H, H-11), 2.52 (t, 1.3H, *J* = 7.3 Hz, keto-H-7), 2.17 (t, 0.7H, *J* = 7.6 Hz, enol-H-7), 1.98 (m, 3H, H-14), 1.58 (m, 2H, H-6), 1.33 -1.20 (m, 8H, H-2, H-3, H-4, H-5), 0.89 (m, 3H, H-1); ¹³C NMR (125 MHz, CDCl₃) 202.3, 194.3, 192.4, 177.7, 170.4, 170.2, 99.1, 57.2, 43.5, 39.9, 39.2, 34.9, 31.7, 31.6, 29.3, 29.1, 29.0, 28.9, 27.9, 26.3, 23.5, 23.3, 23.2, 22.67, 14.1; HRMS (ES) *m/z* calculated for C₁₄H₂₅NSO₃Na 310.1447, found 310.1447 [M+Na]⁺.

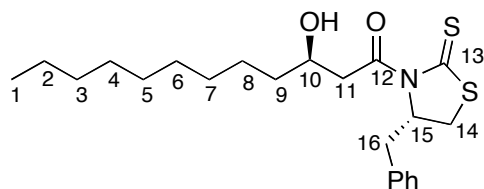
(S)-1-((S)-4-Benzyl-2-thioxothiazolidin-3-yl)-3-hydroxydodecan-1-one (**77**)
and **(R)-1-((S)-4-Benzyl-2-thioxothiazolidin-3-yl)-3-hydroxydodecan-1-one** (**78**)

Compounds **77** and **78** were synthesized from decanal by the similar method for synthesizing **65** and **66** where the auxiliary was changed to (*S*)-4-benzyl-*N*-acetyl-1, 3-thiazolidine-2-thione.



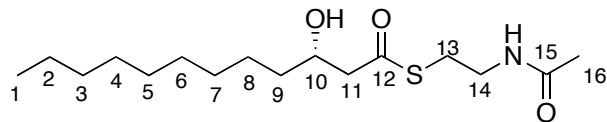
77: 203 mg, yellow oil, 50% yield. IR (CHCl₃, cast film) 3451, 2925, 2854, 1695, 1496 cm⁻¹; ¹H NMR (500 MHz, CDCl₃) δ 7.37-7.25 (m, 5H, Ph), 5.40 (ddd, 1H, *J*

= 10.6, 6.9, 4.04 Hz, H-15), 4.05 (m, 1H, H-10), 3.64 (dd, 1H, $J = 17.7, 2.3$ Hz, H-11), 3.40 (dd, 1H, $J = 11.5, 7.3$ Hz, H-14), 3.23 (dd, 1H, $J = 13.2, 3.7$ Hz, H-16), 3.13 (dd, 1H, $J = 17.7, 9.3$ Hz, H-11), 3.05 (dd, 1H, $J = 13.1, 10.5$ Hz, H-16), 2.89 (d, 1H, $J = 11.6$ Hz, H-14), 1.60 - 1.22 (m, 16H, H-2, H-3, H-4, H-5, H-6, H-7, H-8, H-9), 0.86 (t, 3H, $J = 6.6$ Hz, H-1); ^{13}C NMR (125 MHz, CDCl_3) 201.4, 173.4, 136.4, 129.5, 128.9, 127.3, 68.4, 67.9, 45.9, 36.9, 36.4, 32.1, 31.9, 29.6, 29.5, 29.5, 29.3, 25.6, 22.7, 14.1; $[\alpha]_{\text{D}}^{25} = 123$ (c = 0.280, CHCl_3); HRMS (ES) m/z calculated for $\text{C}_{22}\text{H}_{33}\text{NS}_2\text{O}_2\text{Na}$ 430.1845, found 430.1847 $[\text{M}+\text{Na}]^+$.



78: 38.0 mg, yellow oil, 10% yield. IR (CHCl_3 , cast film) 3449, 2925, 2854, 1697, 1496 cm^{-1} ; ^1H NMR (500 MHz, CDCl_3) δ 7.37-7.27 (m, 5H, Ph), 5.40 (ddd, 1H, $J = 10.6, 6.9, 4.0$ Hz, H-15), 4.05 (m, 1H, H-10), 3.46 (dd, 1H, $J = 17.4, 9.2$ Hz, H-11), 3.40 (dd, 1H, $J = 11.5, 7.2$ Hz, H-14), 3.34 (dd, 1H, $J = 17.4, 2.5$ Hz, H-11), 3.23 (dd, 1H, $J = 13.3, 3.3$ Hz, H-16), 3.09 (s, 1H, OH), 3.05 (dd, 1H, $J = 13.2, 10.5$ Hz, H-16), 2.91 (d, 1H, $J = 11.6$ Hz, H-14), 1.60 - 1.20 (m, 16H, H-2, H-3, H-4, H-5, H-6, H-7, H-8, H-9), 0.86 (t, 3H, $J = 6.9$ Hz, H-1); ^{13}C NMR (125 MHz, CDCl_3) 201.5, 173.9, 136.4, 129.5, 128.9, 127.3, 68.5, 68.3, 45.5, 36.8, 36.7, 32.1, 31.9, 29.6, 29.5, 29.5, 29.3, 25.5, 22.7, 14.1; $[\alpha]_{\text{D}}^{25} = 61.6$ (c = 0.260, CHCl_3); HRMS (ES) m/z calculated for $\text{C}_{22}\text{H}_{33}\text{NS}_2\text{O}_2\text{Na}$ 430.1845, found 430.1847 $[\text{M}+\text{Na}]^+$.

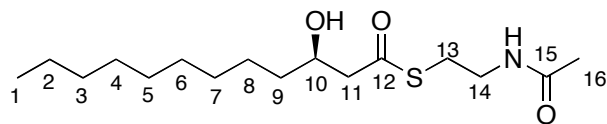
(S)-S-2-Acetamidoethyl 3-hydroxydodecanethioate (37D)



Compound **37D** was synthesized from **77** according to the procedure used to prepare **31L**.

37D: 90.0 mg, white solid, 58% yield. IR (CHCl₃, cast film) 3408, 3281, 3230, 2954, 2917, 2849, 1683, 1658, 1631, 1557 cm⁻¹; ¹H NMR (500 MHz, CDCl₃) δ 6.02 (s, 1H, NH), 4.04 (m, 1H, H-10), 3.45 (m, 1H, H-14), 3.04 (m, 2H, H-13), 2.80 (d, 1H, *J* = 4.4 Hz, OH), 2.87 (d, 1H, *J* = 4.2 Hz OH), 2.73 (dd, 1H, *J* = 15.3, 3.4 Hz, H-11), 2.67 (dd, 1H, *J* = 15.3, 8.7 Hz, H-11), 1.97 (s, 3H, H-16), 1.53 - 1.23 (m, 16H, H-2, H-3, H-4, H-5, H-6, H-7, H-8, H-9), 0.86 (t, 3H, *J* = 6.8 Hz, H-1); ¹³C NMR (125 MHz, CDCl₃) 199.5, 170.5, 68.8, 51.1, 39.3, 36.8, 31.9, 29.6, 29.5, 29.5, 29.3, 28.9, 25.4, 23.2, 22.7, 14.1; [α]_D²⁵ = 29.2 (c = 0.150, CHCl₃); HRMS (ES) *m/z* calculated for C₁₆H₃₁NSO₃Na 340.1917, found 340.1919 [M+Na]⁺.

(R)-S-2-Acetamidoethyl 3-hydroxydodecanethioate (37L)

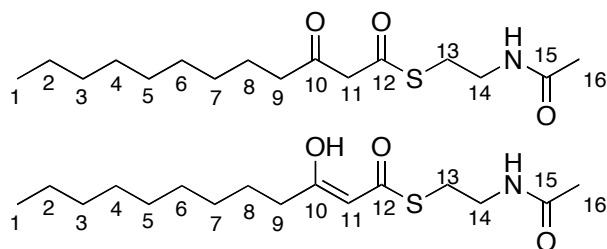


Compound **37L** was synthesized from **78** according to the procedure used to prepare **31L**.

37L: 22.0 mg, white solid, yield 81%. IR (CHCl₃, cast film) 3406, 3313, 2954, 2917, 2845, 1683, 1659, 1638, 1557 cm⁻¹; ¹H NMR (500 MHz, CDCl₃) δ 5.86 (s,

1H, NH), 4.06 (m, 1H, H-10), 3.45 (m, 1H, H-14), 3.04 (m, 2H, H-13), 2.87 (d, 1H, $J = 4.2$ Hz OH), 2.75 (dd, 1H, $J = 15.4, 3.3$ Hz, H-11), 2.67 (dd, 1H, $J = 15.5, 8.5$ Hz, H-11), 2.66 (d, 1H, $J = 4.2$ Hz, OH), 1.97 (s, 3H, H-16), 1.53 - 1.23 (m, 16H, H-2, H-3, H-4, H-5, H-6, H-7, H-8, H-9), 0.86 (t, 3H, $J = 6.8$ Hz, H-1); ^{13}C NMR (125 MHz, CDCl_3) 199.6, 170.5, 68.9, 51.1, 39.3, 36.8, 31.9, 29.6, 29.5, 29.5, 29.3, 28.9, 25.4, 23.2, 22.7, 14.1; $[\alpha]_{\text{D}}^{25} = -14.3$ ($c = 0.260$, CHCl_3); HRMS (ES) m/z calculated for $\text{C}_{16}\text{H}_{31}\text{NSO}_3\text{Na}$ 340.1917, found 340.1918 $[\text{M}+\text{Na}]^+$.

***S*-2-Acetamidoethyl 3-oxododecanethioate and *S*-2-Acetamidoethyl 3-hydroxydodec-2-enethioate (37)**

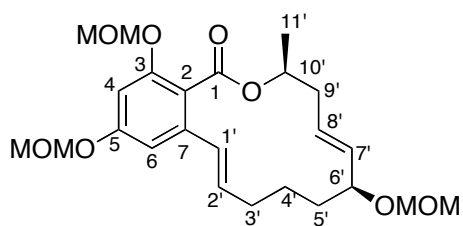


Compound **37** were synthesized from **37D** according to the procedure used to prepare **31**.

37: 35.0 mg, white solid, 64% yield. IR (CHCl_3 , cast film) 3279, 3104, 2948, 2920, 2849, 1717, 1687, 1636, 1565 cm^{-1} ; ^1H NMR (500 MHz, CDCl_3) δ 5.86 (s, 1H, NH), 5.45 (s, 0.3H, enol-H-11), 3.69 (s, 1.4H, keto-H-11), 3.46 (m, 2H, H-14), 3.09 (m, 2H, H-13), 2.52 (t, 1.3H, $J = 7.4$ Hz, keto-H-9), 2.17 (t, 0.7H, $J = 7.6$ Hz, enol-H-9), 1.96 (m, 3H, H-16), 1.58 (m, 2H, H-8), 1.33 - 1.20 (m, 12H, H-2, H-3, H-4, H-5, H-6, H-7), 0.89 (m, 3H, H-1); ^{13}C NMR (125 MHz, CDCl_3)

202.3, 194.3, 192.4, 177.7, 170.4, 170.2, 99.1, 57.2, 43.5, 39.9, 39.2, 34.9, 31.9, 31.3, 29.4, 29.4, 29.3, 29.3, 29.2, 29.2, 29.1, 29.0, 27.9, 26.3, 23.5, 23.3, 23.2, 22.7, 14.1; HRMS (ES) m/z calculated for $C_{16}H_{29}NSO_3Na$ 338.1760, found 338.1763 $[M+Na]^+$.

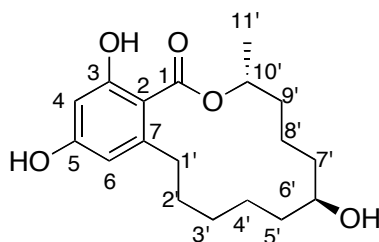
MOM-DHZ (80)



To a stirred solution of DHZ (8.00 mg, 25.1 μ mol) in 5 mL DMF was added iPr_2EtN (0.02 mL, 113 μ mol) at 0 $^{\circ}C$ under Ar. After stirring for 10 min at 0 $^{\circ}C$, methoxymethyl chloride (MOMCl) (0.01 mL, 131 μ mol) was added and the reaction was warmed up to 25 $^{\circ}C$. After stirring for 12 h, the reaction was diluted with Et_2O (100 mL) and washed with NH_4Cl (100 mL), brine (100 mL) and then dried over Na_2SO_4 . The solvent was removed *in vacuo* and the residue was purified using flash column chromatography (1:1 EtOAc/ hexanes) to give the product (8.00 mg, 76%) as a white solid. IR ($CHCl_3$, cast film) 2928, 2852, 1723, 1601, 1578, 1448, 1043 cm^{-1} ; 1H NMR (600 MHz, $CDCl_3$) δ 6.85 (d, 1H, J = 2.1 Hz, H-4), 6.67 (d, 1H, J = 2.1 Hz, H-6), 6.31 (d, 1H, J = 15.9 Hz, H-2'), 6.17 (ddd, 1H, J = 15.9, 7.1, 5.2 Hz, H-1'), 5.67 (ddd, 1H, J = 15.0, 10.2, 4.3 Hz, H-8'), 5.44-5.35 (m, 2H, H-7', H-10'), 5.17-5.10 (m, 4H, OCH_2O), 4.68 (d, 1H, J = 6.7 Hz, OCH_2O), 4.50 (d, 1H, J = 6.7 Hz, OCH_2O), 4.00-3.95 (m, 1H, H-6'), 3.46

(s, 3H, OCH₃), 3.45 (s, 3H, OCH₃), 3.36 (s, 3H, OCH₃), 2.46-2.23 (m, 4H, H-3', H-9'), 1.67-1.57 (m, 4H, H-4', H-5'), 1.37 (d, 3H, *J* = 6.2 Hz, H-11'); ¹³C NMR (125 MHz, CDCl₃) δ 167.8, 158.7, 154.8, 136.7, 133.2, 132.7, 130.0, 126.7, 118.4, 104.8, 102.1, 94.60, 94.41, 93.4, 75.5, 70.9, 56.20, 56.09, 55.2, 39.4, 32.6, 29.7, 22.7, 20.9; HRMS (ES) *m/z* calculated for C₂₄H₃₅O₈ 451.2326, found 451.2320 [M-H]⁻.

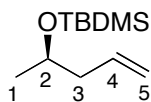
(3R,7S)-7,14,16-trihydroxy-3-methyl-3,4,5,6,7,8,9,10,11,12-decahydro-1H-benzo[*c*][1]oxacyclotetradecin-1-one (83)



To a stirred solution of *epi*-DHZ (1.00 mg, 3.10 μmol) in 1 mL CD₃OD was added Rh on alumina (700 μg, 5 wt%). The resulting solution was stirred under 1 atm H₂. The reaction was monitored by NMR until all starting material was consumed. The solvent was removed *in vacuo* and the residue was purified using preparative TLC (2:1 Hexane/ EtOAc) to give the product (0.8 mg, 80% yield). IR (MeOH, cast film) 3362, 2924, 2854, 1646, 1610, 1582, 1436, 1259 cm⁻¹; ¹H NMR (500 MHz, CD₃OD) δ 6.19 (d, 1H, *J* = 2.4 Hz, H-4), 6.15 (d, 1H, *J* = 2.4 Hz, H-6), 5.16 (m, 2H, H-10'), 3.75 (m, 1H, H-6'), 3.17 (td, 1H, *J* = 12.1, 4.2 Hz, H-1'), 2.42 (td, 1H, *J* = 12.5, 5.2 Hz, H-1'), 1.86-1.75 (m, 2H, H-9', H-2'), 1.72-1.66 (m, 1H, H-5'), 1.66-1.56 (m, 3H, H-4', H-7', H-8'), 1.56-1.46 (m, 4H, H-3',

H-6', H-7', H-8'), 1.46-1.36 (m, 2H, H-3', H-4'), 1.35-1.30 (m, 1H, H-5'), 1.33 (d, 3H, $J = 6.2$ Hz, H-11'), 1.20-1.30 (m, 1H, H-2'); ^{13}C NMR (125 MHz, CD_3OD) 173.0, 166.0, 163.7, 149.1, 111.7, 106.0, 102.0, 74.3, 69.2, 37.6, 36.6, 36.2, 32.6, 32.3, 28.2, 24.5, 22.7, 21.5; HRMS (ES) m/z calculated 321.1707 for $\text{C}_{18}\text{H}_{25}\text{O}_5$, found 321.1706 $[\text{M}-\text{H}]^-$.

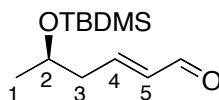
(*R*)-*tert*-Butyldimethyl(pent-4-en-2-yloxy)silane (86)



The known compound²⁰³ was synthesized from (*R*)-pent-4-en-2-ol according to the procedure used to prepare **17**.

86: 4.60 g, a colorless oil, quant. yield. IR (CHCl_3 , cast film) 2957, 2930, 2897, 2858, 1472 cm^{-1} ; ^1H NMR (500 MHz, CDCl_3) δ 5.81 (ddt, 1H, $J = 17.2, 10.1, 7.1$ Hz, H-4), 5.06-5.00 (m, 2H, H-5), 3.84 (sextet, 1H, $J = 6.1$ Hz, H-2), 2.25-2.12 (m, 2H, H-3), 1.13 (d, 3H, $J = 6.1$ Hz, H-1), 0.90 (s, 9H, $\text{Si}-\text{C}(\text{CH}_3)_3$), 0.05 (s, 3H, SiCH_3), 0.04 (s, 3H, SiCH_3); ^{13}C NMR (100 MHz, CDCl_3) δ 135.6, 116.4, 68.4, 44.3, 25.8, 23.4, -4.56, -4.75; $[\alpha]_{\text{D}}^{25} = -4.07$ ($c = 1.82$, CHCl_3).

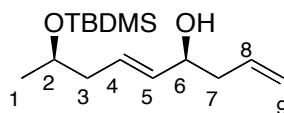
(*R, E*)-5-(*tert*-Butyldimethylsilyloxy)hex-2-enal (87)



The known compound²⁰⁴ was synthesized from **86** according to the procedure used to prepare **18**.

87: 4.10 g, a colorless oil, 78% yield. IR (CHCl₃, cast film) 2957, 2930, 2887, 2858, 2808, 2725, 1697, 1472 cm⁻¹; ¹H NMR (500 MHz, CDCl₃) δ 9.51 (d, 1H, *J* = 7.9 Hz, H-6), 6.86 (dt, 1H, *J* = 15.6, 7.4 Hz, H-4), 6.13 (ddt, *J* = 15.7, 7.9, 1.3 Hz, H-5), 4.00 (sextet, 1H, *J* = 5.9 Hz, H-2), 2.46-2.43 (m, 2H, H-3), 1.18 (d, 3H, *J* = 5.9 Hz, H-1), 0.85 (s, 9H, Si-C(CH₃)₃), 0.03 (s, 3H, SiCH₃), 0.01 (s, 3H, SiCH₃) ; ¹³C NMR (100 MHz, CDCl₃) δ 193.9, 155.4, 134.8, 67.4, 42.8, 25.9, 23.8, 18.1, -4.4, -4.8; [α]_D²⁵ = - 5.08 (c = 1.48, CHCl₃); HRMS (ES) *m/z* calculated for C₁₂H₂₄SiO₂Na 251.1438 found 251.1438 [M+Na]⁺.

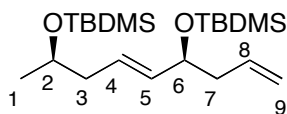
(4*S*, 8*R*, *E*)-8-(*tert*-Butyldimethylsilyloxy)nona-1,5-dien-4-ol (88)



Compound **88** was synthesized from **87** according to the procedure used to prepare **19**.

88: 3.30 g, colorless liquid, 73% yield. IR (CHCl₃, cast film) 3354, 3077, 2957, 2929, 2897, 2858, 1472, 1466 cm⁻¹; ¹H NMR (600 MHz, CDCl₃) δ 5.80 (m, 1H, H-8), 5.66 (m, 1H, H-4), 5.52 (ddt, 1H, *J* = 15.3, 6.6, 1.2 Hz, H-5), 5.12 (m, 2H, H-9), 4.12 (m, 1H, H-6), 3.85 (sextet, 1H, *J* = 6.1 Hz, H-2), 2.30–2.15 (m, 4H, H-3, H-7), 1.12 (d, 3H, *J* = 6.1 Hz, H-1), 0.88 (s, 9H, Si-C(CH₃)₃), 0.05 (s, 3H, SiCH₃), 0.04 (s, 3H, SiCH₃) ; ¹³C NMR (125 MHz, CDCl₃) δ 134.4, 134.3, 128.8, 118.0, 71.9, 68.5, 42.6, 41.9, 25.9, 23.5, 18.2, -4.5, -4.8; [α]_D²⁵ = -12.7 (c = 1.13, CHCl₃); HRMS (ES) *m/z* calculated for C₁₅H₃₀SiO₂Na 293.1907, found 293.1906 [M+Na]⁺.

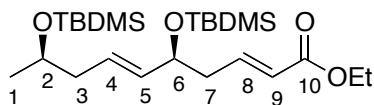
(5*S*, 9*R*, *E*)-5-Allyl-2, 2, 3, 3, 9, 11, 11, 12, 12-nonamethyl-4, 10-dioxa-3, 11-disilatridec-6-ene (89)



Compound **89** was synthesized from **88** according to the procedure used to prepare **20**.

89: 2.10 g, colorless liquid, quant. IR (CHCl₃, cast film) 3078, 2957, 2930, 2897, 2858, 1472, 1463, 1257 cm⁻¹; ¹H NMR (600 MHz, CDCl₃) δ 5.78 (m, 1H, H-8), 5.55 (m, 1H, H-4), 5.45 (ddt, 1H, *J* = 15.4, 6.5, 1.2 Hz, H-5), 5.03 (m, 2H, H-9), 4.09 (m, 1H), 3.80 (sextet, 1H, *J* = 6.1 Hz, H-2), 2.27–2.11 (m, 4H, H-3, H-7), 1.10 (d, 3H, *J* = 6.0 Hz, H-1), 0.88 (s, 18H, Si-C(CH₃)₃), 0.06 (s, 6H, SiCH₃), 0.05 (s, 3H, SiCH₃), 0.03 (s, 3H, SiCH₃); ¹³C NMR (125 MHz, CDCl₃) δ 135.4, 135.3, 126.9, 116.6, 73.5, 68.6, 43.1, 42.6, 26.0, 25.9, 23.2, 18.2, 18.1, -4.2, -4.5, -4.6, -4.7; [α]_D²⁵ = -2.16 (*c* = 1.64, CHCl₃); HRMS (ES) *m/z* calculated for C₂₁H₄₄Si₂O₂Na 407.2772, found 407.2769 [M+Na]⁺.

(2*E*, 5*S*, 6*E*, 9*R*)-Ethyl 5,9-bis(*tert*-butyldimethylsilyloxy) deca-2,6-dienoate (90)

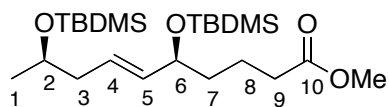


Compound **90** was synthesized from **89** according to the procedure used to prepare **21**.

90: 2.10 g, colorless liquid, 75% yield. IR (CHCl₃, cast film) 2957, 2930, 2897,

2858, 1725, 1657, 1472, 1463 cm^{-1} ; ^1H NMR (600 MHz, CDCl_3) δ 6.94 (m, 1H, H-8), 5.83 (dt, 1H, $J = 15.6, 1.3$ Hz, H-9), 5.60 (m, 1H, H-4), 5.45 (ddt, 1H, $J = 15.5, 6.6, 1.1$ Hz, H-5), 4.18 (m, 3H, H-6, OCH_2CH_3), 3.82 (sextet, 1H, $J = 6.0$ Hz, H-2), 2.38-2.12 (m, 4H, H-3, H-7), 1.28 (t, 3H, $J = 7.1$ Hz, OCH_2CH_3) 1.10 (d, 3H, $J = 6.1$ Hz, H-1), 0.89 (s, 9H, $\text{Si-C}(\text{CH}_3)_3$), 0.88 (s, 9H, $\text{Si-C}(\text{CH}_3)_3$), 0.05 (s, 6H, SiCH_3), 0.04 (s, 3H, SiCH_3), 0.02 (s, 3H, SiCH_3); ^{13}C NMR (125 MHz, CDCl_3) δ 166.5, 145.9 134.9 127.8 123.6 72.7 68.7 60.1 42.8 41.7 26.1 26.0 23.6 18.2 18.1 14.4 -4.3 -4.5 -4.7 -4.8; $[\alpha]_{\text{D}}^{25} = -3.34$ (c = 1.39, CHCl_3); HRMS (ES) m/z calculated for $\text{C}_{24}\text{H}_{48}\text{Si}_2\text{O}_4\text{Na}$ 479.2983, found 479.2987 $[\text{M}+\text{Na}]^+$.

(5*S*, 9*R*, *E*)-Methyl 5,9-bis(*tert*-butyldimethylsilyloxy)dec-6-enoate (91**)**

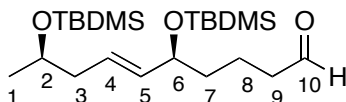


Compound **91** was synthesized from **90** according to the procedure used to prepare **22**.

91: 100 mg, colorless liquid, 90% yield. IR (CHCl_3 , cast film) 2956, 2930, 2897, 2858, 1744, 1472, 1463 cm^{-1} ; ^1H NMR (600 MHz, CDCl_3) δ 5.55 (m, 1H, H-4), 5.42 (m, 1H, H-5), 4.08 (m, 1H, H-6), 3.82 (sextet, 1H, $J = 6.0$ Hz, H-2), 3.68 (s, 3H, OCH_3), 2.32 (t, 2H, $J = 7.1$ Hz, H-9), 2.15 (m, 2H, H-3), 1.70-1.45 (m, 4H, H-7, H-8), 1.11 (d, 3H, $J = 6.0$ Hz, H-1), 0.89 (s, 9H, $\text{Si-C}(\text{CH}_3)_3$), 0.88 (s, 9H, $\text{Si-C}(\text{CH}_3)_3$), 0.05 (s, 6H, SiCH_3), 0.04 (s, 3H, SiCH_3), 0.02 (s, 3H, SiCH_3); ^{13}C NMR (125 MHz, CDCl_3) δ 174.1, 135.4, 126.8, 73.3, 68.5, 51.4, 42.5, 37.7, 34.0, 26.0, 25.8, 23.2, 20.9, 18.2, 18.1, -4.2, -4.6, -4.7, -4.8; $[\alpha]_{\text{D}}^{25} = -0.77$ (c = 0.71,

CHCl₃); HRMS (ES) m/z calculated for C₂₃H₄₈Si₂O₄Na 467.2983, found 467.2977 [M+Na]⁺.

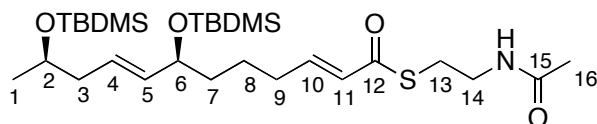
(5*S*, 9*R*, *E*)-5, 9-bis(*tert*-Butyldimethylsilyloxy)dec-6-enal (92**)**



Compound **92** was synthesized from **91** according to the procedure used to prepare **23**.

92: 70.0 mg, colorless liquid, 93% yield. IR (CHCl₃, cast film) 2956, 2930, 2897, 2858, 2710, 1730, 1473, 1255 cm⁻¹; ¹H NMR (500 MHz, CDCl₃) δ 9.76 (t, 1H, J = 1.8 Hz, H-10), 5.55 (m, 1H, H-4), 5.40 (m, 1H, H-5), 4.08 (m, 1H, H-6), 3.82 (sextet, 1H, J = 6.1 Hz, H-2), 2.42 (td, 2H, J = 7.3, 1.8 Hz, H-9), 2.16 (m, 2H, H-3), 1.70-1.45 (m, 4H, H-7, H-8), 1.11 (d, 3H, J = 6.0 Hz, H-1), 0.89 (s, 18H, Si-C(CH₃)₃), 0.06 (s, 3H, SiCH₃), 0.05 (s, 3H, SiCH₃), 0.04 (s, 3H, SiCH₃), 0.02 (s, 3H, SiCH₃); ¹³C NMR (125 MHz, CDCl₃) δ 202.6, 135.4, 127.0, 73.2, 68.5, 43.8, 42.6, 37.7, 25.9, 25.8, 23.1, 18.1, 18.0, -4.2, -4.5, -4.7, -4.8; $[\alpha]_D^{25}$ = -5.64 (c = 0.33, CHCl₃); HRMS (ES) m/z calculated for C₂₂H₄₆Si₂O₃Na 437.2878, found 437.2872 [M+Na]⁺.

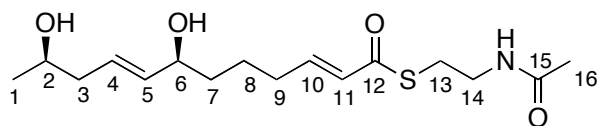
(2*E*, 7*S*, 8*E*, 11*R*)-*S*-2-Acetamidoethyl 7,11-bis(*tert*-butyldimethylsilyloxy)dodeca-2,8-dienethioate (93**)**



Compound **93** was synthesized from **92** according to the procedure used to prepare **26**.

93: 150 mg, colorless liquid, 78% yield. IR (CHCl₃, cast film) 3289, 2955, 2929, 2896, 2857, 1664, 1635, 1558, 1472, 1289 cm⁻¹; ¹H NMR (600 MHz, CDCl₃) δ 6.92 (dt, 1H, *J* = 15.4, 6.8 Hz, H-10), 6.13 (dt, 1H, *J* = 15.5, 1.5 Hz, H-11), 5.86 (s, 1H, NH), 5.54 (m, 1H, H-4), 5.40 (ddt, 1H, *J* = 15.3, 6.7, 1.2 Hz, H-5), 4.05 (dt, 1H, *J* = 6.4, 6.4 Hz, H-6), 3.82 (sextet, 1H, *J* = 6.0 Hz, H-2), 3.47 (dt, 2H, *J* = 5.9, 5.9 Hz, H-14), 3.10 (t, 2H, *J* = 6.5 Hz, H-13), 2.25 - 2.10 (m, 4H, H-3, H-9), 1.97 (s, 3H, H-16), 1.45 - 1.56 (m, 4H, H-7, H-8), 1.10 (d, 3H, *J* = 6.2 Hz, H-1), 0.88 (s, 18H, Si-C(CH₃)₃), 0.05 (s, 3H, SiCH₃), 0.05 (s, 3H, SiCH₃), 0.04 (s, 3H, SiCH₃), 0.02 (s, 3H, SiCH₃); ¹³C NMR (125 MHz, CDCl₃) δ 190.4, 170.2, 146.5, 135.5, 128.4, 126.9, 73.3, 68.5, 42.6, 39.8, 37.8, 32.2, 28.3, 25.9, 25.8, 23.6, 23.4, 23.2, 18.2, 18.1, -4.2, -4.5, -4.7, -4.8; [α]_D²⁵ = -3.21 (c = 1.56, CHCl₃); HRMS (ES) *m/z* calculated for C₂₈H₅₅Si₂O₄SNNa 580.3283, found 580.3280 [M+Na]⁺.

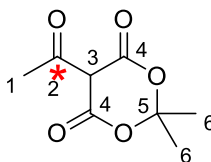
(2*E*, 7*S*, 8*E*, 11*R*)-*S*-2-Acetamidoethyl 7,11-dihydroxydodeca-2,8-dienethioate (94**)**



Compound **94** was synthesized from **93** according to the procedure used to prepare **27**.

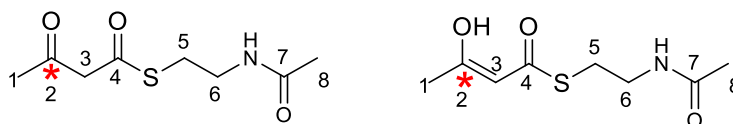
94: 70.0 mg, colorless liquid, 98% yield. IR (CHCl₃, cast film) 3300, 3089, 2965, 2927, 2854, 1660, 1633, 1556, 1436, 1292 cm⁻¹; ¹H NMR (600 MHz, CDCl₃) δ 6.92 (dt, 1H, *J* = 15.4, 6.8 Hz, H-10), 6.13 (dt, 1H, *J* = 15.4, 1.4 Hz, H-11), 5.96 (s, 1H, NH), 5.67 (m, 1H, H-4), 5.58 (m, 1H, H-5), 4.10 (dt, 1H, *J* = 6.4, 6.4 Hz, H-6), 3.85 (sextet, 1H, *J* = 6.2 Hz, H-2), 3.45 (dt, 2H, *J* = 5.9, 5.9 Hz, H-14), 3.09 (t, 2H, *J* = 6.2 Hz, H-13), 2.27-2.15 (m, 4H, H-3, H-9), 1.95 (s, 3H, H-16), 1.87 (s, 2H, OH), 1.62-1.48 (m, 4H, H-7, H-8), 1.10 (d, 3H, *J* = 6.3 Hz, H-1); ¹³C NMR (100 MHz, CDCl₃) δ 190.4, 170.4, 146.2, 136.3, 128.6, 128.0, 72.5, 67.3, 42.1, 39.8, 36.5, 32.1, 28.3, 23.9, 23.3, 23.1; [α]_D²⁵ = -5.58 (c = 0.24, CHCl₃); HRMS (ES) *m/z* calculated for C₁₆H₂₇SO₄Na 352.1553, found 352.1551 [M+Na]⁺.

5-([1-¹³C]-1-Hydroxyethylidene)-2,2-dimethyl-1,3-dioxane-4,6-dione (108)



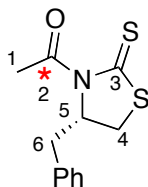
To a stirred solution of Meldrum's acid (1.82 g, 12.7 mmol) in dry CH₂Cl₂ (20 mL) was added dimethylaminopyridine (3.09 g, 25.3 mmol) at 0 °C under Ar. The reaction mixture was stirred for 5 min, and then [1-¹³C]-acetyl chloride (1.00 g, 12.7 mmol) was added. The resulting yellow solution was stirred at 0 °C for another 30 min, and then warmed to 23 °C for another 30 min of stirring. About 10 mL of 1 N HCl was added. The layers were separated, and the aqueous layer was extracted with CH₂Cl₂ (3 x 10 mL). The combined organic layers were washed with 1 N HCl (10 mL), brine (20 mL) and dried over Na₂SO₄. The solvent was removed *in vacuo* to give the product (2.28 g, 97% yield) as a yellow solid. IR (CHCl₃, cast film) 3200 - 2200, 3012, 2986, 2942, 2885, 1732, 1670, 1552 cm⁻¹; ¹H NMR (500 MHz, CDCl₃) δ 2.69 (d, 3H, *J*_{H-13C} = 6.2 Hz, H-1), 1.75 (s, 6H, H-6); ¹³C NMR (125 MHz, CDCl₃) δ 194.6 (enriched), 170.2, 160.5, 104.9, 91.8 (d, *J*_{13C-13C} = 69.8 Hz), 26.8, 23.5 (d, *J*_{13C-13C} = 45.4 Hz); HRMS (ES) *m/z* calculated for C₇[¹³C]H₁₀O₅Na 210.0454, found 210.0452 [M+Na]⁺.

***S*-2-Acetamidoethyl [3-¹³C]-3-oxobutanethioate and *S*-2-Acetamidoethyl [3-¹³C]-3-hydroxybut-2-enethioate (95)**



To a stirred solution of **108** (2.21 g, 11.9 mmol) in dry benzene (60 mL) was added *N*-acetylcysteamine (1.69 g, 14.3 mmol) under Ar. The reaction mixture was heated to reflux for 12 h. The solvent was removed *in vacuo* and the residue was purified using flash column chromatography (9:1 EtOAc/MeOH) to give the product (2.03 g, 84% yield, keto:enol = 4.5:1) as a white solid. IR (CHCl₃, cast film) 3291, 3076, 2932, 1722, 1665, 1548 cm⁻¹; ¹H NMR (500 MHz, CDCl₃) δ 6.02 (br s, 1H, NH), 5.45 (d, 0.20H, *J*_{1H-13C} = 4.0 Hz, enol-H-3), 3.69 (d, 1.80H, *J*_{1H-13C} = 6.1 Hz, keto-H-3), 3.45 (m, 2H, H-6), 3.05 (m, 2H, H-5), 2.25 (d, *J*_{1H-13C} = 6.1 Hz, H-1), 3.05 (m, 2H, H-5), 1.96 (s, 3H, H-8); ¹³C NMR (125 MHz, CDCl₃) δ 199.8 (enriched), 194.1, 192.2, 173.9 (enriched), 170.5, 170.3, 99.8 (d, *J*_{13C-13C} = 69.7 Hz), 57.9 (d, *J*_{13C-13C} = 36.7 Hz), 39.9, 39.2, 30.3 (d, *J*_{13C-13C} = 42.6 Hz), 29.2, 27.8, 23.2, 23.1, 21.2; HRMS (ES) *m/z* calculated for C₇[¹³C]H₁₃NSO₃Na 227.0542, found 227.0538 [M+Na]⁺.

(S)-[1-¹³C]-1-(4-benzyl-2-thioxothiazolidin-3-yl)ethanone (109)



To a stirred solution of 20 mL THF was added NaH (60% wt in mineral oil, 756 mg, 18.9 mmol) at 0 °C under Ar. After stirring for 10 min at 0 °C, Crimmins auxiliary (3.16 g, 15.1 mmol) was added and the mixture was stirred for 10 min at 0 °C. [1-¹³C]acetyl chloride (1.00 g, 12.6 mmol) was added and the mixture was stirred for another 1 h at the same temperature. The reaction was quenched by the addition of sat. NH₄Cl (10 mL). THF was removed *in vacuo* and EtOAc (50 mL) was added to the residue. The layers were separated and the organic layer was dried over Na₂SO₄. The crude product was filtered, concentrated *in vacuo* and purified by flash chromatography (1:7 hexanes:EtOAc) to give the product (2.53 g, 80%) as a yellow solid. IR (CDCl₃, cast film) 3026, 2927, 1697, 1495, 1368 cm⁻¹; ¹H NMR (500 MHz; CDCl₃): δ 7.36-7.26 (m, 5H, PhH), 5.40-5.35 (m, 1H, H-5), 3.38 (ddd, 1H, *J* = 11.5, 7.3, 1.0 Hz, H-4), 3.21 (dd, 1H, *J* = 13.2, 3.8 Hz, H-6), 3.03 (dd, 1H, *J* = 13.2, 10.6 Hz, H-6), 2.88 (d, 1H, *J* = 11.5 Hz, H-4), 2.79 (d, *J*_{13C-1H} = 6.9 Hz, 3H); ¹³C NMR (125 MHz, CDCl₃) δ 196.2 (d, *J*_{13C-13C} = 3.2 Hz), 165.3 (enriched), 131.1, 124.1, 123.5, 121.8, 62.8 (d, *J*_{13C-13C} = 1.0 Hz), 31.3, 26.49 (d, *J*_{13C-13C} = 2.0 Hz), 21.7 (d, *J*_{13C-13C} = 52.7 Hz); [α]_D²⁵ = 240.57 (c = 0.810, CHCl₃); HRMS (EI) *m/z* calculated for C₁₁[¹³C]H₁₃NOS₂ 252.0472, found 252.0469 [M]⁺.

(S)-[1-¹³C]-1-((S)-4-Benzyl-2-thioxothiazolidin-3-yl)-3-hydroxybutan-1-one

(110) and (R)-[1-¹³C]-1-((S)-4-Benzyl-2-thioxothiazolidin-3-yl)-3-hydroxybutan-1-one (111)



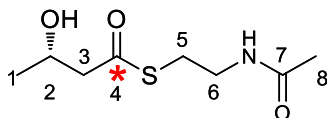
To a stirred solution of **109** (252 mg, 1.00 mmol) in dry CH₂Cl₂ (10 mL) was added TiCl₄ (1.0 M solution in CH₂Cl₂, 1.10 mL, 1.10 mmol) at 0 °C under Ar. The reaction mixture was stirred for 5 min and then cooled to -78 °C. A solution of diisopropylethylamine (DIPEA) (129 mg, 1.00 mmol) in CH₂Cl₂ (2 mL) was added. The reaction mixture was stirred at -78 °C for 2 h. Acetaldehyde (0.50 mL, 8.90 mmol) was then added to the reaction mixture, which was then stirred for 15 min at -78 °C. The reaction was quenched by the addition of 10 mL of saturated ammonium chloride. The layers were separated, and the aqueous layer was extracted with EtOAc (3 x 10 mL). The combined organic layers were washed with brine (20 mL) and dried over Na₂SO₄. The solvent was removed *in vacuo* and the residue was purified using flash column chromatography (1:6 EtOAc/hexanes) to give two diastereomers **110** (120 mg, 41% yield) and **111** (90 mg, 31% yield) as yellow oils.

110: IR (CHCl₃, cast film) 3433, 2966, 2925, 1693 cm⁻¹; ¹H NMR (500 MHz, CDCl₃) δ 7.37-7.25 (m, 5H, Ph), 5.40 (ddd, 1H, *J* = 10.6, 7.3, 4.0 Hz, H-7), 4.32 (m, 1H, H-2), 3.64 (ddd, 1H, *J* = 17.7, 3.0 Hz, *J*_{1H-13C} = 7.0 Hz, H-3), 3.40 (ddd,

1H, $J = 11.6, 7.2, 0.8$ Hz, H-6), 3.22 (dd, 1H, $J = 13.2, 3.9$ Hz, H-8), 3.13 (ddd, 1H, $J = 17.7, 9.2$ Hz, $J_{\text{1H-13C}} = 6.0$ Hz, H-3), 3.05 (dd, 1H, $J = 13.2, 10.4$ Hz, H-8), 2.89 (d, 1H, $J = 11.6$ Hz, H-6), 1.27 (d, 3H, $J = 6.3$ Hz, H-1); ^{13}C NMR (125 MHz, CDCl_3) δ 201.4 (d, $J_{\text{13C-13C}} = 3.4$ Hz), 173.1(enriched), 136.4, 129.4, 128.9, 127.3, 68.3, 64.1(d, $J_{\text{13C-13C}} = 2.1$ Hz), 47.3(d, $J_{\text{13C-13C}} = 49.6$ Hz), 36.8, 32.1, 22.3 (d, $J_{\text{13C-13C}} = 5.4$ Hz); $[\alpha]_{\text{D}}^{25} = 123$ (c = 0.280, CHCl_3); HRMS (ES) m/z calculated for $\text{C}_{13}[^{13}\text{C}]\text{H}_{17}\text{NS}_2\text{O}_2\text{Na}$ 319.0626, found 319.0627 $[\text{M}+\text{Na}]^+$.

111: IR (CHCl_3 , cast film) 3429, 2970, 2929, 1651cm^{-1} ; ^1H NMR (500 MHz, CDCl_3) δ 7.37-7.25 (m, 5H, Ph), 5.40 (ddd, 1H, $J = 10.6, 7.1, 4.0$ Hz, H-7), 4.24 (m, 1H, H-2), 3.45 (ddd, 1H, $J = 17.7, 9.2$ Hz, $J_{\text{1H-13C}} = 6.4$ Hz, H-3), 3.40 (dd, 1H, $J = 11.4, 7.2$ Hz, H-6), 3.32 (ddd, 1H, $J = 17.6, 2.7$ Hz, $J_{\text{1H-13C}} = 6.6$ Hz, H-3), 3.22 (dd, 1H, $J = 13.2, 3.8$ Hz, H-8), 3.05 (dd, 1H, $J = 13.2, 10.4$ Hz, H-8), 2.89 (d, 1H, $J = 11.5$ Hz, H-6), 1.27 (d, 3H, $J = 6.3$ Hz, H-1); ^{13}C NMR (125 MHz, CDCl_3) δ 201.4 ((d, $J_{\text{13C-13C}} = 3.4$ Hz), 173.6 (enriched), 136.3, 129.4, 128.9, 127.3, 68.2, 64.6 (d, $J_{\text{13C-13C}} = 2.0$ Hz), 47.0 (d, $J_{\text{13C-13C}} = 49.7$ Hz), 36.8, 32.1, 22.3 (d, $J_{\text{13C-13C}} = 5.1$ Hz); $n_D^{20} = 153.76$ (c = 0.380, CHCl_3); HRMS (ES) m/z calculated for $\text{C}_{13}[^{13}\text{C}]\text{H}_{17}\text{NS}_2\text{O}_2\text{Na}$ 319.0626, found 319.0624 $[\text{M}+\text{Na}]^+$.

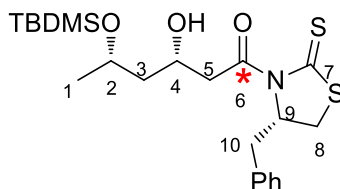
(S)-S-(2-Acetamidoethyl) [1- ^{13}C]-3-hydroxybutanethioate (96)



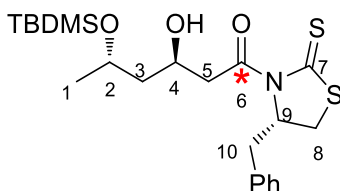
To a stirred solution of **110** (105 mg, 0.355 mmol) in 5 mL MeCN was added K₂CO₃ (188 mg, 1.24 mmol) and *N*-acetylcysteamine (50.8 mg, 0.426 mmol). The reaction mixture was stirred until the yellow color disappeared (about 5 min). The solvent was removed *in vacuo* and the residue was purified using flash column chromatography (EtOAc) to give the product (49.0 mg, 67% yield) as a white solid. IR (CHCl₃, cast film) 3296, 3087, 2970, 2929, 1653, 1658, 1553 cm⁻¹; ¹H NMR (500 MHz, CDCl₃) δ 6.32 (s, 1H, NH), 4.22 (m, 1H, H-2), 3.39 (m, 2H, H-6), 3.23 (br s, 1H, OH), 3.03 (m, 2H, H-5), 2.68 (dd, 2H, *J* = 5.7 Hz, *J*_{1H-13C} = 5.7 Hz, H-3), 1.96 (s, 3H, H-8), 1.20 (d, 3H, *J* = 6.3 Hz, H-1); ¹³C NMR (125 MHz, CDCl₃) δ 199.1(enriched), 170.8, 64.9 (d, *J*_{13C-13C} = 2.3 Hz), 52.2 (d, *J*_{13C-13C} = 44.3 Hz), 39.2, 28.7, 23.1, 22.7 (d, *J*_{13C-13C} = 4.6 Hz); [α]_D²⁵ = 31.49 (c = 0.200, CHCl₃); HRMS (ES) *m/z* calculated for C₇[¹³C]H₁₅NSO₃Na 229.0698, found 229.0696 [M+Na]⁺.

(3*S*, 5*S*)-[1-¹³C]-1-((*S*)-4-Benzyl-2-thioxothiazolidin-3-yl)-5-(*tert*-butyldimethylsilyloxy)-3-hydroxyhexan-1-one (**112**) and (3*R*, 5*S*)-[1-¹³C]-1-((*S*)-4-Benzyl-2-thioxothiazolidin-3-yl)-5-(*tert*-butyldimethylsilyloxy)-3-hydroxyhexan-1-one (**113**)

Compounds **112** and **113** were synthesized from **15** and **109** according to the procedure used to prepare **110** and **111**.



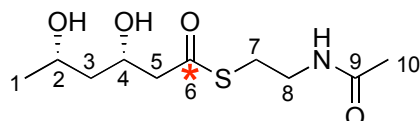
112: 139.0 mg, yellow oil, 31% yield. IR (CHCl₃, cast film) 3489, 2955, 2928, 1647 cm⁻¹; ¹H NMR (500 MHz, CDCl₃) δ 7.37-7.25 (m, 5H, Ph), 5.40 (m, 1H, H-9), 4.35 (m, 1H, H-4), 4.12 (m, 1H, H-2), 3.50 (ddd, 1H, *J* = 17.6, 3.4 Hz, *J*_{1H-13C} = 7.2 Hz, H-5), 3.48 (m, 1H, OH), 3.38 (ddd, 1H, *J* = 11.4, 7.1, 0.8 Hz, H-8), 3.27 (ddd, 1H, *J* = 17.6, 8.6 Hz, *J*_{1H-13C} = 6.2 Hz, H-5), 3.23 (dd, 1H, *J* = 13.3, 3.8 Hz, 10), 3.04 (dd, 1H, *J* = 13.2, 10.6 Hz, H-10), 2.88 (d, 1H, *J* = 11.5 Hz, H-8), 1.73 (m, 1H, H-3), 1.62 (ddd, 1H, *J* = 14.0, 4.5, 3.5 Hz, H-3), 1.20 (d, 3H, *J* = 6.1 Hz, H-1), 0.89 (s, 9H, Si-C(CH₃)₃), 0.087 (s, 3H, SiCH₃), 0.082 (s, 3H, SiCH₃); ¹³C NMR (125 MHz, CDCl₃) δ 201.2 (d, *J*_{13C-13C} = 3.4 Hz), 172.4 (enriched), 136.5, 129.4, 128.9, 127.2, 68.6, 68.4, 67.0 (d, *J*_{13C-13C} = 1.6 Hz), 46.3 (d, *J*_{13C-13C} = 50.8 Hz), 45.5 (d, *J*_{13C-13C} = 4.1 Hz), 36.7, 32.0 (d, *J*_{13C-13C} = 1.3 Hz), 25.8, 24.2, 18.0, -3.97, -4.72; [α]_D²⁵ = 253.80 (c = 0.130, CHCl₃); HRMS (ES) *m/z* calculated for C₂₂[¹³C]H₃₅NO₂S₂SiNa 477.1756, found 477.1750 [M+Na]⁺.



113: 100 mg, yellow oil, 22% yield. IR (CHCl₃, cast film) 3433, 2966, 2925, 1693 cm⁻¹; ¹H NMR (500 MHz, CDCl₃) δ 7.37-7.25 (m, 5H, Ph), 5.40 (ddd, 1H, *J* = 10.6, 7.3, 4.0 Hz, H-9), 4.37 (m, 1H, H-4), 4.18 (m, 1H, H-2), 3.56 (d, 1H, *J* = 2.8 Hz, OH), 3.48 (m, 1H, H-5), 3.38 (m, 1H, H-8), 3.34 (m, 1H, H-5), 3.23 (dd, 1H, *J* = 13.3, 2.8 Hz, 10), 3.03 (dd, 1H, *J* = 13.0, 10.5 Hz, H-10), 2.88 (d, 1H, *J* = 11.5 Hz, H-8), 1.68 (ddd, 1H, *J* = 13.7, 9.8, 2.9 Hz, H-3), 1.54 (ddd, 1H, *J* = 14.0, 7.4, 2.3 Hz, H-3), 1.21 (d, 3H, *J* = 6.2 Hz, H-1), 0.88 (s, 9H, Si-C(CH₃)₃), 0.087

(s, 3H, SiCH₃), 0.082 (s, 3H, SiCH₃); ¹³C NMR (125 MHz, CDCl₃) δ 202.9 (d, *J*_{13C-13C} = 3.1 Hz), 173.1 (enriched), 136.5, 129.4, 128.9, 127.2, 68.3 (d, *J*_{13C-13C} = 3.1 Hz), 66.2, 65.1 (d, *J*_{13C-13C} = 1.8 Hz), 46.3 (d, *J*_{13C-13C} = 50.6 Hz), 44.9 (d, *J*_{13C-13C} = 4.4 Hz), 36.7, 31.9 (d, *J*_{13C-13C} = 2.1 Hz), 25.8, 23.6, 18.0, -4.45, -4.86; = 95.8 (c = 0.400, CHCl₃); HRMS (ES) *m/z* calculated for C₂₂[¹³C]H₃₅NO₂S₂SiNa 477.1756, found 477.1746 [M+Na]⁺.

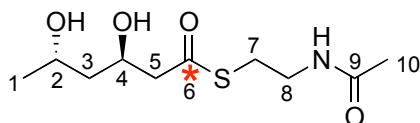
(3*S*, 5*S*)-*S*-(2-Acetamidoethyl) [1-¹³C]-3,5-dihydroxyhexanethioate (97)



To a stirred solution of **112** (6.00 mg, 132 μmol) in 0.5 mL MeCN was added K₂CO₃ (3.00 mg, 198 μmol) and *N*-acetylcysteamine (HSNAC) (2.40 mg, 198 μmol). The reaction mixture was stirred until the yellow color disappeared (about 5 min). The reaction was quenched by the addition of 1 mL saturated ammonium chloride. The layers were separated and the aqueous layer was extracted with EtOAc (3x2 mL). The combined organic layers were washed with brine (5 mL) and dried over Na₂SO₄. The solvent was removed *in vacuo*. The residue was dissolved in 1 mL of a solution of 3:3:1 AcOH/H₂O/THF. The resulting solution was stirred at 25 °C for 2 h. The solvent was removed *in vacuo* and the residue was purified using flash column chromatography (9:1 EtOAc/MeOH) to give the product (2.00 mg, 61% yield) as a white solid. IR (CHCl₃, cast film) 3300, 3093, 2967, 2931, 1686, 1657, 1554 cm⁻¹; ¹H NMR (500 MHz, CD₂Cl₂) δ 5.80 (br s, 1H, NH), 4.30 (m, 1H, H-4), 4.13 (m, 1H, H-2), 3.46-3.36 (m, 2H, H-8), 3.10-

2.95 (m, 2H, H-7), 2.72-2.65 (m, 2H, H-5), 1.96 (s, 3H, H-10), 1.55 (m, 2H, H-3), 1.23 (d, 3H, $J = 6.2$, H-1); ^{13}C NMR (125 MHz, CD_2Cl_2) δ 199.0 (enriched), 170.2, 69.9 (d, $J_{13\text{C}-13\text{C}} = 2.3$ Hz), 68.6, 51.9 (d, $J_{13\text{C}-13\text{C}} = 45.6$ Hz), 44.6 (d, $J_{13\text{C}-13\text{C}} = 4.1$ Hz), 39.2, 29.5, 24.1, 23.3; $[\alpha]_{\text{D}}^{25} = 24.6$ ($c = 0.460$, CHCl_3); HRMS (ES) m/z calculated for $\text{C}_9[^{13}\text{C}]\text{H}_{19}\text{NSO}_4\text{Na}$ 273.0961, found 273.0955 $[\text{M}+\text{Na}]^+$.

(3*R*, 5*S*)-*S*-2-Acetamidoethyl [1- ^{13}C]-3,5-dihydroxyhexanethioate (98**)**

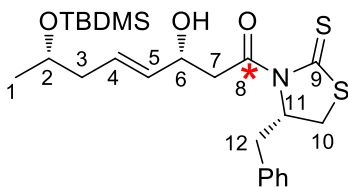


Compound **98** was synthesized from **113** according to the procedure used to prepare **97**.

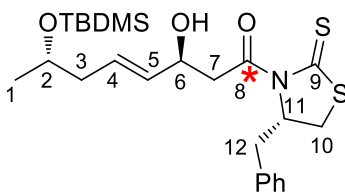
98: 4.00 mg, white solid, 62% yield. IR (CHCl_3 , cast film) 3302, 3093, 2965, 2931, 1686, 1658, 1555, cm^{-1} ; ^1H NMR (500 MHz, CD_2Cl_2) δ 5.90 (br s, 1H, NH), 4.40 (m, 1H, H-4), 4.13 (m, 1H, H-2), 3.46-3.36 (m, 2H, H-8), 3.39 (d, 1H, $J = 6.3$ Hz, OH), 3.10-2.90 (m, 2H, H-7), 2.70-2.60 (m, 2H, H-5), 2.27 (d, 1H, $J = 4.5$ Hz, OH), 1.96 (s, 3H, H-10), 1.65-1.55 (m, 2H, H-3), 1.23 (dd, 3H, $J = 6.3$, $J_{\text{H}-13\text{C}} = 0.8$ Hz, H-1); ^{13}C NMR (125 MHz, CDCl_3) δ 199.2 (enriched), 170.5, 66.9 (d, $J_{13\text{C}-13\text{C}} = 2.1$ Hz), 65.4, 51.6 (d, $J_{13\text{C}-13\text{C}} = 45.9$ Hz), 44.1 (d, $J_{13\text{C}-13\text{C}} = 3.9$ Hz), 39.2, 29.5, 23.8, 23.3; $[\alpha]_{\text{D}}^{25} = -5.42$ ($c = 0.550$, CHCl_3); HRMS (ES) m/z calculated for $\text{C}_9[^{13}\text{C}]\text{H}_{19}\text{NSO}_4\text{Na}$ 273.0961, found 273.0955 $[\text{M}+\text{Na}]^+$.

(3*R*, 7*S*, *E*)- [1-¹³C]-1-((*S*)-4-Benzyl-2-thioxothiazolidin-3-yl)-7-(*tert*-butyldimethylsilyloxy)-3-hydroxyoct-4-en-1-one (**114**) and (3*S*, 7*S*, *E*)-[1-¹³C]-1-((*S*)-4-Benzyl-2-thioxothiazolidin-3-yl)-7-(*tert*-butyldimethylsilyloxy)-3-hydroxyoct-4-en-1-one (**115**)

Compounds **114** and **115** were synthesized from **18** according to the procedure used to prepare **110** and **111**.

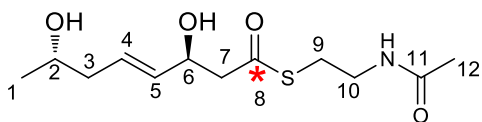


114: 143 mg, yellow oil, 30% yield. IR (CHCl₃, cast film) 3440, 2955, 2927, 2855, 1654 cm⁻¹; ¹H NMR (500 MHz, CDCl₃) δ 7.37-7.25 (m, 5H, Ph), 5.76 (dtd, 1H, *J* = 15.4, 7.2, 1.1 Hz, H-4), 5.59 (ddt, 1H, *J* = 15.4, 6.3, 1.3 Hz, H-5), 5.39 (m, 1H, H-11), 4.69 (m, 1H, H-6), 3.85 (sextet, 1H, *J* = 6.1 Hz, H-2), 3.62 (ddd, 1H, *J* = 17.6, 2.8 Hz, *J*_{H-13C} = 7.0 Hz, H-7), 3.40 (ddd, 1H, *J* = 11.5, 7.2, 1.0 Hz, H-10), 3.30 (ddd, 1H, *J* = 17.6, 9.2 Hz, *J*_{H-13C} = 6.0 Hz, H-7), 3.23 (dd, 1H, *J* = 13.2, 3.9 Hz, H-12), 3.05 (dd, 1H, *J* = 13.3, 10.5 Hz, H-12), 2.91 (d, 1H, *J* = 11.6 Hz, H-10), 2.23-2.10 (m, 2H, H-3), 1.15 (d, 1H, *J* = 6.0 Hz, H-1) 0.88 (s, 9H, Si-C(CH₃)₃), 0.05 (s, 6H, SiCH₃); ¹³C NMR (125 MHz, CDCl₃) δ 201.4 ((d, *J*_{13C-13C} = 3.1 Hz), 172.6 (enriched), 136.5, 132.7 (d, *J*_{13C-13C} = 4.6 Hz), 129.4, 129.3, 128.9, 127.3, 68.6 (d, *J*_{13C-13C} = 2.1 Hz), 68.4, 68.3, 45.7 (d, *J*_{13C-13C} = 50.3 Hz), 42.6, 36.8, 32.1 (d, *J*_{13C-13C} = 1.8 Hz), 25.9, 23.5, 18.2, - 4.42, - 4.56; [α]_D²⁵ = 106.53 (*c* = 0.800, CHCl₃); HRMS (ES) *m/z* calculated for C₂₄[¹³C]H₃₇NO₂S₂SiNa 503.1912, found 503.1902 [M+Na]⁺.



115: 82 mg, yellow oil, 17% yield. IR (CHCl₃, cast film) 3438, 2955, 2927, 2855, 1654 cm⁻¹; ¹H NMR (500 MHz, CDCl₃) δ 7.37 – 7.25 (m, 5H, Ph), 5.75 (dtd, 1H, *J* = 15.4, 7.1, 1.1 Hz, H-4), 5.57 (ddt, 1H, *J* = 15.4, 6.2, 1.2 Hz, H-5), 4.58 (m, 1H, H-6), 3.83 (sextet, 1H, *J* = 6.1 Hz, H-2), 3.62 (ddd, 1H, *J* = 17.3, 9.0 Hz, *J*_{1H-13C} = 6.2 Hz, H-7), 3.42-3.32 (m, 2H, H-10, H-7), 3.23 (dd, 1H, *J* = 13.3, 3.9 Hz, H-12), 3.05 (dd, 1H, *J* = 13.3, 10.4 Hz, H-12), 3.00 (d, 1H, *J* = 7.3 Hz, OH), 2.91 (d, 1H, *J* = 11.5 Hz, H-10), 2.19 (m, 2H, H-3), 1.12 (d, 1H, *J* = 6.1 Hz, H-1) 0.88 (s, 9H, Si-C(CH₃)₃), 0.05 (s, 6H, SiCH₃); 201.4 ((d, *J*_{13C-13C} = 3.1 Hz), 173.1 (enriched), 136.4, 132.7 (d, *J*_{13C-13C} = 4.9 Hz), 129.5, 129.3, 129.0, 127.3, 69.2 (d, *J*_{13C-13C} = 1.6 Hz),, 68.4, 68.3, 45.5 (d, *J*_{13C-13C} = 50.3 Hz), 42.6, 36.8, 32.0 (d, *J*_{13C-13C} = 1.8 Hz), 25.9, 23.6, 18.2, - 4.42, - 4.58; [α]_D²⁵ = 72.9 (c = 1.100, CHCl₃); HRMS (ES) *m/z* calculated for C₂₄ [¹³C]H₃₇NO₂S₂SiNa 503.1912, found 503.1903 [M+Na]⁺.

(3*S*, 7*S*, *E*)-*S*-2-Acetamidoethyl [1-¹³C]-3,7-dihydroxyoct-4-enethioate (101)



Compound **101** was synthesized from **115** according to the procedure used to prepare **97**.

101: 8.00 mg, white solid, 60% yield. IR (CHCl₃, cast film) 3296, 3094, 2967, 2925, 1687, 1658, 1555 cm⁻¹; ¹H NMR (500 MHz, CDCl₃) δ 6.00 (s, 1H, NH), 5.75 (m, 1H, H-4), 5.58 (ddt, 1H, *J* = 15.5, 6.3, 1.1 Hz, H-5), 4.56 (m, 1H, H-6), 3.82 (m, 1H, H-2), 3.44 (m, 2H, H-10), 3.04 (m, 2H, H-9), 2.80 (m, 2H, H-7), 2.30-2.10 (m, 2H, H-3), 1.97 (s, 3H, H-12), 1.19 (d, 3H, *J* = 6.2 Hz, H-1); ¹³C NMR (125 MHz, CDCl₃) δ 198.5 (enriched), 170.6, 134.1 (d, *J*_{13C-13C} = 3.3 Hz), 128.7, 69.5 (d, *J*_{13C-13C} = 1.8 Hz), 67.0, 51.0 (d, *J*_{13C-13C} = 45.7 Hz), 42.0, 39.2, 29.1, 23.2, 23.0; [α]_D²⁵ = 31.3 (c = 0.310, CHCl₃); HRMS (ES) *m/z* calculated for C₁₁[¹³C]H₂₁NSO₄Na 299.1117, found 299.1111 [M+Na]⁺.

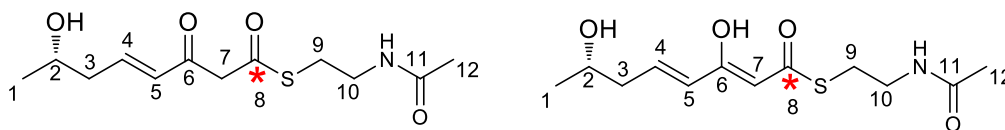
(*S*, *E*)-*S*-2-Acetamidoethyl [1-¹³C]-7-(*tert*-butyldimethylsilyloxy)-3-oxooct-4-enethioate and (*S*, 2*Z*, 4*E*)-*S*-2-Acetamidoethyl [1-¹³C]-7-(*tert*-butyldimethylsilyloxy)-3-hydroxyocta-2,4-dienethioate (**116**)



To a stirred solution of **114** (160 mg, 0.340 mmol) in 5 mL MeCN were added K₂CO₃ (78.6 mg, 0.510 mmol) and *N*-acetylcysteamine (48.6 mg, 0.408 mmol). The reaction mixture was stirred until the yellow color disappeared (about 5 min). The reaction was quenched by the addition of 5 mL saturated ammonium chloride. The layers were separated and the aqueous layer was extracted with EtOAc (3 x 10 mL). The combined organic layers were washed with brine (20 mL) and dried over Na₂SO₄. The solvent was removed *in vacuo*. To the resulting residue was added 10 mL CH₂Cl₂ and Dess-Martin periodinane (92.0 mg, 0.216

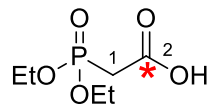
mmol). The resulting solution was stirred at 0 °C for 1 h. The reaction was quenched by the addition of 10 mL of 1:1 10% Na₂S₂O₃: saturated aqueous NaHCO₃. The layers were separated and the aqueous layer was extracted with EtOAc (3 x 10 mL). The combined organic layers were washed with brine (20 mL) and dried over Na₂SO₄. The solvent was removed *in vacuo* and the residue was purified using flash column chromatography (EtOAc) to give the product (28.0 mg, 21% yield, keto:enol = 2:3) as a colorless oil. IR (CHCl₃, cast film) 3287, 3079, 2956, 2930, 2857, 1724, 1656, 1623, 1553 cm⁻¹; ¹H NMR (500 MHz, CDCl₃) δ 6.92 (m, 0.4H, keto-H-4), 6.76 (m, 0.6H, enol-H-4), 6.16 (dt, 0.4H, *J* = 15.9, 1.4 Hz, keto-H-5), 6.14 (br s, 1H, NH), 5.74 (m, 0.6H, enol-H-5), 5.43 (d, 0.6H, *J*_{H-13C} = 4.5 Hz, enol-H-7), 3.98 – 3.89 (m, 1H, H-2), 3.86 (d, 0.8H, *J*_{H-13C} = 6.3 Hz, keto-H-7), 3.48 (m, 2H, H-10), 3.11 (m, 2H, H-9), 2.42-2.30 (m, 2H, H-3), 1.97 (s, 3H, H-12), 1.25 (d, 1.2H, *J* = 6.2 Hz, keto-H-1), 1.23 (d, 1.8H, *J* = 6.2 Hz, enol-H-1), 0.88 (m, 9H, Si-C(CH₃)₃), 0.04 (m, 6H, SiCH₃); ¹³C NMR (125 MHz, CDCl₃) δ 194.8 (enriched), 192.6 (enriched), 191.4, 170.6, 170.5, 167.3, 147.1, 139.6, 131.3, 126.6 (d, *J*_{13C-13C} = 5.7 Hz), 100.3 (d, *J*_{13C-13C} = 63.8 Hz), 67.8, 67.4, 54.8 (d, *J*_{13C-13C} = 46.3 Hz), 43.1, 42.7, 40.0, 39.2, 29.6, 27.9, 23.8, 23.2, 23.1, 23.3, 18.1, 18.0, - 4.47, - 4.56, - 4.80, -4.81; HRMS (ES) *m/z* calculated for C₁₈[¹³C]H₃₃NSSiO₄Na 411.1828, found 411.1820 [M+Na]⁺.

(*S*, *E*)-*S*-2-Acetamidoethyl [1-¹³C]-7-hydroxy-3-oxooct-4-enethioate and (*S*,2*Z*,4*E*)-*S*-2-Acetamidoethyl [1-¹³C]-3,7-dihydroxyocta-2,4-dienethioate (100)



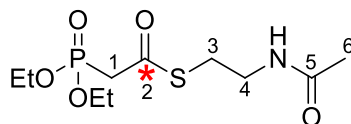
To compound **116** (4.00 mg, 10.4 μmol) was added 0.5 mL AcOH/H₂O/THF in a 3:3:1 solution. The solution was stirred at 25 °C for 4 h. The solvent was removed *in vacuo*, and the residue was purified using flash column chromatography (EtOAc) to give the product (2.00 mg, keto:enol = 2:3, 70% yield) as a colorless oil. IR (CHCl₃, cast film) 3296, 3086, 2969, 2930, 1657, 1583 cm⁻¹; ¹H NMR (500 MHz, CDCl₃) δ 6.95 (m, 0.4H, keto-H-4), 6.78 (m, 0.6H, enol-H-4), 6.22 (m, 0.4H, keto-H-5), 5.90 (br s, 1H, NH), 5.82 (m, 0.6H, enol-H-5), 5.46 (d, 0.6H, $J_{\text{H-13C}}$ = 4.5 Hz, enol-H-7), 3.95 (m, 1H, H-2), 3.86 (d, 0.8H, $J_{\text{H-13C}}$ = 6.4 Hz keto-H-7), 3.48 (m, 2H, H-10), 3.09 (m, 2H, H-9), 2.40 (m, 2H, H-3), 1.97 (s, 3H, H-12), 1.25 (d, 1.2H, J = 6.2 Hz, keto-H-1), 1.23 (d, 1.8H, J = 6.2 Hz, enol-H-1); ¹³C NMR (125 MHz, CDCl₃) δ 194.8 (enriched), 192.6(enriched), 191.4, 170.6, 170.5, 166.8, 147.1, 139.6, 131.8, 126.6 (d, $J_{\text{13C-13C}}$ = 5.6 Hz), 100.3 (d, $J_{\text{13C-13C}}$ = 63.5 Hz), 67.1, 66.8, 55.1 (d, $J_{\text{13C-13C}}$ = 45.6 Hz),, 42.6, 42.3, 40.0, 39.2, 29.5, 28.2, 23.6, 23.4, 23.4, 21.3; HRMS (ES) m/z calculated for C₁₁[¹³C]H₁₉NSO₄Na 297.0961, found 297.0955 [M+Na]⁺.

[1-¹³C]-2-(Diethoxyphosphoryl)acetic acid (118)



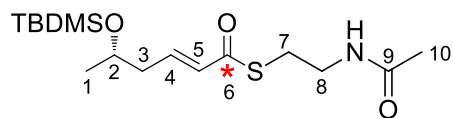
The known compound (unlabeled)²⁰⁵ was prepared according to literature method. To a stirred solution of 1M NaOH (3.6 mL), ethyl (diethoxyphosphono)-[1-¹³C]-acetate (0.630 mL, 3.20 mmol) was added dropwise. After 3 hours at room temperature, ethanol produced in the reaction was removed under reduced pressure. The remaining aqueous solution was acidified to pH = 1 using concentrated HCl and extracted with EtOAc (3x5 mL). The combined organic extracts were washed with brine (10 mL), dried with Na₂SO₄, filtered and concentrated under reduced pressure to give the product as a colorless liquid (450 mg, 73% yield). IR (CHCl₃, cast film) 2987, 1689, 1224 cm⁻¹; ¹H NMR (500 MHz, CDCl₃) δ 9.48 (br s, 1H, COOH), 4.22-4.15 (m, 4H, OCH₂CH₃), 2.98 (dd, 2H, *J*_{1H-13C} = 7.3 Hz, *J*_{1H-31P} = 21.8 Hz, H-1), 1.34 (t, 6H, *J* = 7.1 Hz, OCH₂CH₃); ¹³C NMR (125 MHz, CDCl₃) δ 167.8 (enriched, d, *J*_{13C-31P} = 5.4 Hz), 63.2 (d, *J*_{13C-31P} = 6.5 Hz), 34.2 ppm (dd, *J*_{13C-31P} = 134.5 Hz, *J*_{13C-13C} = 55.2 Hz), 16.3; HRMS calculated for C₅[¹³C]H₁₂O₅P 196.0461, Found 196.0464 [M-H]⁻.

***S*-2-Acetamidoethyl [1-¹³C]-2-(diethoxyphosphoryl)ethanethioate (119)**



In a flame-dried flask under argon, **118** (330 mg, 1.70 mmol) was dissolved in 10 mL of CH₂Cl₂ and cooled to 0 °C. Dimethylaminopyridine (20.0 mg, 0.163 mmol) and dicyclohexylcarbodiimide (DCC) (385 mg, 1.85 mmol) were added, followed by an excess of *N*-acetylcysteamine (0.500 mL, 4.70 mmol). The reaction mixture was stirred at 0 °C for 30 min, then warmed to room temperature and stirred for an additional 22 hours. The solvent was removed under reduced pressure, and the crude reaction mixture was redissolved in EtOAc/EtO₂ = 1:1 (10 mL) and filtered to remove precipitated dicyclohexylurea. The filtrate was concentrated under reduced pressure, and then purified by flash column chromatography (EtOAc to 10% MeOH/EtOAc) to give the product as a white solid (315 mg, 62% yield). IR (CHCl₃, cast film) 3294, 2983, 1648, 1548, 1255 cm⁻¹; ¹H NMR (500 MHz, CDCl₃) δ 6.65 (br s, 1H, NH), 4.20 (m, 4H, OCH₂CH₃), 3.45 (dt, 2H, *J* = 6.2, 6.2 Hz, H-4), 3.22 (dd, 2H, *J*_{1H-31P} = 21.2 Hz, *J*_{1H-13C} = 6.4 Hz, H-1), 3.09 (2H, dt, *J* = 6.5 Hz, *J*_{1H-13C} = 5.6 Hz, H-3), 2.00 (s, 3H, H-6), 1.34 (t, 6H, *J* = 7.1 Hz, OCH₂CH₃); ¹³C NMR (125 MHz, CDCl₃) δ 190.5 (enriched, d, *J*_{13C-31P} = 7.0 Hz), 170.5, 62.9 (d, *J*_{13C-31P} = 6.2 Hz), 43.0 (dd, *J*_{13C-31P} = 131.0 Hz, *J*_{13C-13C} = 44.7 Hz), 39.0, 29.5, 23.1, 16.3 (d, *J*_{13C-31P} = 6.2 Hz); HRMS (ES) *m/z* calculated for C₉[¹³C]H₂₁NO₅PS 299.0906, found 299.0909 [M+H]⁺.

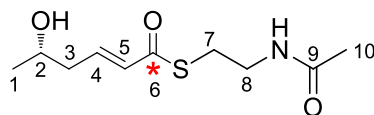
(*S*, *E*)-*S*-2-Acetamidoethyl [1-¹³C]-(5-(*tert*-butyldimethylsilyloxy)hex-2-enethioate (120)



To a stirred solution of LiBr (252 mg, 3.00 mmol) in dry THF, compound **119** (280 mg, 0.950 mmol) was added. The solution was stirred for 10 min at 25 °C, followed by the addition of Et₃N (0.400 mL, 3.00 mmol). The solution was stirred for an additional 10 min and then aldehyde **15** (404 mg) in 2 mL dry THF was added. After 12 hours at room temperature, the reaction was quenched by the addition of 15 mL of water, and the resulting solution was extracted with EtOAc (3 x 10 mL). The combined organic extracts were washed with brine (20 mL), dried over Na₂SO₄ and concentrated under reduced pressure. The residue was purified by flash column chromatography (1:1 EtOAc/hexanes to 2:1 EtOAc/hexanes) to give the product as a yellow oil (241 mg, 76 % yield). IR (CHCl₃, cast film) 3289, 2956, 2929, 1651, 1619, 1552, 1462; ¹H NMR (500 MHz, CDCl₃) δ 6.94 (dddd, 1H, *J* = 15.6, 7.3, 7.3 Hz, *J*_{1H-13C} = 7.3 Hz, H-4), 6.14 (ddt, 1H, *J* = 15.6, 1.3 Hz, *J*_{1H-13C} = 6.1 Hz, H-5), 6.1 (br s, 1H, NH), 3.95 (sextet, 1H, *J* = 6.1 Hz, H-2), 3.46 (dt, 2H, *J* = 6.1, 6.1 Hz, H-8), 3.10 (dt, 2H, *J* = 6.6, 4.9 Hz, H-7), 2.32 (t, 2H, *J* = 6.6 Hz, H-3), 1.97 (s, 3H, H-10), 1.17 (d, 3H, *J* = 6.1 Hz, H-1), 0.88 (s, 9H, Si-C(CH₃)₃), 0.05 (s, 3H, Si-CH₃), 0.04 (s, 3H, Si-CH₃). ¹³C NMR (125 MHz, CDCl₃) δ 190.3 (enriched), 170.4, 143.6, 130.1 (d, *J*_{13C-13C} = 61.4 Hz), 67.5, 42.5 (d, *J*_{13C-13C} = 6.7 Hz), 39.9, 28.2, 25.8, 23.9, 23.1, 18.0, -

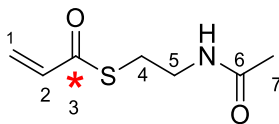
4.80; $\alpha_D^{25} = 7.88$ ($c = 0.510$, CHCl_3); HRMS (ES) m/z calculated for $\text{C}_{15}[^{13}\text{C}]\text{H}_{32}\text{NO}_3\text{SSi}$ 347.19, found 347.1896 $[\text{M}+\text{H}]^+$.

(*S, E*)-*S*-2-Acetamidoethyl [1- ^{13}C]-5-hydroxyhex-2-enethioate (99**)**



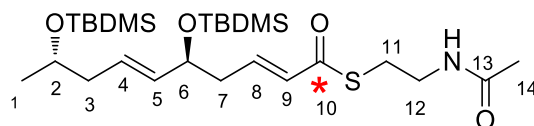
The known compound (unlabeled)¹⁰³ was synthesized as follows. To a solution of $\text{AcOH}/\text{H}_2\text{O}/\text{THF}$ (3:3:1, 7 mL) was added compound **120** (225 mg, 0.650 mmol). The mixture was stirred at room temperature for 19 hours, after which the volatile components were removed under high vacuum. The residue was diluted with 5 mL water, and the solution was extracted with EtOAc (3x5 mL). The combined organic portions were washed with brine (20 mL) and dried over Na_2SO_4 , filtered and concentrated under reduced pressure to give the product as a white solid (125 mg, 83%). IR (cast film) 3295, 3086, 2968, 2930, 1650, 1617, 1553 cm^{-1} ; ^1H NMR (500 MHz, CDCl_3) δ 6.92 (dddd, 1H, $J=15.4, 7.3, 7.3$, $J_{\text{H-}^{13}\text{C}} = 7.30$, H-4), 6.20 (ddt, 1H, $J = 15.4, 1.5$ Hz, $J_{\text{H-}^{13}\text{C}} = 6.10$ Hz, H-5), 6.00 (br s, 1H, NH), 3.96 (sextet, 1H, $J = 6.10$ Hz, H-2), 3.46 (dt, 2H, $J = 6.1, 6.1$ Hz, H-8), 3.10 (dt, 2H, $J_{\text{H-}^{13}\text{C}} = 5.6$ Hz, $J = 4.9$ Hz, H-7), 2.34 (t, 2H, $J = 7.4$ Hz, H-3), 1.94 (s, 3H, H-10), 1.22 (d, 3H, $J = 6.2$ Hz); ^{13}C NMR (125 MHz, CDCl_3) δ 190.3 (enriched), 170.6, 142.6, 130.5 (d, $J_{^{13}\text{C-}^{13}\text{C}} = 61.3$ Hz), 66.6, 41.8 (d, $J_{^{13}\text{C-}^{13}\text{C}} = 6.7$ Hz), 39.7, 28.3, 23.4, 23.2; $\alpha_D^{25} = 0.0944$ ($c = 0.780$, CHCl_3); HRMS (ES) m/z calculated for $\text{C}_9[^{13}\text{C}]\text{H}_{18}\text{NO}_3\text{S}$ 233.1035, found 233.1034 $[\text{M}+\text{H}]^+$.

***S*-2-Acetamidoethyl [1-¹³C]-prop-2-enethioate (122)**



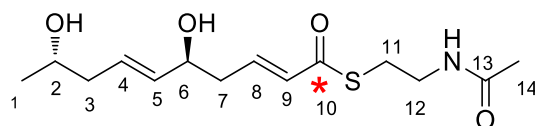
The known compound (unlabeled)²⁰⁶ was as follows. To a stirred solution of [1-¹³C]-acrylic acid (72.1 mg, 1.00 mmol) in 5 mL CH₂Cl₂ was added dimethylaminopyridine (12.2 mg, 0.100 mmol) at 0 °C. Then DCC (227 mg, 1.10 mmol) and *N*-acetylcysteamine (119 mg, 1.00 mmol) were added to the solution sequentially. The mixture was stirred at 0 °C for 30 min, then warmed to 25 °C and stirred for a further 12 h. The solvent was removed *in vacuo* and then 10 mL 1:1 EtOAc/Et₂O was added. The precipitated dicyclohexylurea (DCU) was removed by filtration; the filtrate was concentrated and then purified using flash column chromatography (10:1 EtOAc/MeOH) to give the product (36.0 mg, 20% yield) as a colorless oil. IR (CHCl₃, cast film) 3285, 3074, 2976, 2933, 1670, 1613, 1549 cm⁻¹; ¹H NMR (500 MHz, CDCl₃) δ 6.36 (m, 2H, H-1), 6.10 (br s, 1H, NH), 5.76 (ddd, 1H, *J* = 14.9, 1.3 Hz, *J*_{1H-13C} = 9.9 Hz, H-2), 3.48 (q, 2H, *J* = 6.3 Hz, H-5), 3.13 (td, 2H, *J* = 6.5 Hz, *J*_{1H-13C} = 4.8 Hz, H-4), 1.98 (s, 3H, H-7); ¹³C NMR (125 MHz, CDCl₃) δ 190.6 (enriched), 171.8, 134.7 (d, *J*_{13C-13C} = 60.1 Hz), 127.0, 39.5, 28.3 (d, *J*_{13C-13C} = 0.9 Hz), 23.2; HRMS (ES) *m/z* calculated for C₁₃[¹³C]H₂₃NO₄SNa 325.1274, found 325.1272 [M+Na]⁺.

(2*E*, 5*S*, 6*E*, 9*S*)-*S*-2-Acetamidoethyl [1-¹³C]-5,9-bis(*tert*-butyldimethylsilyloxy)deca-2,6-dienethioate (123)



To a stirred solution of **20** (115 mg, 0.300 mmol) in 6 mL dry CH₂Cl₂ were sequentially added Hoveyda-Grubbs II catalyst (12.5 mg, 19.9 μmol) and **122** (35.0 mg, 0.202 mmol). The solution was stirred at 25 °C for 18 h. The solvent was removed under vacuum, and the residue was purified by column chromatography on silica gel using a 3:1 = EtOAc/hexanes eluent to afford the product as a colorless oil (61.0 mg, 56% yield). IR (CHCl₃, cast film) 3289, 3079, 2955, 2929, 2895, 2856, 1728, 1665, 1635, 1548 cm⁻¹; ¹H NMR (500 MHz, CDCl₃) δ 6.90 (m, 1H, H-8), 6.13 (ddt, 1H, *J* = 15.5, 1.3 Hz, *J*_{H-13C} = 6.0 Hz, H-9), 5.96 (br s, 1H, NH), 5.60 (m, 1H, H-4), 5.42 (ddt, 1H, *J* = 15.4, 6.4, 1.3 Hz, H-5), 4.20 (q, 1H, *J* = 6.1 Hz, H-6), 3.80 (sextet, 1H, *J* = 6.0 Hz, H-2), 3.44 (q, 2H, *J* = 6.2 Hz, H-12), 3.06 (m, 2H, H-11), 2.36 (t, 2H, *J* = 6.8 Hz, H-7), 2.20-2.10 (m, 2H, H-3), 1.95 (s, 3H, H-14), 1.09 (d, 3H, *J* = 6.1 Hz, H-1), 0.88 (s, 18H, Si-C(CH₃)₃), 0.06 (s, 6H, SiCH₃), 0.05 (s, 3H, SiCH₃), 0.03 (s, 3H, SiCH₃); ¹³C NMR (125 MHz, CDCl₃) δ 190.2 (enriched), 170.2, 143.2, 134.5, 130.2 (d, *J*_{13C-13C} = 61.6 Hz), 127.7, 72.3, 68.4, 42.5, 41.5 (d, *J*_{13C-13C} = 6.7 Hz), 39.9, 28.2, 25.9, 25.9, 23.4, 23.2, 18.2, 18.1, - 4.22, - 4.43, - 4.67, - 4.78; [α]_D²⁵ = -11.9 (c = 0.180, CHCl₃); HRMS (ES) *m/z* calculated for C₂₅[¹³C]H₅₂NO₄SSi₂Na 553.3003, found 553.3002 [M+Na]⁺.

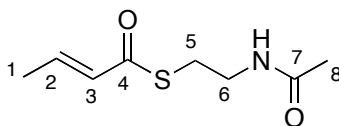
(2*E*, 5*S*, 6*E*, 9*S*)-*S*-2-Acetamidoethyl [1-¹³C]-5,9-dihydroxydeca-2,6-dienethioate (102)



Compound **102** was synthesized from **123** according to the procedure used to prepare **100**.

102: 6.00 mg, white solid, 95% yield. IR (CHCl₃, cast film) 3299, 3089, 2965, 2929, 1649, 1618, 1553 cm⁻¹; ¹H NMR (500 MHz, CDCl₃) δ 6.90 (m, 1H, H-8), 6.19 (m, 1H, H-9), 6.02 (br s, 1H, NH), 5.73 (m, 1H, H-4), 5.58 (m, 1H, H-5), 4.20 (q, 1H, *J* = 6.3 Hz, H-6), 3.80 (sextet, 1H, *J* = 6.1 Hz, H-2), 3.44 (m, 2H, H-12), 3.09 (q, 2H, *J* = 5.8 Hz, H-11), 2.46 (q, 2H, *J* = 5.9 Hz, H-7), 2.30-2.10 (m, 2H, H-3), 1.96 (s, 3H, H-14), 1.19 (d, 3H, *J* = 6.2 Hz, H-1); ¹³C NMR (125 MHz, CDCl₃) δ 190.2 (enriched), 170.5, 141.9, 135.1, 130.6 (d, *J*_{13C-13C} = 61.6 Hz), 128.7, 71.3, 67.2, 41.9, 39.9 (d, *J*_{13C-13C} = 6.2 Hz), 39.6, 28.5, 23.2, 23.0; [α]_D²⁵ = 2.20 (c = 0.150, CHCl₃); HRMS (ES) *m/z* calculated for C₁₃[¹³C]H₂₃NO₄SNa 325.1274, found 325.1272 [M+Na]⁺.

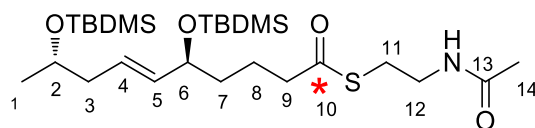
(*E*)-*S*-(2-acetamidoethyl) but-2-enethioate (125)



To a stirred solution of but-2-enoic acid (860 mg, 10.0 mmol) in 50 mL CH₂Cl₂ was added DMAP (122 mg, 1.0 mmol) at 0 °C. Then DCC (2.27 g, 11.0 mmol),

N-acetylcysteamine (1.31 g, 11.0 mmol) were added to the solution sequentially. The mixture was stirred at 0 °C for 30 min, then warmed to 25 °C and stirred for a further 12 h. The solvent was removed *in vacuo* and then 20 mL 1:1 EtOAc/Et₂O was added. The precipitated dicyclohexylurea (DCU) was removed by filtration; the filtrate was concentrated and then purified using flash column chromatography (10:1 EtOAc/MeOH) to give the product (1.50 g, 80% yield) as a white solid. IR (CHCl₃, cast film) 3254, 3075, 2944, 2855, 1661, 1637, 1568 cm⁻¹; ¹H NMR (500 MHz, CDCl₃) δ 6.92 (dq, 1H, *J* = 15.4, 6.9 Hz, H-2), 6.14 (dq, 1H, *J* = 15.4, 1.7 Hz, H-3), 6.10 (br s, 1H, NH), 3.44 (q, 2H, *J* = 6.2 Hz, H-6), 3.07 (t, 2H, *J* = 6.4 Hz, H-5), 1.95 (d, 3H, *J* = 3.3 Hz, H-8), 1.88 (dd, 3H, *J* = 6.9, 1.7 Hz, H-1); ¹³C NMR (125 MHz, CDCl₃) δ 190.2, 170.3, 141.8, 129.9, 39.8, 28.2, 23.2, 18.0; HRMS (EI) *m/z* calculated for C₈H₁₃NO₂S 187.0667, found 187.0669 [M+Na]⁺.

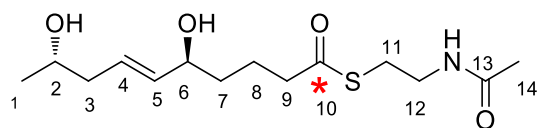
(5*S*, 9*S*, *E*)-*S*-2-Acetamidoethyl [1-¹³C]-5,9-bis(*tert*-butyldimethylsilyloxy)dec-6-enethioate (124**)**



To 0.5 mL of 1:1 = monoglyme:EtOH solution was added InCl₃ (1.50 mg, 6.75 μmol) and NaBH₄ (2.00 mg, 50.0 μmol). The resulting solution was stirred at 25 °C for 5 min. A solution of **123** (8.00 mg, 15.0 μmol) in 0.5 mL of 1:1 = monoglyme:EtOH was added, and the resulting solution was stirred at 25 °C for another 3 h. The reaction was quenched by the addition of 2 mL saturated

ammonium chloride. The layers were separated and the aqueous layer was extracted with EtOAc (3x2 mL). The combined organic layers were washed with brine (5 mL) and dried over Na₂SO₄. The solvent was removed *in vacuo* to give the product (7.00 mg, 87% yield) as a colorless oil. IR (CHCl₃, cast film) 3286, 3079, 2955, 2929, 2896, 2856, 1654, 1553 cm⁻¹; ¹H NMR (500 MHz, CDCl₃) δ 5.80 (br s, 1H, NH), 5.55 (dtd, 1H, *J* = 15.3, 7.2, 0.7 Hz, H-4), 5.39 (ddt, 1H, *J* = 15.4, 6.5, 1.2 Hz, H-5), 4.05 (q, 1H, *J* = 6.2 Hz, H-6), 3.80 (sextet, 1H, *J* = 6.0 Hz, H-2), 3.44 (q, 2H, *J* = 6.2 Hz, H-12), 3.02 (m, 2H, H-11), 2.58 (td, 2H, *J* = 7.4 Hz, *J*_{H-13C} = 5.9 Hz, Hz, H-9), 2.20-2.10 (m, 2H, H-3), 1.96 (s, 3H, H-14), 1.76-1.61 (m, 2H, H-7), 1.53-1.42 (m, 2H, H-8), 1.10 (d, 3H, *J* = 6.1 Hz, H-1), 0.88 (s, 18H, Si-C(CH₃)₃), 0.06 (s, 6H, SiCH₃), 0.05 (s, 3H, SiCH₃), 0.03 (s, 3H, SiCH₃); ¹³C NMR (125 MHz, CD₂Cl₂) δ 199.9 (enriched), 170.1, 135.7, 127.3, 73.4, 68.9, 44.3 (d, *J*_{13C-13C} = 45.9 Hz), 42.9, 39.9, 37.8 (d, *J*_{13C-13C} = 3.6 Hz), 28.8, 26.0, 26.0, 23.5, 23.3, 21.8 (d, *J*_{13C-13C} = 2.0 Hz), 18.4, 18.3, - 4.02, - 4.40, - 4.61, - 4.67; [α]_D²⁵ = -1.46 (c = 0.130, CHCl₃); HRMS (ES) *m/z* calculated for C₂₅[¹³C]H₅₃NO₄SSi₂Na 555.3153, found 555.3160 [M+Na]⁺.

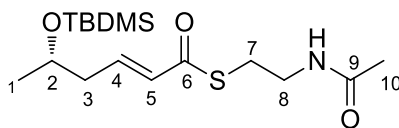
(5*S*, 9*S*, *E*)-*S*-2-Acetamidoethyl [1-¹³C]-5,9-dihydroxydec-6-enethioate (103)



To compound **124** (7.00 mg, 13.1 μmol) was added 2 mL AcOH/H₂O/THF =2:3:1 solution at 0 °C. The resulting solution was stirred at 0 °C for 8 h. The solvent was removed *in vacuo* and the residue was purified using flash column

chromatography (first elute with EtOAc, then with EtOAc/MeOH = 10:1) to give the product (1.70 mg, 43% yield) as a colorless oil. IR (CH₂Cl₂, cast film) 3293, 3089, 2964, 2928, 2865, 1653, 1554 cm⁻¹; ¹H NMR (500 MHz, CD₂Cl₂) δ 5.80 (br s, 1H, NH), 5.65 (dddd, 1H, *J* = 15.4, 7.6, 6.6, 0.9 Hz, H-4), 5.56 (ddt, 1H, *J* = 15.4, 6.6, 1.2 Hz, H-5), 4.05 (q, 1H, *J* = 6.5 Hz, H-6), 3.80 (m, 1H, H-2), 3.32 (q, 2H, *J* = 6.3 Hz, H-12), 3.00 (m, 2H, H-11), 2.59 (td, 2H, *J* = 7.3 Hz, *J*_{H-13C} = 5.9 Hz, H-9), 2.20-2.10 (m, 2H, H-3), 1.89 (s, 3H, H-14), 1.76-1.61 (m, 2H, H-7), 1.53-1.42 (m, 2H, H-8), 1.15 (d, 3H, *J* = 6.2 Hz, H-1), 0.88 (s, 18H, Si-C(CH₃)₃), 0.06 (s, 6H, SiCH₃), 0.05 (s, 3H, SiCH₃), 0.03 (s, 3H, SiCH₃); ¹³C NMR (125 MHz, CD₂Cl₂) δ 199.8 (enriched), 171.2, 136.4, 128.1, 72.5, 67.4, 44.3 (d, *J*_{13C-13C} = 45.6 Hz), 42.4, 39.7, 36.5 (d, *J*_{13C-13C} = 3.3 Hz), 28.9, 23.3, 23.1, 22.0 (d, *J*_{13C-13C} = 2.1 Hz); HRMS (ES) *m/z* calculated for C₁₃[¹³C]H₂₅NO₄SNa 327.1430, found 327.1428 [M+Na]⁺.

(*S,E*)-*S*-2-Acetamidoethyl 5-(*tert*-butyldimethylsilyloxy)hex-2-enethioate (129**)**

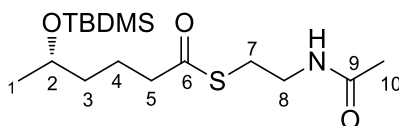


Compound **129** was synthesized from **17** and **122** (unlabeled) according to the procedure used to prepare **123**.

129: 84.0 mg, colorless oil, 70% yield. IR (CHCl₃, cast film) 3286, 3076, 2955, 2929, 2895, 2857, 1662, 1551 cm⁻¹; ¹H NMR (500 MHz, CDCl₃) δ 6.91 (dt, 1H, *J* = 15.4, 7.6 Hz, H-4), 6.12 (dt, 1H, *J* = 15.4, 1.4 Hz, H-5), 6.00 (br s, 1H, NH), 3.92 (sextet, 1H, *J* = 6.0 Hz, H-2), 3.44 (q, 2H, *J* = 6.2 Hz, H-8), 3.07 (t, 2H, *J* =

6.4 Hz, H-7), 2.30 (ddd, 2H, $J = 7.4, 5.9, 1.37$ Hz, H-3), 1.98 (s, 3H, H-10), 1.09 (d, 3H, $J = 6.1$ Hz, H-1), 0.92 (s, 9H, Si-C(CH₃)₃), 0.03 (s, 3H, SiCH₃), 0.02 (s, 3H, SiCH₃); ¹³C NMR (125 MHz, CDCl₃) δ 190.2, 170.3, 143.5, 130.2, 67.4, 42.4, 39.8, 28.2, 25.8, 23.9, 23.2, 18.0, - 4.50, - 4.79; $[\alpha]_D^{25} = 2.00$ (c = 0.320, CHCl₃); HRMS (ES) m/z calculated for C₁₆H₃₂NO₃SSiNa 368.1686, found 368.1686 [M+Na]⁺.

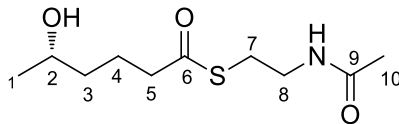
(S)-S-2-Acetamidoethyl 5-(tert-butyldimethylsilyloxy)hexanethioate (130)



Compound **130** was synthesized from **129** according to the procedure used to prepare **124**.

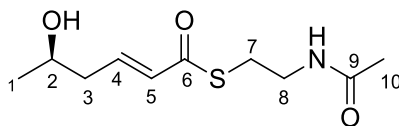
130: 8.00 mg, colorless oil, 87% yield. IR (CHCl₃, cast film) 3290, 3080, 2955, 2929, 2895, 2857, 1693, 1655, 1554 cm⁻¹; ¹H NMR (500 MHz, CDCl₃) δ 5.82 (br s, 1H, NH), 3.77 (sextet, 1H, $J = 6.0$ Hz, H-2), 3.42 (q, 2H, $J = 6.2$ Hz, H-8), 3.02 (t, 2H, $J = 6.4$ Hz, H-7), 2.58 (t, 2H, $J = 7.5$ Hz, H-3), 1.95 (s, 3H, H-10), 1.80 – 1.60 (m, 2H, 3), 1.38 – 1.45 (m, 2H, 4), 1.11 (d, 3H, $J = 6.1$ Hz, H-1), 0.92 (s, 9H, Si-C(CH₃)₃), 0.03 (s, 3H, SiCH₃), 0.02 (s, 3H, SiCH₃); ¹³C NMR (125 MHz, CDCl₃) δ 200.1, 170.2, 68.1, 44.1, 39.8, 38.7, 28.5, 25.9, 23.8, 23.3, 21.9, 18.1, - 4.32, - 4.69; $[\alpha]_D^{25} = 10.2$ (c = 0.320, CHCl₃); HRMS (ES) m/z calculated for C₁₆H₃₃NO₃SSiNa 370.1843, found 370.1839 [M+Na]⁺.

(S)-S-2-Acetamidoethyl 5-hydroxyhexanethioate (105)



To compound **130** (8.00 mg, 23.0 μmol) was added 2 mL AcOH/H₂O/THF =2:3:1 solution at 0 °C. The solution was stirred at 0 °C for 4 h. The solvent was removed *in vacuo*, and the residue was purified using flash column chromatography (first elute with EtOAc/Hexane = 1:1, then with EtOAc) to give the product (2.00 mg, 31% yield) as a colorless oil. IR (CH₂Cl₂, cast film) 3288, 3084, 2964, 2930, 2869, 1690, 1657, 1554 cm⁻¹; ¹H NMR (500 MHz, CD₂Cl₂) δ 5.80 (br s, 1H, NH), 3.76 (sextet, 1H, J = 6.2 Hz, H-2), 3.39 (q, 2H, J = 6.3 Hz, H-8), 3.00 (t, 2H, J = 6.5 Hz, H-7), 2.60 (t, 2H, J = 7.3 Hz, H-3), 1.90 (s, 3H, H-10), 1.80 – 1.65 (m, 2H, 3), 1.45 - 1.40 (m, 2H, 4), 1.11 (d, 3H, J = 6.1 Hz, H-1), 0.92 (s, 9H, Si-C(CH₃)₃), 0.03 (s, 3H, SiCH₃), 0.02 (s, 3H, SiCH₃); ¹³C NMR (125 MHz, CD₂Cl₂) δ 199.9, 170.2, 67.7, 44.2, 39.7, 38.6, 28.9, 23.7, 23.3, 22.2; $[\alpha]_{\text{D}}^{25}$ = 10.0 (c = 0.080, CH₂Cl₂); HRMS (ES) m/z calculated for C₁₀H₁₉NO₃SN⁺ 256.0978, found 256.0975 [M+Na]⁺.

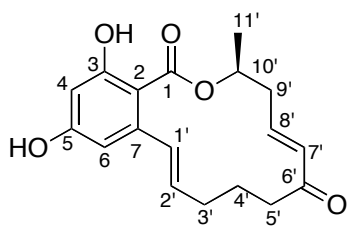
(R, E)-S-2-Acetamidoethyl 5-hydroxyhex-2-enethioate (104)



Compound **104** was synthesized from (*R*)-pent-4-2-ol and **122** according to the procedure used to prepare **123**.

104: 22.0 mg, brown oil, 48% yield. IR (CHCl₃, cast film) 3297, 3086, 2969, 2931, 2857, 1660, 1635, 1551 cm⁻¹; ¹H NMR (500 MHz, CDCl₃) δ 6.93(dt, 1H, *J* = 15.4, 7.5 Hz, H-4), 6.20 (dt, 1H, *J* = 15.4, 1.4 Hz, H-5), 5.95 (brs, 1H, NH), 3.99 (sextet, 1H, *J* = 6.1 Hz, H-2), 3.44 (q, 2H, *J* = 6.2 Hz, H-8), 3.09 (t, 2H, *J* = 6.4 Hz, H-7), 2.38 (m, 2H, H-3), 1.96 (s, 3H, H-10), 1.25 (d, 3H, *J* = 6.2 Hz, H-1); ¹³C NMR (125 MHz, CDCl₃) δ 190.2, 170.3, 142.3, 130.6, 66.7, 41.8, 39.8, 28.4, 23.5, 23.3; [α]_D²⁵ = - 8.69 (c = 0.230, CHCl₃); HRMS (ES) *m/z* calculated for C₁₀H₂₁NO₃SNa 254.0821, found 254.0818 [M+Na]⁺.

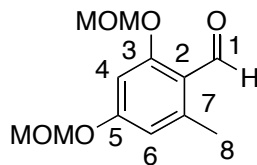
(*S*,5*E*,11*E*)-14,16-dihydroxy-3-methyl-3,4,9,10-tetrahydro-1*H*-benzo[*c*][1]oxacyclotetradecine-1,7(8*H*)-dione (133)



To a stirred solution of DHZ (1.20 mg, 2.77 μmol) in 4 mL CH₂Cl₂ was added Dess-Martin periodinane (2.40 mg, 5.66 μmol). The resulting solution was stirred at 25 °C for 0.5 h. The reaction was quenched by addition of 5 mL of 1:1 10% Na₂S₂O₃ : saturated aqueous NaHCO₃. The layers were separated and the aqueous layer was extracted with EtOAc (3 x 10 mL). The combined organic layers were washed with brine (20 mL) and dried over Na₂SO₄. The solvent was removed *in vacuo* and the residue was purified using flash column chromatography (EtOAc/hexanes = 1:1) to give the product (0.70 mg, 58% yield) as a white solid.

IR (CHCl₃, cast film) 3364, 2926, 2854, 1651, 1618, 1579, 1451, 1259 cm⁻¹; ¹H NMR (600 MHz, CDCl₃) δ 7.02 (ddd, 1H, *J* = 16.2, 8.6, 6.2 Hz, H-8'), 6.94 (d, 1H, *J* = 2.4 Hz, H-2'), 6.43 (d, 1H, *J* = 2.5 Hz, H-4), 6.36 (d, 1H, *J* = 2.6 Hz, H-6), 6.17 (d, 1H, *J* = 16.2 Hz, H-2'), 5.86-5.81 (m, 1H, H-1'), 5.60-5.58 (m, 1H, H-10'), 2.92-2.83 (m, 2H, H-3', H-9'), 2.41-2.33 (m, 2H, H-9', H-5'), 2.31-2.27 (m, 1H, H-3'), 2.14-2.05 (m, 2H, H-4', H-5'), 1.87-1.82 (m, 1H, H-4'), 1.41 (d, 3H, *J* = 6.5 Hz, H-11'). ¹³C NMR (125 MHz, CDCl₃) δ 203.3, 170.2, 164.8, 160.4, 143.4, 143.3, 136.5, 132.9, 132.8, 108.5, 104.6, 102.5, 70.2, 36.4, 34.7, 31.3, 25.9, 19.3; [α]_D²⁵ = -175.30 (c = 0.030, CHCl₃); HRMS (ES) *m/z* calculated for C₁₈H₁₉O₅ 315.1238, found 315.1237 [M-H]⁻.

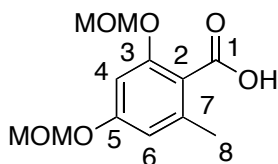
2, 4-bis(Methoxymethoxy)-6-methylbenzaldehyde (138)



To a stirred solution of compound 1-(2,4-Dihydroxy-6-methylphenyl)ethanone (2.28 g, 15.0 mmol) in 40 mL DMF was added 7.80 mL (45.0 mmol) *i*Pr₂EtN at 0 °C under Ar. After stirring for 15 min at 0 °C, 3.40 mL (45.0 mmol) methoxymethyl chloride was added and the reaction was warmed up to 25 °C. After stirring for 12 h, the reaction was diluted with Et₂O (100 mL) and washed with NH₄Cl (100 mL), brine (100 mL) and then dried over Na₂SO₄. The solvent was removed *in vacuo* to give the product (3.58 g, quant.) as a light yellow oil. IR (CHCl₃, cast film) 2960, 2930, 2828, 2782, 1679, 1601, 1573, 1454 cm⁻¹; ¹H

NMR (600 MHz, CDCl₃) δ 10.53 (d, 1H, J = 0.5 Hz, H-1), 6.69 (d, 1H, J = 2.3 Hz, H-4), 6.53 (d, 1H, J = 2.2 Hz, H-6), 5.25 (s, 2H, OCH₂OCH₃), 5.20 (s, 2H, OCH₂OCH₃), 3.52 (s, 3H, OCH₂OCH₃), 3.48 (s, 3H, OCH₂OCH₃), 2.58 (s, 3H, H-8); ¹³C NMR (125 MHz, CDCl₃) δ 190.6, 162.8, 161.8, 144.3, 118.7, 112.3, 100.5, 94.8, 94.0, 56.6, 56.4, 22.2; HRMS (ES) m/z calculated for C₁₂H₁₆O₅Na 263.0890, found 263.0889 [M+Na]⁺.

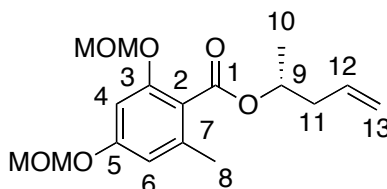
2,4-bis(Methoxymethoxy)-6-methylbenzoic acid (139)



The known compound²⁰⁷ was synthesized as follows. To a stirred solution of compound **138** (3.39 g, 14.2 mmol) in 40 mL DMSO was added sequentially NaHPO₄·H₂O (9.80 g, 71.0 mmol) in 20 mL H₂O, and NaClO₂ (6.40 g, 71.0 mmol) in 20 mL H₂O. After stirring for 12 h, the reaction mixture was diluted with EtOAc (100 mL) and washed with H₂O (100 mL) and brine (100 mL). It was then dried over Na₂SO₄. The solvent was removed *in vacuo* to give the product (3.60 g, quant.) as a light yellow oil. IR (CHCl₃, cast film) 3300-2600, 2958, 2830, 2634, 1679, 1601, 1573, 1454 cm⁻¹; ¹H NMR (400 MHz, CDCl₃) δ 6.72 (d, 1H, J = 2.3 Hz, H-4), 6.62 (d, 1H, J = 2.2 Hz, H-6), 5.26 (s, 2H, OCH₂OCH₃), 5.18 (s, 2H, OCH₂OCH₃), 3.52 (s, 3H, OCH₂OCH₃), 3.48 (s, 3H, OCH₂OCH₃), 2.49 (s, 3H, H-8); ¹³C NMR (100 MHz, CDCl₃) δ 174.6, 159.5, 156.6, 141.7,

116.0, 112.1, 101.4, 95.5, 94.2, 56.7, 56.3, 21.5; HRMS (ES) m/z calculated for $C_{12}H_{15}O_6Na$ 255.0874, found 255.0873 $[M+Na]^+$.

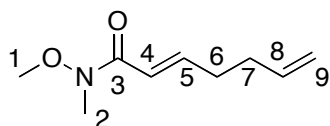
(*R*)-Pent-4-en-2-yl 2,4-bis(methoxymethoxy)-6-methylbenzoate (140)



To a stirred solution of compound **139** (770 mg, 3.00 mmol) in 20 mL CH_2Cl_2 0 °C was added 4-dimethylaminopyridine (DMAP) (36.6 mg, 0.30 mmol), (*R*)-pent-4-en-2-ol (516 mg, 6.00 mmol), and 1-ethyl-3-(3-dimethylaminopropyl)carbodiimide (EDC) (630 mg, 3.30 mmol). After stirring for 12 h, the reaction mixture was diluted with EtOAc (100 mL). The organic phase was washed with H_2O (100 mL) and brine (100 mL). This was then dried over Na_2SO_4 . The solvent was removed *in vacuo* and the residue was purified using flash column chromatography (1:5 EtOAc/hexanes) to give **18** (180 mg, 19%) as a colorless oil. IR ($CHCl_3$, cast film) 3078, 2977, 2957, 2853, 1724, 1607, 1588, 1484 cm^{-1} ; 1H NMR (600 MHz, $CDCl_3$) δ 6.66 (d, 1H, $J = 2.1$ Hz, H-4), 6.54 (d, 1H, $J = 2.2$ Hz, H-6), 5.86 (ddt, 1H, $J = 17.1, 10.2, 6.9$ Hz, H-12), 5.23 (sextet, 1H, $J = 6.3$ Hz, H-9), 5.15-5.06 (m, 6H, OCH_2OCH_3 , H-13), 3.48 (s, 6H, OCH_2OCH_3), 2.53-2.32 (m, 2H, H-11), 2.28 (s, 3H, H-8), 1.33 (d, 1H, $J = 6.4$ Hz, H-10); ^{13}C NMR (125 MHz, $CDCl_3$) δ 167.5, 158.6, 155.2, 137.6, 133.8, 119.1, 117.7, 110.6, 101.2, 94.6, 94.3, 70.9, 56.2, 56.1, 40.3, 19.7, 19.6; $[\alpha]_D^{25} = -$

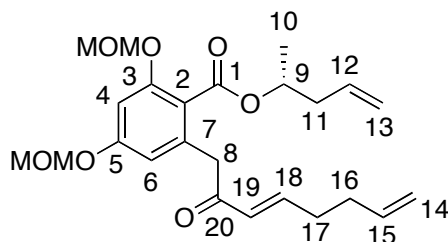
2.69 ($c = 1.07$, CHCl_3); HRMS (ES) m/z calculated for $\text{C}_{17}\text{H}_{24}\text{O}_6\text{Na}$ 347.1465, found 347.1462 $[\text{M}+\text{Na}]^+$.

(E)-N-Methoxy-N-methylhepta-2,6-dienamide (146)



The known compound¹⁵⁰ was synthesized as follows. To a stirred solution of compound diethyl (2-(methoxy(methyl)amino)-2-oxoethyl)phosphonate (841 mg, 10.0 mmol) in 30 mL THF was added 60% NaH (540 mg, 13.5 mmol) at 0 °C under Ar. After stirring for 30 min, compound pent-4-enal (1.85 mL, 9.00 mmol) was added drop wise. The reaction mixture was warmed to 25 °C and was stirred for another 12 h. Then the reaction was quenched with 3.00 mL saturated NH_4Cl , and the mixture was extracted with EtOAc (3×10 mL). The organic layers were combined, washed with brine (10 mL) and then dried over Na_2SO_4 . The solvent was removed *in vacuo* and the residue was purified using flash column chromatography (1:1 EtOAc /hexanes) to give the product (1.50 g, 88%) as a colorless oil. IR (CHCl_3 , cast film) 2975, 2936, 2848, 1665, 1635, 1415 cm^{-1} ; ^1H NMR (500 MHz, CDCl_3) δ 6.93 (dt, 1H, $J = 15.4, 6.8$ Hz, H-5), 6.38 (d, 1H, $J = 15.4$ Hz, H-4), 5.78 (ddt, 1H, $J = 17.0, 10.3, 6.6$ Hz, H-8), 5.01 (dq, 1H, $J = 17.1, 1.7$ Hz, H-9), 4.96 (dq, 1H, $J = 10.2, 1.5$ Hz, H-9), 3.65 (s, 3H, H-1), 3.20 (s, 3H, H-2), 2.33-2.28 (m, 2H, H-6), 2.23-2.17 (m, 2H, H-7); ^{13}C NMR (125 MHz, CDCl_3) δ 166.8, 146.7, 137.3, 119.1, 115.3, 61.6, 32.3, 31.7; HRMS (ES) m/z calculated for $\text{C}_{17}\text{H}_{24}\text{O}_6\text{Na}$ 192.0993, found 192.0995 $[\text{M}+\text{Na}]^+$.

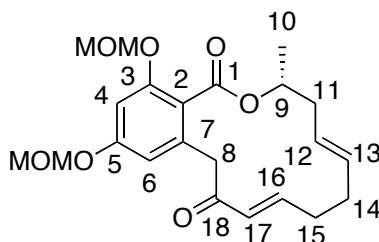
(*R*, *E*)-Pent-4-en-2-yl 2,4-bis(methoxymethoxy)-6-(2-oxoocta-3,7-dienyl)benzoate (141**)**



To a stirred solution of compound **140** (162 mg, 0.500 mmol) in 2 mL THF was added 1.00 mL fresh prepared lithium diisopropylamide (LDA) at -78 °C under Ar. After stirring for 5 min, the Weinreb amide **146** in 1.00 mL THF was added dropwise. The resulting mixture was then stirred for 10 min at -78 °C and the reaction was quenched by addition of 3.00 mL saturated NH₄Cl. The solution was extracted with EtOAc (3×10 mL), and the organic layers were combined, washed with brine (10 mL) and then dried over Na₂SO₄. The solvent was removed *in vacuo* and the residue was purified using flash column chromatography (1:5 EtOAc /hexanes) to give the product (100 mg, 46%) as a colorless oil. IR (CHCl₃, cast film) 3078, 2977, 2932, 2828, 1711, 1606, 1586, 1482 cm⁻¹; ¹H NMR (600 MHz, CDCl₃) δ 6.90 (dt, *J* = 15.7, 6.8 Hz, 1H, H-18), 6.76 (d, 1H, *J* = 2.2, Hz, H-4), 6.52 (d, 1H, *J* = 2.2 Hz, H-6), 6.17 (dt, 1H, *J* = 15.7, 1.5 Hz, H-19), 5.82 (m, 2H, H-12, H-15), 5.20-5.00 (m, 9H, H-9, H-13, H-14, OCH₂OCH₃), 3.88 (d, 1H, *J* = 16.4 Hz, H-8), 3.82 (d, 1H, *J* = 16.3 Hz, H-8), 3.47 (s, 3H, OCH₂OCH₃), 3.45 (s, 3H, OCH₂OCH₃), 2.48-2.18 (m, 6H, H-11, H-16, H-17), 1.29 (d, 1H, *J* = 6.4 Hz, H-10); ¹³C NMR (125 MHz, CDCl₃) δ 196.0, 167.1, 158.9, 156.0, 147.1, 136.9, 134.9, 133.8, 129.5, 118.9, 117.6, 115.6, 111.2, 102.4, 94.6, 94.3, 71.1,

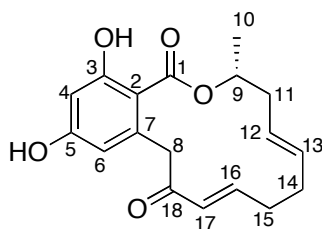
56.2, 56.1, 45.3, 40.2, 32.0, 31.7, 19.4; $[\alpha]_D^{25} = 0.81$ ($c = 1.63$, CHCl_3); HRMS (ES) m/z calculated for $\text{C}_{24}\text{H}_{32}\text{O}_7\text{Na}$ 455.2040, found 455.2036 $[\text{M}+\text{Na}]^+$.

MOM-(*R*) monocillin II (142)



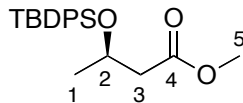
To a stirred solution of **141** (150 mg, 0.350 mmol) in 175 mL dry toluene was added Grubbs II catalyst (29.7 mg, 35.0 μmol). The solution was stirred at 80 $^{\circ}\text{C}$ under Ar for 12 h. The solvent was removed *in vacuo* and the residue was purified using flash column chromatography (1:5 EtOAc/hexanes) to give the product (120 mg, 86%) as a colorless oil. IR (CHCl_3 , cast film) 2929, 2852, 1716, 1606, 1585, 1482, 1437 cm^{-1} ; ^1H NMR (500 MHz, CDCl_3) δ 6.78 (m, 1H, H-16), 6.69 (d, 1H, $J = 2.1$ Hz, H-4), 6.57 (d, 1H, $J = 2.2$ Hz, H-6), 5.99 (d, 1H, $J = 16.1$ Hz, H-17), 5.40-5.29 (m, 2H, H-12, H-13), 5.20-5.09 (m, 5H, H-9, OCH_2OCH_3), 4.05 (d, 1H, $J = 14.7$ Hz, H-8), 3.48–3.42 (m, 7H, H-8, OCH_2OCH_3), 2.40-2.0 (m, 6H, H-11, H-14, H-15), 1.39 (d, 3H, $J = 6.1$ Hz, H-10); ^{13}C NMR (125 MHz, CDCl_3) δ 197.5, 167.6, 158.9, 156.0, 148.9, 135.2, 131.7, 129.9, 128.5, 118.7, 109.8, 102.1, 94.6, 94.3, 71.6, 56.2, 56.1, 44.3 (C-8), 39.6, 30.9, 30.6, 20.2; $[\alpha]_D^{25} = -72.13$ ($c = 0.540$, CHCl_3); HRMS (ES) m/z calculated for $\text{C}_{25}\text{H}_{34}\text{SiO}_3\text{Na}$ 427.1727, found 427.1728 $[\text{M}+\text{Na}]^+$.

(R)-monocillin II (135)



The known compound¹⁵⁰ was prepared according to method different from that reported. To a stirred solution of **142** (7.00 mg, 17.3 μmol) in 5 mL dry MeOH was added Dowex 50W X200 (30.0 mg). The solution was shaken at 25 °C for 12 h. The solvent was removed *in vacuo* and the residue was purified using flash column chromatography (1:5 EtOAc/hexanes) to give the product (4.00 mg, 86%) as a white solid. IR (CHCl_3 , cast film) 3600-3000, 2920, 2849, 1646, 1617, 1262 cm^{-1} ; ^1H NMR (500 MHz, CD_3COCD_3) δ 6.67-6.61 (m, 1H, H-16), 6.33 (d, 1H, J = 2.5 Hz, H-4), 6.31 (d, 1H, J = 2.5 Hz, H-6), 5.84 (d, 1H, J = 15.6 Hz, H-17), 5.35-5.23 (m, 3H, H-9, H-12, H-13), 4.05 (d, 1H, J = 16.8 Hz, H-8), 3.88 (m, 1H, H-11), 2.64 (ddd, 1H, J = 14.5, 8.2, 4.2 Hz, H-11); 2.33 (m, 1H, J = 6.1 Hz, H-11); 1.29 (d, 3H, J = 6.6 Hz, H-10); ^{13}C NMR (125 MHz, CD_3COCD_3) δ 196.5, 171.1, 166.2, 163.2, 147.4, 141.3, 132.6, 131.2, 128.2, 113.2, 106.4, 102.8, 73, 48.9, 37.5, 31.8, 31.7, 18.4; $[\alpha]_{\text{D}}^{25}$ = 70.1 (c = 0.18, CHCl_3); HRMS (ES) m/z calculated for $\text{C}_{18}\text{H}_{20}\text{O}_5\text{Na}$ 339.1203, found 339.1206 $[\text{M}+\text{Na}]^+$.

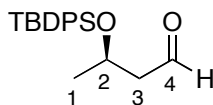
(*R*)-methyl 3-(*tert*-butyldiphenylsilyloxy)butanoate (151)



The known compound²⁰⁸ was synthesized from (*R*)-pent-4-en-2-ol according to the procedure used to prepare **159**.

151: 3.26 g, a colorless oil, quant. yield. IR (CHCl₃, cast film) 2954, 2932, 2894, 2858, 1741, 1111 cm⁻¹; ¹H NMR (500 MHz, CDCl₃) δ 7.76-7.72 (m, 4H, SiPh), 7.48-7.40 (m, 6H, SiPh), 4.35 (m, 1H, H-2), 3.62 (s, 3H, H-5), 2.60 (dd, 1H, *J* = 14.6, 7.0 Hz, H-3), 2.43 (dd, 1H, *J* = 14.6, 5.8 Hz, H-3), 1.16 (d, 3H, *J* = 6.1 Hz, H-1), 1.09 (s, 6H, C(CH₃)₃); ¹³C NMR (125 MHz, CDCl₃) δ 171.8, 135.88, 135.85, 134.3, 133.9, 129.66, 129.60, 127.58, 127.52, 66.9, 51.4, 44.5, 26.9, 23.7, 19.2; [α]_D²⁵ = -2.66 (*c* = 1.92, CHCl₃); HRMS (ES) *m/z* calculated for C₂₁H₂₈SiO₃Na 379.1700, found 379.1698 [M+Na]⁺.

(*R*)-3-(*tert*-butyldiphenylsilyloxy)butanal (152)

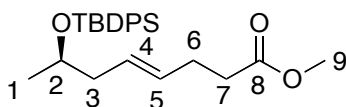


The known compound²⁰⁸ was synthesized from **151** according to the procedure used to prepare **15**.

152: 1.06 g, a colorless oil, 70% yield. IR (CHCl₃, cast film) 2962, 2932, 2895, 2858, 2808, 2724, 1728 cm⁻¹; ¹H NMR (500 MHz, CDCl₃) δ 9.74 (t, 1H, *J* = 2.4 Hz, H-4), 7.69-7.67 (m, 4H, SiPh), 7.46-7.38 (m, 6H, SiPh), 4.33 (sextet, 1H, *J* = 6.2 Hz, H-2), 2.48 (ddd, 2H, *J* = 15.8, 5.8, 2.5 Hz, H-3), 1.16 (d, 3H, *J* = 6.2 Hz,

H-1), 1.03 (s, 6H, C(CH₃)₃); ¹³C NMR (100 MHz, CDCl₃) δ 202.0, 135.8, 134.0, 133.6, 129.8, 129.7, 127.7, 127.6, 65.7, 52.8, 26.9, 23.8, 19.2; [α]_D²⁵ = 6.23 (c = 0.51, CHCl₃); HRMS (ES) *m/z* calculated for C₂₀H₂₆SiO₂Na 349.1594, found 349.1599 [M+Na]⁺.

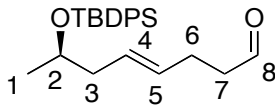
(*R, E*)-Methyl 7-(*tert*-butyldiphenylsilyloxy)oct-4-enoate (155**)**



The known compound¹⁵⁸ was synthesized from **152** according to the procedure used to prepare **161**.

155: 1.06 g, a colorless oil, 71% yield. IR (CHCl₃, cast film) 3074, 2963, 2931, 2896, 2857, 1742, 1428 cm⁻¹; ¹H NMR (600 MHz, C₆D₆) δ 7.79-7.77 (m, 4H, SiPh), 7.23-7.20 (m, 6H, SiPh), 5.34 (dtt, 1H, *J* = 14.7, 7.6, 1.2 Hz, H-4), 5.29-5.25 (m, 1H, H-5), 3.88 (sextet, 1H, *J* = 5.9 Hz, H-2), 3.31 (s, 3H, H-9), 2.21-2.06 (m, 6H, H-3, H-6, H-7), 1.18 (s, 9H, Si-C(CH₃)₃), 1.11 (d, 3H, *J* = 6.1 Hz, H-1); ¹³C NMR (125 MHz, C₆D₆) δ 172.7, 136.3, 136.2, 135.1, 134.9, 131.1, 129.9, 129.8, 128.3, 127.9, 127.9, 127.8, 69.9, 50.9 43.0, 33.9, 28.2, 27.2, 23.0, 19.5; [α]_D²⁵ = 20.91 (c = 0.350, CHCl₃); HRMS (ES) *m/z* calculated for C₂₅H₃₄SiO₃Na 433.2169, found 433.2167 [M+Na]⁺.

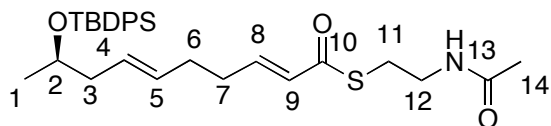
(*R, E*)-7-(*tert*-Butyldiphenylsilyloxy)oct-4-enal (156)



Compound **156** was synthesized from **155** according to the procedure used to prepare **162**.

156: 120 mg, a colorless oil, 70% yield. IR (CHCl₃, cast film) 3071, 2963, 2931, 2893, 2857, 2718, 1728, 1428 cm⁻¹; ¹H NMR (600 MHz, CDCl₃) δ 9.73 (t, 1H, *J* = 1.7 Hz, H-8), 7.67 (m, 4H, SiPh), 7.41 (m, 6H, SiPh), 5.37 (m, 2H, H-4, H-5), 3.86 (sextet, 1H, *J* = 5.9 Hz, H-2), 2.43 (td, 1H, *J* = 7.4, 1.7 Hz, H-7), 2.30 (dt, 2H, *J* = 6.9, 6.9 Hz, H-6), 2.15 (m, 2H, H-3), 1.19 (m, 12H, H-1, Si-C(CH₃)₃); ¹³C NMR (125 MHz, CDCl₃) δ 202.3, 135.9, 134.8, 134.6, 130.2, 129.5, 129.5, 128.1, 127.5, 127.4, 69.5, 43.4, 42.6, 27.1, 25.3, 23.0, 19.3; [α]_D²⁵ = 20.43 (c = 1.93, CHCl₃); HRMS (ES) *m/z* calculated for C₂₄H₃₂SiO₂Na 403.2064, found 403.2061 [M+Na]⁺.

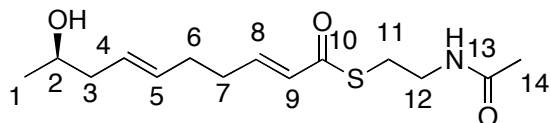
(*R, 2E, 6E*)-S-2-Acetamidoethyl 9-(*tert*-butyldiphenylsilyloxy)deca-2,6-dienethioate (157)



Compound **157** was synthesized from **156** according to the procedure used to prepare **163**.

157: 49.0 mg, a colorless oil, 65% yield. IR (CHCl₃, cast film) 3289, 3071, 2963, 2930, 2895, 2857, 1664, 1634, 1589, 1462, 1288 cm⁻¹; ¹H NMR (600 MHz, CDCl₃) δ 7.67 (m, 4H, SiPh), 7.41 (m, 6H, SiPh), 6.92 (dt, 1H, *J* = 15.5, 6.8 Hz, H-8), 6.13 (dt, 1H, *J* = 15.5, 1.5 Hz, H-9), 5.90 (s, 1H, NH), 5.40 (m, 2H, H-4, H-5), 3.87 (sextet, 1H, *J* = 5.8 Hz, H-2), 3.47 (dt, 2H, *J* = 6.2, 6.2 Hz, H-12), 3.10 (t, 2H, *J* = 6.3 Hz, H-11), 2.26-2.06 (m, 6H, H-3, H-6, H-7), 1.97 (s, 3H, H-14), 1.10 (m, 12H, H-1, Si-C(CH₃)₃); ¹³C NMR (100 MHz, CDCl₃) δ 190.3, 170.3, 145.9, 136.0, 135.9, 134.8, 134.6, 130.6, 129.5, 129.4, 128.6, 128.1, 127.5, 127.4, 69.5, 42.6, 39.9, 32.1, 30.9, 28.3, 27.1, 23.3, 22.9, 19.3; [α]_D²⁵ = 18.75 (c = 0.64, CHCl₃); HRMS (ES) *m/z* calculated for C₃₀H₄₁NSiO₃SNa 546.2469, found 546.2464 [M+Na]⁺.

(*R*, 2*E*, 6*E*)-*S*-2-Acetamidoethyl 9-hydroxydeca-2, 6-dienethioate (149**)**

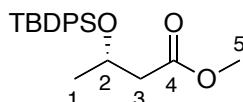


Compound **149** was synthesized from **157** according to the procedure used to prepare **164**.

149: 14.0 mg, a colorless oil, 65%. IR (CHCl₃, cast film) 3296, 3083, 2966, 2926, 2850, 1661, 1634, 1554, 1437, 1290 cm⁻¹; ¹H NMR (600 MHz, CDCl₃) δ 6.92 (dt, 1H, *J* = 15.5, 6.8 Hz, H-8), 6.13 (dt, 1H, *J* = 15.5, 1.5 Hz, H-9), 6.05 (s, 1H, NH), 5.50 (m, 2H, H-4, H-5), 3.85 (sextet, 1H, *J* = 6.1 Hz, H-2), 3.45 (dtd, 2H, *J* = 6.1, 6.1, 2.2 Hz, H-12), 3.10 (t, 2H, *J* = 6.2 Hz, H-11), 2.35-2.10 (m, 6H, H-3, H-6, H-7), 1.97 (s, 3H, H-14), 1.72 (s, 1H, OH), 1.19 (d, 3H, *J* = 6.2 Hz, H-1); ¹³C NMR

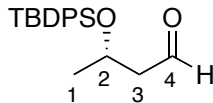
(125 MHz, CDCl₃) δ 190.2, 170.3, 145.6, 132.2, 128.9, 127.8, 67.2, 42.4, 39.6, 31.9, 31.0, 28.4, 23.2, 22.7; $[\alpha]_D^{25} = 2.00$ ($c = 0.100$, CHCl₃); HRMS (ES) m/z calculated for C₁₆H₂₇NSO₄Na 308.1291 found 308.1290 [M+Na]⁺.

(S)-methyl 3-(*tert*-Butyldiphenylsilyloxy)butanoate (159)



The known compound²⁰⁹ was prepared according to literature procedure. To a stirred solution of (*S*)-pent-4-en-2-ol (1.18 g, 10 mmol) in 10 mL dry DMF was sequentially added *tert*-Butyldiphenylsilyloxy chloride (3.10 mL, 12.0 mmol) and imidazole (1.02 g, 15.0 mmol). The solution was stirred for 12 h at 25 °C and then poured into hexanes (100 mL). The layers were separated and the organic layer was washed with H₂O (3 × 100 mL), brine (50 mL), dried over Na₂SO₄ and concentrated *in vacuo* to give the product as a colorless oil (3.56 g, quant.) IR (CHCl₃, cast film) 2956, 2932, 2895, 2858, 1741, 1111 cm⁻¹; ¹H NMR (500 MHz, CDCl₃) δ 7.75-7.72 (m, 4H, SiPh), 7.48-7.40 (m, 5H, SiPh), 4.37 (m, 1H, H-2), 3.63 (s, 3H, H-5), 2.61 (dd, 1H, $J = 14.6, 7.0$ Hz, H-3), 2.44 (dd, 1H, $J = 14.6, 5.8$ Hz, H-3), 1.17 (d, 3H, $J = 6.1$ Hz, H-1), 1.09 (s, C(CH₃)₃); ¹³C NMR (125 MHz, CDCl₃) δ 171.8, 135.88, 135.85, 134.3, 133.9, 129.66, 129.60, 127.58, 127.52, 66.9, 51.4, 44.5, 26.9, 23.7, 19.2; $[\alpha]_D^{25} = 6.31$ ($c = 0.65$, CHCl₃); HRMS (ES) m/z calculated for C₂₁H₂₈SiO₃Na 379.1700, found 379.1700 [M+Na]⁺.

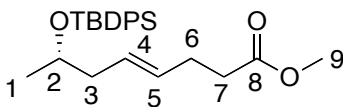
(S)-3-(tert-butylidiphenylsilyloxy)butanal (160)



The known compound²⁰⁹ was synthesized from **159** according to the procedure used to prepare **15**.

160: 700 mg, a colorless oil, 75% yield. IR (CHCl₃, cast film) 2962, 2932, 2895, 2858, 2808, 2724, 1728 cm⁻¹; ¹H NMR (500 MHz, CDCl₃) δ 9.77 (dd, 1H, *J* = 2.9, 2.1 Hz, H-4), 7.69-7.67 (m, 4H, SiPh), 7.46-7.38 (m, 6H, SiPh), 4.36 (sextet, 1H, *J* = 6.2 Hz, H-2), 2.51 (ddd, 2H, *J* = 15.8, 5.8, 2.5 Hz, H-3), 1.19 (d, 3H, *J* = 6.2 Hz, H-1), 1.06 (s, 6H, C(CH₃)₃); ¹³C NMR (125 MHz, CDCl₃) δ 202.0, 135.8, 134.0, 133.6, 129.8, 129.7, 127.7, 127.6, 65.7, 52.8, 26.9, 23.8, 19.2; [α]_D²⁵ = -5.57 (c = 0.42, CHCl₃); HRMS (ES) *m/z* calculated for C₂₀H₂₆SiO₂Na 349.1594, found 349.1597 [M+Na]⁺.

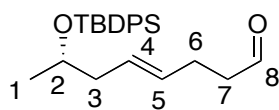
(S, E)-Methyl 7-(tert-butylidiphenylsilyloxy)oct-4-enoate (161)



To a stirred solution of **160** (460 mg, 1.41 mmol) in 15 mL dry THF was added vinylmagnesium bromide (5.60 mL of 1.0 M THF solution, 5.60 mmol) under Ar. The reaction mixture was stirred for 3 h, then quenched with saturated NaHCO₃ (10 mL), and extracted with Et₂O (3×10 mL). The organic phase was washed with brine (20 mL) and dried over Na₂SO₄. The solvent was removed *in vacuo* to give a mixture of diastereomeric allylic alcohols as yellow oil. To this yellow oil in 20

mL xylene was added trimethyl orthoacetate (0.70 mL, 5.51 mmol) and propionic acid (0.02 mL, 262 μ mol). The reaction mixture was heated to reflux for 18 h and quenched with 1.00 mL Et₃N. The solvent was removed *in vacuo* and the residue was purified using flash column chromatography (1:20 Et₂O/hexanes) to give the product (400 mg, 69%) as a colorless oil. IR (CHCl₃, cast film) 3074, 2963, 2931, 2896, 2857, 1742, 1428 cm⁻¹; ¹H NMR (600 MHz, C₆D₆) δ 7.78 (m, 4H, SiPh), 7.22 (m, 6H, SiPh), 5.34 (dtt, 1H, *J* = 14.7, 7.6, 1.2 Hz, H-4), 5.26 (m, 1H, H-5), 3.88 (sextet, 1H, *J* = 5.9 Hz, H-2), 3.31 (s, 3H, H-9), 2.21-2.09 (m, 6H, H-3, H-6, H-7), 1.18 (s, 9H, Si-C(CH₃)₃), 1.11 (d, 3H, *J* = 6.1 Hz, H-1); ¹³C NMR (125 MHz, C₆D₆) δ 172.7, 136.3, 136.2, 135.1, 134.9, 131.1, 129.9, 129.8, 128.3, 127.9, 127.9, 127.8, 69.9, 50.9, 43.0, 33.9, 28.2, 27.2, 23.0, 19.5; [α]_D²⁵ = -46.2 (c = 0.350, CHCl₃); HRMS (ES) *m/z* calculated for C₂₅H₃₄SiO₃Na 433.2169, found 433.2166 [M+Na]⁺.

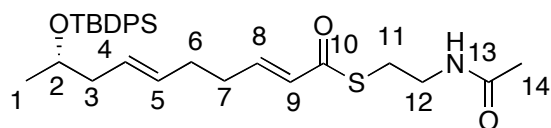
(*S, E*)-7-(*tert*-Butyldiphenylsilyloxy)oct-4-enal (162**)**



To a stirred solution of **161** (288 mg, 0.700 mmol) in 20 mL CH₂Cl₂ was added diisobutyl aluminum hydride (DIBAL) (1.0 M in CH₂Cl₂, 0.300 mL, 0.800 mmol) over 15 min at -78 °C under Ar. The reaction mixture was stirred for 1.5 h at -78 °C, and then 4 mL MeOH was added to quench the excess DIBAL. The solution was diluted with Et₂O, and 20 mL of saturated aqueous potassium sodium tartrate was added. The mixture was stirred until 2 clear layers had formed. The 2 layers

were separated and the organic layer was washed with brine (20 mL) and then dried over Na₂SO₄. The solvent was removed *in vacuo* and the residue was purified using flash column chromatography (1:20 Et₂O /hexanes) to give the product (230 mg, 86%) as a colorless oil. IR (CHCl₃, cast film) 3071, 2963, 2931, 2893, 2857, 2718, 1728, 1428 cm⁻¹; ¹H NMR (600 MHz, CDCl₃) δ 9.73 (t, 1H, *J* = 1.7 Hz, H-8), 7.67 (m, 4H, SiPh), 7.41 (m, 6H, SiPh), 5.37 (m, 2H, H-4, H-5), 3.86 (sextet, 1H, *J* = 5.9 Hz, H-2), 2.43 (td, 1H, *J* = 7.4, 1.7 Hz, H-7), 2.30 (dt, 2H, *J* = 6.9, 6.9 Hz, H-6), 2.15 (m, 2H, H-3), 1.19 (m, 12H, H-1, Si-C(CH₃)₃); ¹³C NMR (125 MHz, CDCl₃) δ 202.3, 135.9, 134.8, 134.6, 130.2, 129.5, 129.5, 128.1, 127.5, 127.4, 69.5, 43.4, 42.6, 27.1, 25.3, 23.0, 19.3; [α]_D²⁵ = -21.7 (c = 1.93, CHCl₃); HRMS (ES) *m/z* calculated for C₂₄H₃₂SiO₂Na 403.2064, found 403.2061 [M+Na]⁺.

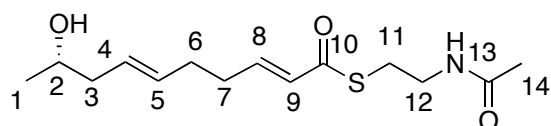
(*S*, 2*E*, 6*E*)-*S*-2-Acetamidoethyl 9-(*tert*-butyldiphenylsilyloxy)deca-2,6-dienethioate (163**)**



To a stirred solution of LiBr (126 mg, 1.46 mmol) in 8 mL dry THF was added **25** (173 mg, 0.580 mmol) under Ar. The solution was stirred for 10 min at 25 °C followed by addition of Et₃N (0.260 mL, 0.730 mmol). The solution was stirred for another 10 min, and then **162** (111 mg, 0.290 mmol) in 2 mL dry THF was added. The solution was stirred at 25 °C for 12 h. The reaction was quenched with saturated NH₄Cl (10 mL) and the mixture was extracted with EtOAc (3×10 mL).

The organic phase was washed with brine (20 mL) and dried over Na₂SO₄. The solvent was removed *in vacuo* and the residue was purified using flash column chromatography (2:1 EtOAc/hexanes) to give the product (80.0 mg, 52%) as a colorless oil. IR (CHCl₃, cast film) 3289, 3071, 2963, 2930, 2895, 2857, 1664, 1634, 1589, 1462, 1288 cm⁻¹; ¹H NMR (600 MHz, CDCl₃) δ 7.67 (m, 4H, SiPh), 7.41 (m, 6H, SiPh), 6.92 (dt, 1H, *J* = 15.5, 6.8 Hz, H-8), 6.13 (dt, 1H, *J* = 15.5, 1.5 Hz, H-9), 5.90 (s, 1H, NH), 5.40 (m, 2H, H-4, H-5), 3.87 (sextet, 1H, *J* = 5.8 Hz, H-2), 3.47 (dt, 2H, *J* = 6.2, 6.2 Hz, H-12), 3.10 (t, 2H, *J* = 6.3 Hz, H-11), 2.26-2.06 (m, 6H, H-3, H-6, H-7), 1.97 (s, 3H, H-14), 1.10 (m, 12H, H-1, Si-C(CH₃)₃); ¹³C NMR (100 MHz, CDCl₃) δ 190.3, 170.3, 145.9 (C-8), 136.0, 135.9, 134.8, 134.6, 130.6, 129.5, 129.4, 128.6, 128.1, 127.5, 127.4, 69.5, 42.6, 39.9, 32.1, 30.9, 28.3, 27.1, 23.3, 22.9, 19.3; [α]_D²⁵ = -20.9 (c = 0.900, CHCl₃); HRMS (ES) *m/z* calculated for C₃₀H₄₁NSiO₃SNa 546.2469, found 546.2462 [M+Na]⁺.

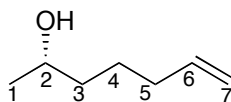
(*S*, 2*E*, 6*E*)-*S*-2-Acetamidoethyl 9-hydroxydeca-2,6-dienethioate(164**)**



To a stirred solution of **163** (59.0 mg, 0.110 mmol) was added 5 mL AcOH/H₂O/THF = 3:3:1 (v/v) solution. Then the solution was stirred at 45 °C for 48 h. The solvent was removed *in vacuo* and the residue was purified using flash column chromatography (10:1 EtOAc/MeOH) to give the product (20.0 mg, 69%) as a colorless oil. IR (CHCl₃, cast film) 3288, 3083, 2966, 2926, 2850, 1661, 1634, 1554, 1437, 1290 cm⁻¹; ¹H NMR (600 MHz, CDCl₃) δ 6.92 (dt, 1H, *J* =

15.5, 6.8 Hz, H-8), 6.13 (dt, 1H, $J = 15.5, 1.5$ Hz, H-9), 6.05 (s, 1H, NH), 5.50 (m, 2H, H-4, H-5), 3.85 (sextet, 1H, $J = 6.1$ Hz, H-2), 3.45 (dtd, 2H, $J = 6.1, 6.1, 2.2$ Hz, H-12), 3.10 (t, 2H, $J = 6.2$ Hz, H-11), 2.35-2.10 (m, 6H, H-3, H-6, H-7), 1.97 (s, 3H, H-14), 1.72 (s, 1H, OH), 1.19 (d, 3H, $J = 6.2$ Hz, H-1); ^{13}C NMR (125 MHz, CDCl_3) δ 190.2, 170.3, 145.6, 132.2, 128.9, 127.8, 67.2, 42.4, 39.6, 31.9, 31.0, 28.4, 23.2, 22.7; $[\alpha]_{\text{D}}^{25} = -8.80$ ($c = 0.200$, CHCl_3); HRMS (ES) m/z calculated for $\text{C}_{16}\text{H}_{27}\text{NSO}_4\text{Na}$ 308.1291 found 308.1288 $[\text{M}+\text{Na}]^+$.

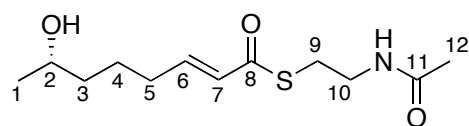
(S)-hept-6-en-2-ol (176)



The known compound was prepared according to literature procedure.²¹⁰ To a stirred solution of (*S*)-propylene oxide (1.00 g, 17.5 mmol) in dry THF (30 mL) was added Li_2CuCl_2 (0.1 M solution in THF, 17.3 mL, 1.73 mmol), followed by a solution of butenylmagnesium bromide (0.5 M solution in THF, 41.5 mL, 20.8 mmol) at $-30\text{ }^\circ\text{C}$ under Ar,. The reaction mixture was stirred for 30 min. The reaction was quenched by the addition of 10 mL saturated ammonium chloride. The layers were separated and the aqueous layer was extracted with Et_2O (3x40 mL). The combined organic layers were washed with brine (20 mL) and dried over Na_2SO_4 . The solvent was removed *in vacuo* to give the product (1.10 g, quant.) as light yellow oils. IR (CHCl_3 , cast film) 3359, 2921, 2851, 1659, 1634, cm^{-1} ; ^1H -NMR (500 MHz; CDCl_3): δ 5.79 (ddt, 1H $J = 17.0, 10.3, 6.7$ Hz, H-6), 4.99 (dq, 1H, $J = 17.1, 1.8$ Hz, H-7), 4.94 (ddt, 1H, $J = 10.2, 2.2, 1.1$ Hz, H-7),

3.81-3.75 (m, 1H, H-2), 2.08-2.02 (m, 2H, H-3), 1.54-1.37 (m, 4H, H-4, H-5), 1.20-1.16 (m, 3H, H-1); ^{13}C NMR (125 MHz, CDCl_3) δ 138.7, 114.6, 68.0, 38.7, 33.7, 25.1; $[\alpha]_{\text{D}}^{25} = 6.53$ ($c = 0.150$, CHCl_3); HRMS (ES) m/z calculated for $\text{C}_7\text{H}_{15}\text{O}$ 115.1117, found 115.1117 $[\text{M}+\text{H}]^+$.

(*S, E*)-*S*-2-Acetamidoethyl 7-hydroxyoct-2-enethioate (177**)**



The known compound¹⁸² was prepared as follows. To a stirred solution of **176** (148 mg, 0.59 mmol) in 5 mL dry CH_2Cl_2 was sequentially added Hoveyda-Grubbs II catalyst (14.0 mg, 23.0 μmol) and **122** (unlabeled, 80.0 mg, 0.46 mmol). The solution was heated to reflux for 12 h. The solvent was removed under vacuum, and the residue was purified by column chromatography on silica gel using EtOAc as eluent to afford the product as a colorless oil (110 mg, 91%). IR (CHCl_3 , cast film) 3289, 3081, 2929, 2860, 1660, 1632, 1435 cm^{-1} ; ^1H NMR (500 MHz, CDCl_3) δ 6.88 (dt, 1H, $J = 15.5$, 6.9 Hz, H-6), 6.10 (dt, 1H, $J = 15.5$, 1.5 Hz, NH), 3.78-3.76 (m, 1H, H-2), 3.40 (q, 2H, $J = 6.2$ Hz, H-10), 3.04 (t, 2H, $J = 6.5$ Hz, H-9), 2.20 (ddd, 2H, $J = 6.8$, 3.2, 1.6 Hz, H-3), 1.92 (s, 3H), 1.48-1.41 (m, 3H, H-12), 1.15 (t, 3H, $J = 5.5$ Hz, H-1); ^{13}C NMR (125 MHz, CDCl_3) δ 190.2, 170.4, 146.2, 128.5, 67.5, 39.7, 38.5, 32.1, 28.2, 24.1, 23.6, 23.1; $[\alpha]_{\text{D}}^{25} = 6.31$ ($c = 0.190$, CHCl_3); HRMS (ES) m/z calculated for $\text{C}_{12}\text{H}_{21}\text{NO}_3\text{SNa}$ 282.1134, found 282.1129 $[\text{M}+\text{Na}]^+$.

5.3 Biological procedures

5.3.1 Strain and general techniques for DNA manipulation

E. coli DH5 α (Invitrogen) was used for cloning following standard techniques. DNA restriction enzymes were purchased from Thermo Science and used as recommended by the manufacturer. PCR was performed using Platinum Taq High Fidelity DNA polymerase (Invitrogen) and PfuUltra II Fusion HS DNA polymerase (Agilent). *S. cerevisiae* strain BJ5464-NpgA (*MAT α ura3-52 his3- Δ 200 leu2- Δ 1 trp1 pep4::HIS3 prb1 Δ 1.6R can1 GAL*) was used for yeast homologous recombination and protein expression host.^{82, 211}

5.3.2 Isolation of *A. cinerariae* genomic DNA & total RNA, and the construction of cDNA library

The cultures of *A. cinerariae* ATCC 11784 was fermented in 500 mL potato dextrose broth (Difco, 6 g/L) at 26 °C and 165 rpm for 7 days in the dark. The cultures were filtered and the mycelium was flash frozen in liquid N₂ for 30 minutes. The protocol developed by Al-Samarrai²¹² was used to obtain the genomic DNA for Illumina sequencing (Ambry Genetics). RNeasy Plant Mini Kit (Qiagen) was used to obtain total RNA. SuperScript II Reverse Transcriptase (Invitrogen) and AccuScript High-Fidelity 1st Strand cDNA Synthesis Kit (Agilent) was used for constructions of the cDNA library GR-cDNA, GzzB1115-cDNA from *A. cinerariae* ATCC 11784, respectively.

5.3.4 Plasmid constructions

Table 5-1 Primers used for cloning

PCR products	Primer names	Primer sequences
<i>dhc3-1</i>	PKS4-fs5	CAT AGA CTA CGC GGA TAC C
	KOSESHP4yr3'	TCG TGA AGG CAT GTT TAA ACC TAG GAT GCA TGT CGA CTA TGA ATT CTT AGT GAT GGT GAT GGT GAT GTC TCT CCC CAT TTC CCA TTG TC
<i>dhc3-2</i>	KOSNP4yr5'	GCA TAC AAT CAA CTA TCA ACT ATT AAC TAT ATC GTA ATA CCA TAT GCC TTC TGC AAC TCC GTC G
	PKS4-rs8	TGGGCGGTCACTCTGATCC
<i>dhc5</i>	XKNP13yr5'	GCA TAC AAT CAA CTA TCA ACT ATT AAC TAT ATC GTA ATA CCA TAT GAA AAC CGG CCA TCG AAC AG
	XKPSHP13yr3'	CTT GAT AAT GAA AAC TAT AAA TCG TGA AGG CAT CGG TCC GCA CGT GTC AGT GAT GGT GAT GGT GAT GTC CCT TGA TAT AGG CAA ATG CCT TC
<i>dhc3</i>	PKS4-N5'	ATA TCA TAT GAT GCC TTC TGC AAC TCC GTC GC
	PKS4-H6ES3'	TATAGAATTCTTAGTGGTGGTGGTGGTGGTGTCT CTCCCCATTTCCTTTCATTGTCACC
<i>dhc5</i>	PKS13-N5'	ATA ACA TAT GAA AAC CGG CCA TCG AAC AGT TCT TC
	PKS13-H6SP3'	TGCTCACGTGTCAGTGGTGGTGGTGGTGGTGTCC CTTGATATAGGCAAATGCCTTCTCC
linearized pGR-1	fsPKS4-PKOS20	GAA AAG ATT GCG GAG AAG AGC
	rsPKS4-PKOS120	CAT GCT AGG CCA ACG ACT
linearized pGR-2	fsPKS13-PXK30	CATGTGCACTTGCTTCATGC
	rsPKS13-PXK30	GTCTCCAAAGAGAAGAACTGTTC
<i>dhc5-p1</i>	PKS13-Exon1-fs	ATGAAAACCGGCCATCGAAC
	PKS13-rs12	ACATCAGCGTTCCTTTCCTTCG
<i>dhc5-p2</i>	PKS13-Exon5-fs	GCGGCAACGCATGCCTATTAC
	PKS13-Exon5-rs	TCCCTTGATATAGGCAAATGC
<i>dhc5</i>	KOS5'	CGA TAC AAT CAA CTA TCA ACT ATT AAC TAT ATC
	XK3'	CTT GAT AAT GAA AAC TAT AAA TCG TGA AGG
<i>dhc5-his</i>	Vectore-pks13-fs	GCTACAAAAAGCATACAATCAAC

	Vectore-pks13- rs	GATAATGAAAAC TATAAATCGTGAAGGCATCGG TCCGCACGTGTCATCCCTTGATATAGGCAAATGC
--	----------------------	--

The *N*-terminal hexahistidine-tagged Dhc3-expression plasmid pGR1 was constructed based on pKOS518-120A. Primers KOSHSHP4yr3' & PKS4-F5 and KOSNP4yr5' & PKS4-RS8 were used to amplify *dhc3-p1* and *dhc3-p2*, respectively, from GR-cDNA. Plasmid pKOS518-120A was digested with *NheI* and *EcoRI*, and the resulting linear vector was co-transformed with *dhc3-p1* and *dhc3-p2* into BJ5464-NpgA using an *S. c.* EasyCompTM Transformation Kit (Invitrogen). After 3 days, a single colony was inoculated in 3 mL SDCt (A, U) [0.5 g Bacto Technical Grade Casamino Acids, 2 g dextrose, and 88 mL Milli-Q water, autoclaved and then supplemented with 10 mL nitrogen base (1.7 g Nitrogen Base without amino acids, 5 g ammonium sulfate and 100 mL Milli-Q water, filtered through 0.2 µ filter), 1 mL adenine (40 mg/20 mL Milli-Q water, filtered through 0.2 µ filter) and 1 mL uracil (40 mg/20 mL Milli-Q water, filtered through 0.2 µ filter)] at 30 °C for 12 h, and plasmid pGR1 was isolated using ZymoprepTM Yeast Plasmid Miniprep kit (Cedarlane). The resulting plasmid was transformed to DH5α for replication to get sufficient amount of plasmid for DNA sequencing (BigDye Terminator v3.1 Cycle Sequencing) to confirm the sequence of the insert.

The *N*-terminal hexahistidine-tagged Dhc5-expression plasmid pGR2 was constructed based on pXK30. Primers XKNP13yr5' and XKNPSHP13yr3' were used to amplify *dhc5* from GR-cDNA. Plasmid pXK30 was digested with *NheI*

and *PmlI*, and the resulting linear vector was co-transformed with *dhc5* into BJ5464-NpgA using an *S. c.* EasyCompTM Transformation kit. After 3 days, a single colony was inoculated in 3 mL SDCt (A, T) [0.5 g Bacto Technical Grade Casamino Acids, 2 g dextrose, and 88 mL Milli-Q water, autoclaved and then supplemented with 10 mL nitrogen base (1.7 g Nitrogen Base without amino acids, 5 g ammonium sulfate and 100 mL Milli-Q water, filtered through 0.2 µ filter), 1 mL adenine (40 mg/20 mL Milli-Q water, filtered through 0.2 µ filter) and 1 mL tryptophan (40 mg/20 mL Milli-Q water, filtered through 0.2 µ filter)] at 30 °C for 12 h, and plasmid pGR2 was isolated using ZymoprepTM Yeast Plasmid Miniprep kit. The resulting plasmid was transformed to DH5α for replication to get sufficient amount of plasmid for DNA sequencing to confirm the sequence of the insert.

The *N*-terminal hexahistidine-tagged Dhc3-expression vector pGzzB221 was constructed based on pGR1. Primers PKS4-H6ES3' and PKS4-N5' were used to amplify *dhc3* from GzzB1115-cDNA. Primers fsPKS4PKOS120 and rsPKS4PKOS120 were used to amplify the linear vector from pGR1. The resulting linear vector was co-transformed with *dhc3* into BJ5464-NpgA using an *S. c.* EasyCompTM Transformation kit. After 3 days, a single colony was inoculated in 3 mL SDCt (A, U) at 30 °C for 12 h, and plasmid pGzzB221 was isolated using ZymoprepTM Yeast Plasmid Miniprep kit. The resulting plasmid was transformed to DH5α to get sufficient plasmid for DNA sequencing to confirm the sequence of the insert.

The *N*-terminal hexahistidine-tagged Dhc5-expression vector pGzzB237-8 was constructed based on pGR2. Primers PKS13-H6ES3' and PKS13-N5' were used to amplify *dhc5* from GzzB1115-cDNA. Primers fsPKS13PXX and rsPKS13PXX were used to amplify the linear vector from pGR2. The resulting linear vector was co-transformed with *dhc3* into BJ5464-NpgA using an *S. c.* EasyCompTM Transformation kit (Invitrogen). After 3 days, a single colony was incubated in 3 mL SDCt (A, T) at 30 °C for 12 h, and plasmid pGzzB237-8 was isolated using ZymoprepTM Yeast Plasmid Miniprep kit. The resulting plasmid was transformed to DH5α for replication to get sufficient amount of plasmid for DNA sequencing to confirm the sequence of the insert.

The *N*-terminal hexahistidine-tagged Dhc5-expression vectors pGzzB255 and pGzzB257 were constructed based on pXK30. Primers XK3' and KOS5' were used to amplify *dhc5* from pGzzB237-8. Plasmid pXK30 was digested with *NheI* and *PmlI*, and the resulting linear vector was co-transformed with *dhc5* into BJ5464-NpgA using an *S. c.* EasyCompTM Transformation kit. After 3 days, two colonies were individually inoculated in 3 mL SDCt (A, T) at 30 °C for 12 h, and plasmids pGzzB255 and pGzzB257 were isolated using ZymoprepTM Yeast Plasmid Miniprep kit. These resulting plasmids were transformed to DH5α for replication to get sufficient amount of plasmid for DNA sequencing to confirm the sequence of the insert.

The *N*-terminal hexahistidine-tagged Dhc5-expression vectors pGzzB255 and pGzzB257 were constructed based on pXK30. Primers XK3' and KOS5' were used to amplify *dhc5* from pGzzB237-8. Plasmid pXK30 was digested with

NheI and *PmlI*, and the resulting linear vector was co-transformed with *dhc5* into BJ5464-NpgA using an *S. c.* EasyComp™ Transformation kit. After 3 days, two colonies were individually inoculated in 3 mL SDCt (A, T) at 30 °C for 12 h, and plasmids pGzzB255 and pGzzB257 were isolated using Zymoprep™ Yeast Plasmid Miniprep kit. These resulting plasmids were transformed to DH5α for replication to get sufficient amount of plasmid for DNA sequencing to confirm the sequence of the insert.

Dhc5-expression vector pGzzB255-ΔHis was constructed based on pXK30. Primers Vector-PKS13-fs and Vector-PKS13-rs were used to amplify *dhc5* from pGzzB237-8. Plasmid pXK30 was digested with *NheI* and *PmlI*, and the resulting linear vector was co-transformed with *dhc5* into BJ5464-NpgA using an *S. c.* EasyComp™ Transformation kit. After 3 days, a single colony was inoculated in 3 mL SDCt (A, T) at 30 °C for 12 h, and plasmid pGzzB255-ΔHis was isolated using Zymoprep™ Yeast Plasmid Miniprep kit. The resulting plasmid was transformed to DH5α for replication to get sufficient amount of plasmid for DNA sequencing to confirm the sequence of the insert.

5.3.5 Protein Expression

N-terminal hexahistidine-tagged Dhc3 and Dhc5 were expressed and purified from *S. cerevisiae* strain BJ5464-NpgA harboring plasmids pGzzB221 and pGzzB255. Plasmids pGzzB221 and pGzzB255 were individually transformed into BJ5464-NpgA using an *S. c.* EasyComp™ Transformation kit. After 3 days, a single colony was picked from a SDCt (A, T) or SDCt (A, U) plate and inoculated in 3 mL SDCt (A, T) or SDCt (A, U) at 28 °C for 72 h. A 1 mL

aliquot of the seed culture was used to inoculate 1 L of YPD (10 g Bacto Yeast extract, 20 g Bacto Peptone and 950 mL Milli-Q water) supplemented with 50 mL 20% dextrose and the culture was shaken at 28 °C for 72 hours. The cells were harvested by centrifugation (4000 g at 4 °C for 15 min) and the cell pellet was resuspended in 25 mL lysis buffer (50 mM NaH₂PO₄, pH 8.0, 0.15 M NaCl, 10 mM imidazole) and lysed with sonication on ice (sonicate for 1 minute, then cool for 1 minute. Repeat 9 - 10 times). Cellular debris was removed by centrifugation (15000 g, 1 hour, 4 °C). Ni-NTA agarose resin was added to the supernatant (2 mL resin/1 L of cell culture) and the solution was stirred at 4 °C for 12 h. The protein/resin mixture was loaded into a gravity flow column and first eluted with 20 mL of Buffer A (50 mM Tris-HCl, pH 7.9, 2 mM EDTA, 2 mM DTT) with 10 mM imidazole. The second elution contained 20 mL of Buffer A with 20 mM imidazole, and the final elution contained 16 mL of Buffer A with 250 mM of imidazole. Purified proteins were concentrated using Amico protein concentrator (100 000 MWCO), which were pre-chilled on ice. The retentate was centrifuged at 4000 g at 4 °C for 45 min until it was under 1 mL. The buffers were exchanged by the addition of 14 mL of Buffer A with 2 mM of imidazole and centrifuged at 3570 g at 4 °C for 45 min until the retentate was less than 1 mL. The aliquots were stored at -80 °C.

Chapter 6: References

1. Staunton, J.; Weissman, K. J., Polyketide biosynthesis: a millennium review. *Nat. Prod. Rep.* **2001**, *18*, 380-416.
2. Hertweck, C., The biosynthetic logic of polyketide diversity. *Angew. Chem., Int. Ed. Engl.* **2009**, *48*, 4688-4716.
3. Weissman, K. J.; Leadlay, P. F., Combinatorial biosynthesis of reduced polyketides. *Nat. Rev. Microbiol.* **2005**, *3*, 925-936.
4. Li, J. W.; Vederas, J. C., Drug discovery and natural products: end of an era or an endless frontier? *Science* **2009**, *325*, 161-165.
5. Zhu, G.; LaGier, M. J.; Stejskal, F.; Millership, J. J.; Cai, X.; Keithly, J. S., *Cryptosporidium parvum*: the first protist known to encode a putative polyketide synthase. *Gene* **2002**, *298*, 79-89.
6. Collie, J. N., Derivatives of the multiple ketene group. *Proc. Chem. Soc.* **1907**, *23*, 230-231.
7. Collie, J. N., Derivatives of the multiple ketene group. *J. Chem. Soc., Trans.* **1907**, *91*, 1806-1813.
8. Collie, J. N.; Myers, W. S., The formation of orcinol and other condensation products from dehydracetic acid. *J. Chem. Soc., Trans.* **1893**, *63*, 122-128.
9. Bentley, R., John Norman Collie: Chemist and mountaineer. *J. Chem. Educ.* **1999**, *76*, 41-47.

10. Birch, A. J.; Massywestropp, R. A.; Moye, C. J., Studies in relation to biosynthesis VII. 2-hydroxy-6-methylbenzoic acid in *Penicillium griseofulvum* dierckx. *Aust. J. Chem.* **1955**, *8*, 539-544.
11. Rawlings, B. J., Biosynthesis of polyketides. *Nat. Prod. Rep.* **1997**, *14*, 523-556.
12. Rawlings, B. J., Biosynthesis of polyketides (other than actinomycete macrolides). *Nat. Prod. Rep.* **1999**, *16*, 425-484.
13. Smith, S.; Tsai, S. C., The type I fatty acid and polyketide synthases: a tale of two megasynthases. *Nat. Prod. Rep.* **2007**, *24*, 1041-1072.
14. Elovson, J.; Vagelos, P. R., Acyl carrier protein. X. Acyl carrier protein synthetase. *J. Biol. Chem.* **1968**, *243*, 3603-3611.
15. Majerus, P. W.; Alberts, A. W.; Vagelos, P. R., The acyl carrier protein of fatty acid synthesis: purification, physical properties, and substrate binding site. *Proc. Natl. Acad. Sci. U. S. A.* **1964**, *51*, 1231-1238.
16. Sauer, F.; Pugh, E. L.; Wakil, S. J.; Delaney, R.; Hill, R. L., 2-Mercaptoethylamine and beta-alanine as components of acyl carrier protein. *Proc. Natl. Acad. Sci. U. S. A.* **1964**, *52*, 1360-1366.
17. Chirala, S. S.; Jayakumar, A.; Gu, Z. W.; Wakil, S. J., Human fatty acid synthase: role of interdomain in the formation of catalytically active synthase dimer. *Proc. Natl. Acad. Sci. U. S. A.* **2001**, *98*, 3104-3108.
18. Soulie, J. M.; Sheplock, G. J.; Tian, W. X.; Hsu, R. Y., Transient kinetic studies of fatty acid synthetase. A kinetic self-editing mechanism for the

- loading of acetyl and malonyl residues and the role of coenzyme A. *J. Biol. Chem.* **1984**, *259*, 134-140.
19. Stern, A.; Sedgwick, B.; Smith, S., The free coenzyme A requirement of animal fatty acid synthetase. Participation in the continuous exchange of acetyl and malonyl moieties between coenzyme a thioester and enzyme. *J. Biol. Chem.* **1982**, *257*, 799-803.
 20. Heath, R. J.; Rock, C. O., The Claisen condensation in biology. *Nat. Prod. Rep.* **2002**, *19*, 581-596.
 21. Hopwood, D. A., Genetic contributions to understanding polyketide synthases. *Chem. Rev.* **1997**, *97*, 2465-2498.
 22. Marsden, A. F.; Caffrey, P.; Aparicio, J. F.; Loughran, M. S.; Staunton, J.; Leadlay, P. F., Stereospecific acyl transfers on the erythromycin-producing polyketide synthase. *Science* **1994**, *263*, 378-380.
 23. Cox, R. J., Polyketides, proteins and genes in fungi: programmed nano-machines begin to reveal their secrets. *Org. Biomol. Chem.* **2007**, *5*, 2010-2026.
 24. Rawlings, B. J., Type I polyketide biosynthesis in bacteria (part B). *Nat. Prod. Rep.* **2001**, *18*, 231-281.
 25. Cortes, J.; Haydock, S. F.; Roberts, G. A.; Bevitt, D. J.; Leadlay, P. F., An unusually large multifunctional polypeptide in the erythromycin-producing polyketide synthase of *Saccharopolyspora erythraea*. *Nature* **1990**, *348*, 176-178.

26. Donadio, S.; Staver, M. J.; McAlpine, J. B.; Swanson, S. J.; Katz, L., Modular organization of genes required for complex polyketide biosynthesis. *Science* **1991**, *252*, 675-679.
27. Donadio, S.; Katz, L., Organization of the enzymatic domains in the multifunctional polyketide synthase involved in erythromycin formation in *Saccharopolyspora erythraea*. *Gene* **1992**, *111*, 51-60.
28. Bevitt, D. J.; Cortes, J.; Haydock, S. F.; Leadlay, P. F., 6-Deoxyerythronolide-B synthase 2 from *Saccharopolyspora erythraea*. Cloning of the structural gene, sequence analysis and inferred domain structure of the multifunctional enzyme. *Eur. J. Biochem.* **1992**, *204*, 39-49.
29. Cane, D. E.; Liang, T. C.; Taylor, P. B.; Chang, C.; Yang, C. C., Macrolide biosynthesis .3. stereochemistry of the chain-elongation steps of erythromycin biosynthesis. *J. Am. Chem. Soc.* **1986**, *108*, 4957-4964.
30. Weissman, K. J.; Timoney, M.; Bycroft, M.; Grice, P.; Hanefeld, U.; Staunton, J.; Leadlay, P. F., The molecular basis of Celmer's rules: the stereochemistry of the condensation step in chain extension on the erythromycin polyketide synthase. *Biochemistry* **1997**, *36*, 13849-13855.
31. Valenzano, C. R.; Lawson, R. J.; Chen, A. Y.; Khosla, C.; Cane, D. E., The biochemical basis for stereochemical control in polyketide biosynthesis. *J. Am. Chem. Soc.* **2009**, *131*, 18501-18511.

32. You, Y. O.; Khosla, C.; Cane, D. E., Stereochemistry of reductions catalyzed by methyl-epimerizing ketoreductase domains of polyketide synthases. *J. Am. Chem. Soc.* **2013**, *135*, 7406-7409.
33. Reid, R.; Piagentini, M.; Rodriguez, E.; Ashley, G.; Viswanathan, N.; Carney, J.; Santi, D. V.; Hutchinson, C. R.; McDaniel, R., A model of structure and catalysis for ketoreductase domains in modular polyketide synthases. *Biochemistry* **2003**, *42*, 72-79.
34. Caffrey, P., Conserved amino acid residues correlating with ketoreductase stereospecificity in modular polyketide synthases. *ChemBioChem* **2003**, *4*, 654-657.
35. Tsai, S. C.; Miercke, L. J.; Krucinski, J.; Gokhale, R.; Chen, J. C.; Foster, P. G.; Cane, D. E.; Khosla, C.; Stroud, R. M., Crystal structure of the macrocycle-forming thioesterase domain of the erythromycin polyketide synthase: versatility from a unique substrate channel. *Proc. Natl. Acad. Sci. U. S. A.* **2001**, *98*, 14808-14813.
36. Piel, J., Biosynthesis of polyketides by trans-AT polyketide synthases. *Nat. Prod. Rep.* **2010**, *27*, 996-1047.
37. Moss, S. J.; Martin, C. J.; Wilkinson, B., Loss of co-linearity by modular polyketide synthases: a mechanism for the evolution of chemical diversity. *Nat. Prod. Rep.* **2004**, *21*, 575-593.
38. Wilkinson, B.; Foster, G.; Rudd, B. A.; Taylor, N. L.; Blackaby, A. P.; Sidebottom, P. J.; Cooper, D. J.; Dawson, M. J.; Buss, A. D.; Gaisser, S.; Bohm, I. U.; Rowe, C. J.; Cortes, J.; Leadlay, P. F.; Staunton, J., Novel

- octaketide macrolides related to 6-deoxyerythronolide B provide evidence for iterative operation of the erythromycin polyketide synthase. *Chem. Biol.* **2000**, *7*, 111-117.
39. Reeves, C. D.; Hu, Z.; Reid, R.; Kealey, J. T., Genes for the biosynthesis of the fungal polyketides hypothemycin from *Hypomyces subiculosus* and radicicol from *Pochonia chlamydosporia*. *Appl. Environ. Microbiol.* **2008**, *74*, 5121-5129.
 40. Zhou, H.; Qiao, K.; Gao, Z.; Vederas, J. C.; Tang, Y., Insights into radicicol biosynthesis via heterologous synthesis of intermediates and analogs. *J. Biol. Chem.* **2010**, *285*, 41412-41421.
 41. Zhou, H.; Qiao, K.; Gao, Z.; Meehan, M. J.; Li, J. W.; Zhao, X.; Dorrestein, P. C.; Vederas, J. C.; Tang, Y., Enzymatic synthesis of resorcylic acid lactones by cooperation of fungal iterative polyketide synthases involved in hypothemycin biosynthesis. *J. Am. Chem. Soc.* **2010**, *132*, 4530-4531.
 42. Scott, A. I.; Beadling, L. C.; Georgopa, N. H.; Subbaray, C. R., Biosynthesis of polyketides. Purification and inhibition studies of 6-methylsalicylic acid synthase. *Bioorg. Chem.* **1974**, *3*, 238-248.
 43. Beck, J.; Ripka, S.; Siegner, A.; Schiltz, E.; Schweizer, E., The multifunctional 6-methylsalicylic acid synthase gene of *Penicillium patulum* - its gene structure relative to that of other polyketide synthases. *Eur. J. Biochem.* **1990**, *192*, 487-498.

44. Spencer, J. B.; Jordan, P. M., Purification and properties of 6-methylsalicylic acid synthase from *Penicillium patulum*. *Biochem. J.* **1992**, 288, 839-846.
45. Kannanga, C. G.; Hennings, K. W.; Stumpf, P. K.; von Wettstein, D., 6-Methylsalicylic acid synthesis by isolated barley chloroplasts. *Eur. J. Biochem.* **1971**, 21, 334-338.
46. Dimroth, P.; Walter, H.; Lynen, F., Biosynthesis of 6-methylsalicylic acid. *Eur. J. Biochem.* **1970**, 13, 98-&.
47. Moriguchi, T.; Kezuka, Y.; Nonaka, T.; Ebizuka, Y.; Fujii, I., Hidden function of catalytic domain in 6-methylsalicylic acid synthase for product release. *J. Biol. Chem.* **2010**, 285, 15637-15643.
48. Maier, T.; Leibundgut, M.; Ban, N., The crystal structure of a mammalian fatty acid synthase. *Science* **2008**, 321, 1315-1322.
49. Keatinge-Clay, A. T., The structures of type I polyketide synthases. *Nat. Prod. Rep.* **2012**, 29, 1050-1073.
50. Ma, S. M.; Tang, Y., Biochemical characterization of the minimal polyketide synthase domains in the lovastatin nonaketide synthase LovB. *FEBS J.* **2007**, 274, 2854-2864.
51. Fisch, K. M.; Bakeer, W.; Yakasai, A. A.; Song, Z.; Pedrick, J.; Wasil, Z.; Bailey, A. M.; Lazarus, C. M.; Simpson, T. J.; Cox, R. J., Rational domain swaps decipher programming in fungal highly reducing polyketide synthases and resurrect an extinct metabolite. *J. Am. Chem. Soc.* **2011**, 133, 16635-16641.

52. McInnes, A. G.; Smith, D. G.; Wat, C. K.; Vining, L. C.; Wright, J. L. C., Tenellin and bassianin, metabolites of *Beauveria* species. Structure elucidation with N-15-enriched and doubly C-13-enriched compounds using C-13 nuclear magnetic-resonance spectroscopy. *J. Chem. Soc., Chem. Commun.* **1974**, 281-282.
53. Heneghan, M. N.; Yakasai, A. A.; Williams, K.; Kadir, K. A.; Wasil, Z.; Bakeer, W.; Fisch, K. M.; Bailey, A. M.; Simpson, T. J.; Cox, R. J.; Lazarus, C. M., The programming role of trans-acting enoyl reductases during the biosynthesis of highly reduced fungal polyketides. *Chemical Science* **2011**, 2, 972-979.
54. Ma, S. M.; Li, J. W.; Choi, J. W.; Zhou, H.; Lee, K. K.; Moorthie, V. A.; Xie, X.; Kealey, J. T.; Da Silva, N. A.; Vederas, J. C.; Tang, Y., Complete reconstitution of a highly reducing iterative polyketide synthase. *Science* **2009**, 326, 589-592.
55. Zhou, H.; Gao, Z.; Qiao, K.; Wang, J.; Vederas, J. C.; Tang, Y., A fungal ketoreductase domain that displays substrate-dependent stereospecificity. *Nat. Chem. Biol.* **2012**, 8, 331-333.
56. Udvary, D. W.; Merski, M.; Townsend, C. A., A method for prediction of the locations of linker regions within large multifunctional proteins, and application to a type I polyketide synthase. *J. Mol. Biol.* **2002**, 323, 585-598.
57. Crawford, J. M.; Dancy, B. C.; Hill, E. A.; Udvary, D. W.; Townsend, C. A., Identification of a starter unit acyl-carrier protein transacylase domain

- in an iterative type I polyketide synthase. *Proc. Natl. Acad. Sci. U. S. A.* **2006**, *103*, 16728-16733.
58. Crawford, J. M.; Thomas, P. M.; Scheerer, J. R.; Vagstad, A. L.; Kelleher, N. L.; Townsend, C. A., Deconstruction of iterative multidomain polyketide synthase function. *Science* **2008**, *320*, 243-246.
59. Crawford, J. M.; Korman, T. P.; Labonte, J. W.; Vagstad, A. L.; Hill, E. A.; Kamari-Bidkorpeh, O.; Tsai, S. C.; Townsend, C. A., Structural basis for biosynthetic programming of fungal aromatic polyketide cyclization. *Nature* **2009**, *461*, 1139-1143.
60. Chooi, Y. H.; Tang, Y., Navigating the fungal polyketide chemical space: from genes to molecules. *J. Org. Chem.* **2012**, *77*, 9933-9953.
61. Crawford, J. M.; Vagstad, A. L.; Whitworth, K. P.; Ehrlich, K. C.; Townsend, C. A., Synthetic strategy of nonreducing iterative polyketide synthases and the origin of the classical "starter-unit effect". *ChemBioChem* **2008**, *9*, 1019-1023.
62. Ma, S. M.; Zhan, J.; Watanabe, K.; Xie, X.; Zhang, W.; Wang, C. C.; Tang, Y., Enzymatic synthesis of aromatic polyketides using PKS4 from *Gibberella fujikuroi*. *J. Am. Chem. Soc.* **2007**, *129*, 10642-10643.
63. Zhang, W.; Li, Y.; Tang, Y., Engineered biosynthesis of bacterial aromatic polyketides in *Escherichia coli*. *Proc. Natl. Acad. Sci. U. S. A.* **2008**, *105*, 20683-20688.

64. Hertweck, C.; Luzhetskyy, A.; Rebets, Y.; Bechthold, A., Type II polyketide synthases: gaining a deeper insight into enzymatic teamwork. *Nat. Prod. Rep.* **2007**, *24*, 162-190.
65. McDaniel, R.; Ebertkhosla, S.; Hopwood, D. A.; Khosla, C., Engineered biosynthesis of novel polyketides. *Science* **1993**, *262*, 1546-1550.
66. Bisang, C.; Long, P. F.; Cortes, J.; Westcott, J.; Crosby, J.; Matharu, A. L.; Cox, R. J.; Simpson, T. J.; Staunton, J.; Leadlay, P. F., A chain initiation factor common to both modular and aromatic polyketide synthases. *Nature* **1999**, *401*, 502-505.
67. Abe, I.; Morita, H., Structure and function of the chalcone synthase superfamily of plant type III polyketide synthases. *Nat. Prod. Rep.* **2010**, *27*, 809-838.
68. Yu, D.; Xu, F.; Zeng, J.; Zhan, J., Type III polyketide synthases in natural product biosynthesis. *IUBMB Life* **2012**, *64*, 285-295.
69. Jez, J. M.; Ferrer, J. L.; Bowman, M. E.; Austin, M. B.; Schroder, J.; Dixon, R. A.; Noel, J. P., Structure and mechanism of chalcone synthase-like polyketide synthases. *J. Ind. Microbiol. Biotechnol.* **2001**, *27*, 393-398.
70. Austin, M. B.; Bowman, M. E.; Ferrer, J. L.; Schroder, J.; Noel, J. P., An aldol switch discovered in stilbene synthases mediates cyclization specificity of type III polyketide synthases. *Chem. Biol.* **2004**, *11*, 1179-1194.

71. Nair, M. S. R.; Carey, S. T., Metabolites of pyrenomycetes .13. structure of (+) hypothemycin, an antibiotic macrolide from *Hypomyces trichothecoides*. *Tetrahedron Lett.* **1980**, *21*, 2011-2012.
72. Agatsuma, T.; Takahashi, A.; Kabuto, C.; Nozoe, S., Revised structure and stereochemistry of hypothemycin. *Chem. Pharm. Bull.* **1993**, *41*, 373-375.
73. Selles, P.; Lett, R., Convergent stereospecific synthesis of C292 (or LL-Z1640-2), and hypothemycin. Part 1. *Tetrahedron Lett.* **2002**, *43*, 4621-4625.
74. Dakas, P.-Y.; Jogireddy, R.; Valot, G.; Barluenga, S.; Winssinger, N., Divergent syntheses of resorcylic acid lactones: L-783277, LL-Z1640-2, and hypothemycin. *Chem.-Eur. J.* **2009**, *15*, 11490-11497.
75. Isaka, M.; Suyarnsestakorn, C.; Tanticharoen, M.; Kongsaree, P.; Thebtaranonth, Y., Aigialomycins A-E, new resorcylic macrolides from the marine mangrove fungus *Aigialus parvus*. *J. Org. Chem.* **2002**, *67*, 1561-1566.
76. Williams, D. H.; Wilkinson, S. E.; Purton, T.; Lamont, A.; Flotow, H.; Murray, E. J., Ro 09-2210 exhibits potent anti-proliferative effects on activated T cells by selectively blocking MKK activity. *Biochemistry* **1998**, *37*, 9579-9585.
77. Camacho, R.; Staruch, M. J.; DaSilva, C.; Koprak, S.; Sewell, T.; Salituro, G.; Dumont, F. J., Hypothemycin inhibits the proliferative response and

modulates the production of cytokines during T cell activation. *Immunopharmacology* **1999**, *44*, 255-265.

78. Tanaka, H.; Nishida, K.; Sugita, K.; Yoshioka, T., Antitumor efficacy of hypothemycin, a new Ras-signaling inhibitor. *Jpn. J. Cancer Res.* **1999**, *90*, 1139-1145.
79. Zhao, A.; Lee, S. H.; Mojena, M.; Jenkins, R. G.; Patrick, D. R.; Huber, H. E.; Goetz, M. A.; Hensens, O. D.; Zink, D. L.; Vilella, D.; Dombrowski, A. W.; Lingham, R. B.; Huang, L., Resorcylic acid lactones: naturally occurring potent and selective inhibitors of MEK. *J. Antibiot.* **1999**, *52*, 1086-1094.
80. Schirmer, A.; Kennedy, J.; Murli, S.; Reid, R.; Santi, D. V., Targeted covalent inactivation of protein kinases by resorcylic acid lactone polyketides. *Proc. Natl. Acad. Sci. U. S. A.* **2006**, *103*, 4234-4239.
81. Rastelli, G.; Rosenfeld, R.; Reid, R.; Santi, D. V., Molecular modeling and crystal structure of ERK2-hypothemycin complexes. *J. Struct. Biol.* **2008**, *164*, 18-23.
82. Lee, K. K.; Da Silva, N. A.; Kealey, J. T., Determination of the extent of phosphopantetheinylation of polyketide synthases expressed in *Escherichia coli* and *Saccharomyces cerevisiae*. *Anal. Biochem.* **2009**, *394*, 75-80.
83. Mootz, H. D.; Schorgendorfer, K.; Marahiel, M. A., Functional characterization of 4'-phosphopantetheinyl transferase genes of bacterial

- and fungal origin by complementation of *Saccharomyces cerevisiae* lys5. *FEMS Microbiol. Lett.* **2002**, *213*, 51-57.
84. Yue, S.; Duncan, J. S.; Yamamoto, Y.; Hutchinson, C. R., Macrolide biosynthesis - ty lactone formation involves the processive addition of 3 carbon units. *J. Am. Chem. Soc.* **1987**, *109*, 1253-1255.
 85. Rathke, M. W.; Nowak, M., The Horner-Wadsworth-Emmons modification of the Wittig reaction using triethylamine and lithium or magnesium salts. *J. Org. Chem.* **1985**, *50*, 2624-2626.
 86. Corey, E. J.; Venkates.A, Protection of hydroxyl groups as tert-butyldimethylsilyl derivatives. *J. Am. Chem. Soc.* **1972**, *94*, 6190-&.
 87. Vulpetti, A.; Gardner, M.; Gennari, C.; Bernardi, A.; Goodman, J. M.; Paterson, I., Origins of stereoselectivity in the addition of chiral allylboranes and crotylboranes to aldehydes - the development and application of a force-field model of the transition-state. *J. Org. Chem.* **1993**, *58*, 1711-1718.
 88. Zhou, H.; Zhan, J.; Watanabe, K.; Xie, X.; Tang, Y., A polyketide macrolactone synthase from the filamentous fungus *Gibberella zeae*. *Proc. Natl. Acad. Sci. U. S. A.* **2008**, *105*, 6249-6254.
 89. Liu, T.; Chiang, Y. M.; Somoza, A. D.; Oakley, B. R.; Wang, C. C., Engineering of an "unnatural" natural product by swapping polyketide synthase domains in *Aspergillus nidulans*. *J. Am. Chem. Soc.* **2011**, *133*, 13314-13316.

90. Zheng, J.; Taylor, C. A.; Piasecki, S. K.; Keatinge-Clay, A. T., Structural and functional analysis of A-type ketoreductases from the amphotericin modular polyketide synthase. *Structure* **2010**, *18*, 913-922.
91. Castonguay, R.; Valenzano, C. R.; Chen, A. Y.; Keatinge-Clay, A.; Khosla, C.; Cane, D. E., Stereospecificity of ketoreductase domains 1 and 2 of the tylactone modular polyketide synthase. *J. Am. Chem. Soc.* **2008**, *130*, 11598-11599.
92. Keatinge-Clay, A. T., A tylosin ketoreductase reveals how chirality is determined in polyketides. *Chem. Biol.* **2007**, *14*, 898-908.
93. Castonguay, R.; He, W.; Chen, A. Y.; Khosla, C.; Cane, D. E., Stereospecificity of ketoreductase domains of the 6-deoxyerythronolide B synthase. *J. Am. Chem. Soc.* **2007**, *129*, 13758-13769.
94. O'Hare, H. M.; Baerga-Ortiz, A.; Popovic, B.; Spencer, J. B.; Leadlay, P. F., High-throughput mutagenesis to evaluate models of stereochemical control in ketoreductase domains from the erythromycin polyketide synthase. *Chem. Biol.* **2006**, *13*, 287-296.
95. Keatinge-Clay, A. T.; Stroud, R. M., The structure of a ketoreductase determines the organization of the beta-carbon processing enzymes of modular polyketide synthases. *Structure* **2006**, *14*, 737-748.
96. Baerga-Ortiz, A.; Popovic, B.; Siskos, A. P.; O'Hare, H. M.; Spiteller, D.; Williams, M. G.; Campillo, N.; Spencer, J. B.; Leadlay, P. F., Directed mutagenesis alters the stereochemistry of catalysis by isolated

- ketoreductase domains from the erythromycin polyketide synthase. *Chem. Biol.* **2006**, *13*, 277-285.
97. Siskos, A. P.; Baerga-Ortiz, A.; Bali, S.; Stein, V.; Mamdani, H.; Spiteller, D.; Popovic, B.; Spencer, J. B.; Staunton, J.; Weissman, K. J.; Leadlay, P. F., Molecular basis of Celmer's rules: Stereochemistry of catalysis by isolated ketoreductase domains from modular polyketide synthases. *Chem. Biol.* **2005**, *12*, 1145-1153.
 98. Hyatt, J. A.; Feldman, P. L.; Clemens, R. J., Thermal-decomposition of "2,2,6-trimethyl-4*H*-1,3-dioxin-4-one and 1-ethoxybutyn-3-one. Acetylketene. *J. Org. Chem.* **1984**, *49*, 5105-5108.
 99. Evans, D. A.; Bartroli, J.; Shih, T. L., Enantioselective aldol condensations .2. erythro-selective chiral alol condensations via boron enolates. *J. Am. Chem. Soc.* **1981**, *103*, 2127-2129.
 100. Zimmerman, H. E.; Traxler, M. D., The stereochemistry of the Ivanov and Reformatsky reactions. I. *J. Am. Chem. Soc.* **1957**, *79*, 1920-1923.
 101. Braun, M., Stereoselective aldol reactions with alpha-unsubstituted chiral enolates. *Angew. Chem., Int. Ed. Engl.* **1987**, *26*, 24-37.
 102. Evans, D. A.; Takacs, J. M.; McGee, L. R.; Ennis, M. D.; Mathre, D. J.; Bartroli, J., Chiral enolate design. *Pure Appl. Chem.* **1981**, *53*, 1109-1127.
 103. Gilbert, I. H.; Ginty, M.; Oneill, J. A.; Simpson, T. J.; Staunton, J.; Willis, C. L., Synthesis of beta-keto and alpha,beta-unsaturated *N*-acetylcysteamine thioesters. *Bioorg. Med. Chem. Lett.* **1995**, *5*, 1587-1590.

104. Nagao, Y.; Yamada, S.; Kumagai, T.; Ochiai, M.; Fujita, E., Use of chiral 1,3-oxazolidine-2-thiones in the diastereoselective synthesis of aldols. *J. Chem. Soc., Chem. Commun.* **1985**, 1418-1419.
105. Crimmins, M. T.; Chaudhary, K., Titanium enolates of thiazolidinethione chiral auxiliaries: Versatile tools for asymmetric aldol additions. *Org. Lett.* **2000**, *2*, 775-777.
106. Crimmins, M. T.; King, B. W.; Tabet, E. A.; Chaudhary, K., Asymmetric aldol additions: Use of titanium tetrachloride and (-)-sparteine for the soft enolization of N-acyl oxazolidinones, oxazolidinethiones, and thiazolidinethiones. *J. Org. Chem.* **2001**, *66*, 894-902.
107. Hodge, M. B.; Olivo, H. F., Stereoselective aldol additions of titanium enolates of N-acetyl-4-isopropyl-thiazolidinethione. *Tetrahedron* **2004**, *60*, 9397-9403.
108. Castonguay, R.; He, W.; Chen, A. Y.; Khosla, C.; Cane, D. E., Stereospecificity of ketoreductase domains of the 6-deoxyerythronolide B synthase. *J. Am. Chem. Soc.* **2007**, *129*, 13758-13769.
109. Wang, S.; Xu, Y.; Maine, E. A.; Wijeratne, E. M.; Espinosa-Artiles, P.; Gunatilaka, A. A.; Molnar, I., Functional characterization of the biosynthesis of radicicol, an Hsp90 inhibitor resorcylic acid lactone from *Chaetomium chiversii*. *Chem. Biol.* **2008**, *15*, 1328-1338.
110. Rossmann, M. G.; Argos, P., Protein folding. *Annu. Rev. Biochem.* **1981**, *50*, 497-532.

111. Filling, C.; Berndt, K. D.; Benach, J.; Knapp, S.; Prozorovski, T.; Nordling, E.; Ladenstein, R.; Jornvall, H.; Oppermann, U., Critical residues for structure and catalysis in short-chain dehydrogenases/reductases. *J. Biol. Chem.* **2002**, *277*, 25677-25684.
112. Pinto, A.; Wang, M.; Horsman, M.; Boddy, C. N., 6-Deoxyerythronolide B synthase thioesterase-catalyzed macrocyclization is highly stereoselective. *Org. Lett.* **2012**, *14*, 2278-2281.
113. Xu, W.; Qiao, K.; Tang, Y., Structural analysis of protein-protein interactions in type I polyketide synthases. *Crit. Rev. Biochem. Mol. Biol.* **2013**, *48*, 98-122.
114. Tosin, M.; Demydchuk, Y.; Parascandolo, J. S.; Per, C. B.; Leeper, F. J.; Leadlay, P. F., In vivo trapping of polyketide intermediates from an assembly line synthase using malonyl carba(dethia)-N-acetyl cysteamines. *Chem. Commun.* **2011**, *47*, 3460-3462.
115. Tosin, M.; Betancor, L.; Stephens, E.; Li, W. M. A.; Spencer, J. B.; Leadlay, P. F., Synthetic chain terminators off-load intermediates from a type I polyketide synthase. *ChemBioChem* **2010**, *11*, 539-546.
116. Tosin, M.; Spiteller, D.; Spencer, J. B., Malonyl carba(dethia)- and malonyl oxa(dethia)-coenzyme A as tools for trapping polyketide intermediates. *ChemBioChem* **2009**, *10*, 1714-1723.
117. Vagstad, A. L.; Bumpus, S. B.; Belecki, K.; Kelleher, N. L.; Townsend, C. A., Interrogation of global active site occupancy of a fungal iterative

- polyketide synthase reveals strategies for maintaining biosynthetic fidelity. *J. Am. Chem. Soc.* **2012**, *134*, 6865-6877.
118. Meehan, M. J.; Xie, X.; Zhao, X.; Xu, W.; Tang, Y.; Dorrestein, P. C., FT-ICR-MS characterization of intermediates in the biosynthesis of the alpha-methylbutyrate side chain of lovastatin by the 277 kDa polyketide synthase LovF. *Biochemistry* **2011**, *50*, 287-299.
 119. Cane, D. E.; Luo, G. L., Biosynthesis of polyketide antibiotics - incorporation of a pentaketide chain elongation intermediate into nargenicin. *J. Am. Chem. Soc.* **1995**, *117*, 6633-6634.
 120. Cane, D. E.; Tan, W. T.; Ott, W. R., Nargenicin biosynthesis - incorporation of polyketide chain elongation intermediates and support for a proposed intramolecular Diels-Alder cyclization. *J. Am. Chem. Soc.* **1993**, *115*, 527-535.
 121. Cane, D. E.; Lambalot, R. H.; Prabhakaran, P. C.; Ott, W. R., Macrolide biosynthesis .7. incorporation of polyketide chain elongation intermediates into methymycin. *J. Am. Chem. Soc.* **1993**, *115*, 522-526.
 122. Cane, D. E.; Yang, C. C., Macrolide biosynthesis .4. intact incorporation of a chain-elongation intermediate into erythromycin. *J. Am. Chem. Soc.* **1987**, *109*, 1255-1257.
 123. Yuzawa, S.; Kapur, S.; Cane, D. E.; Khosla, C., Role of a conserved arginine residue in linkers between the ketosynthase and acyltransferase domains of multimodular polyketide synthases. *Biochemistry* **2012**, *51*, 3708-3710.

124. Kim, C. Y.; Alekseyev, V. Y.; Chen, A. Y.; Tang, Y. Y.; Cane, D. E.; Khosla, C., Reconstituting modular activity from separated domains of 6-deoxyerythronolide B synthase. *Biochemistry* **2004**, *43*, 13892-13898.
125. Liu, Y. Q.; Li, Z.; Vederas, J. C., Biosynthetic incorporation of advanced precursors into dehydrocurvularin, a polyketide phytotoxin from *Alternaria cinerariae*. *Tetrahedron* **1998**, *54*, 15937-15958.
126. Tsantrizos, Y. S.; Zhou, F.; Famili, P.; Yang, X. S., Biosynthesis of the hypotensive metabolite oudenone by *Oudemansiella radicata* .1. intact incorporation of a tetraketide chain elongation intermediate. *J. Org. Chem.* **1995**, *60*, 6922-6929.
127. Brobst, S. W.; Townsend, C. A., The potential role of fatty-acid initiation in the biosynthesis of the fungal aromatic polyketide aflatoxin B1. *Can. J. Chem.* **1994**, *72*, 200-207.
128. Li, Z.; Martin, M.; Vederas, J. C., Biosynthetic incorporation of labeled tetraketide intermediates into dehydrocurvularin, a phytotoxin from *Alternaria cinerariae*, with assistance of beta-oxidation inhibitors. *J. Am. Chem. Soc.* **1992**, *114*, 1531-1533.
129. Yoshizawa, Y.; Li, Z.; Reese, P. B.; Vederas, J. C., Intact incorporation of acetate-derived diketides and tetraketides during biosynthesis of dehydrocurvularin, a macrolide phytotoxin from *Alternaria cinerariae*. *J. Am. Chem. Soc.* **1990**, *112*, 3212-3213.
130. Harrison, P. H.; Noguchi, H.; Vederas, J. C., Biosynthesis of polyene antibiotics - intact incorporation of C-13 labeled octanoate into

- fungichromin by *Streptomyces cellulosa*. *J. Am. Chem. Soc.* **1986**, *108*, 3833-3834.
131. Dumas, A. M.; Fillion, E., Meldrum's acids and 5-alkylidene Meldrum's acids in catalytic carbon-carbon bond-forming processes. *Acc. Chem. Res.* **2010**, *43*, 440-454.
132. Singh, S.; Sharma, V. K.; Gill, S.; Sahota, R. I. K., Reduction of imines using NADH models. *J. Chem. Soc., Perkin Trans.* **1985**, 437-440.
133. Inoue, Y.; Imaizumi, S.; Itoh, H.; Shinya, T.; Hashimoto, H.; Miyano, S., Selective reduction of carbon-carbon double-bonds with an NAD(p)H model-acetic acid system. *Bull. Chem. Soc. Jpn.* **1988**, *61*, 3020-3022.
134. Ranu, B. C.; Samanta, S., Remarkably selective reduction of the alpha,beta-carbon-carbon double bond in highly activated alpha,beta,gamma,delta-unsaturated alkenes by the InCl₃-NaBH₄ reagent system. *J. Org. Chem.* **2003**, *68*, 7130-7132.
135. Tsukamoto, N.; Chuck, J. A.; Luo, G.; Kao, C. M.; Khosla, C.; Cane, D. E., 6-Deoxyerythronolide B synthase 1 is specifically acylated by a diketide intermediate at the beta-ketoacyl-acyl carrier protein synthase domain of module 2. *Biochemistry* **1996**, *35*, 15244-15248.
136. Valenzano, C. R.; You, Y.-O.; Garg, A.; Keatinge-Clay, A.; Khosla, C.; Cane, D. E., Stereospecificity of the dehydratase domain of the erythromycin polyketide synthase. *J. Am. Chem. Soc.* **2010**, *132*, 14697-14699.

137. Kwan, D. H.; Schulz, F., The stereochemistry of complex polyketide biosynthesis by modular polyketide synthases. *Molecules* **2011**, *16*, 6092-6115.
138. Winssinger, N.; Barluenga, S., Chemistry and biology of resorcylic acid lactones. *Chem. Commun.* **2007**, 22-36.
139. Delmotte, P.; Delmotte-Plaqué, J., A new antifungal substance of fungal origin. *Nature* **1953**, *171*, 344.
140. Mirrington, R. N.; Ritchie, E.; Shoppee, C. W.; Taylor, W. C.; Sternhell, S., The constitution of radicicol. *Tetrahedron Lett.* **1964**, 365-370.
141. Lampilas, M.; Lett, R., Convergent stereospecific total synthesis of monochiral monocillin-I related macrolides. *Tetrahedron Lett.* **1992**, *33*, 773-776.
142. Culter, H. G.; Arrendale, R. F.; Springer, J. P.; D., C. P.; Roberts, R. G.; Hanlin, R. T., Monorden from a novel source,. *Agric. Biol. Chem.* **1987**, *51*, 7.
143. Sharma, S. V.; Agatsuma, T.; Nakano, H., Targeting of the protein chaperone, Hsp90, by the transformation suppressing agent, radicicol. *Oncogene* **1998**, *16*, 2639-2645.
144. Schulte, T. W.; Akinaga, S.; Soga, S.; Sullivan, W.; Stensgard, B.; Toft, D.; Neckers, L. M., Antibiotic radicicol binds to the N-terminal domain of Hsp90 and shares important biologic activities with geldanamycin. *Cell. Stress. Chaperon.* **1998**, *3*, 100-108.

145. Workman, P., Overview: translating Hsp90 biology into Hsp90 drugs. *Curr. Cancer Drug Targets* **2003**, *3*, 297-300.
146. Roe, S. M.; Prodromou, C.; O'Brien, R.; Ladbury, J. E.; Piper, P. W.; Pearl, L. H., Structural basis for inhibition of the Hsp90 molecular chaperone by the antitumor antibiotics radicicol and geldanamycin. *J. Med. Chem.* **1999**, *42*, 260-266.
147. Agatsuma, T.; Ogawa, H.; Akasaka, K.; Asai, A.; Yamashita, Y.; Mizukami, T.; Akinaga, S.; Saitoh, Y., Halohydrin and oxime derivatives of radicicol: synthesis and antitumor activities. *Bioorg. Med. Chem.* **2002**, *10*, 3445-3454.
148. Kwon, H. J.; Yoshida, M.; Fukui, Y.; Horinouchi, S.; Beppu, T., Potent and specific inhibition of p60v-src protein kinase both in vivo and in vitro by radicicol. *Cancer Res.* **1992**, *52*, 6926-6930.
149. Barluenga, S.; Fontaine, J. G.; Wang, C.; Aouadi, K.; Chen, R.; Beebe, K.; Neckers, L.; Winssinger, N., Inhibition of Hsp90 with pochoximes: SAR and structure-based insights. *ChemBioChem* **2009**, *10*, 2753-2759.
150. Moulin, E.; Zoete, V.; Barluenga, S.; Karplus, M.; Winssinger, N., Design, synthesis, and biological evaluation of Hsp90 inhibitors based on conformational analysis of radicicol and its analogues. *J. Am. Chem. Soc.* **2005**, *127*, 6999-7004.
151. Wang, C.; Barluenga, S.; Koripelly, G. K.; Fontaine, J.-G.; Chen, R.; Yu, J.-C.; Shen, X.; Chabala, J. C.; Heck, J. V.; Rubenstein, A.; Winssinger,

- N., Synthesis of pochoxime prodrugs as potent Hsp90 inhibitors. *Bioorg. Med. Chem. Lett.* **2009**, *19*, 3836-3840.
152. Wicklow, D. T.; Jordan, A. M.; Gloer, J. B., Antifungal metabolites (monorden, monocillins I, II, III) from *Colletotrichum graminicola*, a systemic vascular pathogen of maize. *Mycol. Res.* **2009**, *113*, 1433-1442.
 153. Hellwig, V.; Mayer-Bartschmid, A.; Muller, H.; Greif, G.; Kleymann, G.; Zitzmann, W.; Tichy, H. V.; Stadler, M., Pochonins A-F, new antiviral and antiparasitic resorcylic acid lactones from *Pochonia chlamydosporia* var. *catenulata*. *J. Nat. Prod.* **2003**, *66*, 829-837.
 154. Chen, R.; Rubenstein, A. E.; Shen, X.; Yu, J.-C.; Giovannini, M. Preparation of radicicol and related macrocyclic compounds which inhibit Hsp90 for therapeutic use in the treatment of neurofibromatosis. PCT Int. Appl. (2008), WO 2008150302 A1 20081211. .
 155. Alhamadsheh, M. M.; Palaniappan, N.; Daschouduri, S.; Reynolds, K. A., Modular polyketide synthases and cis double bond formation: establishment of activated cis-3-cyclohexylpropenoic acid as the diketide intermediate in phoslactomycin biosynthesis. *J. Am. Chem. Soc.* **2007**, *129*, 1910-1911.
 156. Gaffoor, I.; Trail, F., Characterization of two polyketide synthase genes involved in zearalenone biosynthesis in *Gibberella zeae*. *Appl. Environ. Microbiol.* **2006**, *72*, 1793-1799.

157. Chatterjee, A. K.; Choi, T. L.; Sanders, D. P.; Grubbs, R. H., A general model for selectivity in olefin cross metathesis. *J. Am. Chem. Soc.* **2003**, *125*, 11360-11370.
158. Elsworth, J. D.; Willis, C. L., Intramolecular Prins cyclisations for the stereoselective synthesis of bicyclic tetrahydropyrans. *Chem. Commun.* **2008**, 1587-1589.
159. Faulkner, D. J.; Petersen, M. R., Application of the Claisen rearrangement to the synthesis of trans trisubstituted olefinic bonds. Synthesis of squalene and insect juvenile hormone. *J. Am. Chem. Soc.* **1973**, *95*, 553-563.
160. Musgrave, O. C., Curvularin .1. isolation and partial characterisation of a metabolic product from a new species of curvularia. *J. Chem. Soc.* **1956**, 4301-4305.
161. Ghisalberti, E. L.; Rowland, C. Y., 6-Chlorodehydrocurvularin, a new metabolite from *Cochliobolus spicifer*. *J. Nat. Prod.* **1993**, *56*, 2175-2177.
162. Caputo, O.; Viola, F., Isolation of a, beta-dehydrocurvularin from *Aspergillus aureofulgens*. *Planta Med.* **1977**, *31*, 31-32.
163. Kusano, M.; Nakagami, K.; Fujioka, S.; Kawano, T.; Shimada, A.; Kimura, Y., Beta,gamma-dehydrocurvularin and related compounds as nematicides of *Pratylenchus penetrans* from the fungus *Aspergillus* sp. *Biosci., Biotechnol., Biochem.* **2003**, *67*, 1413-1416.
164. Gutierrez, M.; Theoduloz, C.; Rodriguez, J.; Lolas, M.; Schmeda-Hirschmann, G., Bioactive metabolites from the fungus *Nectria galligena*,

- the main apple canker agent in Chile. *J. Agric. Food Chem.* **2005**, *53*, 7701-7708.
165. Aly, A. H.; Debbab, A.; Clements, C.; Edrada-Ebel, R.; Orlikova, B.; Diederich, M.; Wray, V.; Lin, W.; Proksch, P., NF kappa B inhibitors and antitrypanosomal metabolites from endophytic fungus *Penicillium* sp. isolated from *Limonium tubiflorum*. *Bioorg. Med. Chem.* **2011**, *19*, 414-421.
 166. Dai, J.; Krohn, K.; Floerke, U.; Pescitelli, G.; Kerti, G.; Papp, T.; Koeber, K. E.; Benyei, A. C.; Draeger, S.; Schulz, B.; Kurtan, T., Curvularin-type metabolites from the fungus *Curvularia* sp. isolated from a marine alga. *Eur. J. Org. Chem.* **2010**, 6928-6937.
 167. Xie, L. W.; Ouyang, Y. C.; Zou, K.; Wang, G. H.; Chen, M. J.; Sun, H. M.; Dai, S. K.; Li, X., Isolation and difference in anti-*Staphylococcus aureus* bioactivity of curvularin derivatives from fungus *Eupenicillium* sp. *Appl. Biochem. Biotechnol.* **2009**, *159*, 284-293.
 168. Vurro, M.; Evidente, A.; Andolfi, A.; Zonno, M. C.; Giordano, F.; Motta, A., Brefeldin A and alpha,beta-dehydrocurvularin, two phytotoxins from *Alternaria zinniae*, a biocontrol agent of *Xanthium occidentale*. *Plant Sci.* **1998**, *138*, 67-79.
 169. Almassi, F.; Ghisalberti, E. L.; Skelton, B. W.; White, A. H., Structural study of dehydrocurvularin, an inhibitor of microtubule assembly. *Aust. J. Chem.* **1994**, *47*, 1193-1197.

170. Ghisalberti, E. L.; Hockless, D. C. R.; Rowland, C. Y.; White, A. H., Structural study of curvularin, a cell-division inhibitor. *Aust. J. Chem.* **1993**, *46*, 571-575.
171. Arai, K.; Rawlings, B. J.; Yoshizawa, Y.; Vederas, J. C., Biosyntheses of antibiotic a26771b by *Penicillium turbatum* and dehydrocurvularin by *Alternaria cinerariae* - comparison of stereochemistry of polyketide and fatty-acid enoyl thiol ester reductases. *J. Am. Chem. Soc.* **1989**, *111*, 3391-3399.
172. Pirkle, W. H.; Adams, P. E., Broad-spectrum synthesis of enantiomerically pure lactones .1. synthesis of sex-pheromones of the carpenter bee, rove beetle, japanese beetle, black-tailed deer, and oriental hornet. *J. Org. Chem.* **1979**, *44*, 2169-2175.
173. Yao, Y.; Hausding, M.; Erkel, G.; Anke, T.; Forstermann, U.; Kleinert, H., Sporogen, S14-95, and S-curvularin, three inhibitors of human inducible nitric-oxide synthase expression isolated from fungi. *Mol. Pharmacol.* **2003**, *63*, 383-391.
174. Elzner, S.; Schmidt, D.; Schollmeyer, D.; Erkel, G.; Anke, T.; Kleinert, H.; Foerstermann, U.; Kunz, H., Inhibitors of inducible NO synthase expression: Total synthesis of (S)-curvularin and its ring homologues. *ChemMedChem* **2008**, *3*, 924-939.
175. Schmidt, N.; Pautz, A.; Art, J.; Rauschkolb, P.; Jung, M.; Erkel, G.; Goldring, M. B.; Kleinert, H., Transcriptional and post-transcriptional

- regulation of iNOS expression in human chondrocytes. *Biochem. Pharmacol.* **2010**, *79*, 722-732.
176. Schmidt, N.; Art, J.; Forsch, I.; Werner, A.; Erkel, G.; Jung, M.; Horke, S.; Kleinert, H.; Pautz, A., The anti-inflammatory fungal compound (S)-curvularin reduces proinflammatory gene expression in an in vivo model of rheumatoid arthritis. *J. Pharmacol. Exp. Ther.* **2012**, *343*, 106-114.
 177. Rudolph, K.; Serwe, A.; Erkel, G., Inhibition of TGF-beta signaling by the fungal lactones (S)-curvularin, dehydrocurvularin, oxacyclododecindione and galiellalactone. *Cytokine* **2013**, *61*, 285-296.
 178. Santagata, S.; Xu, Y.-m.; Wijeratne, E. M. K.; Kontnik, R.; Rooney, C.; Perley, C. C.; Kwon, H.; Clardy, J.; Kesari, S.; Whitesell, L.; Lindquist, S.; Gunatilaka, A. A. L., Using the heat-shock response to discover anticancer compounds that target protein homeostasis. *ACS Chem. Biol.* **2012**, *7*, 339-348.
 179. Workman, P.; Burrows, F.; Neckers, L.; Rosen, N., Drugging the cancer chaperone Hsp90: combinatorial therapeutic exploitation of oncogene addiction and tumor stress. *Ann. N. Y. Acad. Sci.* **2007**, *1113*, 202-216.
 180. He, J.; Wijeratne, E. M.; Bashyal, B. P.; Zhan, J.; Seliga, C. J.; Liu, M. X.; Pierson, E. E.; Pierson, L. S., 3rd; VanEtten, H. D.; Gunatilaka, A. A., Cytotoxic and other metabolites of *Aspergillus* inhabiting the rhizosphere of Sonoran desert plants. *J. Nat. Prod.* **2004**, *67*, 1985-1991.

181. Birch, A. J.; Musgrave, O. C.; Rickards, R. W.; Smith, H., Studies in relation to biosynthesis .20. the structure and biosynthesis of curvularin. *J. Chem. Soc.* **1959**, 3146-3152.
182. Xu, Y.; Espinosa-Artiles, P.; Schubert, V.; Xu, Y. M.; Zhang, W.; Lin, M.; Gunatilaka, A. A.; Sussmuth, R.; Molnar, I., Characterization of the biosynthetic genes for 10,11-dehydrocurvularin, a heat shock response-modulating anticancer fungal polyketide from *Aspergillus terreus*. *Appl. Environ. Microbiol.* **2013**, *79*, 2038-2047.
183. Kim, Y. T.; Lee, Y. R.; Jin, J.; Han, K. H.; Kim, H.; Kim, J. C.; Lee, T.; Yun, S. H.; Lee, Y. W., Two different polyketide synthase genes are required for synthesis of zearalenone in *Gibberella zeae*. *Mol. Microbiol.* **2005**, *58*, 1102-1113.
184. Medema, M. H.; Blin, K.; Cimermancic, P.; de Jager, V.; Zakrzewski, P.; Fischbach, M. A.; Weber, T.; Takano, E.; Breitling, R., antiSMASH: rapid identification, annotation and analysis of secondary metabolite biosynthesis gene clusters in bacterial and fungal genome sequences. *Nucleic Acids Res.* **2011**, *39*, W339-346.
185. Blin, K.; Medema, M. H.; Kazempour, D.; Fischbach, M. A.; Breitling, R.; Takano, E.; Weber, T., antiSMASH 2.0--a versatile platform for genome mining of secondary metabolite producers. *Nucleic Acids Res.* **2013**, *41*, W204-W212.
186. Xu, Y.; Zhou, T.; Zhou, Z.; Su, S.; Roberts, S. A.; Montfort, W. R.; Zeng, J.; Chen, M.; Zhang, W.; Lin, M.; Zhan, J.; Molnar, I., Rational

- reprogramming of fungal polyketide first-ring cyclization. *Proc. Natl. Acad. Sci. U. S. A.* **2013**, *110*, 5398-5403.
187. Szewczyk, E.; Nayak, T.; Oakley, C. E.; Edgerton, H.; Xiong, Y.; Taheri-Talesh, N.; Osmani, S. A.; Oakley, B. R., Fusion PCR and gene targeting in *Aspergillus nidulans*. *Nat. Protoc.* **2006**, *1*, 3111-3120.
 188. Shuster, J.; Yu, J.; Cox, D.; Chan, R. V.; Smith, M.; Young, E., ADR1-mediated regulation of ADH2 requires an inverted repeat sequence. *Mol. Cell. Biol.* **1986**, *6*, 1894-1902.
 189. Young, E. T.; Sloan, J.; Miller, B.; Li, N.; van Riper, K.; Dombek, K. M., Evolution of a glucose-regulated ADH gene in the genus *Saccharomyces*. *Gene* **2000**, *245*, 299-309.
 190. Walther, K.; Schuller, H. J., Adr1 and Cat8 synergistically activate the glucose-regulated alcohol dehydrogenase gene ADH2 of the yeast *Saccharomyces cerevisiae*. *Microbiology* **2001**, *147*, 2037-2044.
 191. Lee, K. M.; DaSilva, N. A., Evaluation of the *Saccharomyces cerevisiae* ADH2 promoter for protein synthesis. *Yeast* **2005**, *22*, 431-440.
 192. Larionov, V.; Kouprina, N.; Eldarov, M.; Perkins, E.; Porter, G.; Resnick, M. A., Transformation-associated recombination between diverged and homologous DNA repeats is induced by strand breaks. *Yeast* **1994**, *10*, 93-104.
 193. Gibson, D. G.; Benders, G. A.; Andrews-Pfannkoch, C.; Denisova, E. A.; Baden-Tillson, H.; Zaveri, J.; Stockwell, T. B.; Brownley, A.; Thomas, D. W.; Algire, M. A.; Merryman, C.; Young, L.; Noskov, V. N.; Glass, J. I.;

- Venter, J. C.; Hutchison, C. A., 3rd; Smith, H. O., Complete chemical synthesis, assembly, and cloning of a *Mycoplasma genitalium* genome. *Science* **2008**, *319*, 1215-1220.
194. Xu, W.; Chooi, Y. H.; Choi, J. W.; Li, S.; Vederas, J. C.; Da Silva, N. A.; Tang, Y., LovG: the thioesterase required for dihydromonacolin L release and lovastatin nonaketide synthase turnover in lovastatin biosynthesis. *Angew. Chem., Int. Ed. Engl.* **2013**, *52*, 6472-6475.
195. Nunes, C. C.; Dean, R. A., Host-induced gene silencing: a tool for understanding fungal host interaction and for developing novel disease control strategies. *Mol. Plant. Pathol* **2012**, *13*, 519-529.
196. Perrin, D. D. A.; W. L. F., Purification of Laboratory Chemicals. 3ed. *Pergamon Press: New York* **1993**.
197. Burr, D. A.; Chen, X. B.; Vederas, J. C., Syntheses of conjugated pyrones for the enzymatic assay of lovastatin nonaketide synthase, an iterative polyketide synthase. *Org. Lett.* **2007**, *9*, 161-164.
198. Sugimoto, K.; Kobayashi, Y.; Hori, A.; Kondo, T.; Toyooka, N.; Nemoto, H.; Matsuya, Y., Syntheses of aza-analogues of macrophelides via RCM strategy and their biological evaluation. *Tetrahedron* **2011**, *67*, 7681-7685.
199. Marukawa, K.; Mori, K., Pheromone synthesis. Part CCXVIII. Synthesis of (1R,3S,5S)-1,3,8-trimethyl-2,9-dioxabicyclo 3.3.1 non-7-ene, the male pheromone of a hepialid moth, *Endoclita excrescens*, and its enantiomer. *Eur. J. Org. Chem.* **2002**, 3974-3978.

200. Brown, H. C.; Kulkarni, S. V.; Racherla, U. S.; Dhokte, U. P., Chiral synthesis via organoboranes. 47. Efficient synthesis of unsymmetrical ketones and enantiomerically pure spiro ketals using (\pm)-isopinocampheylchloroborane. *J. Org. Chem.* **1998**, *63*, 7030-7036.
201. Savage, I.; Thomas, E. J.; Wilson, P. D., Stereoselective synthesis of allylic amines by rearrangement of allylic trifluoroacetimidates: stereoselective synthesis of polyoxamic acid and derivatives of other α -amino acids. *J. Chem. Soc., Perkin Trans. I* **1999**, 3291-3303.
202. Less, S. L.; Handa, S.; Millburn, K.; Leadlay, P. F.; Dutton, C. J.; Staunton, J., Biosynthesis of tetronasin .6. Preparation of structural analogues of the diketide and triketide biosynthetic precursors to tetronasin. *Tetrahedron Lett.* **1996**, *37*, 3515-3518.
203. Kalivretenos, A.; Stille, J. K.; Hegedus, L. S., Synthesis of beta-resorcylic macrolides via organopalladium chemistry. Application to the total synthesis of (s)-zearalenone. *J. Org. Chem.* **1991**, *56*, 2883-2894.
204. Islam, M. S.; Ishigami, K.; Watanabe, H., Synthesis of (-)-mellein, (+)-ramulosin, and related natural products. *Tetrahedron* **2007**, *63*, 1074-1079.
205. Teichert, A.; Jantos, K.; Harms, K.; Studer, A., One-pot homolytic aromatic substitutions/HWE olefinations under microwave conditions for the formation of a small oxindole library. *Org. Lett.* **2004**, *6*, 3477-3480.
206. Miziorko, H. M.; Behnke, C. E.; Ahmad, F., Chemical events in chloropropionyl-coenzyme A inactivation of acyl-coenzyme A utilizing enzymes. *Biochemistry* **1989**, *28*, 5759-5764.

207. Vu, N. Q.; Chai, C. L. L.; Lim, K. P.; Chia, S. C.; Chen, A., An efficient and practical total synthesis of aigialomycin D. *Tetrahedron* **2007**, *63*, 7053-7058.
208. Jogireddy, R.; Barluenga, S.; Winssinger, N., Molecular editing of kinase-targeting resorcylic acid lactones (RAL): fluoroenone RAL. *ChemMedChem* **2010**, *5*, 670-673.
209. Yoshino, T.; Ng, F.; Danishefsky, S. J., A total synthesis of xestodecalactone A and proof of its absolute stereochemistry: interesting observations on dienophilic control with 1,3-disubstituted nonequivalent allenes. *J. Am. Chem. Soc.* **2006**, *128*, 14185-14191.
210. Dixon, D. J.; Ley, S. V.; Tate, E. W., Diastereoselective oxygen to carbon rearrangements of anomERICALLY linked enol ethers and the total synthesis of (+)-(S,S)-(cis-6-methyltetrahydropyran-2-yl)acetic acid, a component of civet. *J. Chem. Soc., Perkin Trans. I* **2000**, 2385-2394.
211. Jones, E. W., Tackling the protease problem in *Saccharomyces cerevisiae*. *Methods Enzymol.* **1991**, *194*, 428-453.
212. Al-Samarrai, T. H.; Schmid, J., A simple method for extraction of fungal genomic DNA. *Lett. Appl. Microbiol.* **2000**, *30*, 53-56.

Appendix: X-ray crystal structure of dehydrocurvularin

(5)

XCL Code: JCV0903

Date: 14 October 2009

Compound: (5*Z*,11*Z*)-7,14,16-trihydroxy-3-methyl-3,4,7,8,9,10-hexahydro-1*H*-2-benzoxacyclotetradecin-1-one, monohydrate

Formula: C₁₈H₂₄O₆

Supervisor: J. C. Vederas **Crystallographer:** M. J. Ferguson

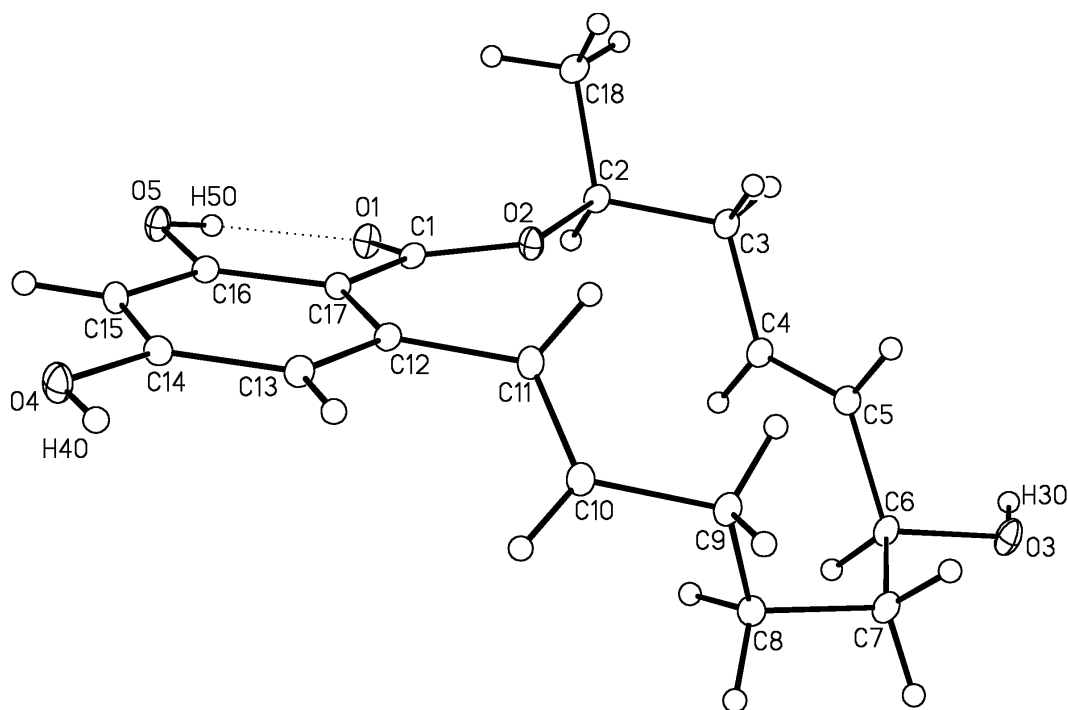


Figure 1. Perspective view of the (5*Z*,11*Z*)-7,14,16-trihydroxy-3-methyl-3,4,7,8,9,10-hexahydro-1*H*-2-benzoxacyclotetradecin-1-one molecule showing the atom labelling scheme. Non-hydrogen atoms are represented by Gaussian ellipsoids at the 20% probability level. Hydrogen atoms are shown with arbitrarily small thermal parameters.

Table 1. Crystallographic Experimental Details*A. Crystal Data*

formula	C ₁₈ H ₂₄ O ₆
formula weight	336.37
crystal dimensions (mm)	0.54 × 0.44 × 0.17
crystal system	orthorhombic
space group	<i>P</i> 2 ₁ 2 ₁ 2 ₁ (No. 19)
unit cell parameters ^a	
<i>a</i> (Å)	8.3124 (3)
<i>b</i> (Å)	9.5889 (3)
<i>c</i> (Å)	21.4172 (6)
<i>V</i> (Å ³)	1707.10 (9)
<i>Z</i>	4
ρ _{calcd} (g cm ⁻³)	1.309
μ (mm ⁻¹)	0.098

B. Data Collection and Refinement Conditions

diffractometer	Bruker D8/APEX II CCD ^b
radiation (λ [Å])	graphite-monochromated Mo Kα
(0.71073)	
temperature (°C)	−100
scan type	ω scans (0.3°) (20 s exposures)
data collection 2θ limit (deg)	55.16
total data collected	15112 (−10 ≤ <i>h</i> ≤ 10, −12 ≤ <i>k</i> ≤ 12, −
27 ≤ <i>l</i> ≤ 27)	
independent reflections	2269 (<i>R</i> _{int} = 0.0118)
number of observed reflections (<i>NO</i>)	2222 [<i>F</i> _o ² ≥ 2σ(<i>F</i> _o ²)]
structure solution method	direct methods (<i>SHELXS</i> −97 ^c)
refinement method	full-matrix least-squares on <i>F</i> ²
(<i>SHELXL</i> −97 ^c)	
absorption correction method	multi-scan (<i>SADABS</i>)
range of transmission factors	0.9836–0.9488
data/restraints/parameters	2269 [<i>F</i> _o ² ≥ −3σ(<i>F</i> _o ²)] / 0 / 221
extinction coefficient (<i>x</i>) ^d	0.0047(10)
Flack absolute structure parameter ^e	0(10)
goodness-of-fit (<i>S</i>) ^f	1.040 [<i>F</i> _o ² ≥ −3σ(<i>F</i> _o ²)]
final <i>R</i> indices ^g	
<i>R</i> ₁ [<i>F</i> _o ² ≥ 2σ(<i>F</i> _o ²)]	0.0276
<i>wR</i> ₂ [<i>F</i> _o ² ≥ −3σ(<i>F</i> _o ²)]	0.0771
largest difference peak and hole	0.272 and −0.155 e Å ⁻³

^aObtained from least-squares refinement of 9798 reflections with $4.66^\circ < 2\theta < 55.08^\circ$.

^bPrograms for diffractometer operation, data collection, data reduction and absorption correction were those supplied by Bruker.

^cSheldrick, G. M. *Acta Crystallogr.* **2008**, *A64*, 112–122.

^d $F_c^* = kF_c[1 + x\{0.001F_c^2\lambda^3/\sin(2\theta)\}]^{-1/4}$ where k is the overall scale factor.

^eFlack, H. D. *Acta Crystallogr.* **1983**, *A39*, 876–881; Flack, H. D.; Bernardinelli, G. *Acta Crystallogr.* **1999**, *A55*, 908–915; Flack, H. D.; Bernardinelli, G. *J. Appl. Cryst.* **2000**, *33*, 1143–1148. The Flack parameter will refine to a value near zero if the structure is in the correct configuration and will refine to a value near one for the inverted configuration. The low anomalous scattering power of the atoms in this structure (none heavier than oxygen) implies that the data **cannot be used for absolute structure assignment**. Friedel pairs were merged prior to final refinement and thus the **Flack parameter is meaningless**. Relative stereochemistry is assigned on the basis of the known stereochemistry of the precursor compound.

$fS = [\Sigma w(F_o^2 - F_c^2)^2/(n - p)]^{1/2}$ (n = number of data; p = number of parameters varied; $w = [\sigma^2(F_o^2) + (0.0493P)^2 + 0.3149P]^{-1}$ where $P = [\text{Max}(F_o^2, 0) + 2F_c^2]/3$).

$gR_1 = \Sigma||F_o| - |F_c||/\Sigma|F_o|$; $wR_2 = [\Sigma w(F_o^2 - F_c^2)^2/\Sigma w(F_o^4)]^{1/2}$.

Table 2. Atomic Coordinates and Equivalent Isotropic Displacement Parameters

Atom	<i>x</i>	<i>y</i>	<i>z</i>	<i>U</i> _{eq} , Å ²
O1	0.33190(14)	0.38686(11)	0.44523(4)	0.0262(2)*
O2	0.19597(13)	0.57572(10)	0.41411(4)	0.0231(2)*
O3	0.33214(16)	1.05653(11)	0.22435(5)	0.0304(3)*
O4	0.25678(15)	0.67778(11)	0.70836(4)	0.0287(2)*
O5	0.33231(14)	0.32491(10)	0.56061(5)	0.0261(2)*
C1	0.26670(17)	0.49946(14)	0.45777(6)	0.0199(3)*
C2	0.18001(18)	0.51441(14)	0.35122(5)	0.0209(3)*
C3	0.13673(19)	0.63501(15)	0.30838(6)	0.0240(3)*
C4	0.26431(19)	0.74467(15)	0.30048(6)	0.0236(3)*
C5	0.23304(18)	0.87986(15)	0.29477(6)	0.0230(3)*
C6	0.35822(18)	0.99002(14)	0.28406(6)	0.0233(3)*
C7	0.3569(2)	1.10660(15)	0.33252(6)	0.0247(3)*
C8	0.38369(18)	1.05146(16)	0.39909(6)	0.0237(3)*
C9	0.22790(18)	1.02929(14)	0.43642(6)	0.0229(3)*
C10	0.25401(18)	0.92687(15)	0.48839(6)	0.0232(3)*
C11	0.18353(17)	0.80265(14)	0.48995(6)	0.0207(3)*
C12	0.22051(16)	0.69526(14)	0.53764(6)	0.0191(3)*
C13	0.22163(18)	0.73646(15)	0.59990(6)	0.0220(3)*
C14	0.25771(17)	0.64112(15)	0.64744(6)	0.0224(3)*
C15	0.29395(18)	0.50377(15)	0.63295(6)	0.0233(3)*
C16	0.29645(16)	0.46170(14)	0.57105(6)	0.0207(3)*
C17	0.25888(16)	0.55486(14)	0.52192(6)	0.0186(2)*
C18	0.0481(2)	0.40550(16)	0.35272(7)	0.0281(3)*
O1S	0.36837(15)	0.88093(13)	0.12449(5)	0.0346(3)*

Anisotropically-refined atoms are marked with an asterisk (*). The form of the anisotropic displacement parameter is: $\exp[-2\pi^2(h^2a^{*2}U_{11} + k^2b^{*2}U_{22} + l^2c^{*2}U_{33} + 2klb^*c^*U_{23} + 2hla^*c^*U_{13} + 2hka^*b^*U_{12})]$.

Table 3. Selected Interatomic Distances (Å)

Atom1	Atom2	Distance	Atom	Atom2	Distance
O1	C1	1.2376(17)	C6	C7	1.5253(19)
O2	C1	1.3247(16)	C7	C8	1.5370(18)
O2	C2	1.4755(14)	C8	C9	1.537(2)
O3	C6	1.4454(15)	C9	C10	1.5002(18)
O4	C14	1.3514(16)	C10	C11	1.3278(19)
O5	C16	1.3636(17)	C11	C12	1.4825(18)
C1	C17	1.4746(17)	C12	C13	1.3908(17)
C2	C3	1.5194(18)	C12	C17	1.4239(18)
C2	C18	1.514(2)	C13	C14	1.4008(19)
C3	C4	1.503(2)	C14	C15	1.386(2)
C4	C5	1.328(2)	C15	C16	1.3859(18)
C5	C6	1.500(2)	C16	C17	1.4151(18)

Table 4. Selected Interatomic Angles (deg)

Atom1 Atom2 Atom3 Angle

C1	O2	C2	117.67(10)
O1	C1	O2	121.52(12)
O1	C1	C17	122.40(12)
O2	C1	C17	116.06(11)
O2	C2	C3	105.63(10)
O2	C2	C18	108.70(10)
C3	C2	C18	111.48(12)
C2	C3	C4	115.68(12)
C3	C4	C5	123.73(15)
C4	C5	C6	124.45(15)
O3	C6	C5	109.99(11)
O3	C6	C7	106.11(11)
C5	C6	C7	114.01(11)
C6	C7	C8	112.21(11)
C7	C8	C9	114.08(12)
C8	C9	C10	110.77(12)

Atom1 Atom2 Atom3 Angle

C9	C10	C11	122.83(13)
C10	C11	C12	123.29(12)
C11	C12	C13	117.69(12)
C11	C12	C17	122.71(12)
C13	C12	C17	119.58(12)
C12	C13	C14	120.86(13)
O4	C14	C13	122.06(13)
O4	C14	C15	117.68(12)
C13	C14	C15	120.26(12)
C14	C15	C16	119.60(12)
O5	C16	C15	116.12(12)
O5	C16	C17	122.24(12)
C15	C16	C17	121.61(13)
C1	C17	C12	124.80(12)
C1	C17	C16	117.11(12)
C12	C17	C16	118.07(12)

Table 5. Torsional Angles (deg)

Atom1	Atom2	Atom3	Atom4	Angle	Atom1	Atom2	Atom3	Atom4	Angle
C2	O2	C1	O1	7.23(19)	C9	C10	C11	C12	173.78(13)
C2	O2	C1	C17	-171.14(11)	C10	C11	C12	C13	48.69(19)
C1	O2	C2	C3	-165.69(12)	C10	C11	C12	C17	-129.44(15)
C1	O2	C2	C18	74.57(15)	C11	C12	C13	C14	-179.13(13)
O1	C1	C17	C12	164.61(14)	C17	C12	C13	C14	-0.9(2)
O1	C1	C17	C16	-13.7(2)	C11	C12	C17	C1	0.0(2)
O2	C1	C17	C12	-17.0(2)	C11	C12	C17	C16	178.34(13)
O2	C1	C17	C16	164.64(12)	C13	C12	C17	C1	-178.06(13)
O2	C2	C3	C4	65.77(15)	C13	C12	C17	C16	0.2(2)
C18	C2	C3	C4	-176.34(12)	C12	C13	C14	O4	-178.77(14)
C2	C3	C4	C5	-143.73(14)	C12	C13	C14	C15	0.4(2)
C3	C4	C5	C6	-177.20(11)	O4	C14	C15	C16	-179.92(13)
C4	C5	C6	O3	116.69(15)	C13	C14	C15	C16	0.9(2)
C4	C5	C6	C7	-124.28(15)	C14	C15	C16	O5	-179.69(13)
O3	C6	C7	C8	-179.91(12)	C14	C15	C16	C17	-1.6(2)
C5	C6	C7	C8	58.87(17)	O5	C16	C17	C1	-2.6(2)
C6	C7	C8	C9	-97.11(15)	O5	C16	C17	C12	179.00(12)
C7	C8	C9	C10	157.70(12)	C15	C16	C17	C1	179.46(13)
C8	C9	C10	C11	-113.78(15)	C15	C16	C17	C12	1.0(2)

Table 6. Anisotropic Displacement Parameters (U_{ij} , Å²)

Atom	U_{11}	U_{22}	U_{33}	U_{23}	U_{13}	U_{12}
O1	0.0337(5)	0.0221(5)	0.0228(4)	-0.0009(4)	0.0030(4)	0.0073(4)
O2	0.0340(5)	0.0202(4)	0.0149(4)	-0.0017(3)	-0.0019(4)	0.0030(4)
O3	0.0519(7)	0.0219(5)	0.0175(4)	0.0024(4)	0.0007(5)	0.0000(5)
O4	0.0424(6)	0.0274(5)	0.0164(4)	-0.0013(4)	-0.0028(4)	-0.0004(5)
O5	0.0365(6)	0.0192(4)	0.0226(4)	0.0030(4)	-0.0011(4)	0.0046(4)
C1	0.0215(6)	0.0188(6)	0.0195(6)	0.0007(5)	0.0025(5)	-0.0015(5)
C2	0.0284(7)	0.0195(6)	0.0148(5)	-0.0034(5)	0.0018(5)	-0.0008(5)
C3	0.0325(7)	0.0220(6)	0.0173(6)	0.0006(5)	-0.0025(5)	-0.0025(6)
C4	0.0284(7)	0.0238(6)	0.0185(5)	0.0019(5)	0.0012(5)	-0.0009(6)
C5	0.0263(7)	0.0238(6)	0.0188(5)	0.0004(5)	-0.0010(5)	-0.0007(6)
C6	0.0306(7)	0.0206(6)	0.0187(6)	0.0035(5)	0.0012(5)	-0.0002(6)
C7	0.0345(7)	0.0190(6)	0.0205(6)	0.0024(5)	0.0001(6)	-0.0019(6)
C8	0.0262(7)	0.0240(6)	0.0207(6)	0.0019(5)	-0.0016(5)	-0.0010(6)
C9	0.0281(7)	0.0193(6)	0.0214(6)	0.0021(5)	0.0008(6)	0.0021(5)
C10	0.0287(7)	0.0232(6)	0.0177(6)	0.0006(5)	-0.0012(5)	0.0002(6)
C11	0.0267(6)	0.0196(6)	0.0158(5)	-0.0004(5)	0.0003(5)	0.0033(5)
C12	0.0208(6)	0.0188(6)	0.0178(5)	0.0006(5)	0.0010(5)	-0.0010(5)
C13	0.0274(6)	0.0203(6)	0.0185(6)	-0.0014(5)	0.0003(5)	-0.0010(6)
C14	0.0237(6)	0.0263(6)	0.0172(6)	0.0005(5)	-0.0015(5)	-0.0038(6)
C15	0.0262(7)	0.0251(6)	0.0185(6)	0.0042(5)	-0.0032(5)	-0.0004(6)
C16	0.0203(6)	0.0198(6)	0.0219(6)	0.0019(5)	-0.0006(5)	-0.0010(5)
C17	0.0202(6)	0.0185(6)	0.0173(5)	0.0000(5)	0.0001(5)	-0.0005(5)
C18	0.0324(7)	0.0244(7)	0.0274(7)	0.0011(6)	-0.0008(6)	-0.0051(6)
O1S	0.0337(6)	0.0360(6)	0.0341(6)	-0.0105(5)	0.0057(5)	-0.0029(5)

The form of the anisotropic displacement parameter is:

$$\exp[-2\pi^2(h^2a^{*2}U_{11} + k^2b^{*2}U_{22} + l^2c^{*2}U_{33} + 2klb^*c^*U_{23} + 2hla^*c^*U_{13} + 2hka^*b^*U_{12})]$$

Table 7. Derived Atomic Coordinates and Displacement Parameters for Hydrogen Atoms

Atom	<i>x</i>	<i>y</i>	<i>z</i>	<i>U</i> _{eq} , Å ²
H3O	0.3374	0.9965	0.1958	0.037
H4O	0.2355	0.7631	0.7116	0.034
H5O	0.3502	0.3126	0.5224	0.031
H2	0.2841	0.4713	0.3379	0.025
H3A	0.1102	0.5967	0.2667	0.029
H3B	0.0385	0.6803	0.3248	0.029
H4	0.3735	0.7156	0.2995	0.028
H5	0.1240	0.9088	0.2977	0.028
H6	0.4668	0.9451	0.2840	0.028
H7A	0.2522	1.1558	0.3307	0.030
H7B	0.4423	1.1748	0.3223	0.030
H8A	0.4422	0.9617	0.3966	0.028
H8B	0.4529	1.1182	0.4220	0.028
H9A	0.1916	1.1195	0.4540	0.028
H9B	0.1426	0.9942	0.4082	0.028
H10	0.3240	0.9520	0.5216	0.028
H11	0.1055	0.7815	0.4590	0.025
H13	0.1976	0.8305	0.6103	0.026
H15	0.3169	0.4389	0.6653	0.028
H18A	0.0792	0.3298	0.3810	0.034
H18B	0.0318	0.3680	0.3106	0.034
H18C	-0.0520	0.4482	0.3675	0.034
H1SA	0.4571	0.8731	0.1047	0.042
H1SB	0.3094	0.8199	0.1075	0.042